Università degli Studi di Milano
Department of Chemistry

Doctorate School in Chemical Science and Technologies
Ph.D Course in Chemistry - XXXIV Cycle

Free-Base Porphyrin for CO_2 Activation

Ph.D Thesis of:
Paolo Sonzini
Matr. n.
R12430

Tutor: Prof. Emma Gallo
Co-Tutor: Dott. Caterina Damiano
Coordinator: Prof. Daniele Passarella

Academic Year 2020/2021

Table of contents

CHAPTER I: INTRODUCTION 5

1. CLIMATE CHANGE IN TODAY'S WORLD 6
2. THE CARBON DIOXIDE PROBLEM 10
3. CARBON DIOXIDE AND ITS ACTIVATION 12
4. CARBON DIOXIDE UTILIZATION (CCU) 15
5. CARBON DIOXIDE CYCLOADDITION TO THREE MEMBERED HETEROCYCLES 19
6. CYCLIC CARBONATES AND OXAZOLIDINONES 25
7. PORPHYRINS AND THEIR COMPLEXES 28
8. HOMOGENOUS CATALYSIS FOR CARBON DIOXIDE CYCLOADDITION TO THREE MEMBERED HETEROCYCLES 34
9. HETEROGENOUS CATALYSIS FOR CARBON DIOXIDE CYCLOADDITION TO THREE MEMBERED HETEROCYCLES 43
10. TANDEM REACTIONS FOR THE SYNTHESIS OF CYCLIC CARBONATES AND OXAZOLIDINONES . 52

CHAPTER II: HOMOGENEOUS CATALYSTS FOR THE CO_2 CYCLOADDITION REACTION 57

1. THE RUTHENIUM *BIS-IMIDO* PORPHYRIN CATALYST 58
2. A NEW CATALYTIC SYSTEM 63
3. OPTIMIZATION OF THE REACTION CONDITIONS 66
4. STUDY OF THE REACTION SCOPE OF THE CARBON DIOXIDE CYCLOADDITION TO *N*-ARYL AZIRIDINES 70
5. TANDEM PROCEDURE FOR OXAZOLIDINONES SYNTHESIS 74
6. MECHANISTIC INSIGHT 77
7. ENLARGING THE REACTION SCOPE 79
8. SYNTHESIS AND CATALYTIC ACTIVITY OF A BIFUNCTIONAL CATALYST 85
9. CARBON DIOXIDE CYCLOADDITION TO EPOXIDES 87
10. CONCLUSIONS 93

CHAPTER III: HETEROGENEOUS CATALYSTS FOR THE CO_2 CYCLOADDITION REACTION .. 95

1. SBA-15 SUPPORTED PORPHYRIN 96
2. CARBON DIOXIDE CYCLOADDITION TO EPOXIDES 105
3. CARBON DIOXIDE CYCLOADDITION TO AZIRIDINES 109

4. CONCLUSIONS 119

CHAPTER IV: EXPERIMENTAL SECTION 121

1. GENERAL AND CHARACTERIZATION 122
2. SYNTHESIS OF THE CATALYSTS 124
3 ^{1}H, ^{13}C AND ^{19}F NMR SPECTRA OF UNPUBLISHED CATALYSTS 146
4 SYNTHESIS OF *N*-ARYL AZIRIDINES 149
5 ^{1}H, ^{13}C AND ^{19}F NMR SPECTRA OF UNREPORTED *N*-ARYL AZIRIDINES 165
6 SYNTHESIS OF *N*-ALKYL AZIRIDINES 175
7 ^{1}H AND ^{13}C SPECTRA OF UNPUBLISHED *N*-ALKYL AZIRIDINES 181
8 CARBON DIOXIDE CYCLOADDITION TO *N*-ARYL AZIRIDINES 182
1. ^{1}H, ^{13}C AND ^{19}F NMR SPECTRA OF UNREPORTED *N*-ARYL OXAZOLIDINONES 196
9 CARBON DIOXIDE CYCLOADDITION TO *N*-ALKYL AZIRIDINES 217
10 ^{1}H AND ^{13}C NMR SPECTRA OF UNREPORTED *N*-ALKYL OXAZOLIDINONES 223
11. CARBON DIOXIDE CYCLOADDITION TO EPOXIDES 224

Chapter I: Introduction

1. Climate change in today's world

The atmospheric concentration of carbon dioxide in 2019 was the highest in the last 2 million years and the human influence in its rising is indisputable.[1]

In the last Assessment Report of the Intergovernmental Panel on Climate Change it is clearly explained how the increase of the atmospheric concentration of greenhouse gas (GHG) since 1750 has undoubtedly an anthropogenic origin.[1] Moreover, the high concentration of GHG leads to a series of other correlated problems as, for instance, global warming with the correlated glacier retreat and arctic sea ice loss, rises in ocean temperature, its acidification, and the rise in sea levels.

The case of global warming may be understood by studying the global mean surface temperature and the global surface air temperature, in fact these two parameters have continuously increased in the last 40 years, reaching the highest temperatures since 1850. Additionally, in the period 1950-2010 the anthropogenic warming is almost the only cause of the rising in temperature.[2]

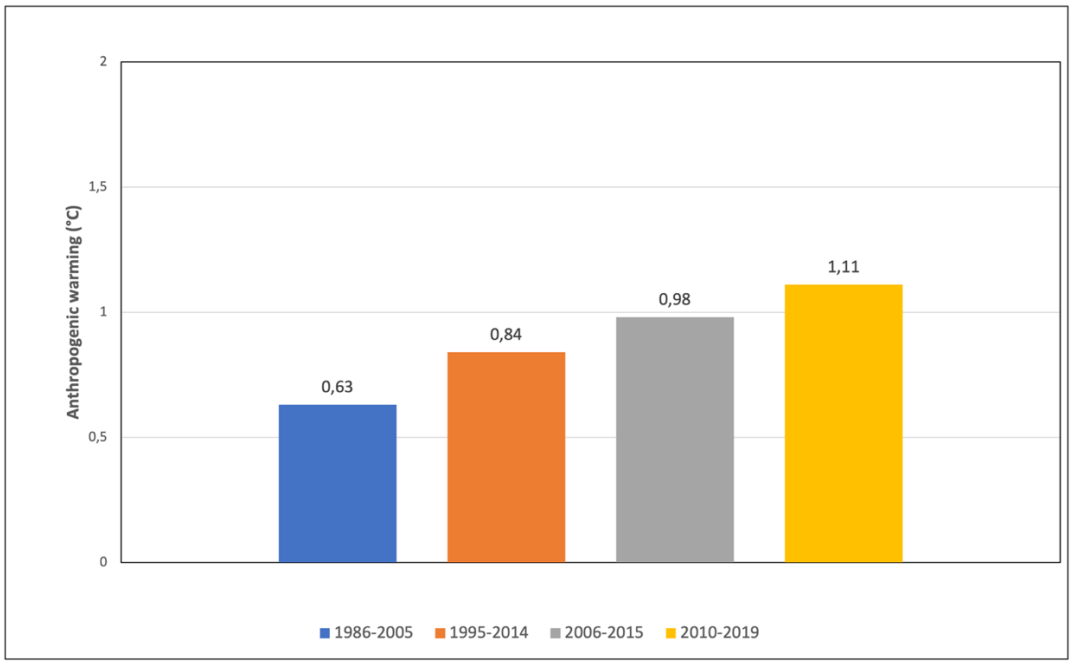

Figure 1: *human influenced global surface air temperature warming with respect to the period 1850-1900.*

Considering the trend represented in figure 1, if nothing is done to turn the tide, temperatures would keep growing at a rate never seen in the last 2000 years. Moreover, global warming will cross the 2 °C over the pre-industrial level by the 21st century, causing bigger and more serious problems unless GHGs emissions are drastically reduced.[1] Naturally, the warming of the surface temperature is not the only problem that arises with high concentration of carbon dioxide; even the temperature of the ocean rose in the last 50 years and the global mean sea level increased too due to the retreat of glaciers and the decrease of the Antarctic sea ice. Another consequence caused by the high concentration of CO_2 in the atmosphere is the acidification of the oceans, which not only has potential harsh effects on the marine ecosystem,[3] but even on the marine capability of exchanging carbon dioxide with the atmosphere and this would lead to the fall of the ocean mitigating potential.[1]

To slow down world pollution and its influence on the climate most of the member states of the United Nations Framework Convention on Climate Change (UNFCCC) have approved the Paris Agreement. This document aims to outline a common path to fight climate change through three fundamental goals: keep global warming under the 2°C, which is the limit to avoid further problems and risks, reduce greenhouse gas emissions, and re-design the economic flows and pathways towards green developments by 2020.[4]

In 2021 the UNFCCC met in Glasgow in order to renew the Paris Agreement and set new and more efficient goals to accelerate the impact on global climate change. The fundamental goal is to limit the rise of global temperature under 1.5°C in four ways: mitigation, adaptation, finance, and collaboration.[5] Focusing on the first point, many countries agreed to fix the 2030 as the limit to reach carbon neutrality by the so called neat zero emission, which means that all the GHG released in the atmosphere by humans has to be balanced by carbon removal (natural or technological). Switch from coal power to a greener energy supplier, stop and reverse deforestation, reduce all the other GHG emissions other than CO_2 ones, and improve the transition to electric vehicles are some of the paths identified to reach this goal. The reduction of carbon dioxide emissions is a fundamental step, but even the ability to catch this gas before or after it is released in the atmosphere is essential and may greatly help reach the fixed purpose.

Throughout the year, these goals gave an intellectual and economic boost to the development of new ideas that can both satisfy the need to reverse the pollution path and to keep alive the economic growth of the planet. Simultaneously to the climate struggle, it became clear that the linear economy based on the "take-make-dispose" chain was ineffective and even harmful. This kind of industrial economy barely moved forward the first steps of the industrialized era, but the linear path brings with it many problems.[6] First, from a merely economic point of view, all the projections indicate that in the next years the request for raw material and energy will rise causing a rise in prices.[7] In the past, the low prices of resources have indeed fed the linear economic pathway, thus the possibility to reuse materials has never been a true necessity. This "take-make-dispose" approach brings with it a very high waste production, not only after the usage of materials (end-of-life waste) but even during all the take-make chain that do not recover and reuse the leftovers.[6] Moreover, exploiting the linear system causes a deep waste of energy not only because disposal is often energy costing, but even because typically the extraction of the material and the first steps of conversion in commercially suitable forms are the most energy-costing steps in the entire chain; all this energy waste may be avoided by reusing the material disposed. Not only do waste production and energy loss bring to economic struggle and raw materials depletion, but they also have a negative influence on climate change.[6]

The solution to the problems raised by the ineffectiveness of linear economy is the so-called circular economy that is based on a restorative intention, wanting to exploit only renewable energy, eliminate toxic chemicals, and remove waste from the chain. The circular economy does not rely only on the need to efficiently use resources, but even completely changes the point of view in the economic system: the focus must be on the system rather than on the components. Looking through the circular economy lenses waste does not exist anymore but becomes part of the product cycle because it is designed for that.[6] Moreover, in the circular economy point of view, waste may be considered as the nutrients that renew the cycle, both biological and technological.[8]

The urgency to find new chemical outcomes fighting climate change and preventing new kinds of pollution led to a great development of the green chemistry. To understand what

green chemistry means, it is possible to refer to the principles stated by Anastas and Warner in 1998.[9] To follow this worthy path is fundamental to eliminate the production of waste using renewable feedstock and energy efficient processes. Moreover, the two authors underline the necessity to avoid hazardous synthesis and prefer catalytic pathways which need to exploit benign solvents and auxiliaries for the synthesis of benign chemicals designed for degradation. Furthermore, it is important to consider the atom economy of the reaction, always targeting the 100%. Finally, a green process must work to prevent damages to humans and to the environment. Applying these principles to the carbon field, the so called green carbon science was born.[10]

Looking to the green chemistry principles analyzed above and to the basis of circular economy already summarized, it is possible to understand how these two fields are deeply connected and have the same goals.

2. The carbon dioxide problem

As stated before, human activities are the main factor in the rise of the atmospheric carbon dioxide concentration in atmosphere and the highest value of all time was registered in the last years.[1] Among all the greenhouse gas, CO_2 is the most present in the atmosphere reaching 76% in the last published IPCC report on the mitigation of climate change.[11] Moreover, almost all the economic sectors play a role in the production of GHG, from energy production to transport, from agriculture to industry.

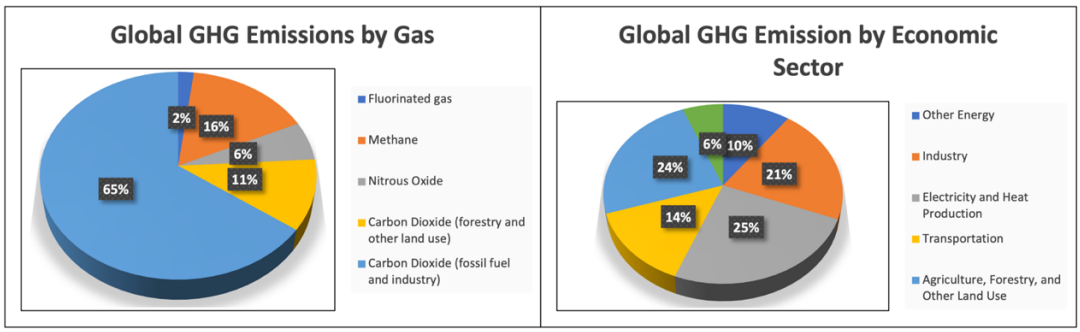

Figure 2: *Global GHG emissions per gas (left) and global GHG emissions per economic sector (right). Based on global emissions from 2010.*[11]

In order to mitigate the anthropogenic effect on the temperature change induced by the GHG emissions and keep the temperature raise under the 2 °C relative to the pre-industrial level, it will be necessary to keep the GHG concentration under 450 ppm CO_2eq (carbon dioxide concentration at the 2018 was of 410 ppm[12]). The reduction of today's emissions in necessary to do so as stated by all the predicted scenarios.[11] To reach this goal it is fundamental to drastically improve the energy production from renewables, improve the planet capacity to seize carbon dioxide by stopping deforestation and starting reforestation, and switching to electric transport.

Reducing carbon dioxide emissions may not be as fast and efficient as needed because the atmospheric concentration of GHG is still very high. However, there are different approaches that may be helpful on the road to carbon neutrality. Three ways have been identified as the most promising and interesting to help solving the CO_2 problem: Carbon

Capture and Storage (CCS), Bioenergy from Carbon Capture and Storage (BECCS) and Carbon Capture and Usage (CCU).

Carbon Capture and Storage has been pinpointed as one of the most promising technologies to meet climate change goals defined by COP26. This process encompasses three different steps: i) CO_2capture, ii) CO_2 transport and iii) CO_2 storage. The second step has already been well developed by utilizing pipelines, tankers, and tank trucks.[13] Then, the storage has been accomplished by exploiting different technologies such as CO_2-enhanced oil recovery and saline formation, moreover different technologies are still in development like enhanced gas recovery, ocean storage and mineral storage.[13–15] Finally, the capture step presents a plethora of different solutions such as chemical and physical absorption or desorption, membrane separation, and capture exploiting micro-algae; from the chemical point of view a lot of different methodologies were proposed which were basing their efforts on the properties of different kinds of molecules like amine, ionic liquids, MOF or metal oxides among others.[13,16]

Bioenergy from Carbon Capture and Storage (BECCS) is the process which allows to take energy from biomass and capture carbon dioxide from the atmosphere. Since the biomass exploits carbon dioxide in its growing through photosynthesis, if during the energy production the GHG are not released back into the atmosphere, it may be considered a negative emission technology (NET). In this case the whole system has to be evaluated very carefully to understand its efficiency and its possible contributions to the global carbon dioxide emission variation.[17,18]

Finally, a third option is Carbon Capture and Usage that aims to convert carbon dioxide into a valuable product removing it from the atmosphere permanently. Studying this field, it was discovered how it is possible to exploit CO_2 as a carbon source to obtain biofuels and fine chemicals.[19–24] Even if carbon dioxide is not very reactive, a plethora of reactions and catalysts have been studied in the last twenty years, as it will be discussed later.

It was estimated that since 1850 land and ocean sink collected from the atmosphere 1430 Gt of carbon dioxide, almost the 60% of emissions.[1] The creation of some human-made sink exploiting CCS and CCU technology is mandatory to meet the goals established by the Paris Agreement.

3. Carbon dioxide and its activation

As stated before, carbon dioxide is a very abundant potential source of C1, noxious for the environment but safe to treat to synthesize added-value products. These characteristics make this greenhouse gas a very interesting molecule to be used following the green chemistry principles. However, CO_2 is very thermodynamically and kinetically stable because its atom of carbon is in the most oxidized state possible. Thus, using it presents different drawbacks that make the processes in which carbon dioxide is involved very energy demanding.[19,25]

Carbon dioxide has 16 electrons and is a $D_{\infty h}$ molecule, thus, in its ground state, is linear. CO_2 is nonpolar and presents two polar carbon-oxygen double bonds that show two sets of orthogonal π orbitals. The lowest unoccupied molecular orbital (LUMO) is centered on the carbon atom, thus it is a Lewis acid and it is an electrophile; on the contrary, the highest occupied molecular orbital (HOMO) lies on the oxygen atoms, thus they are Lewis bases and they are nucleophiles.[26]

In order to avoid very reactive and toxic substrate, it is necessary to activate carbon dioxide and overcome its characteristic stability. To do so, it is possible to utilize cooperatively a catalyst and an energy-rich substrate like three membered heterocycles or strong nucleophile. This will furnish the thermodynamic driving force to form the product through an energy-effective process.

Because of the double electronic nature of carbon dioxide, it is possible to exploit both electron-rich and electron-deficient catalyst even simultaneously. Very good results have been achieved by exploiting organometallic catalysis.[19] Since the two oxygen atoms are weak Lewis base and then nucleophile, while the carbon atom may act as a Lewis acid, thus as an electrophile, carbon dioxide may be activated coordinating a transition metal following five basic modes as shown in figure 3.[27,28] Figure 3a) shows a metallacarboxylate, formed by electron-rich metals through an electron transfer from the metal to the carbon atom; figure 3b) represents the less stable end-on complex due to the interaction between the lone pair of one of the two oxygen atoms and the metal center; then, the complex depicted in figure 3c) is formed when the carbon dioxide acts as a bidentate ligand: this

complex require a more electron-deficient metal and should be more stable than the previous; meanwhile, the metallacycle represented in figure 3d) is formed by the combination of the previous interactions seen: the metal center donates to the carbon atom while one of the two oxygen atoms donates to the metal center; finally, figure 3e) shows the π-complex formed by a side-on interaction between the carbon dioxide double bond and the transition metal.

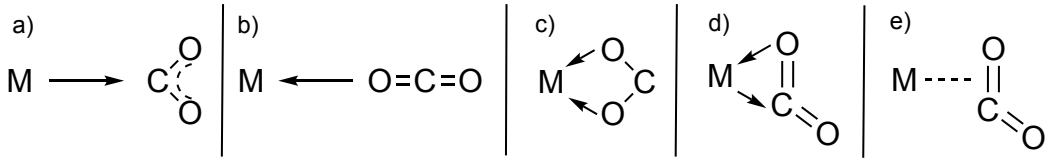

Figure 3: *different modes of metal-carbon dioxide coordination:* ***a)*** *electron transfer metal to carbon,* ***b)*** *electron transfer oxygen to metal,* ***c)*** *electron transfer oxygen to metal,* ***d)*** *electron transfer metal to carbon and oxygen to metal,* ***e)*** *π-complex.*

Keeping in mind these coordination modes, it is possible to design a suitable catalyst to activate CO_2. Knowing these carbon dioxide characteristics, it is easy to understand why different activation routes include a simultaneous and bifunctional double activation exploiting two different catalytic species: the electron-poor carbon atom and one of the electron-rich oxygen atoms give interactions with two molecules that present opposite electronic features. Clearly, it is even possible to design a single bifunctional catalyst that brings both the needed functionalities. Many different metals as chromium, zinc, cobalt and ruthenium have been used as Lewis acid in metalorganic catalysis exploiting a Lewis base as the co-catalyst.[19,29,30] Moreover, to some extent, the organic activation of carbon dioxide has also been achieved exploiting different kinds of bases: the first example has been the Kolbe-Schmitt reaction,[31–33] in which an alkaline base promotes the carboxylation of sp^2 carbon atoms.

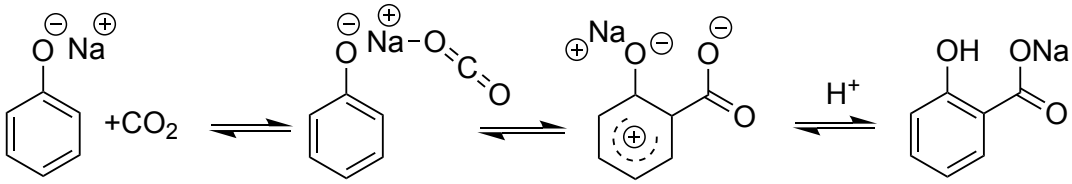

Scheme 1: *Kolbe-Schmitt reaction mechanism.*

From then, other organic bases have been studied as organic catalyst in different carbon dioxide reactions[34] and some of the most efficient ones turned out to be Lewis bases as 1,8-diazabicyclo[5.4.0]undec-7-ene (DBU)[35,36] or 1,5,7-triazabicyclo[4.4.0]dec-5-ene (TBD)[37] that may form covalent zwitterionic adduct with carbon dioxide capable of further reaction, forming new organic compounds like benzoxazinones, chinolines or carboxylated indoles and phenols. Another class of organic molecules that may catalyze carbon dioxide reactions turned out to be the phosphines that may activate CO_2 through the synthesis of carbonates, carbamates, and ureas.[38–40] Since N-heterocyclic carbenes (NHC) present strong basic features when they incorporate electron-donating heteroatoms, like the Lewis base discussed before, they form an adduct with carbon dioxide that may be isolated and used in the synthesis of cyclic carbonates form propargylic alcohols and CO_2.[41]

Finally, a more recent example of organic activation of carbon dioxide is diethyl ammonium iodide as catalyst for the synthesis of oxazolidinones.[42]

4. Carbon Dioxide Utilization (CCU)

During the past twenty years carbon dioxide has been activated through different reactions exploiting the activity of organometallic and organic catalysts or using reactive substrates. As shown in scheme 2, many different classes of compounds can be obtained using carbon dioxide as a building block. For example, CO_2 has been utilized for the carboxylation of phenols, other aromatic compounds, and alkanes through organo-boron, organo-zinc, organo-magnesium, or organo-lithium species or even alkyl halides. Moreover, by exploiting carbon dioxide reactivity, different kinds of cyclization reaction can be targeted using substrates like dienes or propargyls. Then, starting from alcohols it is possible to obtain ketones while, starting from ammonia, it is possible achieving urea. Furthermore, through the reduction of CO_2, carbon monoxide, methanol or, in combination with primary amines, amides and new amines can be produced.[19]

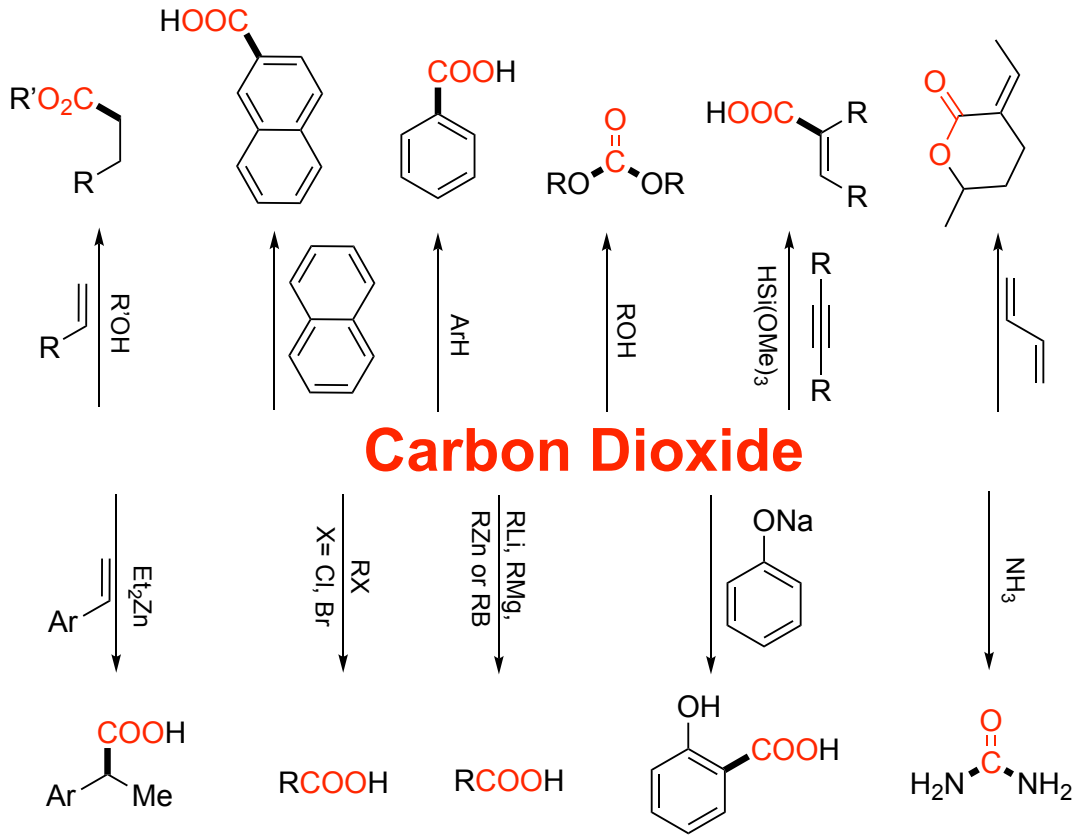

Scheme 2: *some of the possible carbon dioxide reactions.*

Generally, if the reaction substrate is very active, like a Grignard reagent for example, a catalyst would not be needed, otherwise it is possible to exploit one of the possibilities described below.

Another class of compounds that may be obtained from carbon dioxide are five membered heterocycles like cyclic carbonates and oxazolidinones. In this case, usually, a combination of a catalyst and a co-catalyst is necessary to obtain the product without rely on harsh reaction conditions that include very high temperature and/or carbon dioxide pressure.[19,43] In scheme 3 different ways to synthesize these molecules from carbon dioxide are reported.

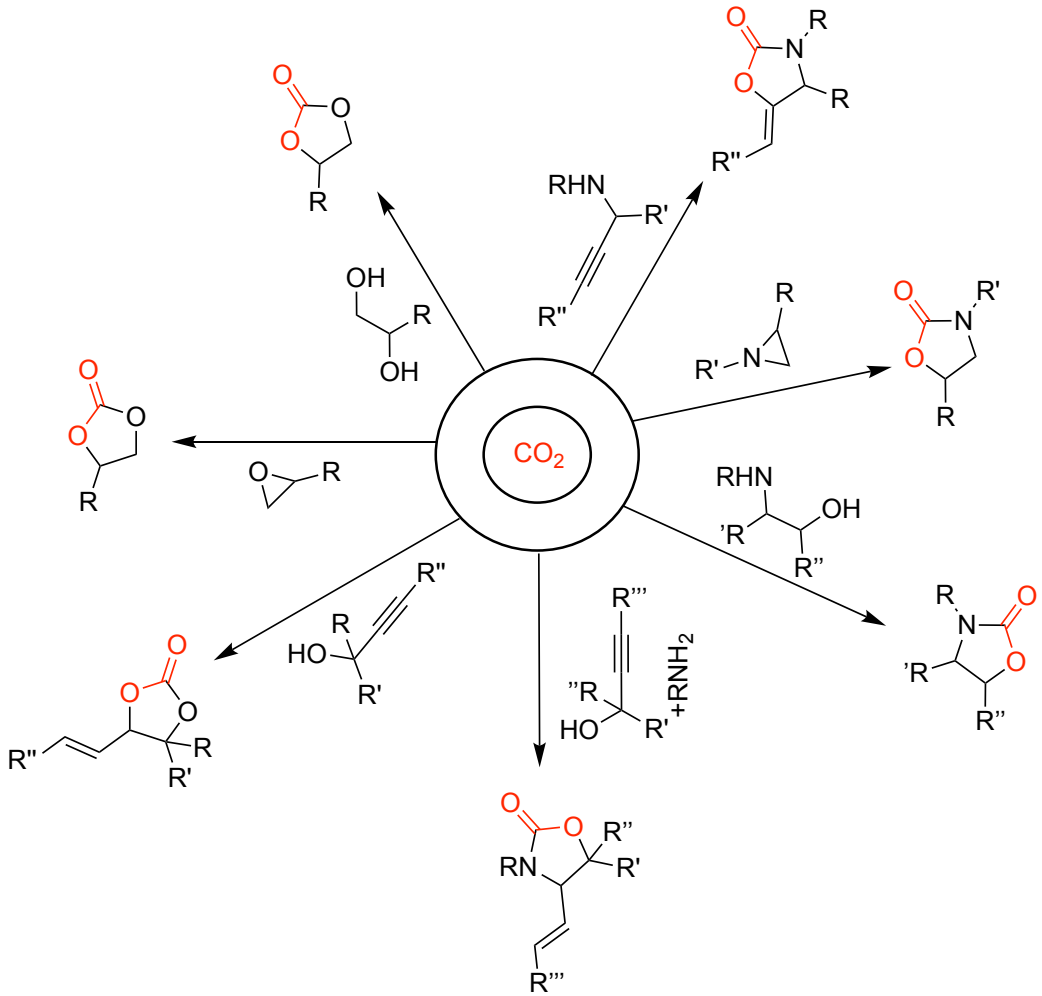

Scheme 3:*examples of synthetic pathways to obtain cyclic carbonates and oxazolidinones exploiting carbon dioxide.*

We can divide all these reactions into two main classes: addiction to alcohols and cycloadditions to three membered heterocycles. First of all cyclic carbonates and oxazolidinones may be obtained from diols or aminoalcohols and carbon dioxide.[44,45] With this methodology it is possible to follow the classic industrial synthesis of these five membered rings avoiding the utilization of phosgene and using CO_2 instead.[46] Moreover, this reaction makes it possible to convert ethylene glycol and propylene glycol, two by-products of the synthesis of dimethyl carbonate (DMC), into useful chemicals. Modulating the activity of the catalyst, utilizing diols and carbon dioxide it is possible to obtain also a copolymerization yielding linear polycarbonates.[47]

Then, cyclic carbonates and oxazolidinones can be produced from propargylic alcohols and amines respectively through a carboxylation followed by an intramolecular cyclization.[43,45,48] Generally, as shown in scheme 4, two consecutive activations are needed: first the activation of the carbon dioxide makes the carboxylation possible, then the activation of the triple bond promotes the intramolecular cyclisation.

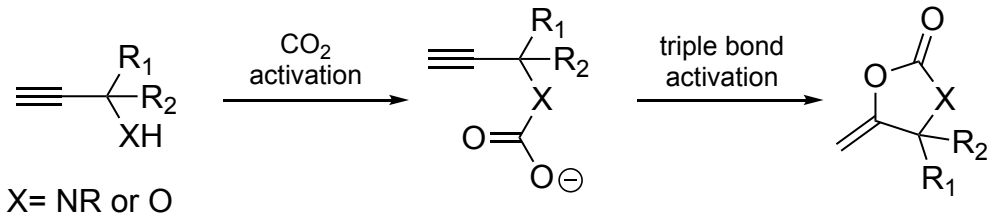

Scheme 4: *synthesis of five membered heterocycles from propargylic alcohols or amines and carbon dioxide.*

Moreover, a third way can be followed to prepare oxazolidinones starting from propargylic alcohols, primary amines, and carbon dioxide.[43]

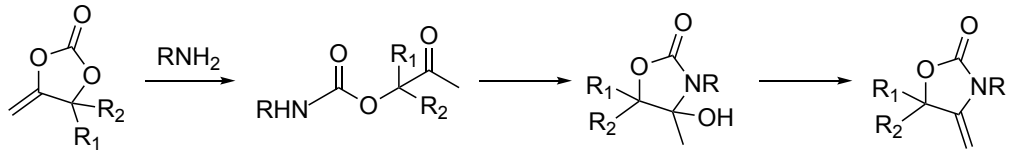

Scheme 5: *second step of the synthesis of oxazolidinones via carbonates opening with primary amines.*

In this case, the first step of the reaction is the formation of the cyclic carbonate as reported in scheme 4, then, the primary amine produces an ring opening reaction followed by a new ring closing step that produce the desired oxazolidinone (scheme 5).[49]

Then, oxazolidinones may be obtained from other three component reactions combining, for example, alkenes, amines, and carbon dioxide[50] or haloalkanes, anilines, and CO_2.[51,52]

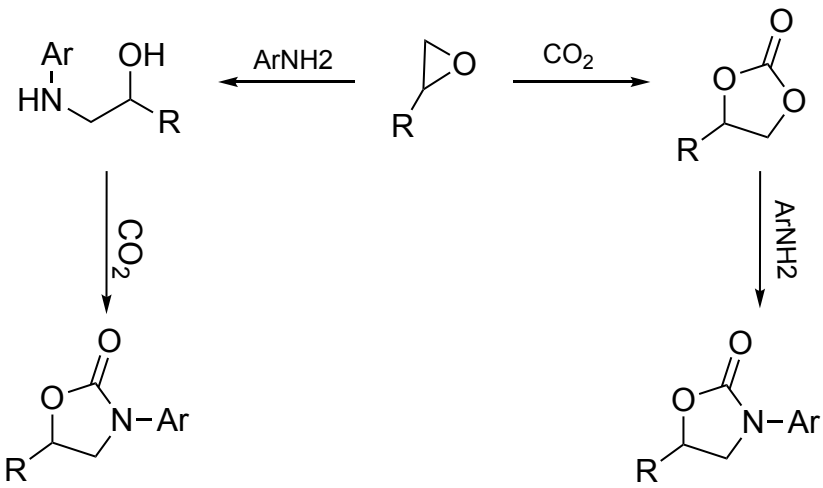

Scheme 6: *simplified possible pathways for the synthesis of oxazolidinones through three components reactions involving epoxides, anilines, and carbon dioxide.*

Moreover, other catalytic systems catalyze the formation of oxazolidinones involving epoxides, amines, and carbon dioxide. In this case the reaction may proceed both through cycloaddition of the carbon dioxide to the epoxide and following nucleophilic attack by the amine, or through the formation of the aminoalcohol intermediate, as reported in scheme 6.[53–58]

Finally, another way to prepare this class of molecules is through the cycloaddition to three membered heterocycles, as it will be more extensively treated in the following pages. All these pathways are very interesting because they exploit carbon dioxide to obtain useful compounds and present a 100% atom economy.

5. Carbon dioxide cycloaddition to three membered heterocycles

The carbon dioxide cycloaddition to three membered heterocycles is another reaction that exploits carbon dioxide and that makes it possible to produce added-value fine chemicals. This reaction has been studied in recent years to obtain a green way to prepare cyclic carbonates and oxazolidinones, in fact, this cycloaddition presents several characteristic suggested by the principle of the green chemistry: first of all, it exploits carbon dioxide, the most important greenhouse gas and an ubiquitous waste of human activity substituting toxic compounds as phosgene;[59] then, it presents a 100% atom economy and does not produce any byproduct; when catalyzed, it may present acceptable reaction condition and the reaction efficiency is enhanced by the substrates inherent reactivity; finally, it is frequently possible working in solvent-free conditions or utilizing small quantity of green solvents.[60,61]

The carbon dioxide cycloaddition to three membered heterocycles has been widely studied both using epoxides[61,62] and *N*-alkyl aziridines,[63,64] while *N*-aryl aziridines gave historically more problems in this reaction and only few methodologies have been published.[65,66] The reactivity trend epoxide, *N*-alkyl aziridines, *N*-aryl aziridines is ruled by the higher electronegativity of the oxygen atom with respect to the nitrogen one. Then, the enhanced stability furnished by the aryl substituent compared to the alkyl one makes *N*-aryl aziridines less reactive trough this pathway.[67] However, the reaction between epoxide and carbon dioxide may result in two different products: cyclic carbonates (scheme 7a) or polycarbonates (scheme 7b). On the other hand, the reaction between aziridines and carbon dioxide produces only oxazolidinones but as two different regioisomers (scheme 7c). Focusing on the reaction between epoxides and CO_2, it should be noted that to afford high reaction selectivity it is necessary avoiding the formation of both the linear and the cyclic carbonate. Indeed, despite cyclic carbonates being the thermodynamic products of the reaction,[68] it is possible to obtain one or the other product even with complete selectivity by modulating the characteristic of the catalyst, the co-catalyst, the substrate, or the reaction conditions.[69] For example, the use of a metalorganic catalyst which forms

strong oxygen-metal bonds favors the formation of linear product, while the use of a catalyst that forms weak metal-oxygen bond eases the formation of cyclic product.

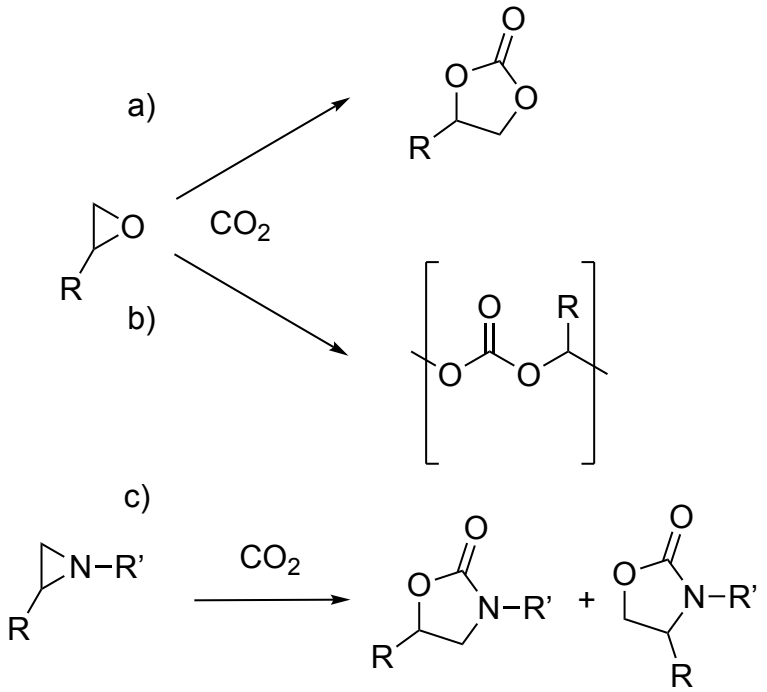

Scheme 7: *general scheme for the reaction between carbon dioxide and epoxides or aziridines.*

Working with aziridines, oxazolidinones are the only obtainable products that are formed as two different regioisomers in a variable ratio and generally the ring-opening reaction on the most encumbered carbon is favorite.[64]

Several mechanistic studies for the catalyzed reaction between epoxides and carbon dioxides has been published but two principal pathways have emerged.

The first and most common one, as reported in scheme 8, starts with the activation of the epoxide through an interaction between the catalyst and the epoxide oxygen atom. Then, a nucleophile attacks the heterocycle, opens it and, at this point, carbon dioxide goes through an insertion between the opened epoxide and the catalyst. If the catalyst presents two different active sites or more than one catalyst is presents, it is possible that one of them activates the CO_2 molecule before the insertion.[69] Finally, a backbiting reaction leads to the cyclization and the formation of the desired cyclic carbonate. In almost all the

reported mechanisms the nucleophilic attack takes place on the less encumbered carbon atom of the three membered ring cycle, however, in the case of styrene oxide, for example, the nucleophilic attack is favored at the phenyl-substituted carbon atom.[64] In order to activate the epoxide, it is possible using metals such as Fe,[70] Co,[71] Cu,[72] Al,[73] Mn,[74] and Zn,[75] or hydrogen bond donors like hydroxy functionalized molecules,[76,77] anilines,[78] carboxylic acids[61] or even the epoxide itself.[79] On the other hand, as nucleophile, the utilization of ammonium salts, phosphonium salts, and imidazolium salts[80,81] takes place or it can be present as the counter ion or ligand of the metal complex utilized.[74] Moreover, it is important to say that this reaction can be carried out even with the sole nucleophile that opens the three membered ring, making possible the addition of the CO_2 molecule.[82]

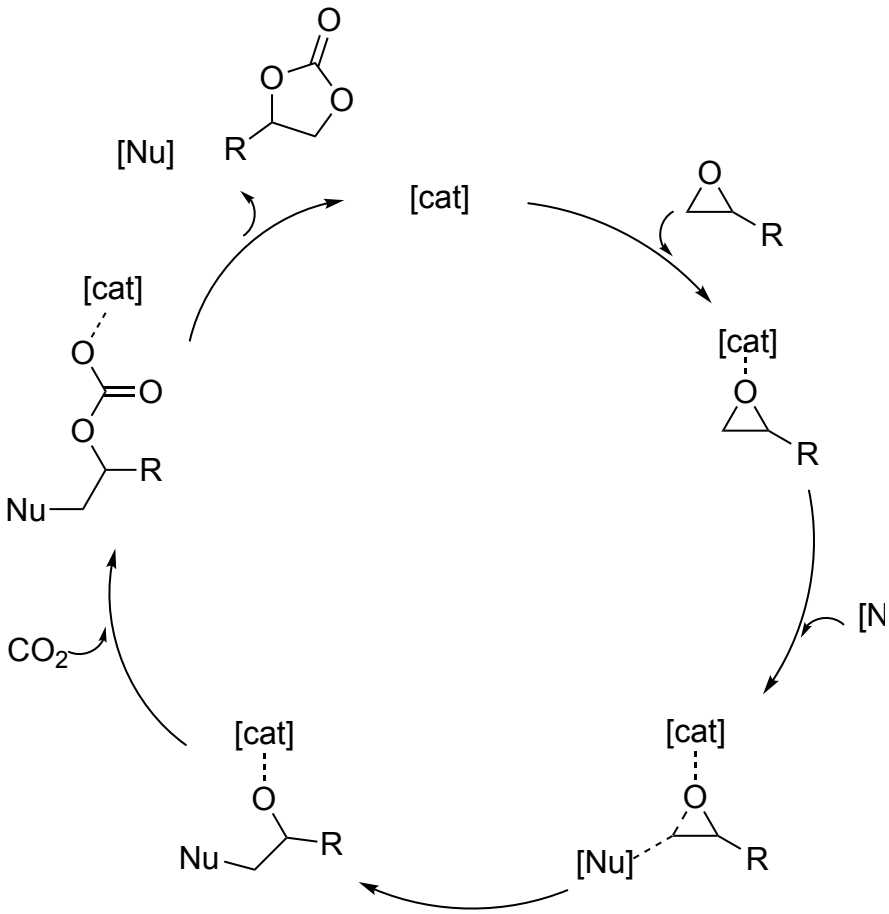

Scheme 8: *general mechanism for the formation of cyclic carbonates from epoxides and CO_2.*

The second possible mechanism involves the activation of the carbon dioxide before the insertion into the heterocycle. In this case, the most efficient carbon dioxide activation takes place with the formation of a zwitterionic adduct with a nucleophile and a further activation of the epoxide by a Lewis acid.[61] As stated before, different molecules can form adducts with carbon dioxide and in this reaction have been used, for example, DBU[83] or NHC (scheme 9).[84]

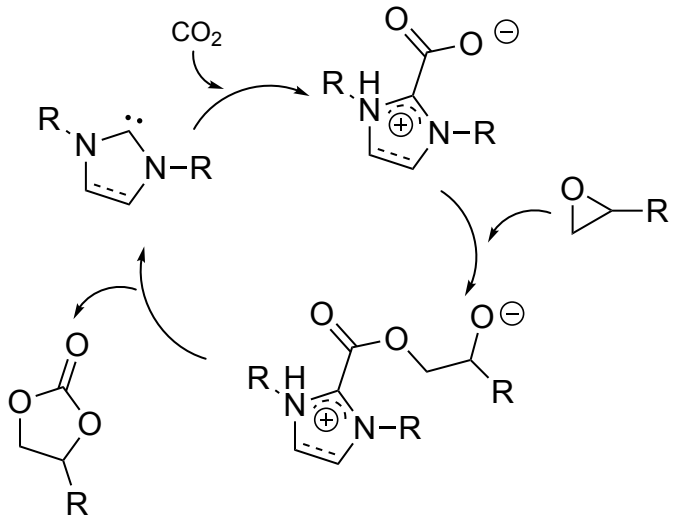

Scheme 9: *NHC catalyzed cycloaddition of carbon dioxide to epoxides.*

When the attention is turned to aziridines it is possible to see how far fewer catalyst have been studied and were efficient in this transformation, moreover also far fewer mechanistic proposals have been made.

The first studies about the carbon dioxide cycloaddition to aziridines report, as in the case of epoxides, the utilization of metal salts as catalysts, e. g. lithium iodide, lithium bromide, or zirconyl chloride, that showed their activity with or without the presence of a nucleophile as the co-catalyst.[85–89] Metalorganic complexes revealed their efficiency in the transformation of aziridines into oxazolidinones; in fact, two of the most active compounds are the Cr(salen) complex active even in the case of epoxide[66] and an aluminum bifunctional catalyst.[90] Starting from the promising results obtained in homogeneous catalysis, some heterogenous catalysts has been developed as mesoporous phosphonates[91,92] or MOFs.[93,94] Moreover, in recent years, even organo-catalysis has tried

to improve the sustainability of this reaction exploiting both homogenous and heterogenous catalyst using, for example, onium salts,[95,96] ionic liquids,[97,98] and amino acids.[99,100]

The mechanism of this reaction is not very clear and seems to be very substrate and catalyst dependent.

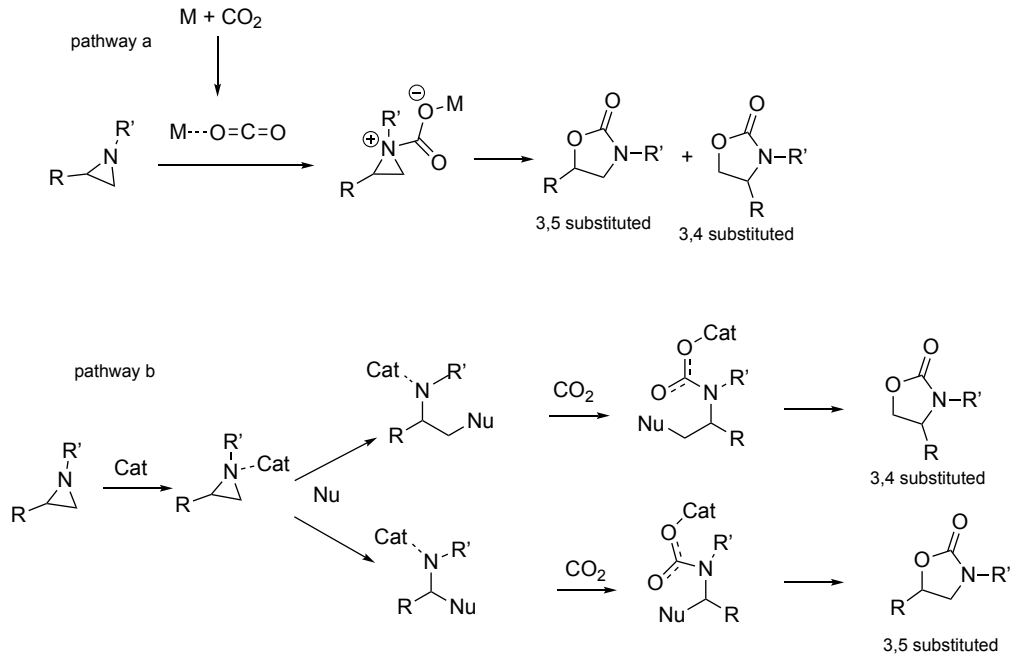

Scheme 10: *possible reaction mechanisms for the carbon dioxide cycloaddition to aziridines.*

Generally, the regioisomer formation seems to be influenced by the steric encumbrance of the nucleophile that performs the opening reaction and from the substituents on the cycle: big nucleophiles favor the attack at the non-substituted carbon, while the presence of a phenyl ring pushes the reaction through the formation of the 3,5-substituted oxazolidinone.[101] Besides these considerations, all the mechanisms proposed may be divided in two classes: 1) the carbon dioxide activation by a metal center makes possible the interaction between the nitrogen atom of the substrates and the carbon atom of CO_2, the successive nucleophilic attack of one of the two oxygen atom to the favored carbon on the cycle leads to the oxazolidinones formation[102] (scheme 9, pathway a), this is the case of the Chromium(salen) complex; 2) the catalyst activates the aziridine molecule and the

nucleophile operates the ring-opening reaction followed by the carbon dioxide insertion and the following closing of the cycle[42,103,104] (scheme 9, pathway b).

It is important to underline that in in all the reported mechanisms the nucleophilic attack takes place with an S_N2 mechanism. In the case of pathway b, the activation of the aziridine may be performed by a metal[101,103,104] or by H-bonding[42] but it is generally less efficient than in the case of epoxides. Moreover, even in this latest case, a carbon dioxide activation may be performed by metal salts.[101]

6. Cyclic carbonates and oxazolidinones

During the years cyclic carbonates have shown great utility in a wide range of applications;[105,106] first of all, many cyclic carbonates have found usage as polar aprotic solvents in synthesis and catalysis[107] and probably the most used in this field is the propylene carbonate (PC).[108] However, even if they may be considered green solvents, one of the most important drawbacks in using cyclic carbonates as solvents is the high boiling point that rises problems during the product purification. Others applications for cyclic carbonates are as lubricants[105] or non-aqueous electrolytes for lithium batteries[109] and once again one of the most used is PC.[110] Moreover, cyclic carbonates find applications as monomer for the preparation of polymers,[111] in particular of polycarbonates and polyurethanes, and as intermediates in organic synthesis.[112] In this latter case, they are used both to retain the cyclic carbonate structure making further modification of the substituents on the cycle, or to form new molecules after the opening of the cycle exploiting a plethora of different reagents like carboxylic acids or amines. In fact, complex cyclic carbonates present in Nature[113] have been partially mimicked to obtain synthetic analogs by modifying vinyl and alkynyl substituted cyclic carbonates.[114] Moreover, α-alkylidene cyclic carbonates are useful for the preparation of α-hydroxy ketones and 5-methylene-oxazolidin-2-one derivatives.[45]

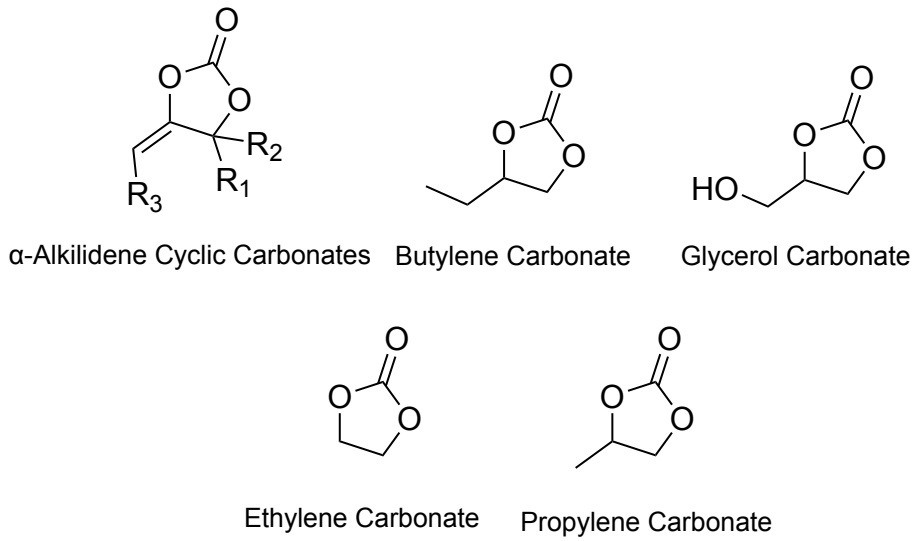

Figure 4: *most used cyclic carbonates.*

Another important role played by cyclic carbonates in organic synthesis is the improvement of the sustainability of the dimethyl carbonate (DMC) production.[45] Indeed, as stated before, the possibility to convert by-product of the DMC synthesis into useful carbonates, like propylene carbonate and glycerol carbonate, makes the whole process for the production of dimethyl carbonate greener. This is an important results since DMC is one of the most used organic carbonates in industry due to its applications as electrolyte,[109] methylating agent,[115] and alternative to phosgene.[116] It is important to note that few industrial processes exploit cyclic carbonates. For example, the Shell-Omega process produces ethylene glycol from ethylene carbonate, while the Ashai-Kesei requires the cleavage of ethylene carbonate with methanol obtaining DMC and ethylene glycol.[61]

On the other hand, oxazolidinones constitute a very interesting and promising class of molecules that has been studied for their applications as chiral auxiliaries in organic synthesis and for their pharmacological potential.[117–119]

Evans was the first to discover the potential of oxazolidinones in the enantioselective aldol condensation,[120] and, since then, this class of molecules has been applied to different classes of reactions.[121,122] Moreover, since the early 1990s, oxazolidinones have been studied as pharmacologically active compounds and *N*-aryl oxazolidinones have shown the most interesting properties due to their ability to interact with RNA and proteins. In addition, they show a reversible and selective inhibition of monoamine oxidase A (MOA), an enzyme that may degrade different amine neurotransmitters.[123] Then, similar molecular scaffolds have shown their potential as antibacterial agents becoming an important resource to exploit against the development of antibiotic resistance.[124,125]

Toloxatone was one of the first oxazolidinones to be introduced as a drug; it was studied as an antidepressant during the effort to find alternatives to first monoamine oxidase inhibitors (MAOIs) to avoid the many drawbacks that those molecules presented.[123] Starting from toloxatone, different new antidepressants have been synthesized throughout the years like 3-(1*H*-pyrrol-1-yl)-2-oxazolidinones.[126] In recent years, molecules containing the oxazolidinone moiety have been studied even as HIV-1 protease inhibitors; the five membered heterocycle was identified to overcome the drug resistance developed for Amprenavir and to mimic Darunavir, two FDA approved protease inhibitors.[127]

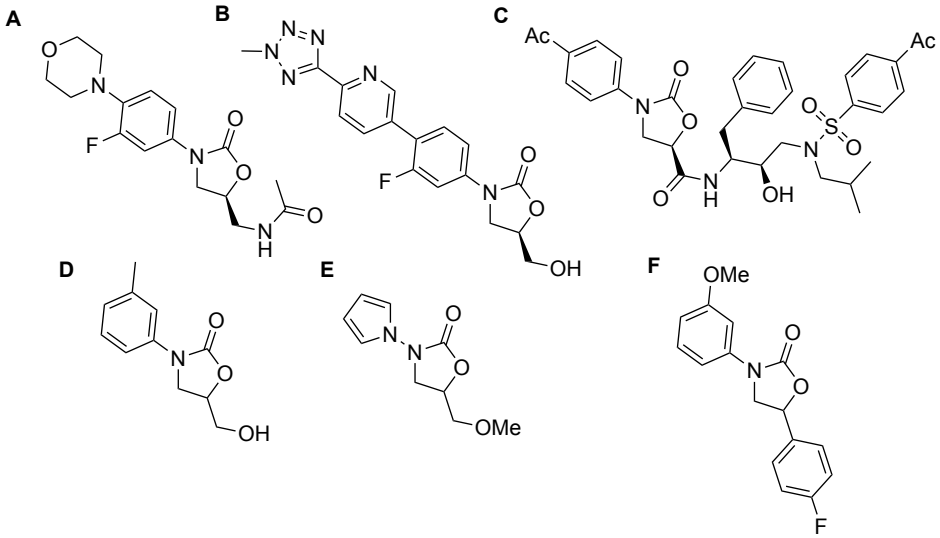

Figure 5: *some pharmaceutically important oxazolidinones; A) Linezolid and B) Tedizolid are used as antimicrobial agents, C) has been studied as HIV-1 protease inhibitor, D) Toloxatone and E) are used as antidepressant while F) is a D5D inhibitor.*

The most studied oxazolidinone is probably Linezolid, an antimicrobial agent used to treat infections provoked by Gram-positive bacteria like staphylococci, streptococci, and enterococci. It has been approved in the 2000s after the need to discover new antibiotics after the development of multidrug resistance by *enterococci faecalis* and *enterococcus faecium*.[128,129] Then, studying Linezolid and its drawbacks, Tedizolid was discovered. This is another oxazolidinone molecule used to treat bacterial skin infections and, with respects to Linezolid, it presents longer life and a broader spectrum of activity. These features allow lower dosage and overcome the Linezolid-resistance showed by some Gram-positive pathogens.[130]

Lastly, some oxazolidinones have demonstrated an anti-inflammatory activity being delta-5-desaturase (D5D) inhibitors. This class of compounds, in fact, prevents the production of arachidonic acid from the desaturation of dihomo-γ-linolenic acid (DGLA) accomplished by D5D, where DGLA is a precursor of anti-inflammatory eicosanoids.

7. Porphyrins and their complexes

Between all the catalysts utilized in the carbon dioxide cycloaddition to three membered heterocycles, porphyrin metal complexes play an important role.[29] Porphyrin ligands are a very versatile class of high stable macrocycles formed by four pyrrolic units connected by methine bridges. Since these heterocycles possess 11 conjugate double bonds and 26 π-electrons, they respect the Hückel's rule. Moreover, it is possible to vastly modify the porphyrins carbon skeleton. In fact, many different substituents may be linked at the β pyrrolic carbon atoms or in the *meso* positions (the naming of the carbon atoms is shown in figure 6). Along with porphyrins, other tetrapyrrolic related macrocycles have been studied.

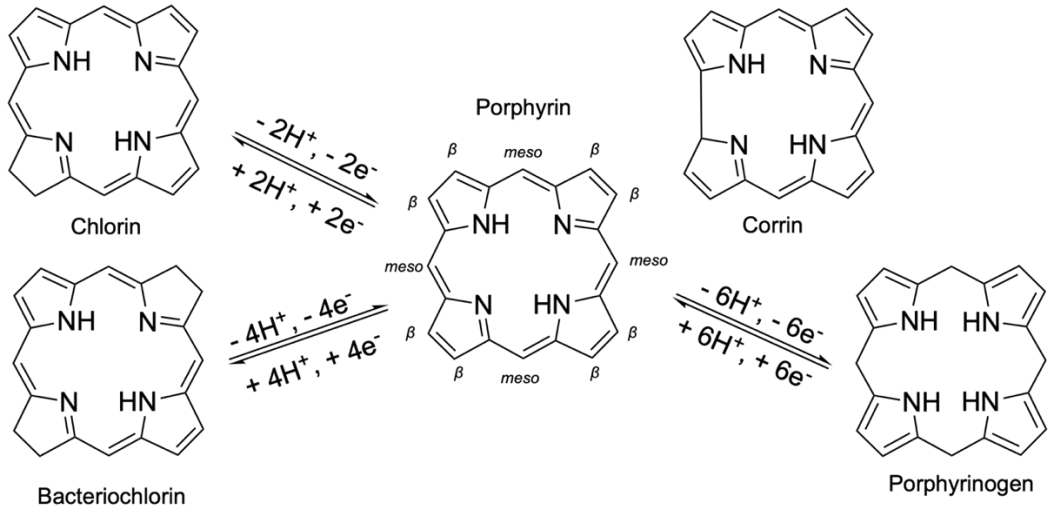

Scheme 11: *porphyrin and related tetrapyrrolic macrocycles.*

The porphyrin ring is largely present in Nature in molecules like chlorophyll, hemoglobin, and cytochromes, this is enough to make this ligand gain the name of "the pigment of life". Besides that, this class of ligands and its complexes are widely used in all the chemistry related fields, from catalysis[131] to medicine,[132,133] from optical[134] to sensing applications.[135] In order to obtain porphyrins, the purification from natural sources has revealed itself to be very expensive and time consuming, thus, since the early 1900s, considerable efforts have been devoted to find suitable synthetic pathways to obtain these compounds by finding different routes to achieve the functionalization of choice.[136] Due to their

prominent presence in Nature, the synthesis of β-substituted porphyrins was the first to be attempted by Hans Fischer, who exploited the reactivity of dipyrromethenes (scheme 12, a).[137] However, the severe reaction conditions prevented a wide application of this synthetic route. Thus, in 1960, MacDonald and co-workers published a new methodology that takes advantage of the usage of dipyrromethanes, the so-called "2+2 procedure"(scheme 12, b).[138] Up to now, this is the most used methodology to obtain β-substituted porphyrins with its variation introduced by Momentau's work which involves 2,5-diformylpyrroles and tripyrrane and for this reason has been called "3+1 procedure" (scheme 12, c).[139]

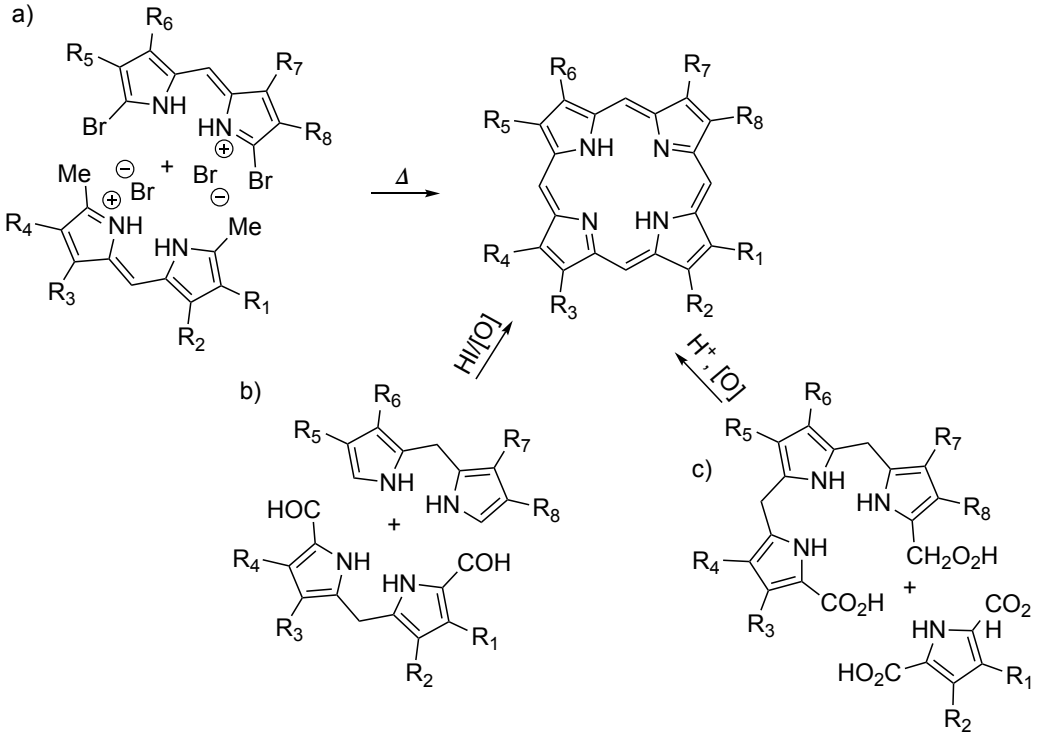

Scheme 12: *Synthetic pathways for the preparation of β-substituted porphyrins.*

Nonetheless, all these syntheses are quite complicated, require many synthetic steps and difficult purifications. Thus, *meso*-substituted porphyrins have found wider applications due to the easier pathways to synthesize them and thanks to the interesting properties demonstrated. The first synthetic pattern was proposed by Rothemund, who obtained bot *meso*-tetramethylporphyrin and *meso*-tetraphenylporphyrin ($TPPH_2$) refluxing pyrrole and

the corresponding aldehyde in methanol in a sealed tube (scheme 13).[140,141] After this groundbreaking work, this approach was modified by Adler and Longo by using refluxing propionic acid as the solvent at atmospheric pressure (scheme 13). This novelty permitted to extend the protocol to a wider number of substituted benzaldehydes, making it possible to obtain quickly relatively pure porphyrins in good amounts (yield up to the 20%).[142] However, this methodology has some limitations. First of all, the purification may be hard due to the large amount of by-products obtained, then, the harsh reaction conditions prevent the utilization of acid-sensitive functional groups. Additionally, removing the high boiling solvent from the reaction may be tricky. Thus, to reduce these problems, in some cases it is possible to use lower boiling solvents as acetic acid or exploit microwave irradiations obtaining softer reaction conditions.[143]

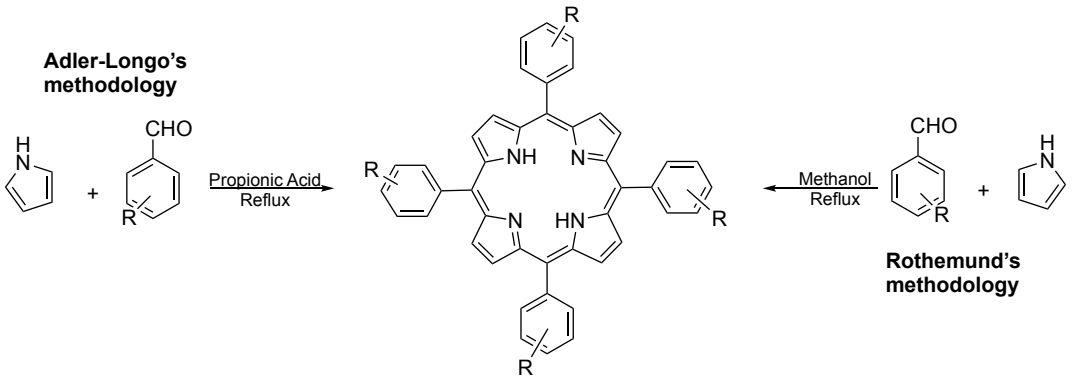

Scheme 13: *Adler-Longo's and Rothemund's methodology for the synthesis of meso-substituted porphyrins.*

A great improvement to the synthesis of porphyrins has been made with the publication of Lindsey's work in 1987.[144] The proposed protocol suggests a two-step one-pot preparation of meso-substituted porphyrins from pyrrole and benzaldehyde. The starting reagents dissolved in chlorinated solvents, as dichloromethane or chloroform, initially form the porphyrinogen at the thermodynamic equilibrium thanks to a Lewis catalyst as $BF_3 \cdot Et_2O$. Then, exploiting an oxidant as 2,3-dichloro-5,6-dicyano-1,4-benzoquinone (DDQ), the wanted porphyrin can be obtained (scheme 14). Considering that high dilution conditions (10^{-2} M) are necessary to foster the formation of the porphyrinogen over the formation of

polymers, it is not easy to apply this methodology on a large scale. Nonetheless, the dilution issue has been partially overcome for the synthesis of some simple *meso*-substituted porphyrins by following studies conducted by the same author in which concentrations higher than 0.1 M and different oxidants have been studied.[145] By exploiting this pathway it is possible to obtain a plethora of porphyrins that exhibit different electronic, optical and structural properties.

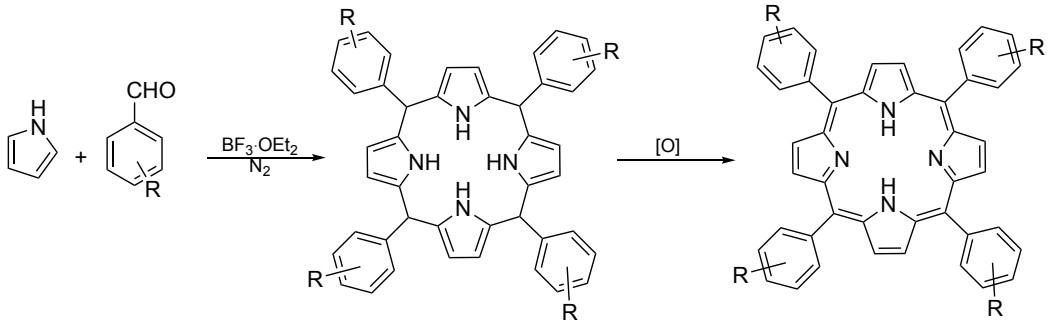

Scheme 14: *Lindsey's methodology for the synthesis of meso-substituted porphyrins.*

Porphyrins are extensively used as ligands in metalorganic chemistry. As shown before, when they are not coordinated to any metal, they present two protonated pyrrolic moieties and they are usually called "free-base". If these two protons are removed, porphyrins become tetradentate dianionic ligands and may accommodate a variety of metals and semi-metals in different shapes forming porphyrin complexes.[146]

Depending on the nature of the metal ion and its configuration, oxidation state, and spin state, these complexes present many differences in structure and reactivity. To classify the porphyrin complexes, it is possible to refer either to geometry, stoichiometry, or both. The metal ions generally fit into the porphyrin core generating square planar or octahedral complexes. If this is not possible due to the dimension of the metal ion or its electronic properties, less common geometries may be found. This is the case of the so-called "out of plane" complexes.[147] Porphyrin metal complexes may be prepared in several different ways exploiting different reactivities, like coordination, reduction, and oxidation; the choice of the reaction pathway would be determined by the nature of the metal sources. It is possible to identify four different classes of reactions that make the complexes synthesis possible: A) metal coordination from a MX_2-type salt, B) metal salt reduction, C) spontaneous

oxidation of the metal starting from a M(0) cluster and D) external agent mediated oxidation.[148]

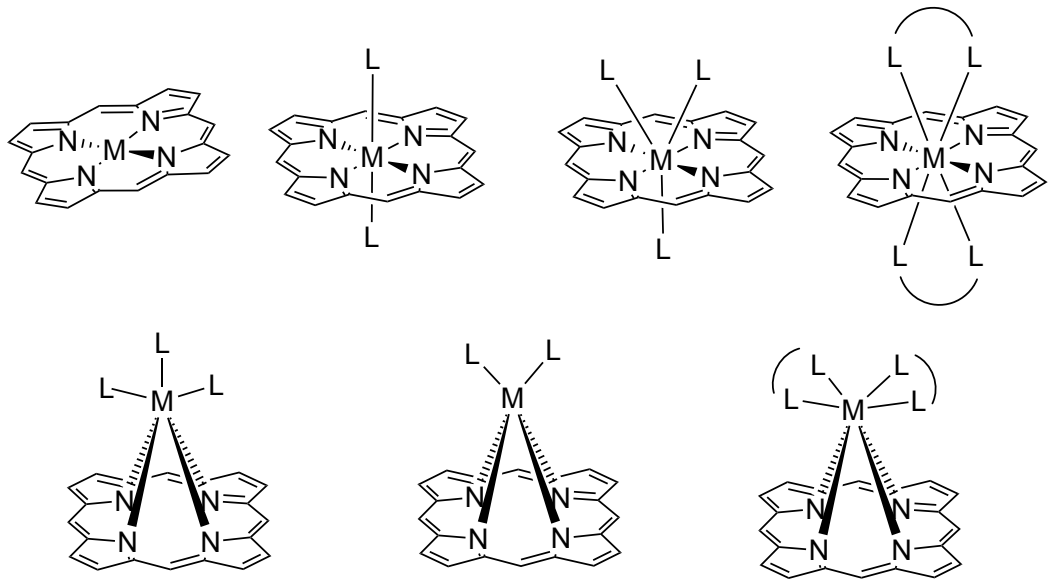

Figure 6: *possible geometries of porphyrin metal complexes.*

A) Metal coordination from a MX_2-type salt: in this reaction a divalent metal salt reacts directly with the porphyrin ligand in the opportune reaction conditions. The biggest problem is finding the right solvent that solubilizes both the metal salt and ligand. The most effective is generally *N,N*-dimethylformamide (DMF). This methodology is effective for a variety of metals such as Zn, Co, Cu, Ni, Fe, and others, forming the desired product with generally good to excellent yields. To speed up the reaction it is possible to use weak Brønsted bases that are capable of deprotonating the porphyrin pyrroles.[149]

B) Metal salt reduction: this procedure works through the insertion of the metal ion starting from a precursor in higher oxidation state. In this case a reducing agent is needed.

C) Spontaneous metal oxidation from a M(0) cluster: this synthesis is based on the reaction between $M(CO)_{12}$ clusters and the porphyrin in high boiling solvents where the metal oxidation is promoted by the displacing of the two protons of the

inner pyrroles as molecular hydrogen. This procedure is used almost exclusively for the synthesis of ruthenium and osmium derivatives and, in this case, the solubility does not interfere with the reaction productivity.

D) **External agent mediated oxidation:** exploiting this methodology, the addition of an external agent is needed to oxidize the metal ion coordinated to the porphyrin in order to obtain a stable complex. The most common oxidants utilized are oxygen and iodine; the oxidation may occur *in situ* or during the work up

8. Homogenous catalysis for carbon dioxide cycloaddition to three membered heterocycles

The carbon dioxide cycloaddition to epoxides, as stated before, has been widely and extensively studied since the second half of the 20th century, exploiting the reactivity of many different catalysts.[150] Since the first studies, metalorganic catalysis took a prominent role in this field and during the years two classes of compounds proved to be the most used: salen metal complexes[151] and metalloporphyrins.[29] The first class cited has been studied since Paddock and Nguyen discovered the activity of a Cr(III) complex in the coupling of CO_2 and epoxide.[152] From then, a lot of studies have been carried out designing very active catalysts to be used for very interesting applications, such as the kinetic resolution of racemic epoxides.[153]

On the other hand, porphyrin-based catalysts have been widely applied to promote the cycloaddition of carbon dioxide to epoxides due to their promising features. Several of the studied catalysts turned out to be very active and stable, ensuring good sustainability. Moreover, the versatility of this class of ligands allowed the synthesis of bifunctional or dimeric and trimeric catalysts. The first porphyrin complex to be used in the preparation of cyclic carbonates was (TPP)Al(OR) (TPP= dianion of the *meso*-tetraphenylporphyrin)[154] and in particular (TPP)Al(OMe) (figure 7, a), that showed its activity in the presence of 1-methylimidazole (NMI) by inserting CO_2 between the aluminum atom and the OR moiety before carrying out the cycloaddition. Starting from this point other aluminum complexes were studied changing the axial ligand (figure 7, b) and the co-catalyst[155] or the porphyrin itself (figure 7, c).[156]

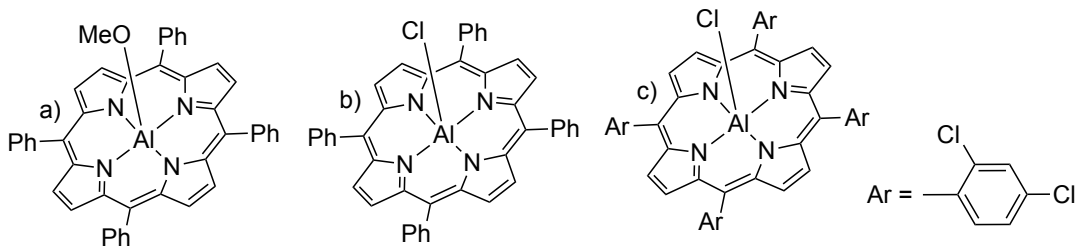

Figure 7: *aluminum-based porphyrin complexes used in the cycloaddition reaction of carbon dioxide to epoxides.*

The importance of the Lewis acidity of the metal center in the reaction productivity has been investigated through the comparison of the activity of Sn(II) and Sn(IV) TPP complexes. The results gathered from these studies proved that $Sn(TPP)Cl_2$ showed the best catalytic performances in combination with 4-dimethylammoniumpyridine (DMAP).[155] Even in this case the influence of the axial ligand was investigated and $Sn^{IV}(TPP)(OTf)_2$ in combination with tetrabutylphosphoniumbromide (TBPB) showed an improved activity converting the desired epoxides at only 50 °C and 0.1 MPa of carbon dioxide.[157] To conclude the discussion about main group metal porphyrin complex, Bi^{III}(porphyrin)X complexes have been tested in combination with TBAI as the co-catalyst that showed a promising activity even at only 0.1 MPa of carbon dioxide pressure.[158]

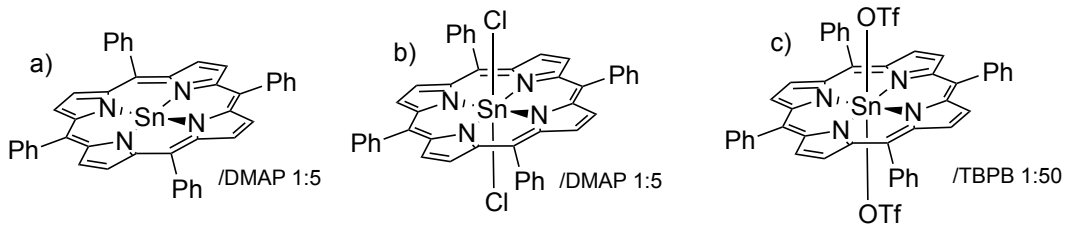

Figure 8: *Sn based catalytic system for the conversion of epoxides to carbonates.*

All the studies carried out about the reaction mechanism involved when these catalysts were used showed that the reaction proceeds through i) the initial activation of the epoxide by the metal site, ii) the nucleophilic attack on the heterocycle, iii) the carbon dioxide bonding and, finally, iv) the ring closure step by an S_N2 reaction (scheme 8). Moreover, even if it is possible to obtain the desired products using all these catalysts, any of them has shown activity at room pressure and temperature at the same time.

Switching to the transition metals that may be obtained in various different oxidation states, the first studied porphyrin complexes were $Cr^{III}(TPP)Cl$ and $Cr^{IV}(TPP)O$, which were effective in combination with NMI or DMAP, but only under harsh experimental conditions.[159] Another metal that has been studied in this reaction was cobalt, due to the possibility to easily achieve both Co(II) and Co(III) porphyrins. While $Co^{II}(TPP)$ showed a poor catalytic efficiency, $Co^{III}(TPP)Cl$, in combination with DMAP, afforded terminal and internal cyclic carbonates successfully.[160] Starting from these results, the catalytic system

was improved by utilizing as co-catalyst phenyltrimethyl ammonium tribromide (PTAT) and tetrabutyl ammonium bromide (TBAB) and switching the axial ligand from chloride to acetate.[161] In this case the Br_3^- anion gave better results probably because it is a better leaving group than the simple bromide, resulting in the activity of the catalytic combination even at 25 °C and 0.7 MPa of CO_2.

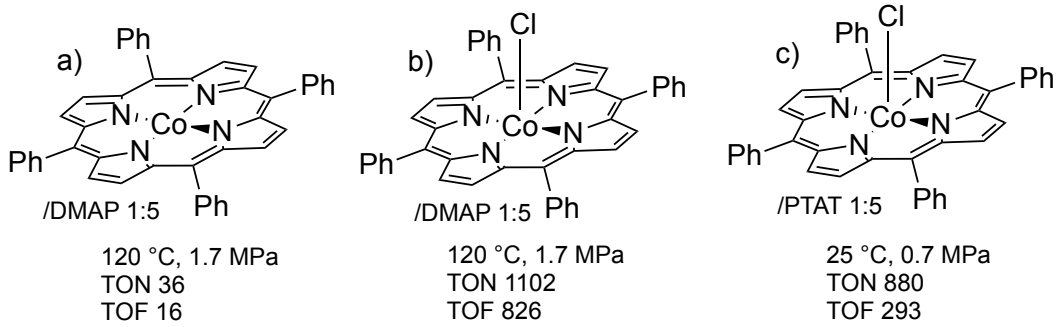

Figure 9: *cobalt-based porphyrin active in the cycloaddition of carbon dioxides to epoxides. TON and TOF reported are referred to the conversion of propylene oxide to propylene carbonate.*

Another catalyst that presented interesting properties in term of sustainability, performing well at 70 °C and at only 0.1 MPa of CO_2, is Mn^{III}(*p*-OMe-TPP)(Cl) (*p*-OMe-TPP is the dianion of tetra(4-methoxyphenyl)porphyrin) in combination with TBAB, which converted both internal and terminal epoxides with excellent yields.[162]

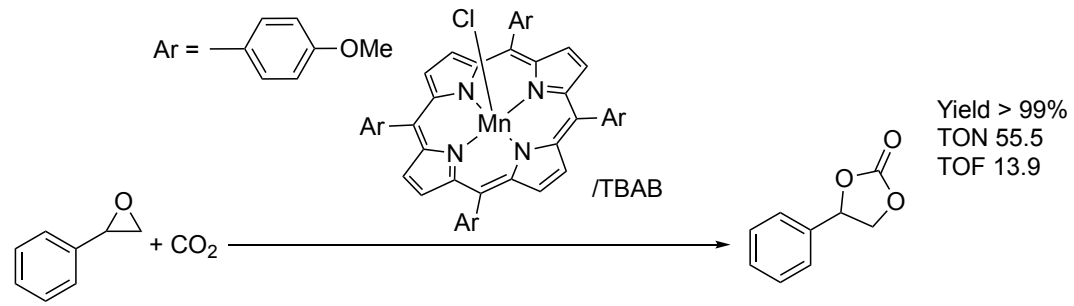

Scheme 15: *Mn^{III}(p-OMe-TPP)(Cl)/TBAB/SO = 1.0:1.3:55.5, 0.1 MPa CO_2 70 °C, 4h.*

Moreover, even Ru[161,163] has been studied in different oxidation states showing a good reactivity at only 50 °C and 0.67 MPa of CO_2 when the catalytic Ru(TPP)$(PPh_3)_2$/PTAT/EDA (EDA = ethyldiazoacetate) combination was employed. This system is inactive in the absence of EDA to suggest that the active center is the Ru^{IV} that is formed *in situ* thanks to

the presence of the oxidant. However, even if these results are encouraging, it is necessary to improve the sustainability of the reaction avoiding catalysts based on this expensive metal.

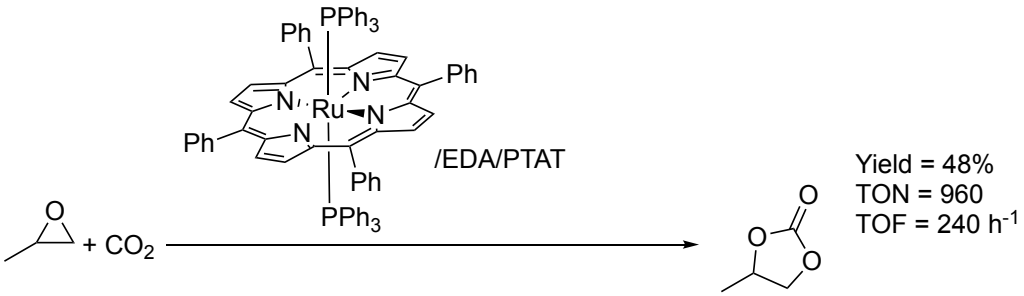

Scheme 16: *Ru(TPP)(PPh$_3$)$_2$/EDA/PTAT/PO = 1:1:2:100, 0.67 MPa, 50 °C, 4 h.*

The catalytic mechanism of the reaction promoted by the ruthenium complex is analogous to that reported in scheme 8.

As stated before, usually two elements are needed to catalyze the reaction between epoxides and carbon dioxide, a Lewis acid to activate the epoxide and a Lewis base as the co-catalyst. The two moieties may be combined designing a new bifunctional molecule. Bearing this idea in mind, H. Jing and co-authors proposed a series of metal porphyrins bearing an ammonium moiety on the porphyrin skeleton. Different M^{III}(TTMAPP)I_4(X) (TTMAPPI_4= dianion of tetra-(*p-N*,*N*,*N*-trimethyl-phenylammonium iodide)porphyrin) were tested and the Co(III) acetate complex (figure 10, a) proved to be the most active species by working in the following conditions: 0.001 mol% of catalyst, 0.67 MPa CO_2, 80 °C.[164]

In order to enhance the poor catalytic activity of cheap and sustainable Zn and Mg porphyrins when used in combination with a co-catalyst, different bifunctional catalysts have been synthesized and tested.[165,166] The most efficient one was proposed by T. Ema and co-workers, in fact, different Zn and Mg porphyrin complexes bearing onium salts at the end of an alkyl chain of the porphyrin skeleton demonstrated to be very efficient if the CO_2 cycloaddition to epoxides. The magnesium based catalyst functionalized with TBAB (figure 10, b) on the *meta* position of the *meso* phenyl rings of the porphyrin showed outstanding TON and TOF values up to 103.000 and 12.000 h^{-1}.[167]

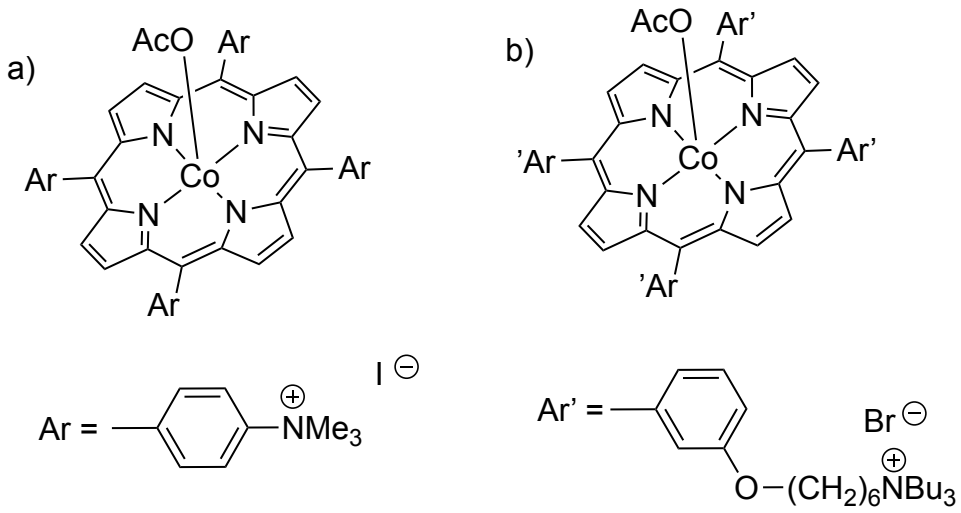

Figure 10: *bifunctional porphyrin-based catalyst for the cycloaddition reaction of carbon dioxide to epoxide.*

Another class of bifunctional porphyrinic catalysts exploits the possibility to prepare multi-porphyrin complexes by augmenting metal active sites and nucleophilic functionalities. Zn and Mg porphyrin dimers and trimers were synthesized using this approach and these catalysts showed an improved catalytic activity with respect those reported for the previous presented bifunctional porphyrins.[168]

To improve the reaction sustainability avoiding the use of metals, during the past years several organic catalysts have been tested. Many of them have been previously used as the co-catalyst of the reaction but it emerged that the use of these nucleophilic species alone allowed obtaining the desired product. In these cases, their activity was lower than that observed if used in combination with a metal center, but it is possible to get an overall gain by avoiding the complex synthesis of the catalyst and the use of expensive materials. Four main classes of organic catalysts have emerged through the years: ammonium salts, phosphonium salts, imidazolium based ionic liquids, and hydrogen bond donors.[169]

Tetrabutyl ammonium halides are widely used as co-catalysts thanks to the good nucleophilic and leaving group ability of the halide anions. The first application as catalyst has been reported by Calo et al.[170] Tetrabutyl ammonium iodide (TBAI) alone, and in combination with TBAB, was exploited to synthesize desired cyclic carbonates. They

proposed a four-step mechanism that basically reproduces the one reported in scheme 8, without the epoxide activation by a Lewis acid. The suggested mechanism was supported by DFT studies[171] and the reactivity of different anions was determined as follow: $Cl^->Br^->I^->F^-$.[172] These reactivity scales followed the nucleophilicity of the anion; note that the scarce activity of fluorine derivatives was due to its poor ability as leaving group. Moreover, the increase of the steric hindrance of the alkyl chain was responsible for an increase of the salt activity because the interaction between the anion and the cation in the salt diminished with the encumbrance of the cation and this lead to an increment of the nucleophilic character of the anion.[173]

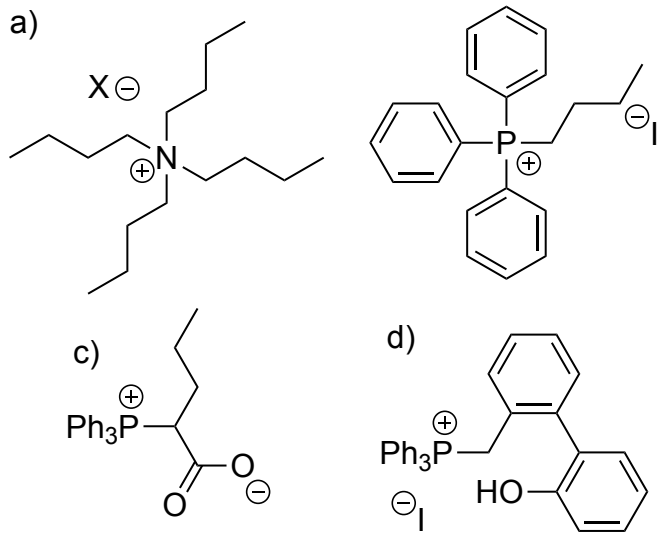

Figure 11: *onium catalysts utilized in the coupling reaction between CO_2 and epoxides.*

Besides ammonium salts, phosphonium salts also demonstrated their activity as co-catalysts and consequently their activity as the sole catalytic species has been studied. Different salts have been tested such as butyl triphenyl phosphonium iodide (figure 11, b), phosphorous ylides[174] (figure 11, c), tetraaryl phosphonium salts[175] and even a bifunctional phosphonium salt bearing an hydrogen bond donor moiety (figure 11, d).

Even if the first catalyst cited required the harshest reaction conditions, it has been successfully tested in the cycloaddition reaction in water medium.[176] On the other hand, considering the most accessible reaction parameters, the most performative catalyst resulted to be bifunctional phosphonium species.[177]

Ionic liquids (IL) represent another widely used class of organic catalysts that show a good activity in the cycloaddition reaction of epoxide with CO_2. They have been studied because of their peculiar ability to work both as solvent and catalyst and because of the high possibility to functionalize their structure that led to the preparation of many kinds of different molecules, even exploiting the possibility to prepare bifunctional catalysts inserting Lewis acid moiety onto the IL scaffold.[169]

Then, hydrogen bond donor (HBD) species have been studied because of their ability to activate the epoxide as a substitute of a metal center. Considering that the presence of a nucleophilic additive to accomplish the desired transformation is required, they have been used in combination with co-catalysts such as TBAX.[178]

Finally, another class of organocatalysts is represented by nitrogen donor bases, like DMAP and DBU, that can activate carbon dioxide by forming an adduct, as stated in chapter I.5. However, these molecules need harsh experimental conditions to catalyze the coupling between CO_2 and epoxides, diminishing drastically the sustainability of the methodology.[82]

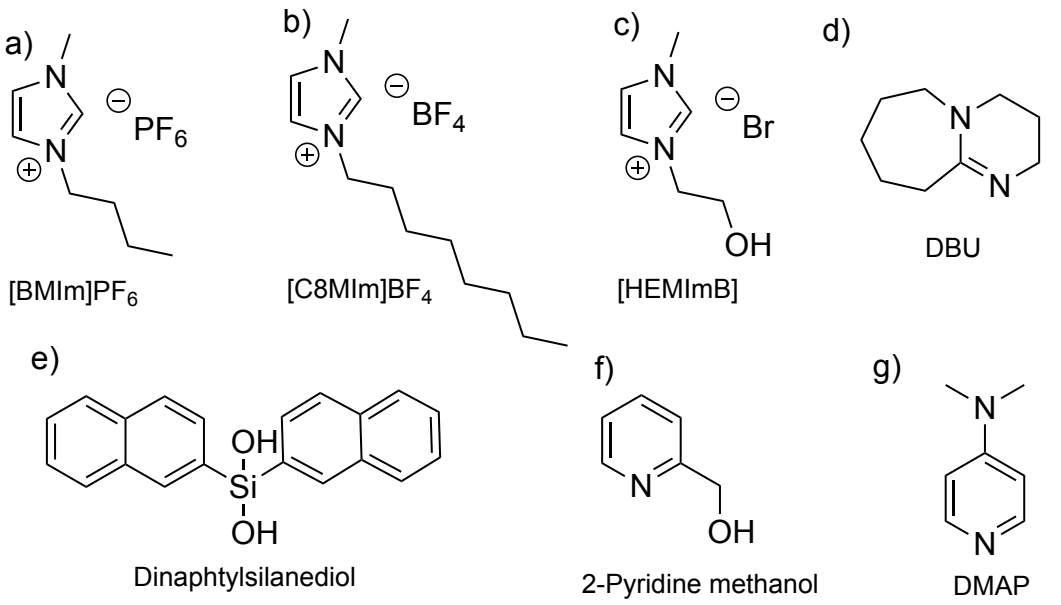

Figure 12: *some IL (a, b, c), HBD (e, f) and nitrogen donor base (d, g) active in the cycloaddition reaction between CO_2 and epoxides.*

Even if the coupling reaction between aziridine and carbon dioxide has been less studied then the analogous reaction involving epoxides, different catalysts, such as IL[85,86], metal halides[87] and organotin or organoantimony compounds[85] have been tested. However, the need of high quantity of the catalyst, the harsh experimental conditions needed and the toxicity of some of these compounds limited their large application. Despite salen complexes demonstrated a good reactivity both with *N*-alkyl[66,90] and *N*-aryl aziridines,[65] it has been demonstrated that the reaction may also occur in the absence of any catalytic species.[179]

It is interesting to notice that even if porphyrins found large application as homogenous catalysts of the cycloaddition of CO_2 to epoxides, only few examples are present in literature concerning their use in the analogous reaction using aziridines. In 2018 H. Ji and co-authors reported the activity of a bifunctional imidazolium-based ionic liquid decorated with Zn porphyrin that catalyzed the cycloaddition reaction of CO_2 to both epoxides and *N*-alkylaziridines.[180]

This catalyst efficiently converted eight different epoxides with good yields at 60 °C, 2.0 MPa of carbon dioxide in 8-48 h and eight different aziridines with good yields at 90 °C and 2.0 MPa CO_2 in 2-10 h. The proposed mechanism implies the substrate activation by interaction of the three-membered ring with the zinc center, the following nucleophilic attack, and the ending backbiting ring closure, as shown in schemes 17.

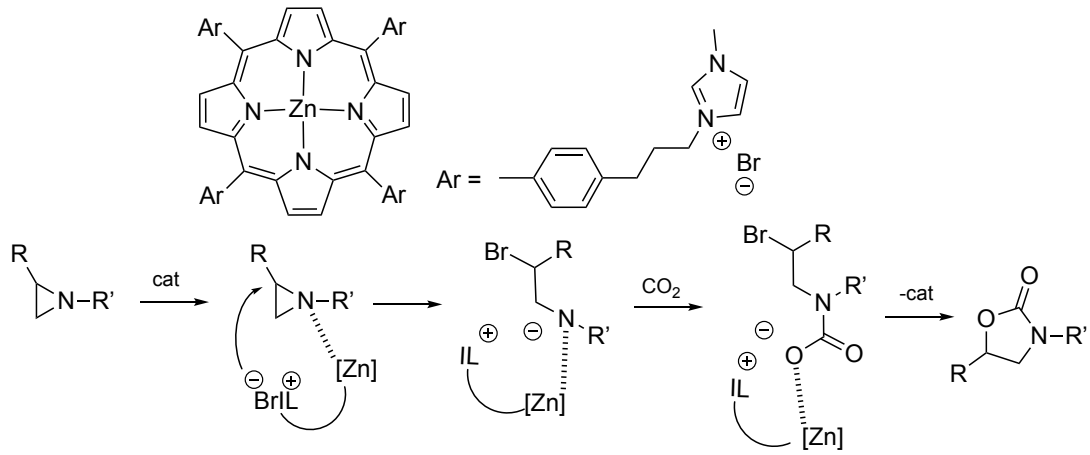

Scheme 17: *Zn-based bifunctional catalyst and proposed mechanism for the formation of oxazolidinones from aziridines and carbon dioxide.*

In the same year, Gallo and co-workers reported the activity of the $Ru^{IV}(TPP)(NAr)_2$/TBACl system, which was active at 0.6 MPa of carbon dioxide and 100°C to convert several aziridines into corresponding oxazolidinones with a regioselectivity of 90:10, favoring the 3,5-substituted product.[181] In this case the proposed mechanism involved the formation of a Ru^{V} intermediate that was responsible for the carbon dioxide activation.

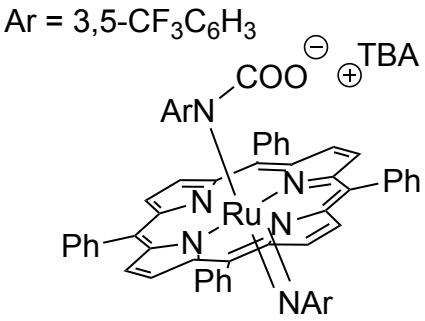

Figure 13: *Ru^{V} intermediate formed by $Ru(TPP)(NAr)_2$, tetrabutyl ammonium chloride and carbon dioxide.*

As already stated for metalorganic catalysis, also organocatalysis has been less studied for the conversion of aziridines into oxazolidinones by utilizing CO_2. The first reported catalyst was L-histidine in 2010,[99] that worked only under harsh experimental conditions for the conversion of *N*-alkyl substituted aziridines. In this case the amino acid serves both as nucleophile species and HBD for the aziridine activation. The following year, Bhanage an co-authors reported the activity of a PEG functionalized phosphonium bromide[182] that converted thirteen *N*-alkyl aziridines in the corresponding oxazolidinones at 50 °C and 5.0 MPa of carbon dioxide. More recently, Marchetti et al. reported the efficiency of diethyl ammonium iodide in the synthesis of oxazolidinones from aziridines and carbon dioxide at room temperature and pressure.[182] Even without achieving high yields and the possibility to use this protocol for a broad scope of substrates, this work confirmed the potential use of ammonium salts as catalysts of this reaction.

9. Heterogenous catalysis for carbon dioxide cycloaddition to three membered heterocycles

On the path towards green chemistry, heterogeneous catalysis offers different technical improvements compared to homogenous catalysis to simplify and optimize the product purification. For example, an heterogenous catalyst is easier to recover compared to a homogeneous one, then the catalyst recycle is simpler and it can be done more efficiently. Moreover, this kind of catalysts are usually more stable and even the product isolation requires a lower number of steps. In addition, the design of the reactor is simpler when a heterogenous catalyst is employed. Thus, even if homogeneous catalysts normally show higher catalytic activity,[183] all the characteristics described above significantly improve the overall process by reducing the production costs.

One of the first class of compounds used as heterogeneous catalysts in the cycloaddition of carbon dioxide to epoxides has been Mg[184,185] and Nb[186] oxide. However, this class of compounds did not show good catalytic activities and required the utilization of toxic solvents such as DMF. More recently, metal organic frameworks (MOFs) have been studied for their promising features.[169] In fact, the catalytic activity or CO_2 affinity can be fine-tuned by modifying the organic ligand, by changing the metal center, by controlling the MOF porosity, and by stabilizing the MOF structure.[187] Since the work of Han and co-workers[188] has been published, this class of compounds have been deeply studied as catalysts of the reaction between epoxides and carbon dioxide. In particular, thanks to their high versatility, salen-[189,190] and porphyrin-[191] based MOFs have been synthesized in order to take advantage for the good reactivity showed by these compounds under homogeneous conditions. Moreover, porphyrins have been used as building blocks for other heterogeneous catalysts such as covalent organic frameworks (COFs) and porous organic polymers (POPs).[191] Despite all these materials showed better activity compared to that of the simpler metal oxides, their difficult and time demanding syntheses has to be considered an important drawback. Moreover, the synthesis may be very expensive on the basis of the used metal and the building blocks needed for the preparation.[192]

In order to overcome the lack of activity of some heterogeneous catalysts, the preparation of supported homogeneous catalysts may be explored by linking active homogeneous catalyst directly onto a solid support. Exploiting this strategy, it is possible keeping the advantages of using heterogeneous catalysts by maintaining the activity of the starting homogeneous one. In addition, solid support may play a synergistic catalytic role in the reaction.[60] Many different types of supports have been studied in the carbon dioxide cycloaddition to epoxides like polyethylene glycol (PEG),[193,194] polystyrene (PS),[195,196] nanoparticles,[197–199] and biopolymers.[200,201] Another interesting solid support is silica, which shows different chemical and physical properties on the basis of the protocol applied for its preparation. For example Ozin,[202] Stein[203] and Inagaki[204] prepared periodic mesoporous organosilicas (PMOs) that can bear numerous organic functionalities thanks to the presence of organically bridged silica precursors. Other two types of silica exploited as support are the so-called MCM (mobile composition of matter)[205] and Santa Barbara amorphous material (SBA).[206] These last two classes of materials are usually functionalized by grafting methods, and the range of functional groups and moieties that may be exploited is wide. Moreover, silica based materials may exhibit a synergistic behavior with the supported molecule in the reaction between epoxides and CO_2 with the consequent improvement of the catalytic performances.[207] In fact, the presence of Si-OH groups on the silica surface enhances the activity of the catalyst *via* epoxide activation through H-bonding.[207–209]

Through the years different molecules have been supported on silica in order to accomplish the transformation of epoxides into cyclic carbonates by using carbon dioxide. For example Ratnasamy and co-workers prepared aluminum and titanium modified SBA-15 materials grafted with organic bases,[210,211] whereas Garcia and co-workers supported Cr(salen) complexes onto MCM-41 materials.[212,213] In this last case a recyclability issue emerged due to catalyst leaching attributable to the coordinative nature of the complex-silica bond. Thus, the recyclability has been successively improved by covalently bonding the salen complex to silica using different grafting methodology.[214]

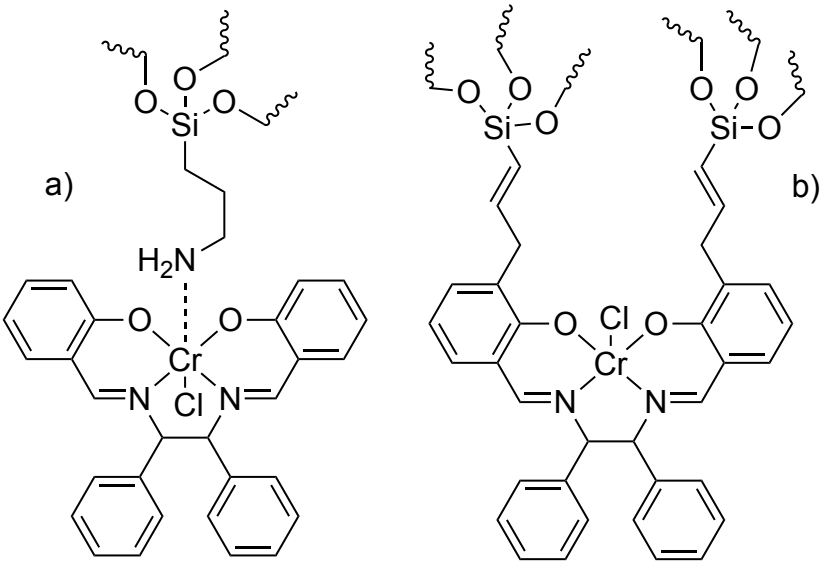

Figure 14: *a) silica coordinated complex and b) silica covalently bonded complex.*

Moreover, even metalloporphyrins, due to their good catalytic activity in the studied transformation, has been supported onto solid surface. For example, M. M. Pereira and co-authors reported the catalytic activity of hybrid materials based on a magnetic core of Fe_3O_4 covered by a silica layer functionalized with different metalloporphyrins.[199] Once again, the chromium catalyst showed promising activity in the conversion of styrene oxide in the corresponding carbonate with 52% of yield in 24 h at 80°C and 1.0 MPa of carbon dioxide. Moreover, 4,4',4'',4'''-(porphyrin-5,10,15,20- tetrayl)tetrakis (benzoic acid) ($TCPPH_2$) has been used as an organic supported catalyst thanks to its linkage to a PMO.

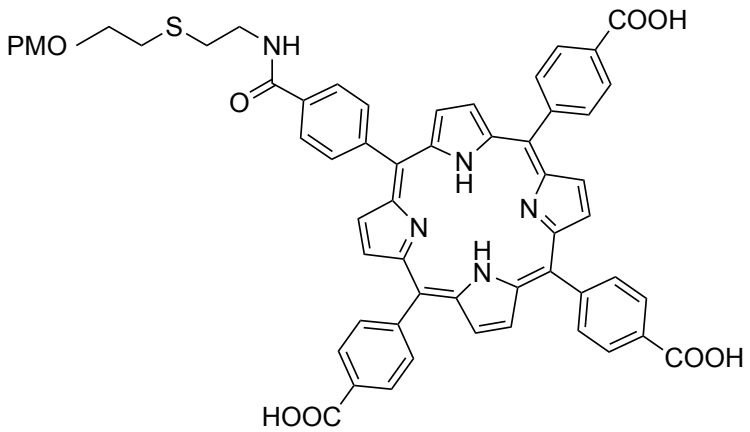

Figure 15: *$TCPPH_2$@PMO.*

The resulting material, in combination with DMAP converted in good yields epichlorohydrin in 2 h, 120°C and 0.6 MPa of CO_2. It should be noted that the organic catalyst improved its activity when supported onto silica.[215]

Then, another example of silica-supported porphyrin has been published by Q. Yhang and her research group who immobilized 5,10,15,20-tetrakis(4-pyridyl)porphyrin zinc(II) (ZnTPy) onto SBA-15 silica exploiting 3-(trimethoxysilyl)propyl bromide obtaining cationic ZnTPy@SBA-15. The so-obtained bifunctional catalyst, presenting both a Lewis acid, the zinc atom, and a nucleophile, the bromine anion, showed interesting activity in the coupling of carbon dioxide with different epoxides at 1.5 MPa of CO_2 and 120 °C.[216]

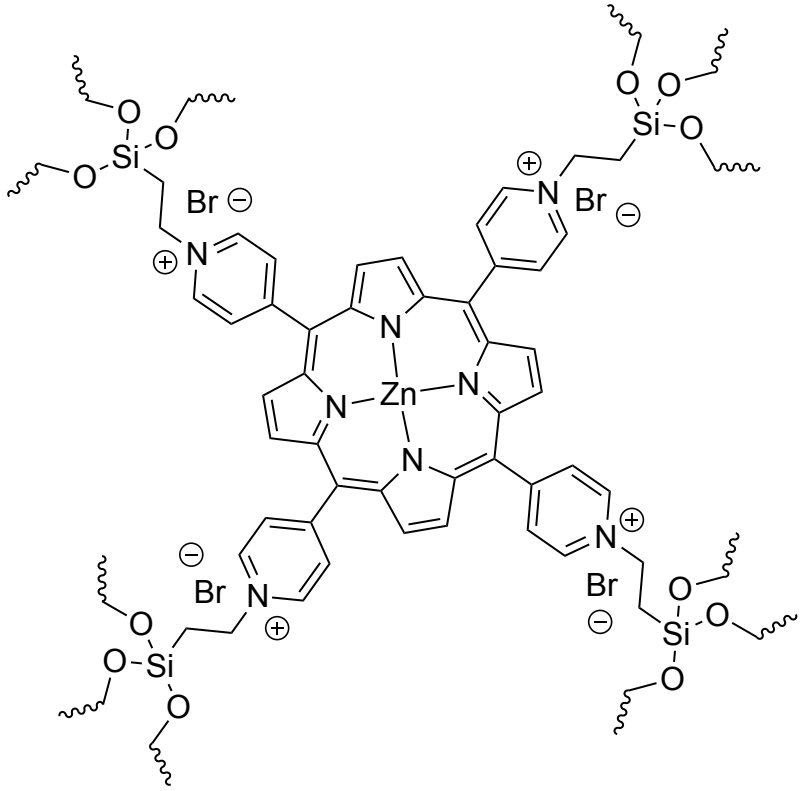

***Figure 16**: ZnTPy@SBA-15.*

However, these three catalysts worked under quite harsh conditions and the most promising seems to be the $TCPPH_2$-based one since it is a metal-free catalyst, even if it has been tested only with epichlorohydrin, one of the most reactive epoxides.

Other organic compounds have been grafted onto silica for achieving efficient metal-free heterogeneous catalysts for the cycloaddition of carbon dioxide to three membered heterocycles. Supported hydrogen bond donors were prepared in order to exploit the activity of guanidine[217] or other amines[218] in this transformation, but in both cases the prepared catalysts needed harsh reaction conditions to be active. Thanks to their activity under homogeneous condition, IL has also been supported onto silica. The first example was proposed in 2007 by employing very harsh experimental conditions like 8.0 MPa of CO_2 and 160 °C.[219] Supported ionic liquid were then modified by adding acid moieties on the IL backbone[220] and then studied by Breitzke and co-workers to better understand the influence of different functionalizations of the supported molecules and the role of the solid support.[221] Another category of organic catalysts studied and supported onto silica are onium salts. The catalytic activity of supported phosphonium salt in promoting this reaction was first reported in 2006 and the synergic role of both the catalyst and the solid support was underlined.[207] Then, the phosphonium salt 3-(triethoxysilyl)propyltriphenylphosphonium bromide supported on SBA-15 silica was studied. The reported catalyst displayed good robustness and a synergistic activity of the organic and inorganic components was demonstrated by converting different epoxides in the corresponding cycling carbonates at 1.0 MPa of CO_2 and 90 °C.[222]

Ammonium salt has also been supported on surfaces and the resulting catalytic activity has been extensively investigated. Different ammonium salts have been tested as catalysts in the coupling reaction between epoxides and carbon dioxide by starting from aminopyridinium iodide, which showed a good efficiency even under atmospheric pressure.[223] The synergic effect of the onium salt with silica has been highlighted in this case as well. Recently, kinetic studies revealed that by using this catalyst the cycloaddition reaction of CO_2 to styrene oxide (SO) shows a first order dependency with respect to SO, CO_2 and the catalyst itself.[224]

However, the *N*-Benzyl DABCO bromide-based ammonium salt (DABCO = 1,4-diazabicyclo [2.2.2]octane), grafted on 3-chloropropyl silica, showed poorer activity compared to that of the previously presented catalyst[208] as well as TBAB supported onto silica that needs very harsh condition, as supercritical CO_2, to produce cyclic carbonates in

good yields.[225] Recently, Dufaud and co-workers prepared a series of different materials to investigate under heterogeneous phase the effectiveness of tetraphosphonate cavitand in the activation of ammonium halides in the cycloaddition reaction of carbon dioxide to epoxides.[226] Firstly, they synthesized a series of materials by supporting the cavitand or the ammonium halide onto ultra large SBA-15. The study allowed them to conclude that the linkage of the ammonium salt directly onto the silica, even if the iodide anion may experience an enhancement of its nucleophilicity, produced a material less active than that obtained by linking tetraphosphonate. In fact, the linkage of the host onto silica brought results comparable with those obtained under homogeneous condition.[227] In addition, the same authors have recently studied the role of SBA-15 silica on the activity of quaternary ammonium halides in the coupling of epoxides and CO_2.[209] In particular, they found that over the activation of epoxides through the silanol moieties, the same functional group may interact with the halide anion and its nucleophilicity may be drastically reduced depending on the nature of the halide (chloride anion suffers from the deactivation the most) and the number of silanol moieties present in the neighborhood of the ammonium salt.

Once again, the reaction between aziridine and CO_2 has been much less studied than the corresponding one with epoxides. In particular, only *N*-alkyl aziridines were tested in the studies by using heterogeneous catalysts. Some of the simplest catalytic species studied were zirconyl chloride $ZrOCl_2 \cdot 8H_2O$,[89] mesoporous zirconium phosphonates[92] and titanium phosphonates[91] that however worked only under harsh experimental conditions as in presence of more than 2.0 MPa of carbon dioxide and more than 100 °C. It should be noted that MOF, widely used in the conversion of epoxides into cyclic carbonates, were scarcely employed and there are only few examples of their use in the synthesis of oxazolidinones.[187] The first example was proposed by He and co-workers, who studied MOF-based [Cu_{30}] nanocages. Nevertheless, this compound worked only at high catalytic loading (10 mol% of Cu) in the presence of TBAB (5 mol%) and at high pressures of carbon dioxide (2.0 MPa).[94] Then, the activity of copper derivatives was confirmed by S. Ma and co-authors, who prepared a metal-metalloporphyrin framework that worked even at room temperature and in a lower loading (0.625 mol%) but in very long reaction times.[93]

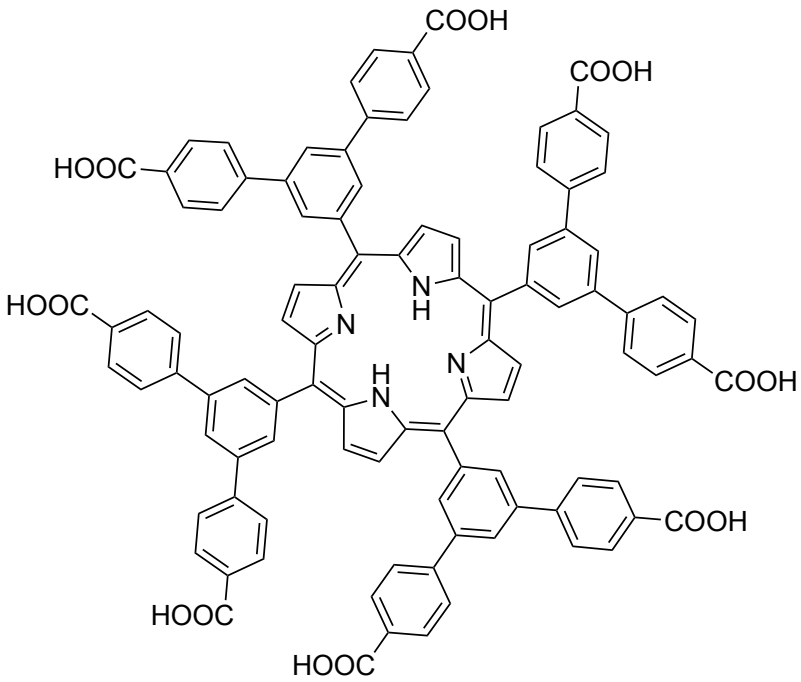

Figure 17: *Tetrakis-3,5-bis[(4-carboxy)phenyl]phenyl porphyrin, the ligand used to build the Cu-based MOF by S. Ma.*

More recently, a bifunctional heterogeneous aminopyridinium-based POP has been tested in the cycloaddition reaction of carbon dioxide to 1-butyl-2-phenyl aziridine, giving encouraging results. However, more studies need to be done in order to expand the scope and improve reaction conditions.[228]

In addition, different supports have been tested to prepare heterogenized catalytic systems, such as polystyrene-supported ionic liquid[98,229] or amino acids,[100] ion exchange resins,[230] and chitosan.[231,232] Nonetheless, in all these cases of at least 2.0 MPa of CO_2 pressure were needed.

Another interesting solid support tested was PEG, which has been used in combination with ammonium salts, phosphonium salts[182] and IL.[233]

The heterogenized ammonium bromide showed a promising activity converting different aziridines in the corresponding oxazolidinones in very short times and with low catalyst loadings (0.25 mol %). However, 100 °C and 8.0 MPa of carbon dioxide were needed. It is

interesting to notice that L.-N. He and co-authors also tested *N*-phenyl-2-phenyl aziridine obtaining as the only product the homocoupling of the aziridine.[95]

Finally, silica-based materials, and in particular MCM-41, have been used as solid supports for grafting two different organic catalysts. In 2011, X.-B. Lu and co-workers studied the catalytic activity of MCM-41 functionalized with *N*-heterocyclic carbene (NHC). As already discussed, NHCs can form adducts with carbon dioxide activating it through the cycloaddition to epoxides and aziridines. This catalyst promoted the reactions of CO_2 with both epoxides and *N*-alkyl aziridines even at low catalyst loadings (0.5 mol %), but in long reaction times and more than 100 °C and 2.0 MPa of CO_2 were required.[234]

Moreover, an amine functionalized MCM-41 demonstrated to be active at 40 °C but high catalytic loadings and 5.0 MPa of CO_2 were necessary to make the reaction proceed. The proposed mechanism involves the activation of carbon dioxide *via* the formation of a carbamate moiety, the activation of the aziridine through H-bonding and the following ring opening reaction in which the nucleophile is the carbamate itself (scheme 18).[235]

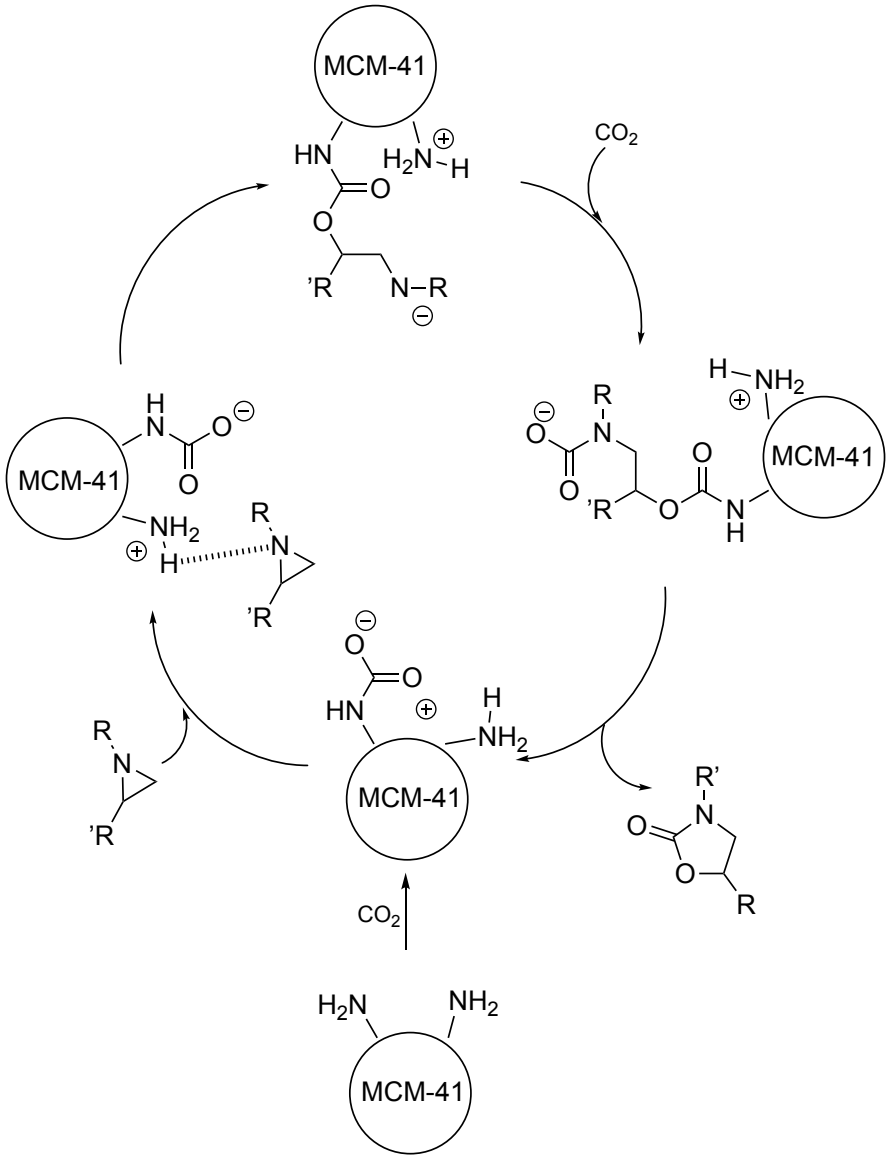

Scheme 18: *proposed mechanism for the formation of oxazolidinones catalyzed by amine functionalized MCM-41.*

10. Tandem reactions for the synthesis of cyclic carbonates and oxazolidinones

The formation of cyclic carbonates and oxazolidinones directly from alkenes, which are first transformed into epoxides or aziridines and then reacted with carbon dioxide, is an interesting pathway to improve the sustainability of their synthesis. Aresta proposed the tandem synthesis of cyclic carbonate in 1987 by first utilizing a rhodium catalyst[236] and then exploiting the catalytic activity of Nb_2O_5.[237,238] Unfortunately the formation of styrene carbonate directly from styrene, molecular oxygen, and carbon dioxide occurred in moderate yields due to the formation of large amount of oxidation by-products. Since then, the production of cyclic carbonate from alkenes and CO_2 has been widely studied by testing many different catalysts and experimental conditions in order to overcome the low reaction productivity that had initially emerged.[239–241]

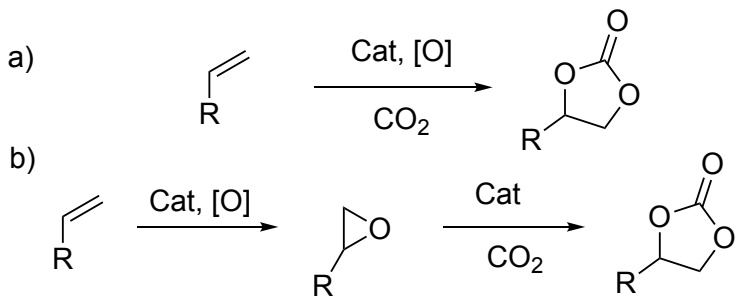

Scheme 19: *mono e multi step reactions to produce cyclic carbonates from alkenes.*

The desired cyclic carbonate was obtained either by directly mixing all the needed reagents and catalyst or by performing a step-by-step reaction, in which the epoxide intermediate, that was neither isolated or purified to avoid time and energy demanding work-up, was directly reacted with CO_2.[240]

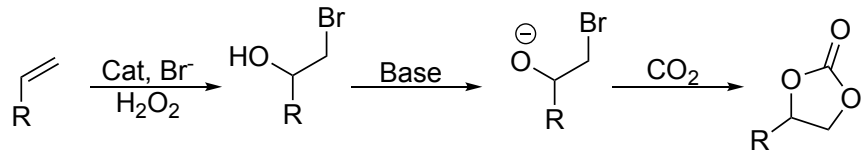

Scheme 20: *formation of cyclic carbonates from alkenes via bromohydrin intermediate.*

Two different mechanisms have been envisaged, the first passing through the epoxide formation and the second *via* bromohydrin intermediate (scheme 20).[239]

In 2010 H. Jing reported the catalytic activity of Ru-porphyrin catalyst that, in the presence of onium salts co-catalyst, promoted the tandem synthesis of cyclic carbonates from alkenes in yields up to 89% and high selectivity. Unfortunately the high catalytic loading of 4 mol% was needed.[242]

The synthesis of cyclic carbonates was also performed by applying multistep reactions that had the drawback to occur with the contemporary formation of several by-products. However, the first example of multi-step reaction was proposed by reacting alkene in the presence of methyltrioxorhenium, urea hydrogen peroxide and IL as the catalytic system.[243] Despite the obvious problems that the utilization of multiple reagents may involve, in this way the applicability and efficiency of multi-step protocols were demonstrated.

Starting from these studies, a plethora of catalysts have been tested, improving the reaction productivity and sustainability by exploiting the catalytic activity of noble metals,[244–246] transition metals,[247–249] and IL.[250] To further improve the recyclability of the catalyst and the product purification, different heterogeneous material has been tested such as MOFs[251–253] and titanium and aluminum silicates.[254–256] Finally, a flow protocol[257] and an asymmetric transformation[258] have been developed as well.

It should be noted that only two examples of tandem reaction producing oxazolidinones from alkenes have been reported. The first one presented the synthesis of *N*-tosyl oxazolidinones from alkenes, chloramine-T and carbon dioxide catalyzed by the TBAB/$TBAB_3$ system.[259]

The proposed mechanism run through the initial bromine-catalyzed aziridination of the alkene[260] followed by the carbon dioxide cycloaddition catalyzed by TBAB.

However, this methodology presented different drawbacks. First, only tosyl oxazolidinones may be prepared, then, at the end of the reaction, different by-products may be detected such as unreacted aziridine and the corresponding tosylamino ethanol; finally, the catalytic system only works in the presence of 8.0 MPa of carbon dioxide.

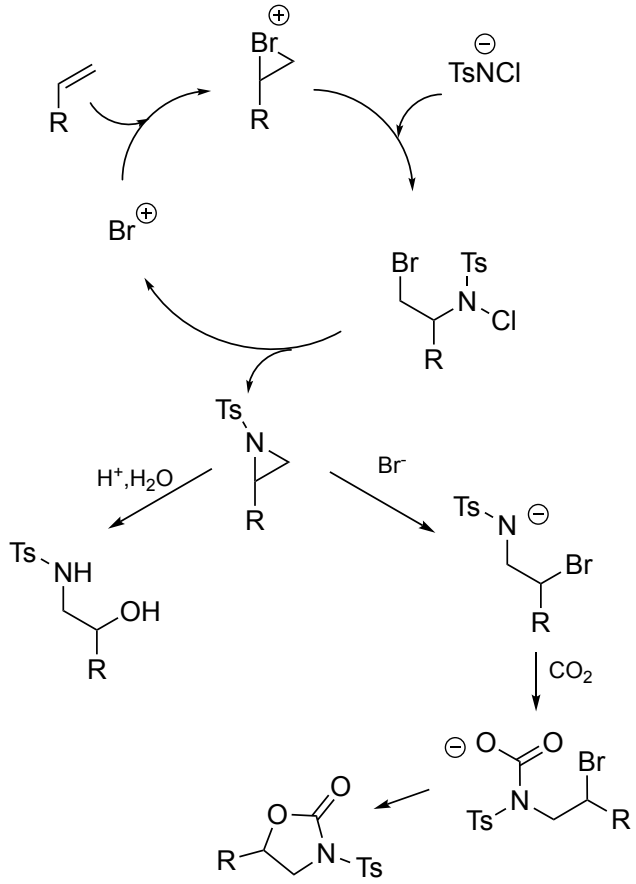

Scheme 21: *mechanism proposed for the synthesis of oxazolidinones from alkenes, chloramine-T and* CO_2

On the other hand, a dendritic fibrous nanonsilica functionalized with $Dy_2Ce_2O_7$ nanoparticles catalyzes the formation of *N*-aryl oxazolidinones from carbon dioxide, styrene, and anilines in the presence of *tert*-butyl hydroperoxide (TBHP) as the oxidant. The reaction proceeds with good yields utilizing different anilines and the catalyst resulted stable for at least 10 runs with a low leaching. In this case the unique catalyst carries out the initial epoxidation and the following formation of oxazolidinones through the three component mechanism that involves epoxides, amines and carbon dioxide.[57,261]

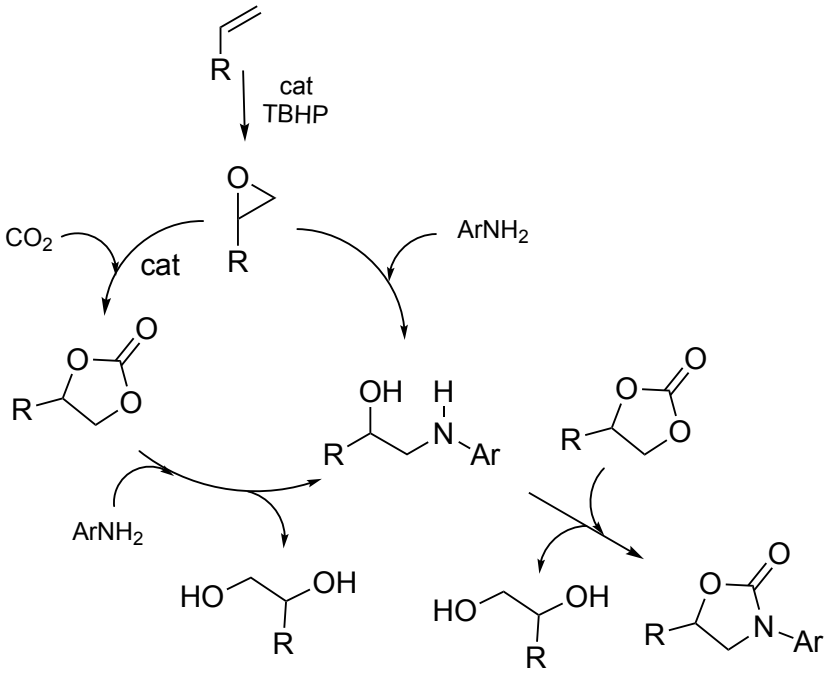

Scheme 22: *production of oxazolidinones from alkenes, anilines, and CO_2 trough the formation of epoxides.*

11. Aim of the thesis

As presented in the previous pages, the carbon dioxide cycloaddition to three membered heterocycles can be a valuable tool to produce useful cyclic carbonates and oxazolidinones exploiting carbon dioxide as a carbon source. Moreover, this reaction is a simple and effective way to apply the green chemistry and CCU principles and may be industrialized to improve the sustainability of the synthetic pathways currently exploited. The utilization of this reaction, for example, makes possible to avoid toxic reactants as phosgene and, at the same time, gives an added value to an ubiquitous waste and greenhouse gas as CO_2 helping to reduce its concentration in the atmosphere.

This work is devoted to the study of sustainable organic catalysts, both homogeneous and heterogeneous, for the production of cyclic carbonates and oxazolidinones from epoxides and aziridines respectively. Two different ways was followed to improve the sustainability of this reaction: the utilization of organic catalysts, that makes possible to avoid the presence of metal traces in the final products and to use less toxic solvents, and the preparation of a hybrid heterogeneous material, that simplifies the purification protocols and enables an easy recovery of the catalyst. Here will be presented the study of the activity of free-base porphyrins in this class of reactions and the role of the porphyrin itself in the activation of the ammonium salts. This study paved the way to the presentation of the first general methodology for the preparation of *N*-aryl oxazolidinones from the corresponding aziridine and carbon dioxide. Moreover, a tandem procedure for the synthesis of these useful organic compounds was developed

Chapter II: Homogeneous catalysts for the CO_2 cycloaddition reaction

1. The ruthenium *bis-imido* porphyrin catalyst

In this chapter the activity of the homogeneous catalytic system *meso*-tetraphenyl porphyrin/TBACl will be discussed.

Keeping in mind the previously reported study that exploited the reactivity of porphyrin metal complexes and ammonium salts in the carbon dioxide cycloaddition to three membered heterocycles, free-base porphyrins have been tested in order to improve the reaction sustainability. The possibility to avoid the utilization of metals combined with the necessity to improve the activity of organic catalysts utilized to promote this transformation produced the efforts devoted to this project.

In the last years, the experience of the research group in the synthesis of aziridines from styrenes and aryl azides *via* the nitrene transfer reaction generated the interest in further reactions that may involve these organic molecules. At the same time, the abundancy of studies about the reaction between epoxides and carbon dioxide exploiting porphyrin-based catalysts and the concomitant lack of general methodologies for the corresponding reaction between *N*-aryl aziridines and CO_2 raised the interest in this field. In particular, the clear advantages presented by the utilization of carbon dioxide as an organic synthon and the necessity to improve the synthetic pathways for the production of *N*-aryl oxazolidinones make this topic interesting and worth of study.

Two previous PhD thesis carried out in the research group established the ability of ruthenium *bis-imido* porphyrins in combination with ammonium salts to catalyze the cycloaddition reaction of carbon dioxide to epoxides[262] and *N*-alkyl aziridines[181] as a starting point for further investigations.

First, different catalysts have been tested to understand the role of the imido moieties and how they are involved in the reaction mechanism. Both the porphyrin ligand and the imido moieties have been modified to produce a library of electronically different metalorganic compounds and, among all the complex applied to the studied reaction, $Ru^{IV}(TPP)(NAr)_2$ (Ar = 3,5-$(CF_3)C_6H_3$ **1**), in combination with the co-catalyst tetrabutyl ammonium chloride (TBACl), was identified as the most active catalyst.

By reacting *N*-alkyl aziridines with carbon dioxide in the presence of this catalyst/co-catalyst combination for 6 h, at 100 °C and 0.6 MPa and with a catalyst/co-catalyst/aziridine ratio of 1:5:100, different *N*-alkyl oxazolidinones were produced obtaining yields up to 99% and regioselectivities for the 3,5-substituted regioisomer (product a, table 1) up to 99:1, as reported in table 1.

Table 1: *Synthesis of oxazolidinones catalyzed by* ***1****.*

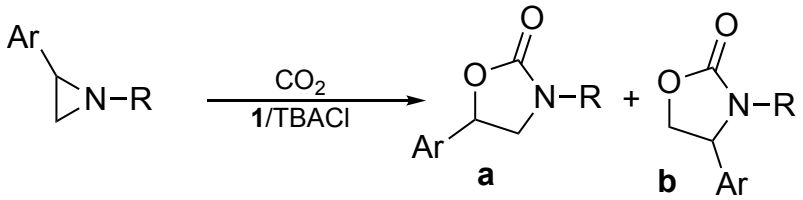

Entry	Ar	R	Yield (%)[a]	a/b[b]
1	-Ph	-Et	65	95:5
2	-Ph	-^{n}Pr	60	90:10
3	-Ph	-^{n}Bu	71	95:5
4	-Ph	-^{i}Pr	20	90:10
5	-Ph	-^{i}Amyl	81	92:8
6	-Ph	-Allyl	70	94:6
7	-Ph	-^{n}Hex	55	94:6
8	-Ph	-Cyp	10	99:1
9	-Ph	-CH_2Cy	55	94:6
10	-Ph	-Bn	85	99:1
11	-Ph	-(2-OMe)Bn	64	99:1
12	-Ph	-(4-OMe)Bn	60	99:1
13	-(2-Me)Ph	-^{n}Bu	92	90:10
14	-(3-Me)Ph	-^{n}Bu	96	90:10
15	-(4-Me)Ph	-^{n}Bu	90	90:10

Reactions carried out in a steel autoclave at 100 °C and, 0.6 MPa of carbon dioxide for 6 h. ***1****/TBACl/Aziridine = :1:5:100. a) Isolated yields. b) Determined by* ^{1}*H NMR spectroscopy using 2,4-dinitrotoluene as the internal standard.*

In general, the catalyst displayed worse activity with the increase of the bulkiness on the nitrogen atom substituent. On the contrary, the presence of electron rich aryl ring on the carbon atom improved the reaction productivity. Moreover, it is possible to notice this effect independently from the position of the EDG group on the phenyl substituent.

In addition, the catalytic system resulted active in the conversion of epoxides into the corresponding cyclic carbonates with yields up to 99 %, as reported in chart 1.

Chart 1: *Synthesis of cyclic carbonates catalyzed by* ***1.***

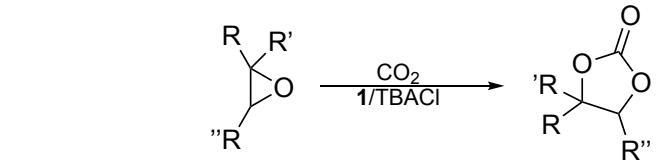

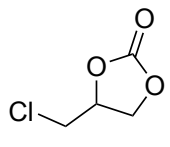

Conversion: 100%
Selecitivity: 99%
Yield: 99%

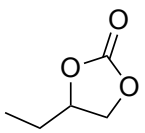

Conversion: 100%
Selecitivity: 65%
Yield: 65%

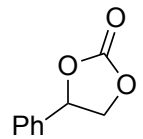

Conversion: 100%
Selecitivity: 99%
Yield: 99%

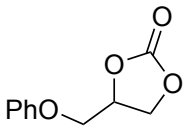

Conversion: 100%
Selecitivity: 94%
Yield: 94%

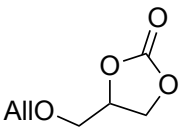

Conversion: 100%
Selecitivity: 99%
Yield: 99%

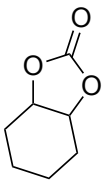

Conversion: 100%
Selecitivity: 17%
Yield: 17%

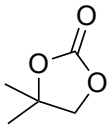

Conversion: 100%
Selecitivity: 15%
Yield: 15%

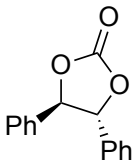

Conversion: 100%
Selecitivity: 15%
Yield: 15%

Reactions carried out in a steel autoclave at 100 °C and, 0.6 MPa of carbon dioxide for 8 h. ***1****/TBACl/epoxide = 1:5:100. Yields and conversions determined by* ^{1}*H NMR spectroscopy using 2,4-dinitrotoluene as the internal standard.*

The reported catalytic combination resulted effective in the conversion of terminal epoxides but demonstrated poor activity when applied to disubstituted or internal epoxides. It is worth of notice that the reported oxiranes reacted with CO_2 also in the presence of the sole TBACl obtaining only slightly worse results with overall good yields: just in a few cases an important decrease of the selectivity was detected. These results confirm the good activity of ammonium salts in the carbon dioxide cycloaddition reactions. After the isolation of the intermediate $\mathbf{I_3}$ (scheme 23), a general mechanism for the cycloaddition of carbon dioxide to three membered heterocycles catalyzed by complex **1** was hypothesized (scheme 23). First, the nitrogen atom of the imido moiety activates the carbon dioxide molecule forming a reactive intermediate $\mathbf{I_1}$. The so-formed complex may go through two different processes with opposite results. Either it may be deactivated by reacting with TBACl and forming a stable salt $\mathbf{I_3}$ that leaves the catalytic cycle or $\mathbf{I_1}$ may be responsible for the ring-opening reaction of the three membered heterocycle, yielding the charged intermediate $\mathbf{I_2}$. Then, the ring-closing step brings to the formation of the five membered heterocycle and the regeneration of the catalyst.

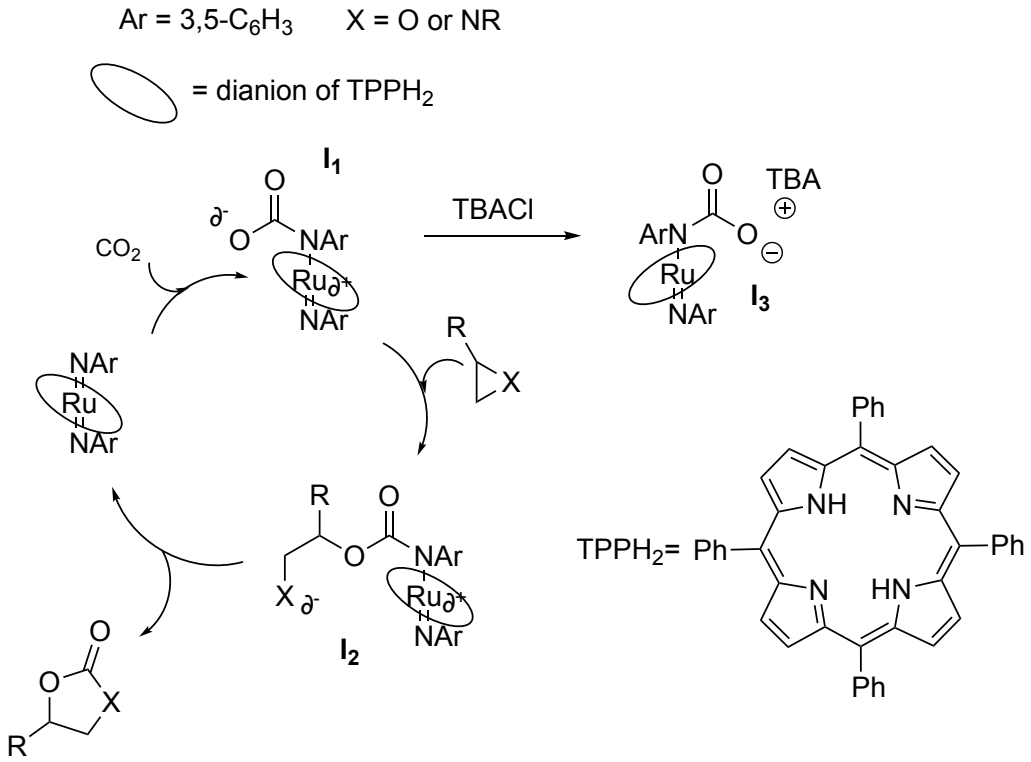

Scheme 23: *proposed mechanism for the formation of cyclic carbonates and oxazolidinones catalyzed by* ***1****.*

2. A new catalytic system

Considering the results obtained using **1** with *N*-alkyl aziridines and epoxides, the activity of the *bis-imido* catalyst was evaluated in the reaction between 1-(3,5-trifluoromethylphenyl)-2-phenyl aziridine **2**. After 15 h at 100 °C and 1.2 MPa of carbon dioxide in benzene, 60% of the aziridine was converted but the obtained selectivity was very low (table 2, entry 1), in fact, many different unidentified by-products were presents in the reaction mixture.

To investigate the role of the metal center and of the imido moieties, catalyst **1** was substituted with the ligand *meso*-tetraphenyl porphyrin ($TPPH_2$, **3**) in combination with TBACl. The catalytic system **3**/TBACl showed reduced activity but increased selectivity for the production of the desired oxazolidinone (table 2, entry 2). Thus, the benefit in term of sustainability to replace a ruthenium-based catalyst with an organic and cheap molecule like $TPPH_2$ attracted our attention. Then, deeper studies were carried out to fine tune the catalytic system that displayed such good selectivity for the synthesis of *N*-aryl oxazolidinones, which are a tricky class of compounds to be obtained through carbon dioxide cycloaddition. First, since the reaction was carried out in the absence of a metal atom, it was possible using a coordinating solvent that otherwise would deactivate the catalytic center. Thus, we replaced benzene with tetrahydrofuran (THF), which solubilizes better carbon dioxide[263] and also the catalyst and co-catalyst. The improvement of the catalytic performances was evident since the first reaction (table 2, entry 3), the conversion remarkably increased even if a slight decrease of the selectivity was detected. In fact, the use of THF guaranteed a higher concentration of carbon dioxide into the mixture, improving the product yield of the coupling reaction between CO_2 and **2**. Afterwards, two different organic co-catalysts, used in literature in the cycloaddition of carbon dioxide to aziridines and oxiranes such as PPNCl (*bis*(triphenylphosphine) iminium chloride) and DMAP,[264] were tested in the same reaction in combination with **3**: lower or no results were obtained (table 2, entries 4 and 5). In the first case, PPNCl produced worse results probably because the phosphonium cation is bigger than the ammonium one, as indicated also by the low regioselectivity; usually the regioisomer a is the favored reaction product but the

encumbrance of the onium salt may turn the regioselectivity toward the product b. On the other hand, DMAP generally needs a synergic nucleophile species, and this role cannot be played by the porphyrin with the consequent observed lack of activity. Thus, the best co-catalyst resulted to be TBACl, which produced the best values for conversion, selectivity, and regioselectivity.

***Table 2**: cycloaddition reaction to produce **4a/4b**.*

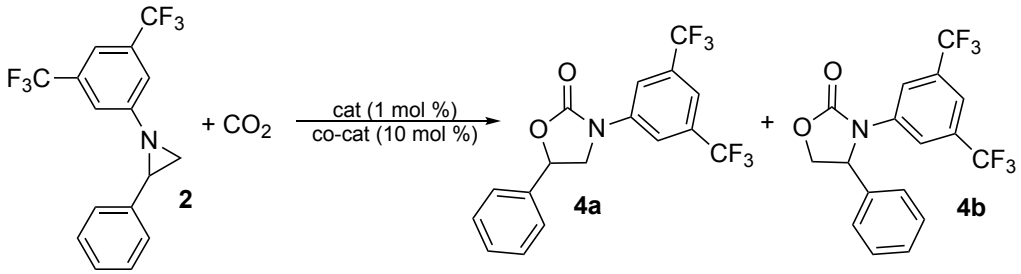

Entry	Catalyst	Co-catalyst	Conversion (%)[d]	Selectivity (%)[d]	Yield (%)[d]	**4a/4b**[d]
1[a]	**1**	TBACl	60	40	24	97:3
2[a]	$TPPH_2$	TBACl	20	90	18	90:10
3[b]	$TPPH_2$	TBACl	61	80	49	90:10
4[b]	$TPPH_2$	PPNCl	49	78	38	65:35
5[b]	$TPPH_2$	DMAP	/	/	/	/
6[b]		TBACl	63	79	50	74:26
7[b]	$TPPH_2$		/	/	/	/
8[c]	$TPPH_2$	TBACl	20	80	16	90:10
9[c]		TBACl	5	79	4	76:24

a) *Reaction performed in a steel autoclave: 0.11 M benzene N-aryl aziridine solution for 15 h at 1.2 MPa, 100 °C and cat/co-cat/aziridine ratio 1:10:100. b) Reaction performed in THF. c) Reaction run for 6 h. d) Determined by ^1H NMR by using 2,4-dinitrotoluene as the internal standard.*

Then, to understand the porphyrin catalytic role, a reaction with the sole TBACl was run (table 2, entry 6), obtaining very similar conversion and selectivity with respect to the combination **3**/TBACl; however, the a/b ratio improved in the presence of the porphyrin. Note that **3** alone was not active in this transformation (table 2 entry 7) to underline the

pivotal role played by the ammonium salt in this reaction. Finally, to improve our knowledge about the $TPPH_2$ role in synthesis of oxazolidinones, two more reactions were carried out by reacting aziridine with CO_2 for a reduced time. The reaction catalyzed by the system **3**/TBACl was more productive than the reaction carried out with the ammonium salt alone to underline that after a short reaction time the presence of the porphyrin improves both the regioselectivity and the rate of the substrate conversion.

3. Optimization of the reaction conditions

Once the catalytic activity of the system $TPPH_2$/TBACl was confirmed, the interest in applying such a convenient methodology to synthesize *N*-aryl oxazolidinones (NAOs) resulted evident. Thus, this pathway was investigated in depth starting from the optimization of the reaction conditions.

As a model reaction, the cycloaddition of carbon dioxide to **2** was chosen, producing oxazolidinones **4a** and **4b,** and the reaction parameters were tuned one by one to maximize the reaction productivity.

Initially, seven experiments at different substrate concentrations were performed by utilizing the following reaction conditions: the THF solution of **2** at the desired concentration was stirred for 15 h at 100 °C and 1.2 MPa of CO_2 in a steel autoclave with a **3**/TBACl/**2** ratio of 1:10:100. The gathered results are reported in figure 18.

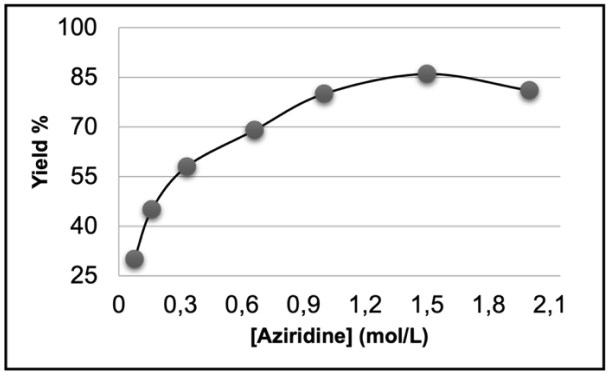

Entry	Conc (M)	Yield (%)
1	0.075	30
2	0.16	45
3	0.33	58
4	0.66	69
5	1.00	80
6	1.50	86
7	2.00	81

Figure 18: *optimization of the aziridine concentration.*

As shown in figure 18, the best result was obtained at 1.50 M of aziridine in THF. The reaction yields growth continuously up to 86%, then a slight decrease at higher concentration was detected that can be also due to the increase of the reaction mixture density at concentrations higher than 2.0 M. A regioisomeric ratio **4a**/**4b** of 86:14 corresponds to the yield reported in entry 6 of figure 18. In addition, using the same experimental conditions, a solvent free reaction was performed, obtaining the good conversion of 88% but with the lower selectivity towards the desired product of 77%, probably due to the occurrence of the aziridine homocoupling. Then, once the aziridine

concentration was fixed at 1.5 mol/L and without changing the other parameters, five different pressure values were tested.

The best result was obtained using 1.2 MPa of CO_2. It is important to note that at higher pressures the reaction yield decreased probably due to the small volumetric expansion that occurs at high pressures and the consequent aziridine dilution was responsible for the decrease of the catalytic efficiency.[265] Moreover, it is important to underline that the system was quite effective even at lower pressures (entry 1 and 2, table of figure 19) but those conditions would require very long reaction times. Considering that less reactive substrates may not give satisfying results in such soft conditions, we decided to proceed in our study by fixing the pressure at 1.2 MPa.

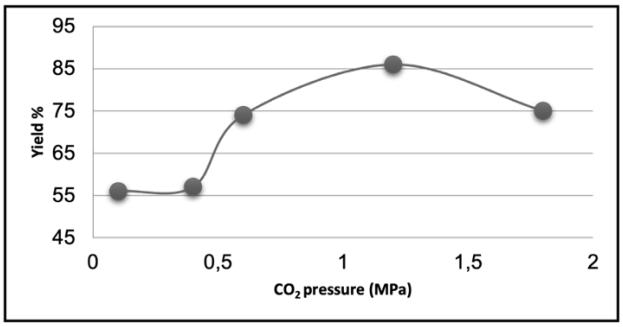

Entry	CO_2 pressure (MPa)	Yield (%)
1	0.1	56
2	0.4	57
3	0.6	74
4	1.2	86
5	1.8	75

***Figure 19**: carbon dioxide pressure optimization.*

Then, the effect of the temperature was studied by applying the values of pressure and concentration optimized up to know (1.5 M aziridine in THF and 1.2 MPa of CO_2) and by running reactions for 15 h.

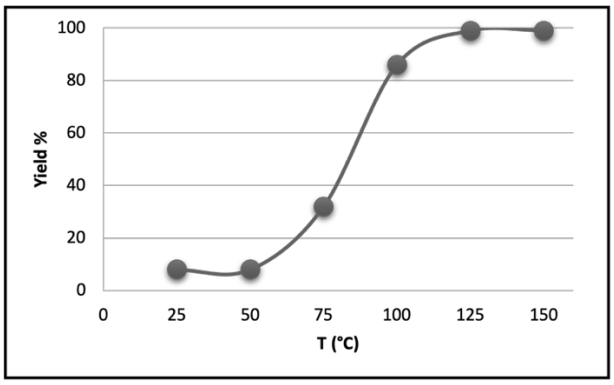

Entry	T (°C)	Yield (%)
1	25	8
2	50	9
3	75	32
4	100	86
5	125	99
6	150	99

***Figure 20:** temperature optimization.*

Raising the temperature up to 125 °C the complete conversion of the substrate was obtained, reaching 99% of yield with a **4a**/**4b** regioisomeric ratio of 86:14. It is important to note that up to 75 °C the reaction productivity was quite low. This result indicated the presence of quite a high energy barrier, which must be surpassed to produce oxazolidinones from aziridines and CO_2.

Then, some other reactions were carried out to further improve the reaction conditions, as shown in table 3.

Table 3

Entry	$TPPH_2$ mol %	TBACl mol %	Solvent	Conversion (%)[a]	Selectivity (%)[a]	**4a**/**4b**[a]
1	1	10	THF	100	99	86:14
2	1	5	THF	100	99	86:14
3	0	5	THF	84	72	80:20
4	1	5	2-MeTHF	99	81	80:20

Reactions performed in a steel autoclave: 1.5 M N-aryl aziridine solution for 8 h at 1.2 MPa, 125 °C.
a) Determined by ^1H NMR using 2,4-dinitrotoluene as the internal standard

First, the time was reduced from 15 h to 8 h, achieving again the complete conversion of the substrate (table 3, entry 1). Then the quantity of TBACl was halved. Once again, this change does not affect the catalytic productivity neither the regioselectivity (table 3, entry 2). In the optimized conditions the porphyrin role was investigated one more time running a reaction with the sole ammonium salt as the catalytic species (table 3, entry 3): conversion and selectivity fell to 84% and 72 % respectively, underlining the importance of the macrocyclic molecule in the catalytic system. Finally, in order to improve the sustainability of this methodology, THF was replaced by the more benign 2-methyl THF, which is a stable and water-immiscible green solvent derived from natural sources like corncobs and bagasse.[266] However, its use was thwarted by the decrease of selectivity detected (table 3, entry 4).

Then, the following optimized reaction conditions were used to study the reaction scope: 1.5 M aziridine solution in THF, 125 °C, 1.2 MPa of carbon dioxide, and 8 h in a steel autoclave utilizing a $TPPH_2$/TBACl/aziridine ratio of 1:5:100.

4. Study of the reaction scope of the carbon dioxide cycloaddition to *N*-aryl aziridines

The data gathered during the study of the reaction scope are reported in table 4. They indicated that the reaction productivity was affected by both steric and electronic factors. When R_1 was an electron withdrawing group (EWG) the reaction experienced a beneficial effect, as proven by the complete conversion of the aziridine into the desired oxazolidinone, as reported in entries 1 and 2 of table 4. Then, it was noticeable that the addition of a methyl or bromine substituent on the R_3 position of aziridine, bearing an EWG as R_1, did not affect the reaction productivity (table 4, entries 3, 5 and 6). On the contrary, the addition of a bulkier moiety, as in the case of aziridine **9**, caused a slight decrease of selectivity and yield.

The simultaneous presence of two EWGs, such as 3,5-$(CF_3)_2C_6H_3$ and C_6F_5, was responsible for a slight decrease of the reaction productivity (table 4, entry 7). On the other hand, it is important to note that when EWG and electron donating groups (EDG) are both present on the two different phenyl rings, the reaction productivity improved compared with that of the previous case (table 4, entry 8). In fact, when aziridine **17** was reacted, 92% of conversion with 86% of selectivity was observed with a 91:9 regioisomeric ratio by favoring the formation of oxazolidinone **18a**. The obtained data suggested that the C-N bond may be polarized by the presence of two groups with opposite electronic characteristics and this event could help the aziridine opening through the cleavage of the C-N bond. It seems that it is not important on which phenyl ring EWG and EDG are located to induce the bond polarization. Moreover, this can explain the decrease of reaction productivity noted for the reaction described in entry 7 of table 4. Thus, when any R_3 substituent is present and R_1 is an EWG, the aziridine conversions and oxazolidinone yield increased due to the bond polarization. This suggestion is in accordance with the reduction of the reaction productivity that was observed when EDG substituted aziridines **19** and **21** were reacted (table 4, entries 9 and 10). The data gathered during the study of the reaction scope are reported in table 4. They indicated that the reaction productivity was affected by both steric and electronic factors. When R_1 was an electron withdrawing group (EWG) the

reaction experienced a beneficial effect, as proven by the complete conversion of the aziridine into the desired oxazolidinone, as reported in entries 1 and 2 of table 4.

Table 4: *synthesis of N-aryl oxazolidinones catalyzed by the $TPPH_2$/TBACl system.*[a]

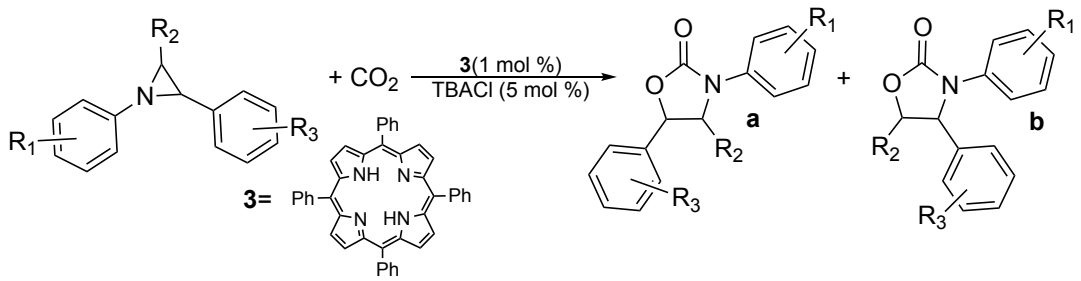

Entry	Aziridine	R^1	R^2	R^3	Conv. %[b]	Sel. %[c]	Yield %[c]	a/b[b]
1	**2**	3,5-$(CF_3)_2$	H	/	>99	>99	>99	**4a**/**4b**=86:14
2	**5**	4-NO_2	H	/	>99	>99	>99	**6a**/**6b**=78:22
3	**7**	3,5-$(CF_3)_2$	H	4-Me	>99	90	>99	**8a**/**8b**=80:20
4	**9**	3,5-$(CF_3)_2$	H	4-^{t}Bu	98	86	84	**10a**/**10b**=99:1
5	**11**	4-NO_2	H	4-Me	>99	90	90	**12a**/**12b**=85:15
6	**13**	3,5-$(CF_3)_2$	H	4-Br	>99	>99	>99	**14a**/**14b**=80:20
7	**15**	3,5-$(CF_3)_2$	H	F_5	80	80	64	**16a**/**16b**=82:18
8	**17**	4-^{t}Bu	H	F_5	92	86	79	**18a**/**18b**=91:9
9	**19**	4-OMe	H	/	85	23	19	**20a**/**20b**=99:1
10	**21**	4-^{t}Bu	H	/	95	57	54	**22a**/**22b**=96:4
11	**23**	4-Br	H	/	>99	50	50	**24a**/**24b**=90:10
12	**25**	4-Cl	H	/	97	74	72	**26a**/**26b**=89:11
13	**27**	2-NO_2	H	/	>99	60	60	**28a**/**28b**=64:36
14	**29**	3-OMe	H	/	80	trace	trace	/
15	**30**	3,5-Cl_2	H	/	94	>99	94	**31a**/**31b**=81:19
16	**32**	3,5-$(NO_2)_2$	H	/	>99	30	30	**33a**/**33b**=76:24
17	**34**	3,5-$(CF_3)_2$	Me	/	73	71	52	**35a**/**35b**=94:6
18	**36**	4-^{t}Bu	Me	/	70	40	28	**37a**/**37b**=83:17

*a) Reaction performed in a steel autoclave with the following conditions: 1.5 M N-aryl aziridine solution in THF for 8 h with **3**/TBACl/aziridine = 1:5:100 at 125 °C and 1.2 MPa of CO_2. b) Determined by ^{1}H NMR using 2,4-dinitrotoluene as the internal standard. c) Isolated by flash chromatography.*

Then, it was noticeable that the addition of a methyl or bromine substituent on the R_3 position of aziridine, bearing an EWG as R_1, did not affect the reaction productivity (table 4, entries 3, 5 and 6). On the contrary, the addition of a bulkier moiety, as in the case of aziridine **9**, caused a slight decrease of selectivity and yield.

The simultaneous presence of two EWGs, such as 3,5-$(CF_3)_2C_6H_3$ and C_6F_5, was responsible for a slight decrease of the reaction productivity (table 4, entry 7). On the other hand, it is important to note that when EWG and electron donating groups (EDG) are both present on the two different phenyl rings, the reaction productivity improved compared with that of the previous case (table 4, entry 8). In fact, when aziridine **17** was reacted, 92% of conversion with 86% of selectivity was observed with a 91:9 regioisomeric ratio by favoring the formation of oxazolidinone **18a**. The obtained data suggested that the C-N bond may be polarized by the presence of two groups with opposite electronic characteristics and this event could help the aziridine opening through the cleavage of the C-N bond. It seems that it is not important on which phenyl ring EWG and EDG are located to induce the bond polarization. Moreover, this can explain the decrease of reaction productivity noted for the reaction described in entry 7 of table 4. Thus, when any R_3 substituent is present and R_1 is an EWG, the aziridine conversions and oxazolidinone yield increased due to the bond polarization. This suggestion is in accordance with the reduction of the reaction productivity that was observed when EDG substituted aziridines **19** and **21** were reacted (table 4, entries 9 and 10).

It is interesting to note that the presence of halide substituents reduced the reaction productivity, oxazolidinone **26** was obtained with 72% of yield (table 4, entry 12) and the bromine substituted was isolated with the moderate yield of 50% (table 4, entry 11).

The position of the substituent on the phenyl ring also plays an important role in the reaction. In fact, when the nitro group was moved from the *para* position with respect the nitrogen atom to the *ortho* one, the selectivity decreased to 60% yield, but the obtained regioisomeric ratio **28a**/**28b** of oxazolidinone resulted 64:36 (entry 13, table 4). An even worse result was obtained by reacting aziridine **29** with carbon dioxide: only traces of the desired oxazolidinone were detected between many not-isolated side-products due to the very low registered selectivity.

Then, even if the aziridine bearing on the nitrogen atom a 3,5-dichloro substituted phenyl ring was efficiently converted (table 4, entry 15), the reaction between aziridine **32** and CO_2 produced only 30% yield of oxazolidinone **33** (a/b ratio = 76:24). Despite the complete aziridine conversion, a plethora of non-characterized side-products was detected. This behavior may be caused by the poor solubility of the dinitro substituted aziridine that may disfavor the reaction with carbon dioxide.

Then, the study of the reactivity of di-substituted aziridines revealed that the presence of a further substituent on the three-membered heterocycle has a negative effect (table 4, entries 17 and 18). The reaction of substrates **34** and **36** occurred with low conversion and selectivity and, accordingly with data reported above, the presence of an EWGs improved the reaction productivity and oxazolidinones **35** and **37** were isolated in 52% and 28% yield, respectively.

In all the reactions reported in table 4, regioisomer a was the favorite one to point out that the ring opening event is always favored on the more substituted carbon atom. This hypothesis was supported by the lack of reactivity of the aziridine **38** towards carbon dioxide probably due to the too high steric hindrance on the carbon bearing the phenyl group. Despite the complete conversion of the substrate, no oxazolidinone was formed and among many side-products formed, the only one that was isolated and characterized was the corresponding allyl amine, as reported in scheme 24.

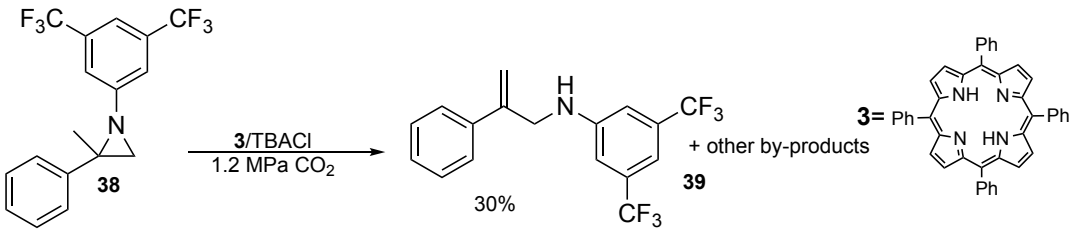

Scheme 24: *Reaction performed in a steel autoclave with the following conditions: 1.5 M N-aryl aziridine solution in THF for 8 h with **3**/TBACl/aziridine = 1:5:100 at 125 °C and 1.2 MPa of CO_2.*

5. Tandem procedure for oxazolidinones synthesis

Starting from Professor Gallo's group expertise in the synthesis of aziridines from alkenes and aryl azides, a tandem procedure was developed to improve the reaction sustainability. The first step of the reaction consisted in the preparation of *N*-aryl aziridines *via* a nitrene transfer reaction from aryl azides to styrenes catalyzed by Ru(TPP)(CO) **40**.[267] The aziridination yield was determined by ^{1}H NMR by using 2,4-dinitrotoluene as the internal standard after the evaporation of the reaction solvent and low-boiling unreacted liquid alkenes such as styrene. At this point, the reaction mixture was solubilized in THF, transferred in a steel autoclave, and reacted with carbon dioxide after adding the catalytic **3**/TBACl system.

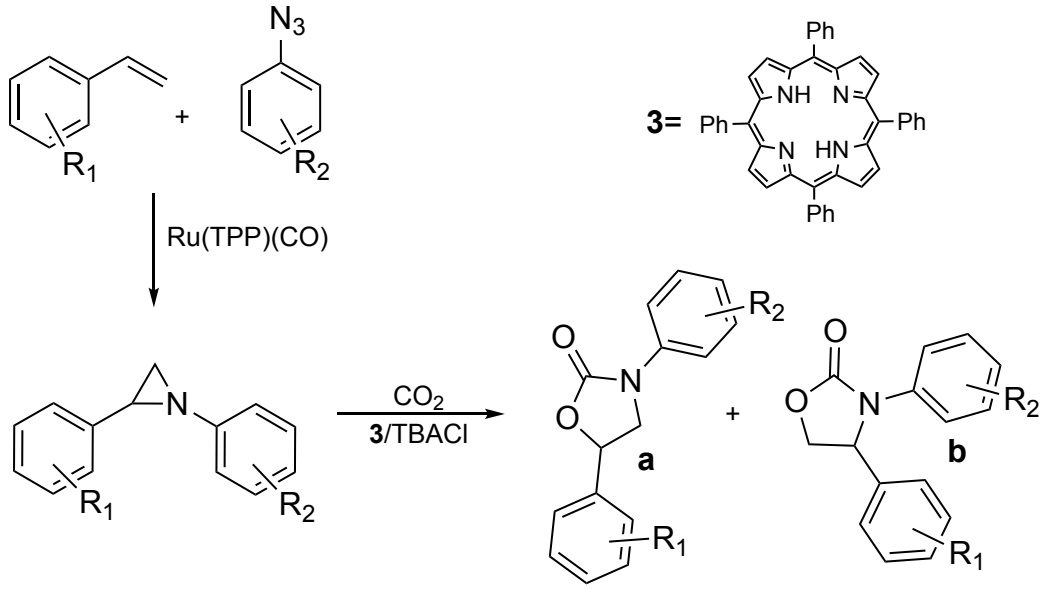

Scheme 25: *tandem procedure for the preparation of oxazolidinones from styrenes, aryl azides and carbon dioxide.*

To study the applicability of this tandem procedure three different oxazolidinones were prepared. Compounds **4a**/**4b** and **20a**/**20b** were formed by reacting the corresponding aziridines with CO_2 in order to investigate opposite reactivities. As reported in table 5, the first oxazolidinone was obtained in more than 99% yield while the second in only 18%. Furthermore, the study of these two syntheses allows understanding the eventual

influence of unreacted species formed during the first step of the tandem reaction on the second step of the process. In fact, the preparation of aziridines **2** and **19** are the most and the worst effective among those reported in the reaction scope, while **2** was obtained in 99% of yield, aziridine **19** was formed in the moderate yield of 65%. As reported in figure 21, the presence of unreacted material did not influence the oxazolidinone formation and the tandem reaction produced the two desired products with yields and regioselectivities were very similar to those obtained by starting from the purified aziridine to underline the effectiveness of this new protocol.

It is important to highlight that the catalyst of the first step, **Ru(TPP)CO**, did not have any influence on the reaction between aziridine and carbon dioxide as well as the presence of unreacted azide. These results underlined the stability and activity of the reported catalytic system.

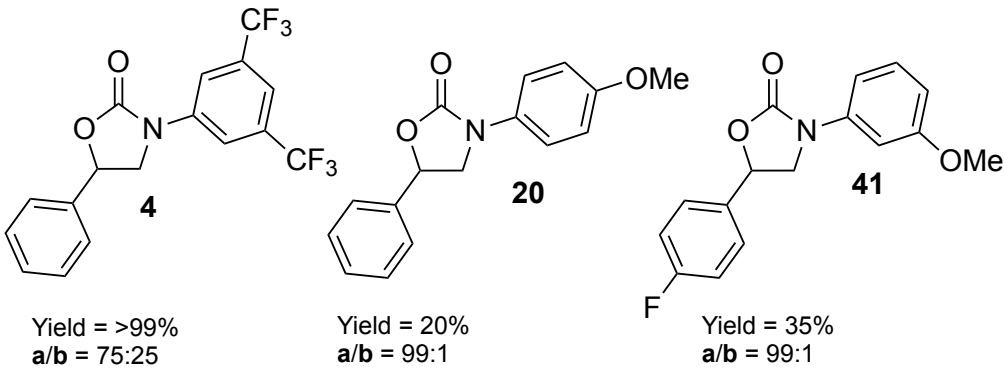

Figure 21: *oxazolidinones produced by the tandem methodology.*

Another important result obtained by using this tandem protocol is the production of compound **41** as the only regioisomer. This molecule is a Δ-5 desaturase (D5D) inhibitor, a potent anti-inflammatory[268] and even if the obtained yield was not very high (35%), this result is worth of mention because of the high *in vitro* activity of this compound and the lower yield that was reported for the previous synthesis starting from the epoxide (3-4%).[268]

The reported tandem reaction is the first one reported for the synthesis of *N*-aryl oxazolidinones starting directly from alkenes and carbon dioxide and it is an interesting synthetic procedure because **Ru(TPP)(CO)** did not affect the carbon dioxide cycloaddition

to aziridine, the styrene, or other low-boiling alkenes, may be easily eliminated during the purification step and the eventual residue of aril azide did not compromise the oxazolidinone production. This protocol presents different features of green chemistry: a) it is possible to avoid the purification of intermediate by applying the tandem methodology; b) the starting reagents are cheap and easy to obtain; c) the catalytic system is cheap and stable; d) carbon dioxide is exploited as one of the reagents; e) the only reaction by-product is benign molecular nitrogen; f) the atom economy of the reaction is very high.

6. Mechanistic insight

In collaboration with Dr. Gabriele Manca of the ICCCOM-CNR of Sesto Fiorentino, the reaction mechanism was investigated by DFT studies. Previous research about the cycloaddition of carbon dioxide to *N*-alkyl aziridines has been devoted to understanding the role of metal centers.[74,102,261] It is important to note that the mechanism of the uncatalyzed[104,269] reaction was also studied and theoretical investigations showed an energy barrier of almost 50 kcal/mol for the aziridine conversion.

The first goal of the theoretical studies was clarifying the porphyrin role in the reaction. The modelling of the interaction between $TPPH_2$ and the other reaction components revealed that **3** may accommodate the cation of the ammonium salt forming the adduct **A1**. The result of these interactions is the activation of the halide anion that is more prone to attack the aziridine for allowing the ring-opening reaction. The formation of this adduct is exergonic by -7.5 kcal/mol.

Then the comparison between the reaction of **2** with **A1** or TBACl alone, forming respectively adducts **A2** and **A3,** underlined the beneficial role of the porphyrin. While the formation of **A2** is exergonic by -8.4 kcal/mol, **A3** was achieved by an endergonic transformation.

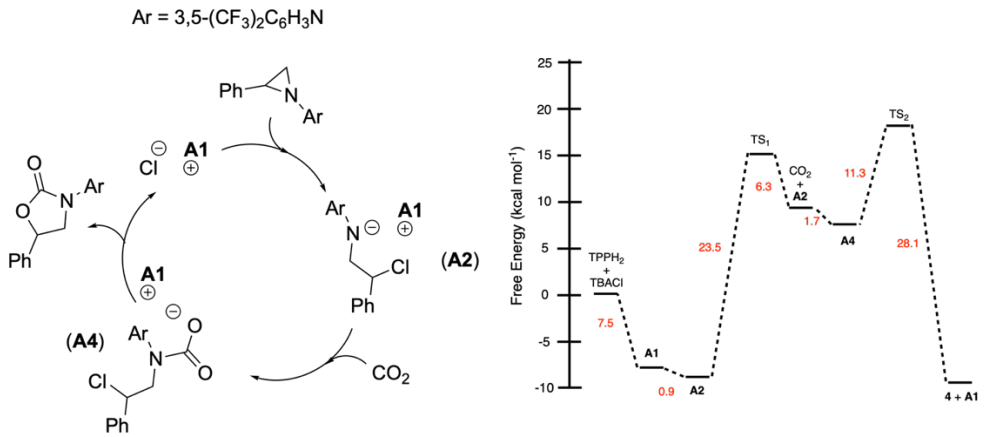

Scheme 26: *proposed mechanism and energy profile for the cycloaddition of carbon dioxide to N-aryl aziridines catalyzed by the system $TPPH_2$/TBACl.*

The proposed mechanism (scheme 26) shows the initial attack of the chloride anion, which was activated by the formation of the **A1** adduct, to the aziridine ring at the more encumbered carbon. A free energy barrier of +23.5 kcal/mol, which is the highest of the catalytic cycle and corresponds to the formation of TS_1, represents the rate determining step (RDS) and it is associated with the ring-opening process. The so-formed opened aziridine can activate carbon dioxide through an interaction between the negatively charged nitrogen atom and the electron deficient carbon atom of the CO_2 molecule forming **A4**. At this point, the negatively charged oxygen atom is responsible for the ring-closing step, which produces the desired oxazolidinone and the initial adduct **A1**, which can start a new catalytic cycle. The whole process occurs with a free energy gain of -2.2 kcal/mol that is consistent with similar reported processes.[102] It is important to note that the highest energy barrier encountered in the reaction catalyzed by the system **3**/TBACl (23.5 kcal/mol) is much lower than the 50 kcal/mol reported for the uncatalyzed reaction.

7. Enlarging the reaction scope

After the study of the catalytic system applied to the conversion of *N*-aryl aziridines, a new study was performed to extend the applicability of the protocol. The **3**/TBACl catalytic system was applied to the conversion of *N*-alkyl aziridines into the corresponding oxazolidinones.

Initially, aziridine **2** and 1-^{n}butyl-2-phenyl aziridine **42** were reacted with carbon dioxide. These two model reactions were used to compare the reactivity of the two classes of aziridines by testing, in combination with TBACl, the catalytic activity of several porphyrins to study the influence of the steric and electronic characteristic of the catalyst on the reaction productivity.

The syntheses of oxazolidinones **4** and 3-butyl-5-phenyl-oxazalidin-2-one **43** were performed in the reduced time of 3 h and 1 h, respectively. These short reaction times were applied in order to magnify the differences arisen from the reactivity of the used catalytic systems without flatten them. In fact, when the two reactions were run for longer time, the complete aziridine conversion was observed in both cases and it was not possible to observe the difference in the porphyrin reactivity under the applied catalytic conditions.

Results reported in table 5 highlight the generally better reactivity of *N*-alkyl aziridines that were converted into corresponding oxazolidinones in higher yields and a/b regioselectivities with respect compounds deriving from *N*-aryl derivatives. The reaction productivity of the synthesis of compounds **43** was less dependent upon the nature of the porphyrin catalyst with respect the synthesis of **4** probably due to the intrinsic higher reactivity of aziridine **42** in this transformation with respect to aziridine **2**. While in the synthesis of oxazolidinone **4**, the best yield and regioselectivity was obtained by using the catalyst **3**, the preparation of **43** was efficiently catalyzed by *meso*-tetrakis(4-carboxyphenyl) porphyrin (4-COOHTPPH_2) **46**. The general trend is similar for both the aziridines tested. Even if electron rich porphyrins seem to be slightly better catalysts for the carbon dioxide cycloaddition to aziridines, acquired data revealed that the presence of either EDG or EWG on the *meso* position of the porphyrin ring (porphyrins **44** and **45**, entries 2 and 3, table 5) poorly influenced reaction yields. In addition, electronic

differences of applied catalysts had a very limited effect on the a/b regioselectivity. On the contrary, the steric encumbrance of the porphyrin plays a more important role, as suggested by the low productivity that was observed in the presence of 5-(pentafluorophenyl)-10,15,20-triphenyl porphyrin (F_5TPPH_2) **47** (entry 5, table 5).

Table 5: *catalytic tests of different porphyrin/TBACl catalytic systems.*

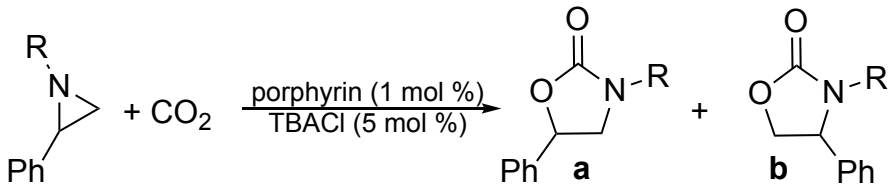

4: R = 3,5-$(CF_3)_2C_6H_3$ **43**: R = ^{n}Butyl

Entry	Porphyrin	Yield **4** (%)[b]	**4a**/**4b** ratio[b]	Yield **43** (%)[b]	**43a**/**43b** ratio[b]
1	**3** $TPPH_2$	95	87:13	95[c]	95:5
2	**44** 4-^{t}BuTPPH_2	69	83:17	94[c]	91:9
3	**45** 4-CF_3TPPH_2	61	85:15	80[c]	92:8
4	**46** 4-COOHTPPH_2	84	86:14	99[c]	86:14
5	**47** F_5TPPH_2	69	87:13	76[c]	88:12
6	**48** $F_{20}TPPH_2$	43	84:16	74[c]	89:11
7	**49** $OEPH_2$	63	84:16	85[c]	93:7

a) Reaction performed in a steel autoclave with the following conditions: 1.5 M aziridine solution in THF for 3 h with porphyrin/TBACl/aziridine = 1:5:100 at 125 °C and 1.2 MPa of CO_2. b) Determined by ^{1}H NMR using 2,4-dinitrotoluene as the internal standard. c) Reaction stopped after 1 h.

The worsening effect of bulky porphyrins on the catalytic activity is well evident when the catalyst *meso*-tetrakis(4-pentafluorophenyl) porphyrin ($F_{20}TPPH_2$) **48**, which bears onto the porphyrinic skeleton four pentafluorophenyl moieties instead of only one, was used. This effect is more evident in the case of the synthesis of aziridine **2** probably due to the higher encumbrance of the phenyl ring compared to that of alkyl substituent on the aziridine nitrogen atom. Utilizing octaethylporphyrin ($OEPH_2$) **49**, which has no *meso* functionalization but shows ethyl groups on *ß*-pyrrolic positions, the reaction productivity

decreases too. In conclusion, reported data indicated that the porphyrin steric and electronic characteristic did not greatly influence the reaction outcome.

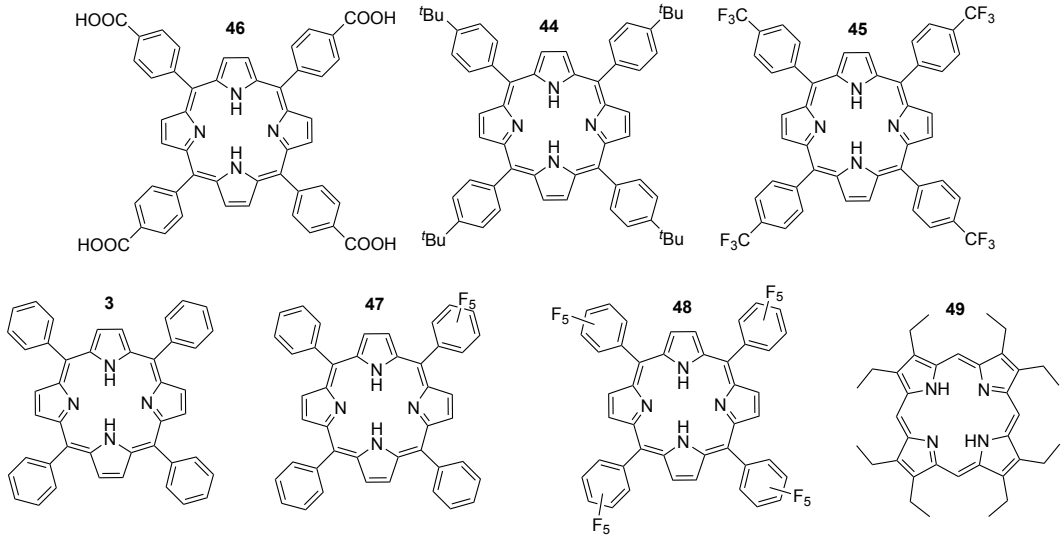

Figure 22: *porphyrins utilized in the reactivity study.*

The catalytic role of the porphyrin was confirmed by running the synthesis of oxazolidinones **4** and **43** in the presence of the sole TBACl and by applying the reaction conditions reported in table 6. In these cases, the products were obtained in 54% and 80% of yield, respectively.

Considering catalytic data and the commercial availability at low costs of $TPPH_2$, this catalyst must be considered the most convenient promoter and, to further enhance its catalytic activity, it was tested in the presence of other ammonium salts as the co-catalyst. Porphyrin **3** was tested alongside tetrabutyl ammonium bromide (TBAB) and tetrabutyl ammonium iodide (TBAI) and the combinations $TPPH_2$/TBAB and $TPPH_2$/TBAI produced after 1 hour compound **43** with 27% and 42% yield, respectively. In view of achieved data, tetrabutyl ammonium chloride was confirmed as the best salt to utilize in this transformation.

Taking into account the obtained results, the catalytic **3**/TBACl system was selected to study the cycloaddition reaction of carbon dioxide to several *N*-alkyl aziridines.

Chart 2: *cycloaddition of carbon dioxide to N-alkyl aziridines.*

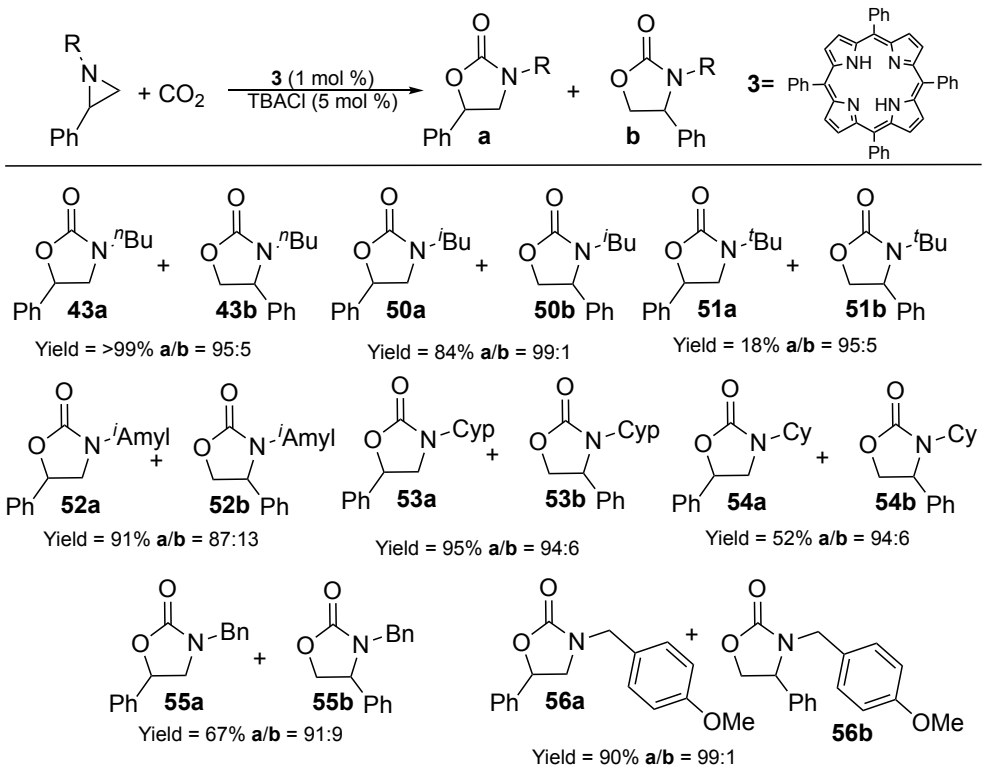

*Reaction performed in a steel autoclave with the following conditions: 1.5 M aziridine solution in THF for 6 h with **3**/TBACl/aziridine = 1:5:100 at 125 °C and 1.2 MPa of CO_2. Yields and a/b ratios determined by ^{1}H NMR using 2,4-dinitrotoluene as the internal standard.*

The products reported in chart 2 were obtained by running the reactions for 6 hours to magnify the catalytic performances even with less reactive substrates. It is important to underline that the regioisomeric ratio is not affected by reaction time, as suggested by the same **43a**/**43b** ratio that was obtained by reacting aziridine for 1 or 6 hours (see table 5, entry 1 and chart 2).

As already stated above, the steric encumbrance on the nitrogen atom determines the reaction productivity. In fact, compounds **43**, **50**, and **51** were formed in >99%, 84% and 18% yield and the decrease of the reaction productivity was ascribed to the increase of the bulkiness on the nitrogen substituent. In addition, the enlargement of the alkyl chain improved the reaction productivity due to the presence of a CH_2 spacer before the chain ramification that reduce the steric hindrance around the nitrogen atom (compare products

50 and **52** in chart 2). The same trend was observed in the case of cyclic alkyl substituent, as shown for the synthesis of products **53** and **54** that have been obtained in 95% and 52% yields, respectively. It is interesting to note that the steric hindrance did not impact on the reaction regioselectivity. The reaction of *N*-benzylic aziridines with carbon dioxide produced compounds **55** and **56** in 67% and 91% yields, respectively and in both cases a very good regioselectivity was observed probably due to the presence of the -CH_2- spacer between the phenyl group and the nitrogen atom of the aziridine.

It is worth mentioning that in all the cases reported in chart 2, oxazolidinones were formed with a 100% of selectivity.

In collaboration with Dr. Gabriele Manca, the cycloaddition reaction of carbon dioxide to *N*-alkyl aziridines was investigated by the DFT studies and it resulted to be very similar to that already described for *N*-aryl aziridines in scheme **26**. Only little energy differences were calculated by modeling aziridine **42** as the starting material. It is interesting to highlight that the ring-opening reaction requires more energy in this latter case because the resulting opened intermediate does not efficiently stabilize the negative charge on the nitrogen atom and this destabilization guarantees an efficient carbon dioxide activation with the following ring-closing step. *N*-butyl oxazolidinone was achieved with an overall energy gain of -4.7 kcal/mol, that is higher than that one calculated for the synthesis of oxazolidinone **4** in accordance with the general higher reactivity of *N*-alkyl aziridines with respect to *N*-aryl aziridines. The overall gain is granted by the very convenient ring-closing reaction step.

In order to study the influence of the porphyrin structure on the reaction productivity, different porphyrins were modelled in combination with TBACl and the energy demand of the formation of adducts with the ammonium salt confirmed the low influence of the porphyrin structure on the reaction productivity. The different obtained adducts were formed with energy profiles very similar to that observed in the formation of the **A1** adduct.

Aziridine **42** was also reacted in the presence of porphyrin **57** to investigate a possible asymmetric version of the carbon dioxide cycloaddition reaction. This catalyst was chosen in view of the good result obtained by using this ligand for the synthesis of chiral iron complexes that was very active in olefin cyclopropanations.[270,271]

The reaction was run for 15 h at 1.2 MPa of CO_2 and 50 °C in the presence of a **57**/TBACl/**42** ratio = 1:10:100 and a racemic mixture of **43** in 99% yield and **43a**/**43b** = 90:10 was produced, confirming the general difficulty to perform stereoselective ring-opening processes. Thus, in the future, it would be necessary to investigate the transformation of enantiopure aziridines into the corresponding oxazolidinones to use the reported procedure for the synthesis of enantiopure products.

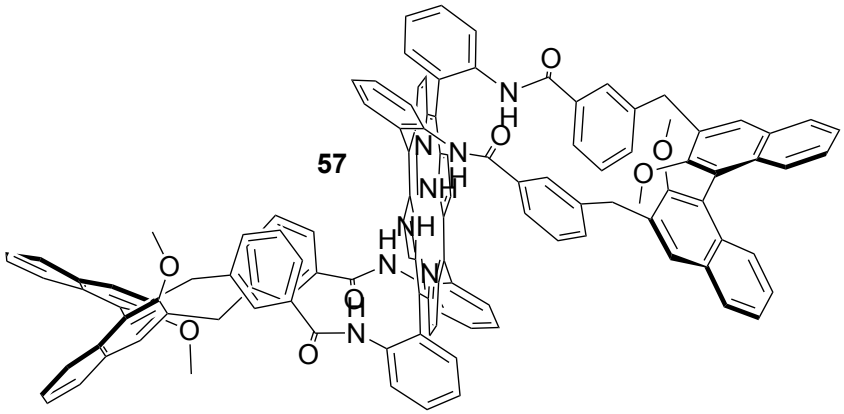

Figure 23: *porphyrin* ***57****.*

8. Synthesis and catalytic activity of a bifunctional catalyst

In view of the excellent result obtained by using porphyrin-based bifunctional catalysts in the cycloaddition reaction of carbon dioxide to epoxides producing cyclic carbonates,[168,272,273] we decided to synthesize a bifunctional organic catalyst bearing the ammonium salt onto the porphyrin skeleton.

We prepared the new porphyrin catalyst starting from compound **48**. One pentafluorophenyl rings was replaced by an aromatic moiety which bears on one *ortho* position a brominated alkyl chain. The so-obtained A_3B porphyrin, prepared by applying a classic Lindsey's procedure, was further modified by reacting it with tributyl amine and KCl to afford catalyst **58** (scheme 27).

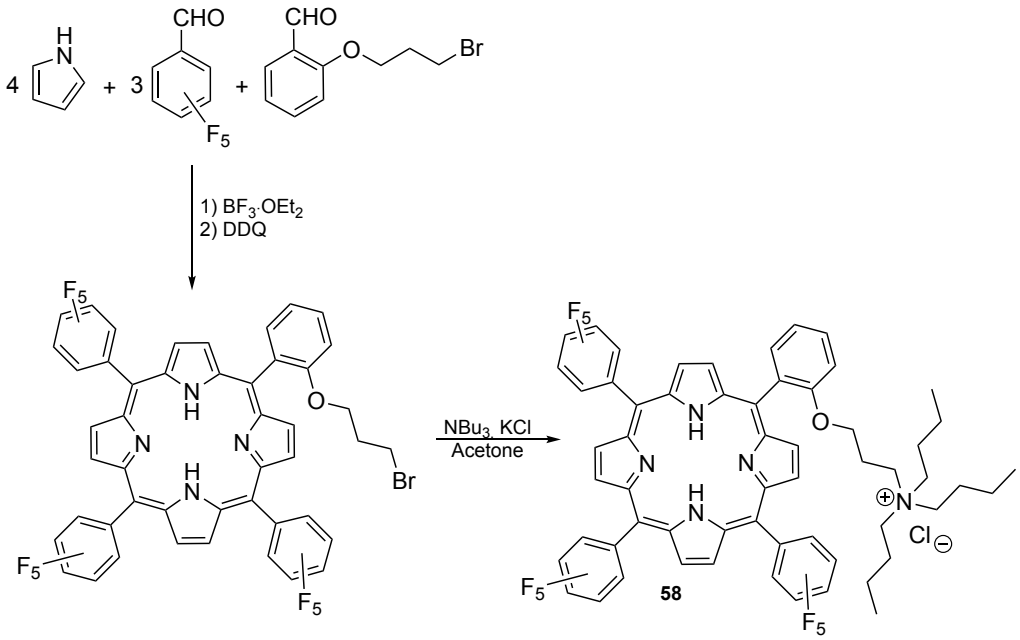

***Scheme 27**: synthesis of catalyst **58**.*

Catalyst **58** displays a good mobility of the ammonium arm due to the three -CH_2- group of the linker and consequently the catalyst may adapt its shape to the incoming substrate during the reaction.

$F_{20}TPPH_2$ was chosen for the preparation of the new bifunctional catalyst because its poor activity, when used in combination with TBACl (entry 6, table 5), allows better

understanding any positive catalytic effect deriving from the introduction of the ammonium salt on the porphyrin skeleton.

Catalyst **58** promoted the formation of the desired oxazolidinone in only 49% of yield with the **43a**/**43b** ratio of 99:1. This reaction was less productive than that performed by employing the catalytic **48**/TBACl system (1:5:100 ratio), which yielded **43** in 74% of yield with a regioisomeric ratio of 89:11. In both cases 1.5 M solution of the corresponding aziridine solution in THF was reacted for 3 h at 125 °C and 1.2 MPa of CO_2. This underwhelming result may be the consequence of an insufficient loading of ammonium salt since when using the binary system, the anion concentration is five time higher than that of the porphyrin.

The low reactivity of the bifunctional porphyrin was confirmed by DFT studies. As in the case of binary catalytic systems, the adduct formed by the interaction of the cation with the porphyrin core must interact with the incoming aziridine to favor the ring-opening step. In the case of the bifunctional porphyrin, the interaction between the adduct and the aziridine produces an energy demanding intermediate (+9.7 kcal/mol) that makes the nucleophilic attack difficult. Considering the experimental and computational results obtained, the mechanism was not investigated further.

9. Carbon dioxide cycloaddition to epoxides

In view of the good activity showed by the **3**/TBACl system in the conversion of aziridines into oxazolidinones, the protocol was also applied to the cycloaddition of CO_2 to epoxides. In order to optimize experimental conditions, the model reaction between CO_2 and styrene oxide (SO) **59** was investigated and since oxiranes are more reactive then aziridines, the reaction was run by testing lower catalyst/co-catalyst loadings (table 6) by keeping the reaction conditions studied for the synthesis of oxazolidinones.

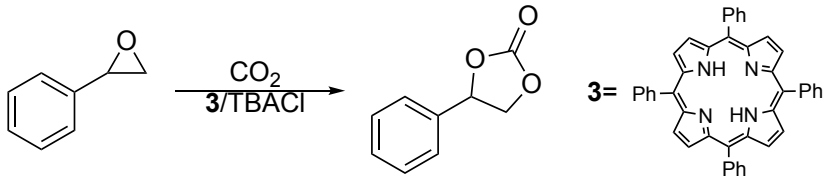

Scheme 28: *synthesis of styrene carbonate.*

Table 6: *study of the catalyst and co-catalyst loading reacting SO with carbon dioxide.*

Entry	**3** (mol%)	TBACl (mol%)	TON[b]	TOF[b] (h^{-1})	Yield[c]
1	1	5	99	25	>99
2	0.1	0.5	792	200	80
3	0.01	0.05	3300	660	33

*a) Reaction performed in a steel autoclave for 4 h at 125°C and 1.2 MPa of CO_2 in solvent free condition. b) Referred to **3**. c) Determined by ^1H NMR utilizing mesitylene as internal standard.*

We decided to use the **3**/TBACl/SO ratio of 1:5:10000 for the following studies because, despite the moderate yield that was observed, this catalytic ratio was responsible for very high TON and TOF values. In addition, the sustainability of this protocol was enhanced by working under solvent-free conditions.

The model reaction was performed several times keeping fixed temperature (125 °C), pressure (1.2 MPa) and the **3**/TBACl/SO ratio (1:5:10000) to identify that 2 h was the most convenient reaction time to maximize the catalytic performance. If the reaction was run

for longer times a decrease of the product yield was observed probably due to a catalyst deactivation.

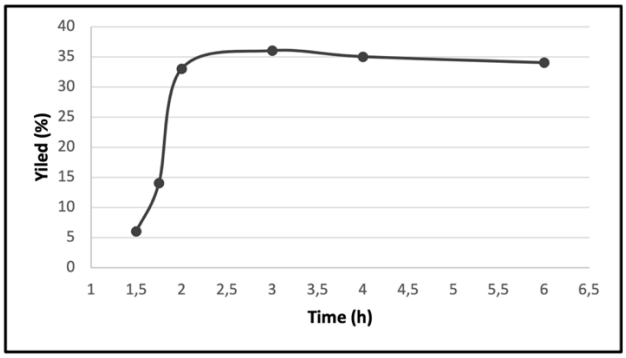

Entry	Time (h)	Yield (%)
1	1.5	6
2	1.75	14
3	2.0	33
4	3.0	36
5	4.0	35
6	6.0	34

Figure 24: *reaction time optimization.*

Then, the temperature effect on the reaction productivity was investigated by reacting SO with carbon dioxide for 1.5 h at 1.2 MPa of CO_2 and **3**/TBACl/SO ratio 1:5:10000 under solvent free conditions. The reaction was run for 1.5 h in order to better understand the effect of the temperature before reaching the plateau.

From gathered data is it possible to conclude that at 125 °C only traces of the desired product were formed and that the best productivity was reached at 150 °C. Then, at higher temperatures the reaction yield decreased.

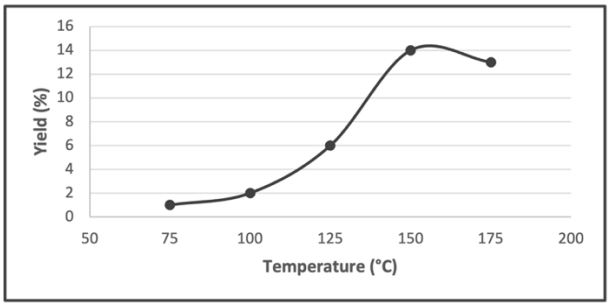

Entry	Temperature (°C)	Yield (%)
1	75	1
2	100	2
3	125	6
4	150	14
5	175	13

Figure 25: *temperature optimization.*

Once the temperature was optimized, the ratio between porphyrin and TBACl was fine-tuned by keeping the ammonium salt concentration at 0.05 mol% and increasing the concentration of **3** each time. Five different reactions were run at 125 °C and 1.2 MPa of carbon dioxide for 1.5 h in order to magnify the effect of the porphyrin concentration on

the reaction productivity. As reported in figure 26, the yield increased by increasing the porphyrin concentration up to the 1:1 $TPPH_2$/TBACl ratio.

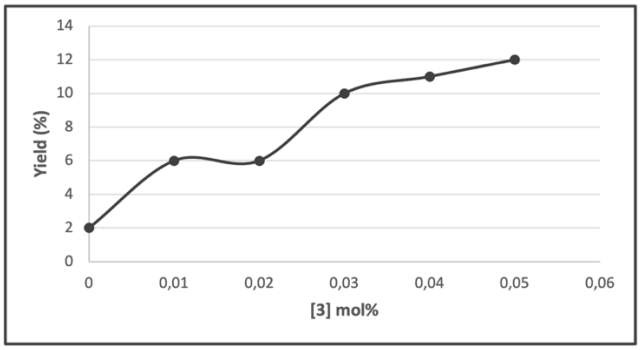

Entry	**3** (mol%)	Yield (%)
1	0	2
2	0.01	6
3	0.02	6
4	0.03	10
5	0.04	11
6	0.05	12

***Figure 26**: Influence of the amount of **3** on the yield of styrene carbonate.*

Finally, the dependence of the reaction productivity on the carbon dioxide pressure was studied performing five reactions at different pressures by fixing the other parameters as 150 °C, 1.0 h, catalyst/co-catalyst/ratio = 1:1:2000.

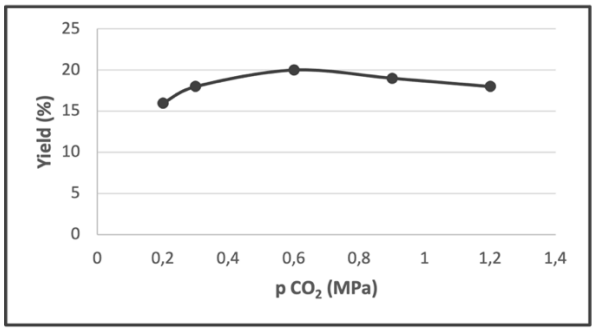

Entry	**p CO_2** (MPa)	Yield (%)
1	0.2	16
2	0.3	18
3	0.6	20
4	0.9	19
5	1.2	18

***Figure 27**: pressure optimization.*

The reduced yields reported for high pressure values (0.9 and 1.2 MPa) could be attributed to the decrease of epoxide concentration in the liquid phase.[78] Since the reaction takes place in this phase, the enhance of the carbon dioxide pressure produced a rise of the gas concentration in the liquid phase with a contemporary decrease of the substrate concentration.

The best reaction conditions identified above were used to study the reactivity of different ammonium salts in order to understand the influence of the halide anion on the reaction productivity.

Table 7: *influence of TBAX on the cycloaddition reaction of carbon dioxide to SO.*

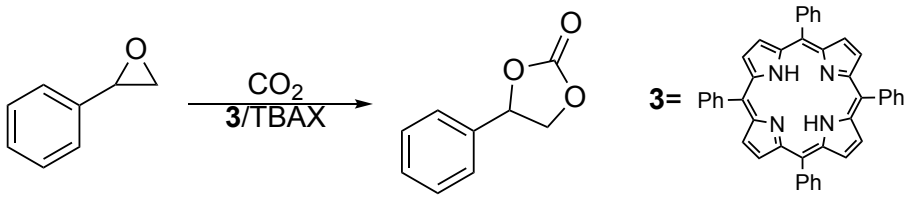

Entry	Porphyrin	TBAX	Yield (%)	TOF (h^{-1})
1	/	/	0	/
2	**3**	/	0	/
3	/	TBACl	11	228
4	**3**	TBACl	20	416
5	**3**	TBAB	14	291
6	**3**	TBAI	9	187

Solvent-free reactions were run for 1.0 h in a steel autoclave by using 0.250 mL of SO, at 150 °C, 0.6 MPa of CO_2 and $TPPH_2$/TBAX/SO = 5:5:10000. Yields were measured by ^1H NMR using mesitylene as the internal standard.

Then, using the optimized condition and the catalytic $TPPH_2$/TBACl system, the reaction scope was investigated by testing different epoxides with carbon dioxide.

Six of these reactions were performed using both 0.250 mL or 5.0 ml of substrate in order to verify if it is possible to use this methodology in a large scale for further process developments.

Even if the yields reported in chart 3 are quite low, the turnover numbers (TON) and turnover frequencies (TOF) values were very high for a full organic catalyst, which allow working in a metal-free conditions. The studied catalytic system was active in the conversion of terminal and mono substituted epoxides. As expected, epichlorohydrin, among the employed oxiranes, was very efficiently converted confirming its high reactivity towards CO_2. Compounds **60** and **61** were obtained in similar yields while the production of compounds **63** and **64** was less efficient (chart 3). These results underlined that steric factor did not strongly influence the conversion of terminal epoxides into the corresponding cyclic carbonate and epoxides bearing alkylic chain with different length gave similar results. On the other hand, electron-poor epoxides were better converted into

corresponding cyclic carbonates because they are more susceptible to the nucleophilic attack of the anion.

Chart 3: *synthesis of cyclic carbonates catalyzed by the system **3**/TBACl.*

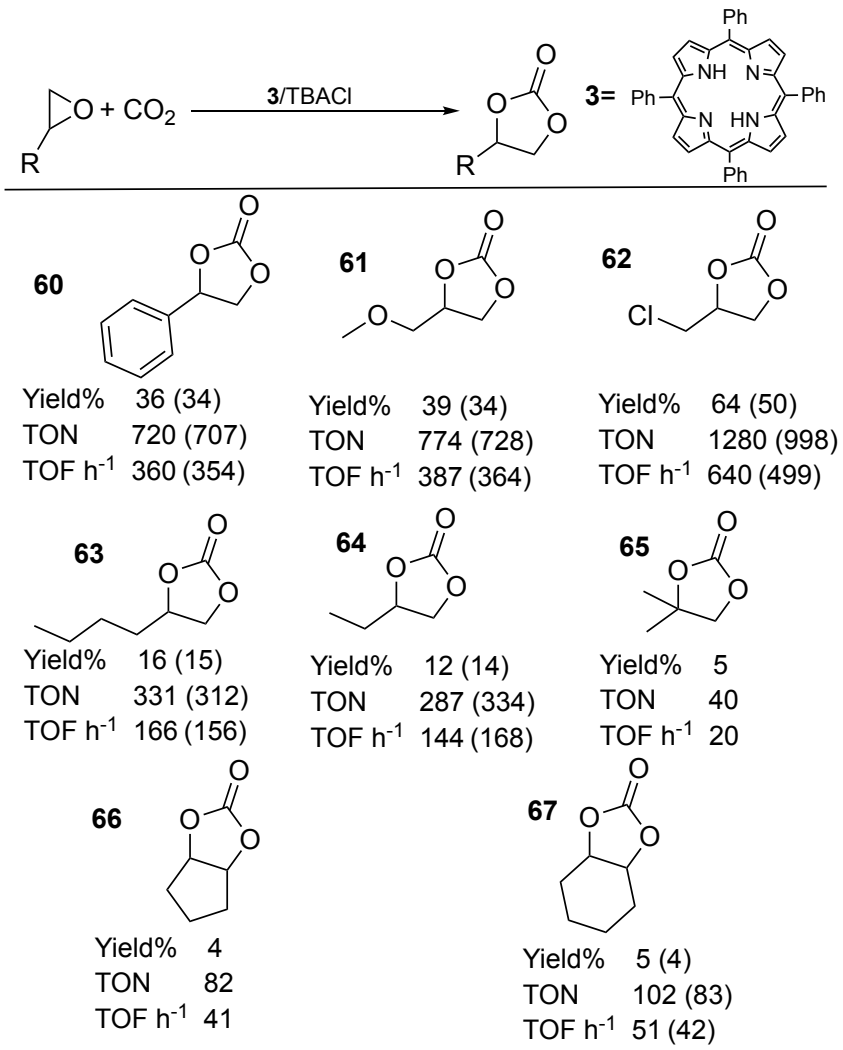

Solvent-free reactions were run for 2.0 h by using 0.250 mL of epoxide at 150 °C, 0.6 MPa and $TPPH_2$/TBACl/epoxide = 5:5:10000 in a steel autoclave. Values in parentheses are obtained with 5.0 mL of epoxide. Yields determined by ^1H NMR using mesitylene as the internal standard.

The presence of quaternary carbon on the epoxide ring provoked a drastic decrease of the performances as stated by the synthesis of product **65** that was obtained in 5% of yield only. Bicyclic epoxides were almost unreactive in the presence of this catalytic system and

compounds **66** and **67** were formed in very low yields probably also because this last class of substrates is more prone to form polycarbonates than cyclic carbonates.

In conclusion, we can state that the catalytic system **3**/TBACl demonstrated good activity in the cycloaddition reaction of carbon dioxide to epoxides even at low catalytic loadings and especially terminal epoxides were successfully converted into corresponding cyclic carbonates.

10. Conclusions

In the previous chapter a new metal-free catalytic system active in the carbon dioxide cycloaddition to three membered heterocycles was presented. The organic nature of the two components, *meso*-tetraphenyl porphyrin and tetrabutyl ammonium chloride, improves the sustainability of the reaction avoiding the presence of any metal in the reaction medium. Additionally, carbon dioxide is a benign reactant and an important waste to convert to a new use. In addition, the porphyrin utilized is not toxic, it is cheap, stable, and also very active. All these features make the reported synthesis of oxazolidinones and cyclic carbonates a green process worth of study.

After the initial optimization of the reaction conditions and the test of the activity of different porphyrins and salts, the best identified combination was employed to promote the reaction of three different classes of substrates. The reaction of epoxides with CO_2 was run under solvent-free conditions, the catalytic system was active at low catalytic loadings and very good TON and TOF values were obtained. Among the substrates tested in the reaction, terminal epoxides were the most active.

The reaction between *N*-alkyl aziridines and carbon dioxide gave interesting results since the catalytic system displayed a good activity by promoting the CO_2 cycloaddition to different substrates. In this case the steric hindrance on the nitrogen atom was the factor that effected the most the catalytic performances. The more the substituent on the nitrogen atom was bulky, the lower was the yield obtained. With this class of substrates, a chiral porphyrin and a bifunctional catalyst were also tested, unfortunately with unsatisfactory results in both cases. Either a racemic product was obtained and the use of a porphyrin bearing the ammonium salt moiety worsened the catalytic productivity.

The most interesting goal achieved by using the $TPPH_2$/TBACl catalytic system was the successful conversion of 19 different *N*-aryl aziridines with yields up to 99% and regioisomeric ratio up to 99:1. This result represents the first general methodology to convert this class of heterocycles to the corresponding oxazolidinones.

The performed study allowed understanding the influence of the different experimental conditions on the reaction productivity. Then, a tandem protocol of the synthesis of

oxazolidinones from alkenes, aryl azides and carbon dioxide was tested. In this reaction the aziridine was formed *in situ* and converted into corresponding oxazolidinone without being purified. In addition, neither the catalyst Ru(TPP)CO nor eventual unreacted starting materials affected the carbon dioxide cycloaddition. Exploiting this methodology 3-(3-methoxyphenyl)-5-(4-fluorophenyl)oxazolidin-2-one was prepared, this oxazolidinone is a potent D5D-inhibitor used for its anti-inflammatory properties.

In collaboration with Dr. Gabriele Manca, a reaction mechanism was proposed underlining the role of the porphyrin in the catalytic system. $TPPH_2$ activates the ammonium salt through the formation of an adduct which improves the activity of the chloride anion in the ring-opening reaction. The DFT calculations highlighted that the studied system halved the free energy barrier of the reaction with respect to the uncatalyzed one.

On the basis of these results, we performed the heterogenization of the porphyrin to improve the sustainability of the reaction, as described in the following section.

Chapter III: Heterogeneous catalysts for the CO_2 cycloaddition reaction

1. SBA-15 supported porphyrin

After the good results obtained with the homogeneous catalytic $TPPH_2$/TBACl system, the heterogenization of the homogeneous catalyst was undertaken to improve the reaction sustainability by combining the advantages of homogeneous and heterogeneous catalytic processes. The activity of the homogenous catalyst was preserved, and, at the same time, an easy catalyst recovery and product purification were possible. Once again, the reaction between *N*-aryl aziridines and carbon dioxide was not studied, then the good activity demonstrated by the catalytic system proposed in the previous chapter paved the way to a possible application in heterogeneous conditions.

The design of the new hybrid organic-inorganic catalyst was performed by considering the textural and structural properties of the host matrix, which must display pores large enough to accommodate the bulky porphyrin molecule. Santa Barbara amorphous materials (SBA) are ideal for this purpose due to the possibility to prepare mesoporous silicas with large surface areas and pore sizes tunable in the range from 2 to 50 nm.[205,206,274] SBA silicas are often functionalized by grafting methods with a plethora of different functional groups. Moreover, as mentioned in the introduction, silica-based materials may improve the reactivity of epoxides towards CO_2 by a hydrogen bond activation, thanks to the presence of hydroxy groups on its surface.[207–209]

Starting from the studies of Dufaud's group, only the porphyrin was linked to the silica matrix and the ammonium salt was solubilized in the reaction medium because it is well known that its activity decreased when linked onto the surface. The chloride anion interacts with silanols through hydrogen bonding which decrease its nucleofilicity.[226] On the contrary, linking a compound that enhances the reactivity of the halide anion towards the ring opening reaction gave good results.[227]

Starting from these considerations, we decided to support **3** onto SBA-15 silica by covalent bonding instead of applying non-covalent approaches such as entrapment, ion pair formation or adsorption. Indeed, it was possible to obtain a tight support of the porphyrin onto the material thanks to a covalent bond, which is more solid in comparison to other interactions and guarantees a high stability of the material obtained. The pathway selected

was a two steps procedure that included a final alkyne-azide cycloaddition between an azide-functionalized SBA-15 silica and an ethynyl-functionalized porphyrin. Thus, it was necessary to initially prepare these two compounds as follows.

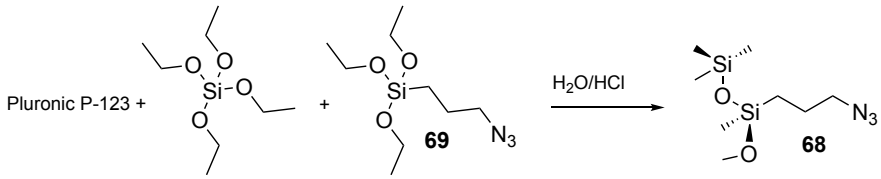

Scheme 29: *preparation of compound* ***68****.*

The first step consisted in the preparation of the azidopropyl-functionalized SBA-15 (N_3@SBA-15) material **68** by a direct co-condensation of 3-azidopropyltriethoxysilane **69**, and tetraethoxysilane (TEOS), as reported in scheme 29. During the preparation of compound **68** pluronic P-123 was used as a templating polymer in acidic aqueous solution. Pluronic P-123 is a linear symmetric copolymer formed by three blocks in alternated fashion PEO-PPO-PEO (PEO = polyethylene oxide, PPO = polypropylene oxide).

This one-pot route for the introduction of azido groups was chosen over the post-grafting method in order to guarantee a better homogeneous distribution of the functional groups. In this way, a high local concentration of silanols can be maintained and they may be exploited for the activation of epoxides. For the same reason 0.2 mmol/g was selected as azide loading as it corresponds to site isolation. The obtained material was fully characterized, and the obtained data will be reported later for the confrontation with the final heterogeneous catalyst.

Then, (5-(4-(3-methyl-3-hydroxybut-1-yn-1yl)phenyl)-10,15,20-triphenylporphyrin) was prepared through a classic Adler-Longo's procedure by refluxing the two aldehydes and pyrrole in propionic acid. Then, the ethynyl moiety was readily deprotected by refluxing the porphyrin with KOH in toluene, following the retro-Favorskij procedure[275] and obtaining (5-(4-ethynylphenyl)-10,15,20-triphenylporphyrin) ($EtTPPH_2$). Finally, the so-obtained porphyrin was reacted with $Zn(OAc)_2{\cdot}2H_2O$ in a 65:35 mixture of chloroform and methanol and the desired metal complex Zn(5-(4-ethynylphenyl)-10,15,20-triphenylporphyrin) **70** was obtained (scheme 30).

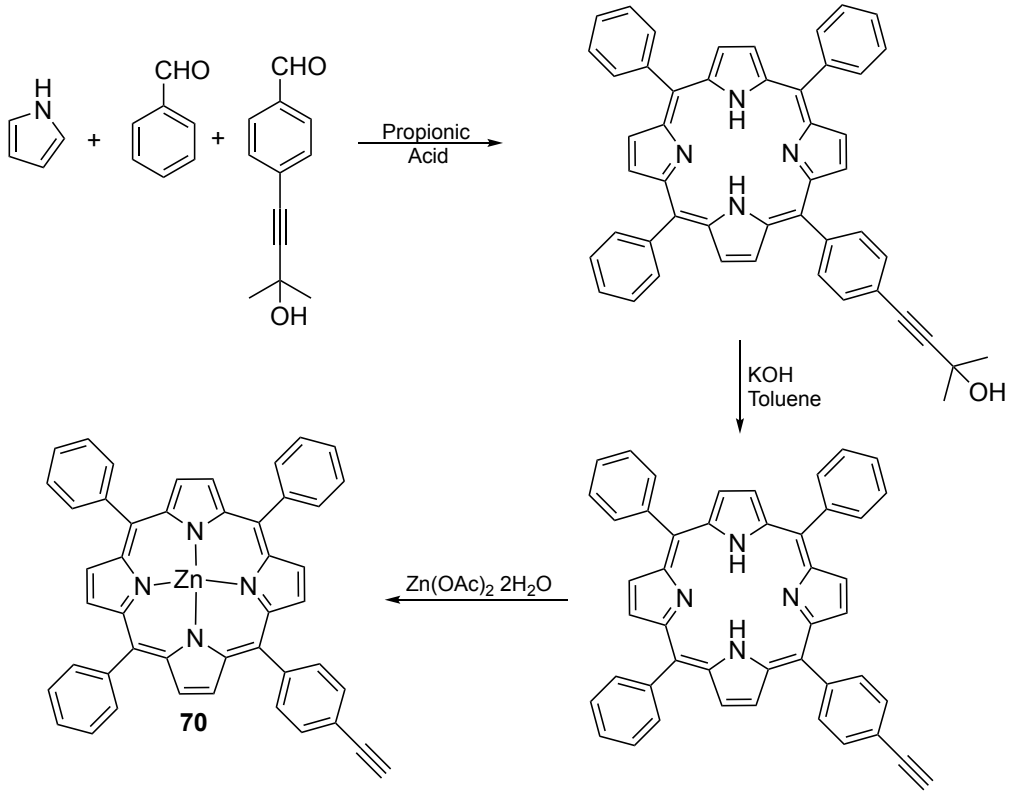

Scheme 30: *synthetic procedure for the preparation of complex* ***70****.*

The complexation of porphyrin with zinc was necessary to proceed with the next alkyne-azide cycloaddition and avoid that the copper catalyst, utilized to promote the "click reaction", can interact with a free-base porphyrin forming Cu-complexes. After the isolation of the desired product, the treatment with a slightly acidic water solution was sufficient to remove the zinc atom from the tetrapyrrolic core and restore the free-base porphyrin.

Then, the last step for the synthesis of the heterogeneous catalyst was the "click reaction". As reported in scheme 31, we followed the classic protocol exploiting the reactivity of copper iodide and triethylamine to synthesize $ZnTPPH_2$@SBA-15. After the reaction, *N*,*N*-diethyldithiocarbamate sodium trihydrate was used to remove the copper catalyst and the excess of porphyrin was recovered. Then, washing the obtained material with slight acidic water and then with water until the neutrality, compound **71** ($TPPH_2$@SBA-15) was isolated.

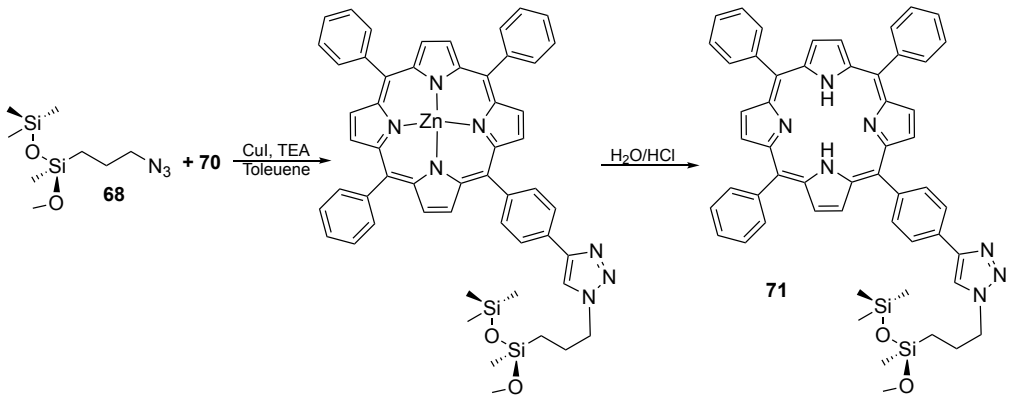

Scheme 31: *Synthesis of material* ***71****.*

UV-Vis analyses were performed to verify the success of the procedure to remove zinc, and the collected spectra are reported in figure 28. Not only the performed analyses indicated that the porphyrin was successfully loaded onto the SBA-15 silica, but also that the zinc removal was effective. Indeed, comparing the spectrum on the left with that one in the center of figure 28, the presence of the same absorption bands was evident. In both spectra the Soret band at 417 nm at the four Q-bands between 500 and 600 nm were visible.

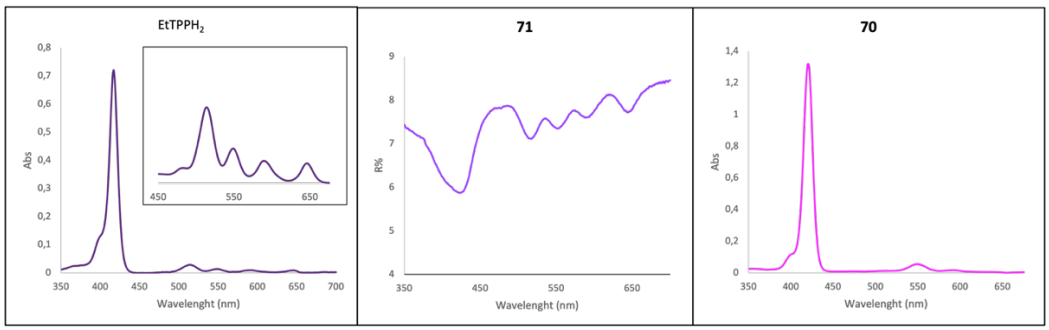

Figure 28: *Liquid (left) and solid (center) UV-Vis spectra of* ***EtTPPH$_2$*** *and* ***71****, respectively. On the right liquid UV-Vis spectrum of compound* ***70*** *for comparison.*

Moreover, the presence of four Q-bands was characteristic of free-base. The slight shift of the Soret band, observed passing from the liquid spectrum of $EtTPPH_2$ (417 nm) to the solid one of compounds **71** (424-nm), could be due to the silica local environment as well as the transformation of the simple alkyne, in the *meso* position of the porphyrin, into the triazole

group linked to the silica surface.[276] In addition, the presence of four Q-bands and not just two, as in the spectrum of metalated compound **70**, confirmed the efficiency of the acidic treatment for the complete Zn removal after the "click" procedure.

Both the hybrid material **68** and **71** were fully characterized with different bulk and molecular techniques not only to investigate textural and structural properties, but also to verify the integrity of the precursor structure.

The diffractograms obtained by small angle powder XRD of both the hybrid materials are reported in figure 29 where the typical profile characteristic of hexagonal mesophases is evident for both solid.

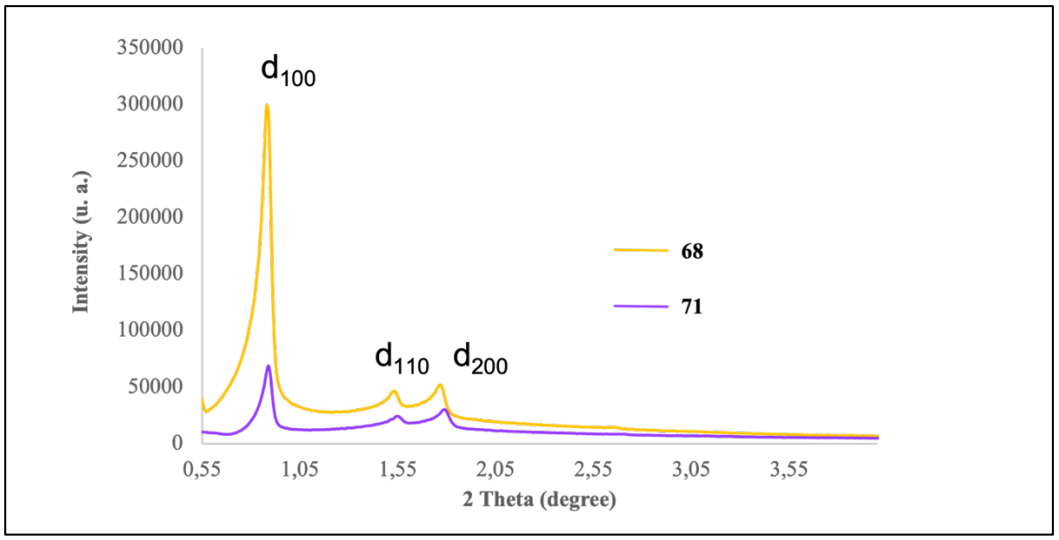

Figure 29: *X-ray powder diffraction patterns of* ***68*** *and* ***71****.*

The presence of the three peaks that correspond to (100), (110) and (200) reflections are well resolved and the unit-cell parameter a_0 did not change to indicate that the porphyrin loading did not worsen the structural long-range ordering of the solid. The decrease of d_{100} intensity after the porphyrin linking was evident and it can be caused by a reduction of the local order introduced by the presence of the porphyrin and/or to a contrast matching between the amorphous silicate framework and the bulky porphyrin that is present in its channels.

In table 8 other collected data from small angle powder XRD and nitrogen sorption measurements are summarized.

Table 2: *XRD and nitrogen sorption derived data.*

	N_3@SBA-15	$TPPH_2$@SBA-15
Surface Area	559 m^2/g	479 m^2/g
Pore Volume[a]	0.76 cm^3/g	0.61 cm^3/g
BET Surface Area	581 cm^3/g	494 cm^3/g
C	95	131
Average Pore Diameter[b]	5.5 nm	5.6 nm
d_{100}[c]	99 Å	99 Å
a_0[d]	114 Å	114 Å
Wall Thickness[e]	59 Å	58 Å

a) Total pore volume at P/P0 = 0.973. b) Pore size from desorption branch applying the BJH pore analysis. c) d(100) spacing. d) a_0 = 2d(100)/√3, hexagonal lattice parameter calculated from XRD. e) Calculated by a_0 – pore size.

The nitrogen sorption/desorption isotherms showed a sharp inflexion in the pressure range between 0.5 and 0.8 P/P_0 for both solids even if a noticeable lowering of the nitrogen uptake was observable for material **71** (figure 30).

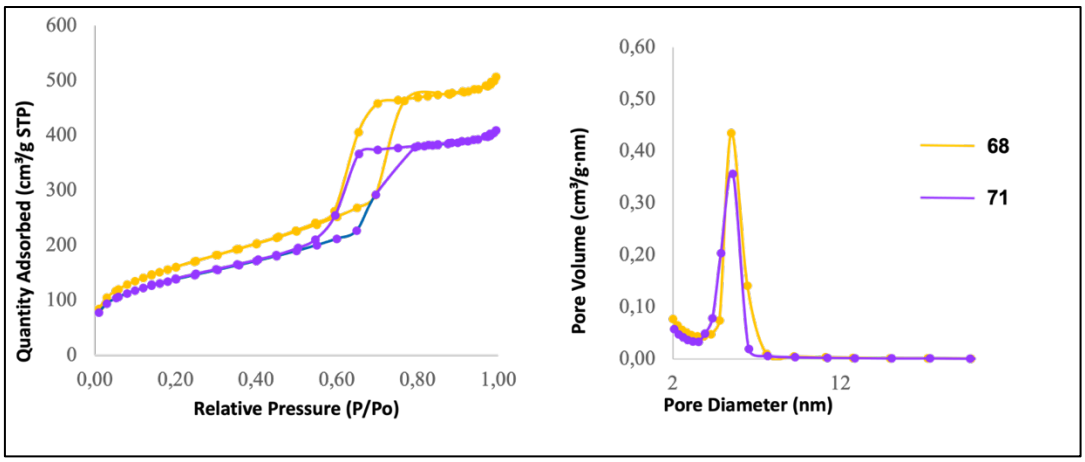

Figure 30: *Nitrogen adsorption/desorption isotherms (left) and pore size distributions (right)* ***68*** *and* ***71****.*

It is possible to ascribe this decrease to the presence of the porphyrin inside the pore channels and this is consistent with the decrease of BET surface area reported in table 11.

For both the prepared materials a fairly narrow pore diameter distribution was detected with an average of 5.5 nm. Another confirmation of the porphyrin loading was the enhanced hydrophobic character of the material, testified by the increase of the C value. Then, the formation of a covalent bond between the porphyrin and the azide functionality was confirmed by IR analyses (figure 31) performed on both the prepared materials. The intensity of the characteristic peak of the azide moiety (2290 cm^{-1}) decreased after the "click" reaction due to the reduction of azide moieties concentration for the formation of the triazole linker.

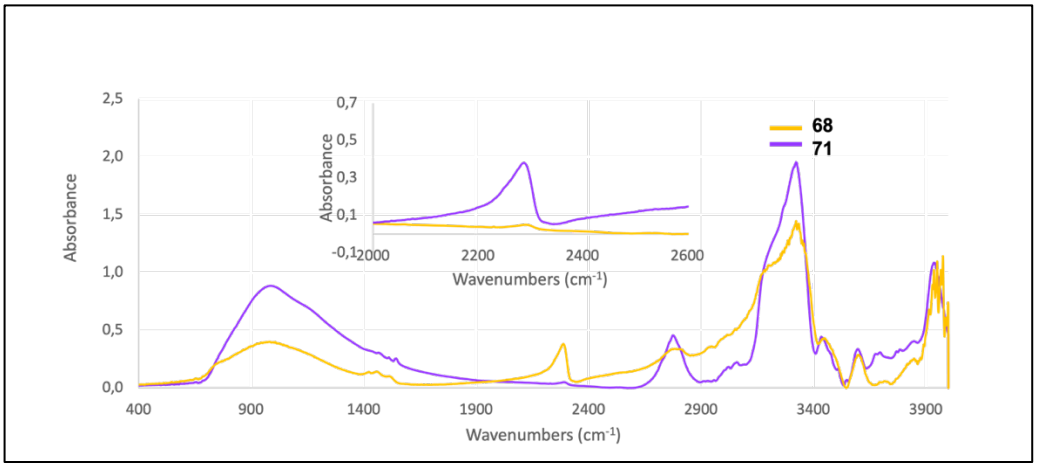

Figure 31: *FT-IR spectra of* ***68*** *and* ***71****.*

^{13}C CP/MAS NMR spectroscopy revealed the presence of peaks originating from the propyl chain in the 5-50 ppm range and those of the porphyrin in the aromatic region (figure 32). The NMR spectroscopic analysis of compound **71** revealed many signals in the region between 100 and 160 ppm and the pattern ascribed to the propyl group appeared different because of the environment variations due to the post-synthetic modifications. It should be noted that signals attributed to the templating polymer P-123 were still present in both spectra due to the washing procedure applied to material **68**. In order to completely remove the polymer from the compound it would be necessary to perform a Soxhlet extraction with ethanol. However, this procedure would produce ethoxy moieties from the silanols and the potential of silica in activating epoxide would be reduced. Thus, a milder

Soxhlet extraction with acetonitrile was applied, which cannot completely remove the P-123 from the silica channel as indicated by a decrease of P-123 NMR signals (figure 32).

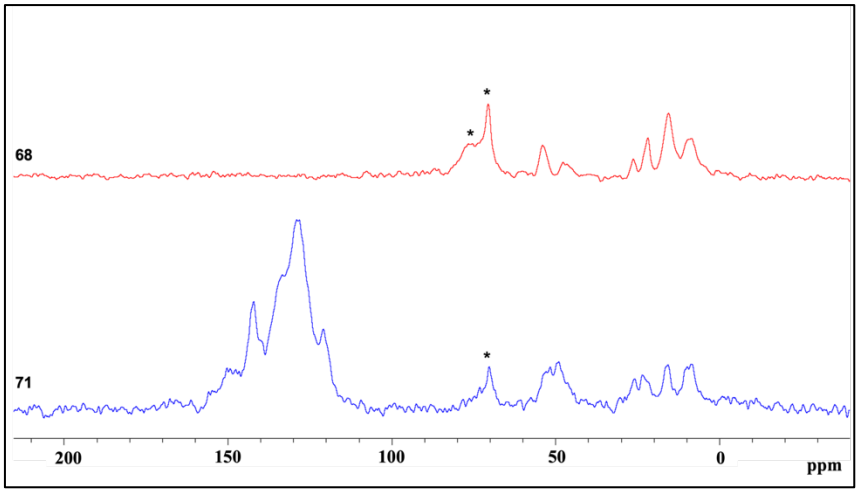

Figure 32: *^{13}C CP/MAS NMR **68** and **71** hybrid materials. * Signals for residual Pluronic P-123.*

It is to be noted that in both the spectra signals attributable to Q^2, Q^3 and Q^4 silicon sites of the silica frameworks from -90 to 110 ppm were visible (figure 33) to suggest that the "click reaction" did not affect the previous formed bonds and the porphyrin introduction has not produced significant changes in the material.

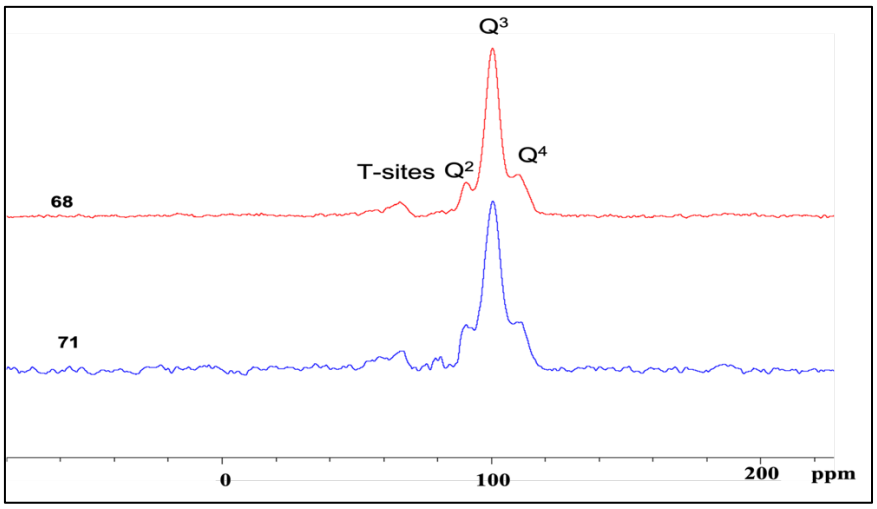

Figure 33*: CP MAS ^{29}Si NMR of **68** and **71**.*

Finally, the organic loading was determined by nitrogen elemental analysis, corrected from sample humidity that was derived from the SiO_2 content calculation by TGA analyses run at 1000 °C. The azidopropyl loading of **68** was calculated as 0.24 mmol/g of dry silica, while that one of **71** was 0.11 mmol/g of dry silica. This data indicated that the "click reaction" occurred in a 46% yield, which is an acceptable result for the preparation of an heterogenous material considering that the yield could be partially affected by the presence of P-123 in the SBA-15 pores.

2. Carbon dioxide cycloaddition to epoxides

The so-prepared heterogeneous catalyst **71** was tested in the carbon dioxide cycloaddition to styrene oxide in order to evaluate the catalytic efficiency of the porphyrin immobilized on the solid surface.

Table 9: *study of the activity of the heterogenous catalyst.*

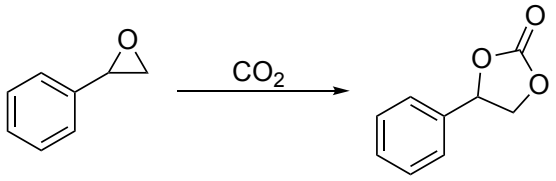

Entry	SBA-15 material	TBAX	Yield (%)	TON	TOF (h^{-1})
1	**71**	TBACl	6	118	59
2	**71**	TBAI	42 (28)[b]	832 (555)[b]	416 (555)[b]
3	**68**	TBAI	34 (15)[b]	674 (297)[b]	337 (297)[b]
4	**68 + 3**	TBAI	23	446	228
5	/	TBAI	15 (5)[b]	297 (99)[b]	148 (99)[b]
6	**68**	/	/	/	/

Reaction carried out in a steel autoclave in solvent-free condition for 2.0 h, at 150 °C, and 0.6 MPa of carbon dioxide with a catalyst/TBAX/SO ratio = 1:1:2000. Yields calculated by ^{1}H NMR using mesitylene as the internal standard. b) Reaction run for 1 h.

As reported in entry 1 of table 9, the reaction conditions applied for the catalytic system **3**/TBACl did not work well under heterogeneous conditions. The low yield detected by using TBACl as the co-catalyst can be due to the interaction between the ammonium salt and the silica material, silanols can reduce the chloride anion nucleophilicity through the formation of hydrogen bonds and the catalytic efficiency of the system drastically dropped.[209] Thus, TBAI was chosen as the partner of hybrid material **71** because the iodide anion is less prone to interact with silanols present on the surface of the solid support and the lack of formation of hydrogen bonds was responsible for a better reactivity (table 9, entry 2) with respect to that observed when TBACl was employed. This result indicated that

when silica-based material are utilized, TBAI is more active than TBACl that is more effective under homogenous conditions, as reported in chapter II.9.

The **71**/TBAI catalytic system was active in promoting the reaction of SO with carbon dioxide and the corresponding cyclic carbonate was formed in a better yield with respect to what obtained under homogeneous condition (42% *vs* 36%). The catalytic role of the porphyrin was confirmed by running a reaction in the presence of material **68** that, bearing only azide moieties, was less active than **71** (table 9, entry 3). Then, in order to understand if it is necessary to covalently link the porphyrin onto the silica support, $TPPH_2$ was simply added to the system **68**/TBAI and even worse result was obtained, underlining the catalytic activity of the heterogenized material (table 9, entry 4). To confirm the activity of the **71**/TBAI system, two other reactions were run by using either **68** or TBAI alone. While the azide-functionalized material was ineffective in the synthesis of styrene carbonate from SO and carbon dioxide, TBAI alone was responsible for the formation of the desired product in low yields to underline the catalytic role of the ammonium salt in the reaction. Finally, in order to better understand the effect of the porphyrin, three model reactions were run for only 1 hour in the presence of **71**/TBAI system, **68** and TBAI alone. As reported in table 9 (values in parenthesis), acquired data confirmed the good activity of the heterogeneous catalytic material both in terms of TOF and TON values.

Once the activity of the catalytic system **71**/TBAI was confirmed, the reaction scope was investigated by testing eight different epoxides and using the reaction conditions reported in chart 4. The general trends discussed in the previous chapter were confirmed also when the heterogeneous catalyst was used. Terminal epoxides were converted more easily than internal and disubstituted ones, which did not display any reactivity towards carbon dioxide under these catalytic conditions. It is reasonable that diffusion constraints play an important role and the lack of reactivity in the formation of products **65**, **66**, and **67** was due to the high steric hindrance of starting epoxide that is not compatible with the free space around the active site in the heterogeneous material. On the other hand, it is very interesting noting that the CO_2 cycloaddition to terminal epoxides was more efficient by using porphyrin-supported on silica as the promoter. Yields, TON and TOF values were higher than those obtained under homogenous conditions (see chapter II.9) to suggest an

active role of silanols that can activate epoxide *via* hydrogen bonding, producing a beneficial effect on the whole reactivity. Note that registered TON and TOF values by using this material were quite high for a metal-free heterogeneous catalyst.

Chart 4: *study of the reaction scope under heterogenous conditions.*

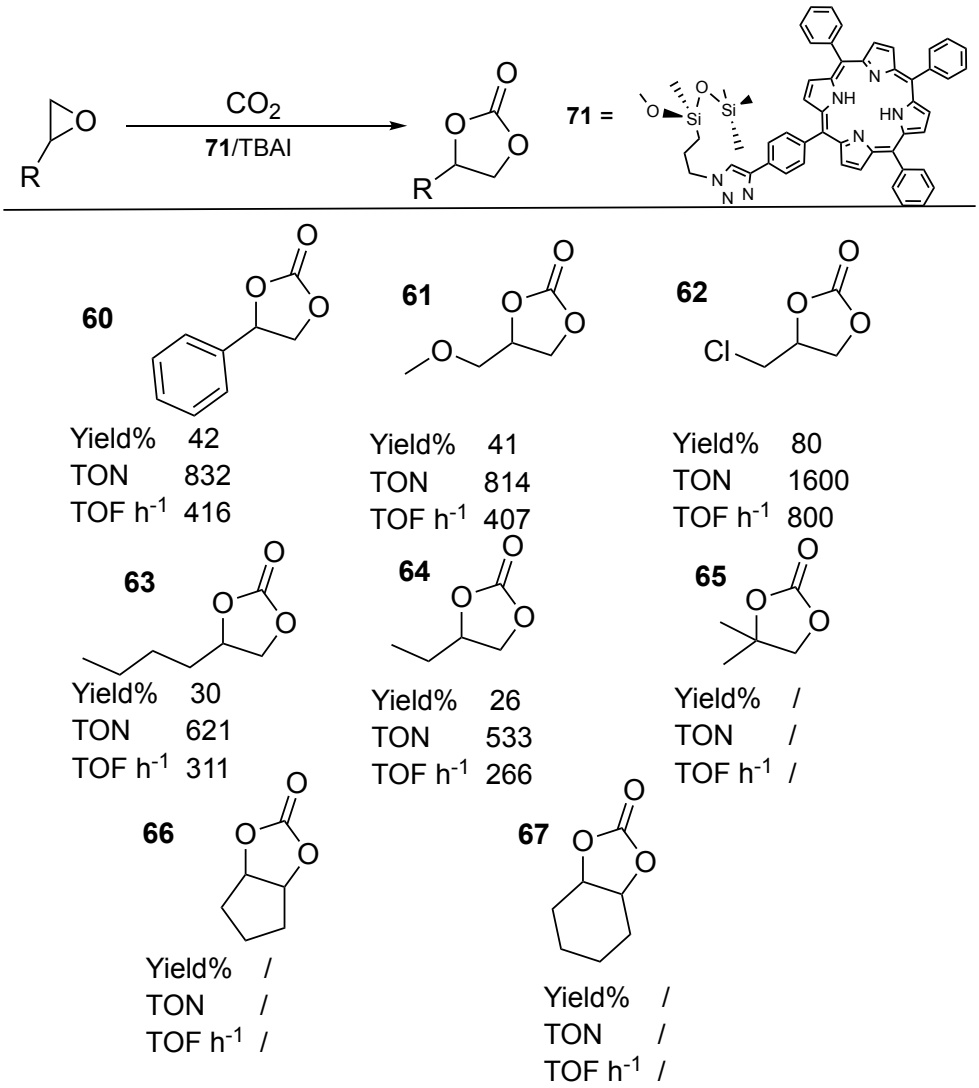

Reaction carried out in a steel autoclave in solvent-free condition for 2.0 h, at 150 °C, and 0.6 MPa of carbon dioxide with a ***71****/TBAI/epoxide ratio = 1:1:2000. Yields calculated by* ^{1}*H NMR using mesitylene as the internal standard.*

Considering that an advantage of using a heterogenous catalyst is the possibility to easily recover it, the recyclability of system **71** was investigated by performing three consecutive gram-scale cycloaddition reactions of carbon dioxide to styrene oxide. The three experiments produced styrene carbonate in 30%, 34% and 31% of yield, respectively. Even if a slight decrease of the yields was detected in all the three performed reactions, these results testified the recyclability and the chemical stability of the hybrid material. Between every reaction the only step needed to recover the catalyst was a simple filtration.

Then, a gram-scale reaction was also performed by utilizing **68**/TBAI system in order to verify one more time the effectiveness of the heterogenized catalyst. The obtained lower yield of 16% confirmed the role of the porphyrin in the carbon dioxide cycloaddition to epoxides.

After one catalytic cycle, the amount of porphyrin detected in solution by UV-Vis analyses was only 0.7% to indicate a low porphyrin leaching from the solid support. Considering that at this low concentration the porphyrin activity is negligible, it is possible to state that the synthesis of epoxides is only mediated by the heterogenized porphyrin.

Thus, it is possible to conclude that the use of **71**/TBAI catalytic system allowed an easy product purification and catalyst recovery and fostered the reactivity of epoxides towards carbon dioxide thanks to an active role of the solid support and the establishment of a very interesting silanols/porphyrin/TBAI synergic catalytic action.

3. Carbon dioxide cycloaddition to aziridines

In view of the good results obtained reacting epoxides and CO_2 in the presence of the heterogeneous **71**/TBAI catalyst, this hybrid material was also tested in the cycloaddition reaction of carbon dioxide to aziridines. First, the reactivity of *N*-alkyl substrates was analyzed exploiting as the model the reaction between carbon dioxide and 1-butyl-2-phenyl aziridine. Since aziridines are generally less reactive than epoxides,[67] the most effective catalytic loading to apply under heterogeneous conditions was identified by first running six reactions with six different catalyst/co-catalyst/substrate ratio under homogeneous conditions (table 10).

Table 10: *catalyst loading optimization.*

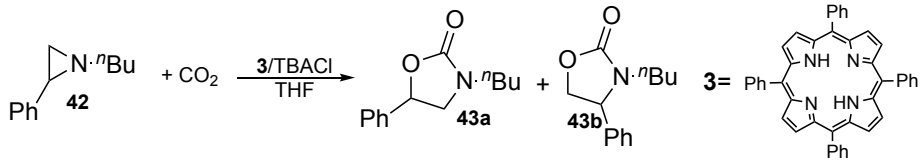

Entry	**3** (mol%)	TBACl (mol%)	Yield (%)	**43a/43b**
1	1.00	5.00	100	90/10
2	0.67	3.33	100	90/10
3	0.50	2.50	100	90/10
4	0.40	2.00	100	91/9
5	0.20	1.00	72	89/11
6	0.050	0.250	/	/

All reactions carried out with 1.5 M aziridine solution in THF in a steel autoclave at 125 °C and 1.2 MPa of CO_2 for 1 h. Yields obtained by NMR using 2,4-dinitrotoluene as internal standard.

The six performed reactions ranged from the conditions utilized in the aziridine study under homogeneous conditions (table 10, entry 1) to those applied in the carbon dioxide cycloaddition to epoxides (table 10, entry 6). The catalytic condition utilized with epoxides (entry 6) were not effective for the synthesis of oxazolidinones to confirm the minor reactivity of aziridines with respect that of oxiranes and the reaction was productive when at least the catalyst and co-catalyst loadings of 0.40 and 2.00 mol%, respectively were used.

It should be noted that while the sole TBAI can activate aziridines towards the formation of the five membered products (table 11, entry 4), the reaction did not proceed in the presence of the sole porphyrin, the hybrid material **71**, or the combination **68**/**3** (entries 1-3, table 11). These results underlined once again the importance of the ammonium salt in this class of reactions. When TBAI was utilized in combination with **68** a yield improvement was obtained with respect to the yield of the reaction performed by using TBAI alone to testify that silica operated synergistically with the ammonium salt also in the case of aziridines (entry 5, table 11). A further increase of the reaction yield was registered by substituting the azido-functionalized silica with **71**, demonstrating the positive porphyrin effect in the reaction outcome (table 11, entry 6).

Table 11: *study of the heterogeneous reaction.*

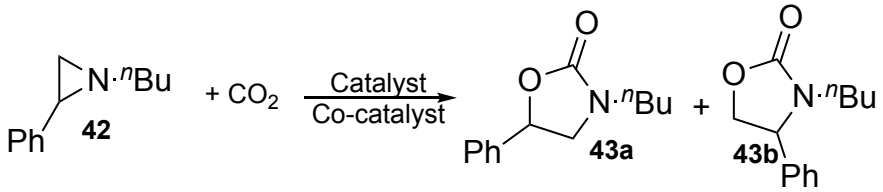

Entry	Catalyst	Co-catalyst	Time (h)	Yield (%)	**43a**/**43b**
1	**3**	/	1	/	/
2	**71**	/	1	/	/
3	**68**/**3**	/	1	/	/
4	/	TBAI	1	9	87/13
5	**68**	TBAI	1	17	90/10
6	**71**	TBAI	1	25	99/1
7	**3**	TBAI	1	42	98/2
8	/	TBACl	1	65	86/14
9	**71**	TBACl	1	20	98/2
10	/	TBAI	6	75	92/8
11	**71**	TBAI	6	95	97/3
12	**71**	TBACl	6	81	95/5

1.5 M aziridine solution in THF in a steel autoclave with catalyst/co-catalyst/aziridine ratio = 1:5:250 at 125 °C and 1.2 MPa of CO_2. Yields obtained by NMR using 2,4-dinitrotoluene as internal standard.

It is interesting to note that the use of **71**/TBAI was responsible for an improvement of both the yield and regioselectivity towards the formation of product **43a** (see entries 4-6 of table 11). In order to understand the difference between the activity of homogenous and heterogeneous catalysts, porphyrin **3** was tested in combination with TBAI instead with TBACl as usually performed under homogeneous conditions. Results of entry 7 (table 11) confirmed that TBAI was less active than TBACl under homogeneous conditions.

Contrarily to that observed in the reaction involving epoxides, the heterogeneous catalyst was less active than the homogeneous one in the CO_2 cycloaddition to *N*-alkyl aziridines. This can be due to a limited aziridine activation through hydrogen bonding from the silanols of the support also due to the higher steric hindrance on the nitrogen atom of the aziridine that limited the interaction with the surface.

In order to understand if TBACl can be deactivated by interacting with the silica matrix, TBACl alone and in combination with **71** was used to synthesize product **43** (entries 8 and 9, table 11). Acquired data indicated that the reaction activity of TBACl was reduced in presence of silica, since the reaction yields felt from 65% to 20% when instead using TBACl alone, a combination of TBACl with the porphyrin-supported silica was employed (compare entries 8 and 9 of table 11). However, the presence of porphyrin had a positive effect on the reaction regioselectivity. As already reported for the cycloaddition to epoxides, also in the reaction involving aziridines TBAI is the more efficient co-catalyst as revealed by the analysis of results reported in entries 10-12 of table 11. The catalytic combination **71**/TBAI was selected as the most efficient for the conversion of *N*-alkyl aziridines to oxazolidinones and used to study the scope of the reaction. These reaction conditions were tested on ten different substrates by running experiments first for 6 h, where only the most reactive substrates gave good results, and then the reaction time was extended to 16 h to improve the substrate conversion. The gathered data are summarized in table 12.

Prolonging the reaction time, very good results both in terms of yields and regioselectivities were obtained with almost all the tested substrates. Considering that the steric encumbrance on the nitrogen atom is the most important factor which determined the reaction productivity, different aziridines presenting different alkyl chains on the nitrogen atom were tested (entries 1-4, table 12).

Table 12: *study of the reaction scope under heterogenous conditions.*

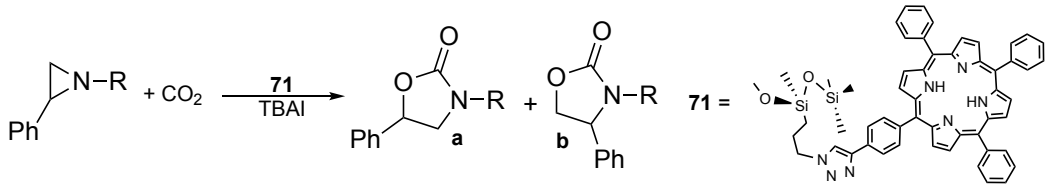

Entry	Aziridine	R	Yield (%)[a]	a/b ratio[a]
1	**42**	^{n}Butyl	100 (95)[b]	**43a**/**43b**=94/6 (97/3)[b]
2	**72**	^{i}Butyl	86 (28)[b]	**50a**/**50b**=99/1 (99/1)[b]
3	**73**	^{s}Butyl	34 (5)[b]	**74a**/**74b**=99/1 (99/1)[b]
4	**75**	^{t}Butyl	/	/
5	**76**	Cyclopenthyl	97 (34)[b]	**53a**/**53b**=99/1 (99/1)[b]
6	**77**	Cyclohexyl	42 (8)	**54a**/**54b**=99/1 (99/1)[b]
7	**78**	Methylcyclohexyl	95 (30)	**79a**/**79b**=99/1 (99/1)[b]
8	**80**	Benzyl	100 (42)	**55a**/**55b**=99/1 (99/1)[b]
9	**81**	4-Methoxy benzyl	100 (48)	**56a**/**56b**=99/1 (99/1)[b]
10	**82**	^{i}Amyl	100 (67)[b]	**43a**/**43b**=93/7 (94/6)[b]
11[c]	**42**	^{n}Butyl	88	**43a**/**43b**=93/7
12[d]	**42**	^{n}Butyl	100	**43a**/**43b**=93/7
13[e]	**42**	^{n}Butyl	100	**43a**/**43b**=94/6
14[f]	**42**	^{n}Butyl	100	**43a**/**43b**=94/6
15[g]	**42**	^{n}Butyl	100	**43a**/**43b**=93/7

*1.5 M aziridine solution in THF in a steel autoclave with **71**/TBAI/aziridine ratio = 1:5:250 at 125 °C and 1.2 MPa of CO_2 for 16h. a) Obtained by NMR using 2,4-dinitrotoluene as the internal standard. b) Reaction run for 6 h. c) Reaction performed under solvent-free condition in a steel autoclave with **71**/TBAI/aziridine ratio = 1:5:400 at 125°C and 1.2 MPa of CO_2. d) First catalyst recycle. e) Second catalyst recycle. f) Third catalyst recycle. g) Reaction performed with 1.0 g of substrate.*

Experimental results showed that augmenting the bulkiness of the substituent on the carbon atom directly bonded to the aziridine nitrogen atom, the reaction yield proportionally decreased. It is interesting to note that 1-^{t}butyl-2-phenyl **75** aziridine did not

evolve to the desired oxazolidinone in the presence of the heterogenous catalyst while, under homogenous conditions, the desired product was isolated in a low yield. These results underlined the importance of having free space around the catalytic site when working with SBA-15 silica to allow the reaction to proceed. Thus, it is possible to attribute the lack of reactivity of aziridine **75** to diffusion constraints as also supported by data acquired in the reaction involving substrates **78**, **80**-**82**. In these cases, a -CH_2- atom is directly bonded to the aziridine nitrogen atom and the presence of this spacer guaranteed a good reactivity when these substrates were reacted for a sufficient long time (entries 7-10, table 12). However, looking at data gathered after 6 h, it is possible to see that all these substrates are less reactive than aziridine **42**. The comparison between entries 2 and 10 (table 12) suggested that the relocation of the steric encumbrance on one carbon atom forward may be sufficient to drastically improve the reaction productivity (enhancement from 28 to 67% yield).

The reaction was also efficient with aziridine bearing cyclic alkyl group on the nitrogen atom. *N*-cyclopentyl substituted product was obtained with a much better yield than the one observed by reacting the *N*-cyclohexyl substituted one because the flatter character displayed by the cyclopentyl substituent, in comparison to that of the cyclohexyl one, allowed a better reactivity. This data was in accordance with the one registered under homogenous conditions indicating that the different nature of the two exploited catalysts did not influence the general trend of the aziridine reactivity. Note that the differences in the reaction performance in the synthesis of compounds **55a**/**55b** and **56a**/**56b** were less evident that in the case of the reactions performed under homogenous conditions. While the two compounds were formed with 67% and 90% yield, respectively by using **3**/TBACl system (chart 2) the reaction promoted by **71**/TBAI formed the two compounds with 42% and 48% yield. Probably, the positive effect of the methoxy group was reduced by the possible interactions between the methoxy group of the aziridine and the silanols present on the hybrid material surface.

It is important to underline that all the examined reactions up to now displayed an excellent selectivity (100%) and a very good regioisomeric ratio, up to 99/1 and never lower than 94/6.

The reaction between **42** and carbon dioxide was also tested under solvent free condition and despite the complete conversion of the substrate and the achieved 88% yield, this result was affected by a reduction of the selectivity (table 12, entry 11). This result could also be due to the variation of the reaction conditions because, to efficiently suspend the catalyst, it was necessary reducing the catalytic loading to 1/5/400. Even if the detected selectivity was slightly worse than the one obtained by working in THF as the reaction solvent, this result may be considered a starting point for further optimization of the protocol for working under solvent-free conditions with a consequent environmental improvement.

The catalyst recyclability was also tested performing four experiments with the same hybrid material (entries 1, 12-14, table 12). After every reaction, the SBA-15-based catalyst was simply filtered, washed with dichloromethane, and dried in the oven. All the reactions occurred with a complete substrate conversion, full selectivity in the desired product and the very good regioselectivity showed by the fresh catalyst was preserved as well.

Finally, the carbon dioxide cycloaddition to **42** was performed in a large scale by using 1.00 gram of substrate and with our delight, the reaction occurred with 100% of yield. The recyclability of the catalyst and its efficiency when working on a large scale testified the potential application for further process developments as a further scale-up or application under flow condition.

Pushed by the good results obtained reacting epoxides and *N*-alkyl aziridines with carbon dioxide, we tested the heterogenous system **71**/TBAI with the more challenging *N*-aryl aziridines as well. The cycloaddition of carbon dioxide to compound **2**, utilizing the same reaction conditions employed before with the **71**/TBAI/substrate ratio = 1:5:100, occurred with a very low selectivity towards the formation of the desired oxazolidinone despite the complete conversion of the starting aziridine observed. Fortunately, the simple replacement of TBAI with TBACl resulted in an enhancement of the catalytic efficiency and a complete conversion of **2** in the desired oxazolidinone was observed.

Thus, in order to better investigate the effect of TBAX in the synthesis of oxazolidinones catalyzed by **71**/TBAX system, compounds **42** and **2** were reacted with carbon dioxide in the presence of both TBACl and TBAI. As reported in figure 34, even if the reaction of **42**

with carbon dioxide performed well in the presence of both the ammonium salts, TBAI resulted more efficient than TBACl (figure 34, a) due to the deactivation of the chloride anion in the presence of silica material with unprotected silanols. On the contrary, observing the result obtained by reacting *N*-aryl aziridines with CO_2 in the reported conditions, it is possible to observe the decrease of the reaction selectivity when TBAI was employed. Considering that the halide reactivity is tightly bonded to many factors such as reaction conditions, substrates, catalyst, and many others,[277] it is necessary to better study the mechanism of this reactions to understand the difference in reactivity that was observed by using either TBAI or TBACl in the CO_2 cycloaddition to *N*-aryl aziridines. Up to now, it is only possible to hypothesize that the minor nucleophilicity of iodide is a more important factor than its good efficiency as leaving group and it is responsible for the observed decrease of the reaction performances.

TBACl

t (h)	Conv (%)	Sel (%)	Yield (%)
1	20	100	20
3	48	100	48
6	83	100	83
9	90	100	90
16	100	100	100

TBAI

t (h)	Conv (%)	Sel (%)	Yield (%)
1	25	100	25
3	77	100	77
6	95	100	95
9	100	100	100
16	100	100	100

TBACl

t (h)	Conv (%)	Sel (%)	Yield (%)
1	14	100	14
3	44	100	44
6	76	100	76
9	100	100	100
16	100	100	100

TBAI

t (h)	Conv (%)	Sel (%)	Yield (%)
1	9	90	8
3	53	51	27
6	60	45	27
9	96	27	26
16	100	20	20

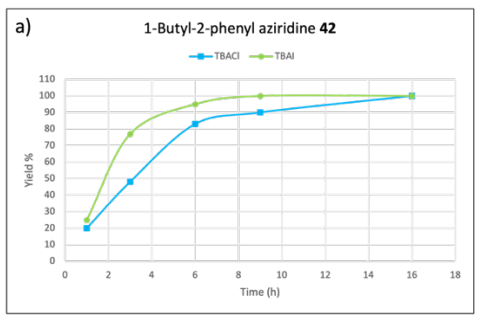

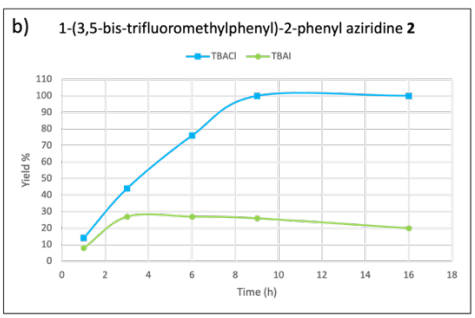

***Figure 34**: ammonium salt reactivity in the cycloaddition reaction of carbon dioxide to aziridines under heterogenous conditions. All the reactions were performed with the following conditions: 1.5 M aziridine solution in THF in a steel autoclave with **71**/TBAX/aziridine ratio = 1:5:250 for figure a) and = 1:5:100 for figure b) at 125 °C and 1.2 MPa of CO_2. Yields obtained by NMR by using 2,4-dinitrotoluene as the internal standard*

In view of previous results, to produce oxazolidinones from *N*-aryl aziridines and carbon dioxide, it was necessary to utilize TBACl in combination with **71** even if the halide efficiency is mitigated by the interaction with the silica matrix. Thus, the heterogeneous catalytic

system **71**/TBACl was tested by reacting ten different substrates with carbon dioxide at 125°C and 1.2 MPa for 16 h with a **71**/TBACl/aziridine ratio of 1:5:100.

As reported in table 13, the employed catalytic system performed better in the conversion of aziridines bearing EWGs, in accordance with the data gathered under homogeneous conditions (see chapter II.4). When the substituent was present only on the Ar moiety, quantitative yields were obtained (entries 1 and 8, table 13). However, the addition of a second substituent on the Ar^2 ring can produce different effects. In particular, if Ar = 3,5-*bis*-trifluoromethyl phenyl and the other aryl ring bears EDG, a slightly reduction of the reaction productivity was observed, as showed in entries 2 and 3 of table 13. However, almost no effects were registered on the reaction regioselectivity. On the contrary, a bromine atom on the *para* position of Ar^2 did not affect the reaction yield but diminished the regioselectivity (**14a**/**14b** = 75:25, entry 4, table 13). The presence of a pentafluorophenyl ring on carbon atom of the heterocycle reduced the reaction productivity and compound **16** was formed in the modest yield of 55%. In this latter case the fluorine atoms modified the electronic features of the C-N bond of the aziridine and augmented the steric hindrance around the carbon atom where the nucleophilic attack takes place. Thus, the low yield reported for the production of product **16** may be the result of the combination of steric and electronic effects. As expected, the regioselectivity diminished for the presence of the pentafluorophenyl ring due to the negative influence of EWGs. As already reported for the reaction promoted by the homogenous **3**/TBACl catalytic system, the presence of halogen atoms on the Ar moiety of the aziridine provoked a drop of the productivity of the reaction catalyzed by the hybrid material **71** (entries 6 and 7, table 13). The presence of EDG as the sole substituent on the phenyl rings was responsible for the decrease of the reaction selectivity (entry 9, table 13). The recyclability of the catalyst and the possibility of performing the reaction in a larger scale were also tested. 1-(3,5-*Bis*-trifluoromethylphenyl)-2-phenylaziridine was reacted with carbon dioxide in the presence of the catalytic system **71**/TBACl for four consecutive times, filtering, washing, and drying the hybrid material before every new reaction cycle. The recycled catalyst produced the desired compound in very good yields and regioselectivities, as reported in entries 10-12 of table 13. Since no major differences were detected in comparison to the

reaction performed with the fresh catalyst (entry 1, table 13), it is possible to state that the studied hybrid material is reusable up to four times without a lack of reactivity.

Table 13: *study of the carbon dioxide cycloaddition to N-aryl aziridines reaction scope.*

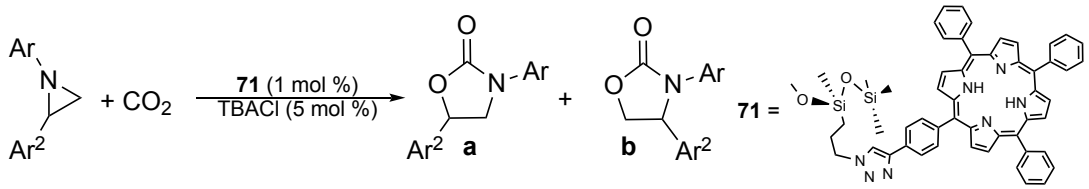

Entry	Ar	Ar^2	Conv. (%)[a]	Sel. (%)[a]	Yield (%)[a]	a/b ratio[a]
1	3,5-$(CF_3)_2C_6H_3$	C_6H_5	100	100	100	**4a**/**4b**=93:7
2	3,5-$(CF_3)_2C_6H_3$	4-^{t}BuC_6H_4	97	100	97	**10a**/**10b**=93:7
3	3,5-$(CF_3)_2C_6H_3$	4-MeC_6H_4	96	99	95	**8a**/**8b**=99:1
4	3,5-$(CF_3)_2C_6H_3$	4-BrC_6H_4	100	100	100	**14a**/**14b**=75:25
5	3,5-$(CF_3)_2C_6H_3$	C_6F_5	55	100	55	**16a**/**16b**=83:17
6	4-BrC_6H_4	C_6H_5	64	98	63	**24a**/**24b**=99:1
7	4-ClC_6H_4	C_6H_5	66	100	66	**26a**/**26b**=98:2
8	4-NO_2 C_6H_4	C_6H_5	100	100	100	**6a**/**6b**=85:15
9	4-^{t}Bu C_6H_4	C_6H_5	100	20	20	**18a**/**18b**=99:1
10[b]	3,5-$(CF_3)_2C_6H_3$	C_6H_5	100	100	100	**4a**/**4b**=92:8
11[c]	3,5-$(CF_3)_2C_6H_3$	C_6H_5	96	100	96	**4a**/**4b**=96:4
12[d]	3,5-$(CF_3)_2C_6H_3$	C_6H_5	100	100	100	**4a**/**4b**=93:7
13[e]	3,5-$(CF_3)_2C_6H_3$	C_6H_5	100	100	100	**4a**/**4b**=86:14

*1.5 M aziridine solution in THF in a steel autoclave with **71**/TBACl/aziridine ratio = 1:5:100 at 125 °C and 1.2 MPa of CO_2 for 16 h. a) Obtained by NMR using 2,4-dinitrotoluene as the internal standard. b) First recycle of the catalyst. c) Second recycle of the catalyst. d) Third recycle of the catalyst. e) Reaction performed on 1.0 gram of substrate.*

Finally, the same reaction was performed on a larger scale by using 1.00 g of substrate and the desired product was formed in a quantitative yield. Only a minor lowering of the regioselectivity was detected (entry 13, table 13). This data suggested the possibility to apply the catalytic system to further process development.

Thus, the porphyrin-functionalized silica displayed very good activity for the conversion of EWGs substituted *N*-aryl aziridines, showing excellent results with different substrates and in large scale reactions. Moreover, the catalyst **71** is recyclable and easy to recover, demonstrating a high applicability in the conversion of this class of substrate into the corresponding oxazolidinones.

4. Conclusions

In this chapter the synthesis, characterization, and catalytic activity of an SBA-15 supported porphyrin in the carbon dioxide cycloaddition reaction to three membered heterocycles were presented. The efficient support of porphyrin on the silica matrix makes it possible to upgrade the catalytic procedure presented in the previous chapter. The use of a heterogeneous catalyst improved the reaction sustainability thanks to an easier product purification, an easier catalyst recovery, and an enhanced recyclability of the material. In addition, this material may synergize with the other components of the catalytic system, improving the substrates reactivity towards carbon dioxide.

The hybrid material was prepared by the one-pot synthesis of the azido functionalized silica to which was linked the porphyrin by alkyne-azide cycloaddition. The silica functionalization occurred with an efficiency of 46%. Both the unfunctionalized and porphyrin-functionalized silica were fully characterized by IR, UV-Vis, solid NMR, TGA, nitrogen absorption, elemental analysis, and XRD in order to determine the efficiency of the linkage and its extent. Acquired data depicted a successful loading of the porphyrin by covalent binding and the maintenance of the mesostructuration of the solid during the material preparation.

The so-obtained hybrid material **71**, in combination with ammonium salts, successfully performed the conversion of three different classes of heterocycles into the desired products, highlighting the synergistic effect of the matrix with the catalyst for the reaction productivity. At first, the reaction between epoxides and CO_2 was studied utilizing TBAI in the place of TBACl due to the interaction between the silanols and the chloride anion, which reduces the ammonium salt reactivity. Exploiting the catalytic system **71**/TBAI, improved TON and TOF values were registered for the conversion of different epoxides into the corresponding cyclic carbonates. These results underlined the positive effect of the silica matrix on the epoxide activation. Moreover, the recyclability showed and the possibility to work in a large scale and solvent free conditions put forward the porphyrin-supported material for further process developments.

Then, the same system demonstrated a good catalytic efficiency in the conversion of *N*-alkyl aziridines to the corresponding oxazolidinones. The same reactivity trends already observed under homogenous conditions were detected by exploiting material **71** and the catalytic performances were dependent on steric factors due to diffusion constraints. In this case, the heterogeneous catalyst showed a reduced activity in comparison with the homogeneous counterparts because the silanols present on the silica surface did not activate aziridines to the same extent that was registered in the cycloaddition to epoxides. However, the reduced reactivity was efficiently overcome by prolonging the reaction time to 16 h.

Finally, compound **71** in combination with TBACl displayed good activity also in the conversion of the less reactive *N*-aryl aziridines. The preparation of ten different oxazolidinones was accomplished, obtaining similar results to those observed by applying the catalytic system **3**/TBACl under homogeneous conditions.

In addition, the porphyrin functionalized SBA-15 material showed good recyclability and activity in the conversion of larger quantity of both classes of aziridines studied.

The effectiveness of the heterogeneous catalyst rewarded the efforts spent for the improvement of the protocol presented in chapter II, underlining the possibility to develop an efficient preparation of oxazolidinones and cyclic carbonates from carbon dioxide by respecting the principles of green chemistry. Moreover, due to the efficiency showed by the heterogeneous catalyst it was possible to imagine further process developments and applications.

Chapter IV: Experimental Section

1. General and characterization

THF and benzene were distilled over sodium and benzophenone and kept under nitrogen. Decalin, hexane, and toluene were distilled over sodium and kept under nitrogen. Acetone were distilled over $MgSO_4$ and kept under nitrogen. Styrene, pyrrole, and α-methyl styrene were distilled over calcium hydride under reduced pressure and kept under nitrogen. Water was removed from dimethylformamide by azeotropic distillation with benzene (10% v/v previously distilled over CaH_2) and further distillation under reduced pressure; the so-obtained dry DMF were stored under argon over molecular sieves. All the other starting materials were commercial products used as received. NMR spectra were recorded at room temperature either on a Bruker Avance 300-DRX, operating at 300 MHz for ^{1}H, at 75 MHz for ^{13}C and at 282 MHz for ^{19}F or on a Bruker Avance 400-DRX spectrometers, operating at 400 MHz for ^{1}H and at 100 MHz for ^{13}C and at 376 MHz for ^{19}F. Chemical shifts (ppm) are reported relative to TMS. The ^{1}H NMR signals of the compounds described in the following were attributed by 2D NMR techniques. Assignments of the resonances in ^{13}C NMR were made by using the APT pulse sequence, HSQC, and HMBC techniques. Solid state CP-MAS experiments were performed on a Bruker Avance II 300 spectrometer using a 4 mm double resonance Bruker MAS probe at spectral frequencies of 75.5 MHz and 59.6 MHz for respectively ^{13}C and ^{29}Si. Chemical shifts were referenced to TMS or external 85% H_3PO_4. The spinning rate was 5 kHz (^{29}Si) or 10 kHz (^{13}C) and samples were spun at the magic angle (MAS) using ZrO_2 rotors. The experimental details for the NMR experiments were as follows: contact time 2 ms, repetition time 2 s, number of scans from 3000 to 25000 depending on the loading and the nature of the sample. Infrared spectra were recorded on a Varian Scimitar FTS 1000 or a JASCO FT/IR-4200 (JASCO) spectrometer in the absorbance mode. UV/Vis spectra were recorded on an Agilent 8453E instrument or on a Perkin Elmer Lambda 1050 spectrometer. Solid UV/Visible spectra were acquired using a PerkinElmer Lambda 1050 UV/VIS/NIR spectrometer equipped with a Praying Mantis equipment (HarrickTM) for solid analysis. Nitrogen adsorption-desorption isotherms at 77 K were measured using a Micromeritics ASAP 2020M physisorption analyzer. The samples were evacuated at 10^{-5} Torr and 150 °C during 15 h before the measurements. Specific surface

areas were calculated by following the BET procedure. Pore size distribution was obtained by using the BJH pore analysis applied to the desorption branch of the nitrogen adsorption-desorption isotherm. A Netzsch thermoanalyser STA 409 PC was used for simultaneous thermal analysis combining thermogravimetric (TGA) and differential thermoanalysis (DTA) at a heating rate of 5 °C min^{-1} in air from 25-900 °C. Small-angle X-ray powder diffraction (XRD) data were acquired on a Bruker D5005 diffractometer using Cu Kα monochromatic radiation (λ = 1.5418 Å). C, N elemental analyses determinations were performed by ICP-AES (Activa Jobin Yvon) spectroscopy from a solution obtained by treatment of the hybrid materials with a mixture of HF, HNO_3 and H_2SO_4 in a teflon reactor at 150°C. Elemental analyses and mass spectra were recorded in the analytical laboratories of Milan University.

2. Synthesis of the Catalysts

2.1 Synthesis of Ru(TPP)CO (40)

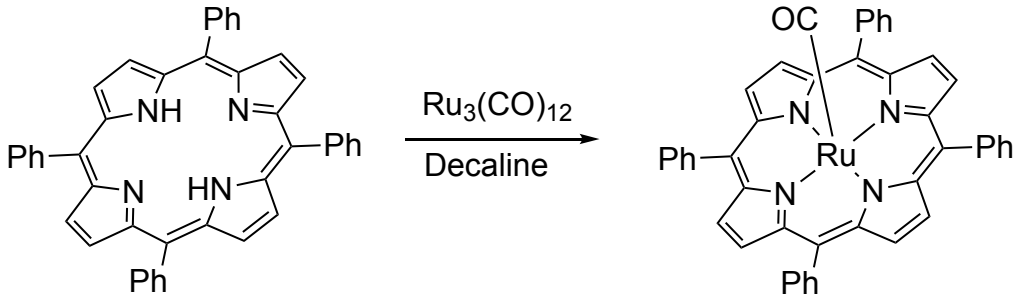

Reaction under nitrogen atmosphere. The metal precursor $Ru_3(CO)_{12}$ (0.626 g, 9.80 x 10^{-1} mol) and the ligand *meso*-tetraphenylporphyrin (1.23 g, 2.00 x 10^{-3} mol) were dissolved in dry decalin (60 mL). Then, the reaction mixture was refluxed for 7 h until to the complete consumption of $TPPH_2$ which was observed by TLC (SiO_2, hexane/CH_2Cl_2 = 80:20). The solvent was removed to dryness under vacuum and the crude was purified by flash chromatography (silica gel, 60 µm, gradient from hexane/CH_2Cl_2 7:3 to CH_2Cl_2). The product fraction was evaporated to dryness under vacuum and dried at 100 °C. The product was obtained as a reddish crystalline solid (yield: 73%). The collected analytical data are in accordance with those reported in literature.[278]

^{1}H NMR (300 MHz, $CDCl_3$): δ 8.68 (s, 8H, $H_{\beta pyrr}$), 8.22 (m, 4H, H_{Ph}), 8.11 (m, 4H, H_{Ph}), and 7.75 - 7.72 ppm (m, 12H, H_{Ph}).

2.2 Synthesis of Ru(TPP)NAr_2 (Ar = 3,5-$(CF_3)_2C_6H_3$) (1)

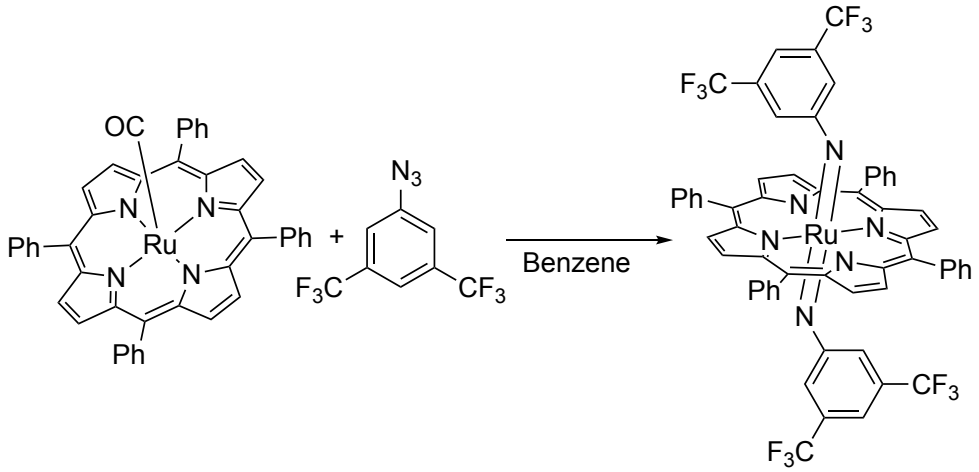

Reaction under nitrogen atmosphere. Ru(TPP)CO (0.150 g, 2.02 x 10^{-4} mol) and 3,5-*bis*(trifluoromethyl)phenyl azide (0.154 g, 6.06 x 10^{-3} mol) was suspended in dry benzene (30 mL). The resulting dark mixture was refluxed for 3 h observing the complete consumption of the starting ruthenium complex by TLC (Al_2O_3, hexane/CH_2Cl_2 1:1). The volume was reduced to about 5 mL and dry hexane (20 mL) was added to precipitate the desired product. A crystalline violet solid was collected by filtration and dried under vacuum (yield: 70%). The collected analytical data are in accordance with those reported in literature.[279]

^{1}H NMR (300 MHz, $CDCl_3$): δ 8.87 (s, 8H, $H_{\beta pyrr}$), 8.08 (d, 8H, *J* = 6.9 Hz, H_{Ar}), 7.83 - 7.76 (m, 12H, H_{Ar}), 6.60 (s, 2H, H_{Ar}), and 2.66 ppm (s, 4H, H_{Ar}).

2.3 Synthesis of *meso*-tetraphenylporphyrin $TPPH_2$ (3)

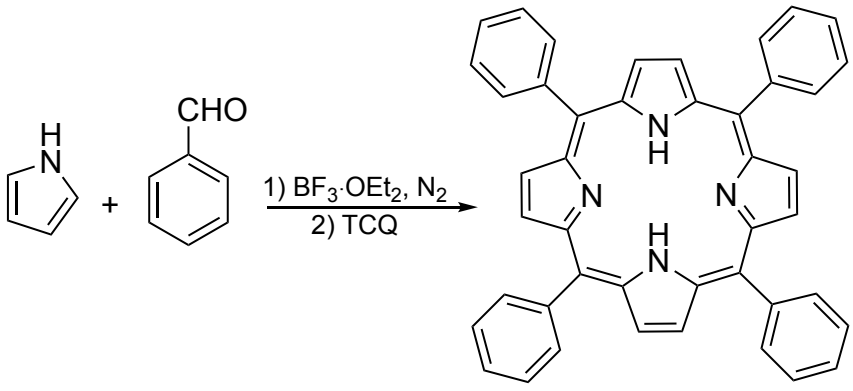

Dry pyrrole (0.54 g, 8.05 x 10^{-3} mol) and benzaldehyde (0.84 g, 7.92 x 10^{-3} mol) were dissolved in dry CH_2Cl_2 (250 mL) under nitrogen atmosphere. The mixture was protected from light, then, $BF_3{\cdot}OEt_2$ (0.34 g, 2.43 x 10^{-3} mol) and tetrachloro-1,4-quinone (TCQ) (1.54 g, 6.23 x 10^{-3} mol) were added under nitrogen atmosphere. The solution was stirred for 2 minutes at 100 °C, then stirred for 45 minutes under nitrogen atmosphere. Finally, the reaction mixture was stirred for 45 minutes in air. The solvent was removed under vacuum to dryness and the crude was purified by silica filtration and successively, by flash chromatography (silica gel, 60 µm, gradient from hexane/CH_2Cl_2 9:1 to hexane/CH_2Cl_2 7:3). The product fraction was evaporated to dryness under vacuum at 100°C. The product was obtained as a purple crystalline solid (yield: 20%). The collected analytical data are in accordance with those reported in literature.[145]

^{1}H NMR (400 MHz, $CDCl_3$, 298 K): δ 8.85 (s, 8H, $H_{\beta pyrr}$), 8.22 (d, *J* = 6.5 Hz, 8H, H_{Ph}), 7.80 - 7.40 (m, 12H, H_{Ph}), and -2.76 ppm (s, 2H, NH).

2.4 Synthesis of *meso*-tetrakis(4-tert-butylphenyl) porphyrin 4-^{t}BuTPPH$_2$ (44)

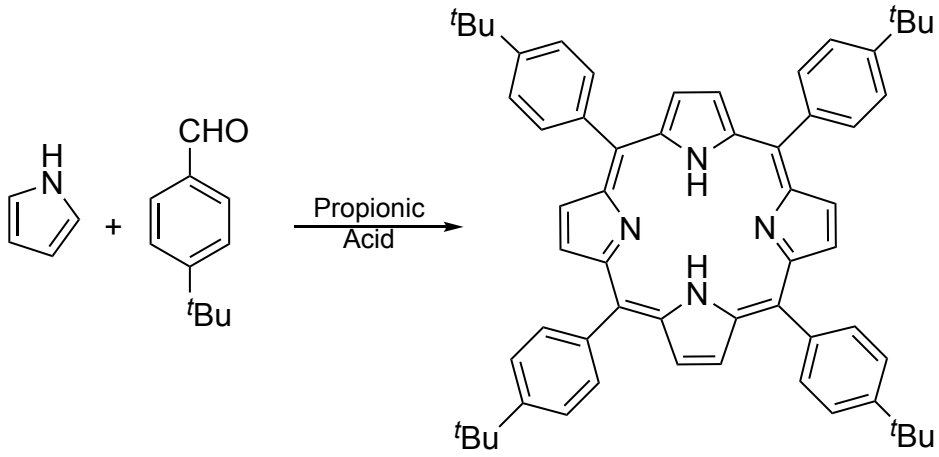

4-^{t}Butyl benzaldehyde (3.20 g, 1.97 x 10^{-2} mol) and dry pyrrole (1.34 g, 2.00 x 10^{-2} mol) were added dropwise in 15 minutes to boiling propionic acid (50 mL). The dark mixture was refluxed for 1 h and then stirred at RT for 24 h. The precipitate was collected in a filter, then washed several times with water and one time with cold methanol. The powder was dried under vacuum at 100 °C. The desired product was obtained as a purple crystalline solid

(yield: 21%). The collected analytical data are in accordance with those reported in literature.[280]

^{1}H NMR (400 MHz, $CDCl_3$): δ 8.88 (s, 8H, $H_{\beta pyrr}$), 8.17 (d, *J* = 7.5 Hz, 8H, H_{Ar}), 7.78 (d, *J* = 7.5 Hz, 8H, H_{Ar}), 1.62 (s, 36H, $H_{t\mathrm{Bu}}$), and -2.74 ppm (s, 2H, NH).

2.5 Synthesis of *meso*-tetrakis(4-trifluoromethylphenyl) porphyrin 4-CF_3-$TPPH_2$ (45)

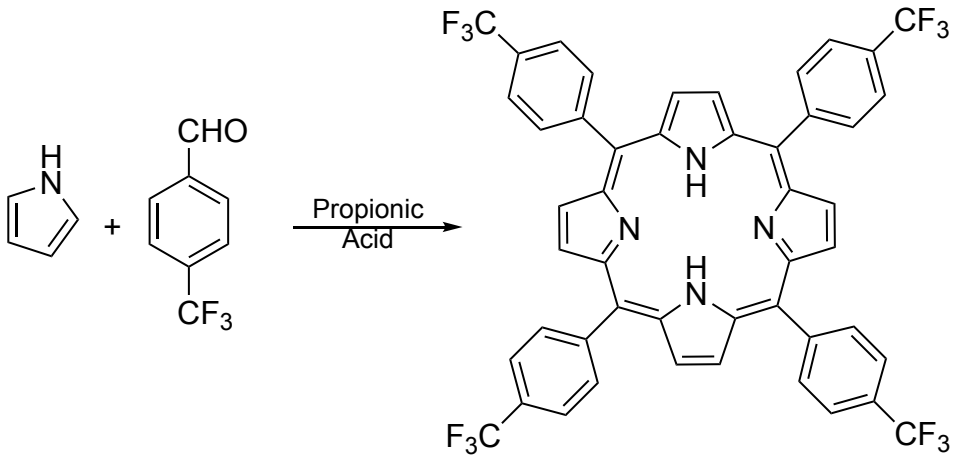

4-Trifluoromethyl benzaldehyde (3.43 g, 1.97 x 10^{-2} mol) and dry pyrrole (1.34 g, 2.00 x 10^{-2} mol) were added dropwise in 15 minutes to boiling propionic acid (50 mL). The dark mixture was refluxed for 30 min and then cooled to RT. The precipitate was collected in a filter, then washed several times with water and one time with cold methanol. The powder obtained was dried under vacuum at 100 °C. The desired product was obtained as a purple crystalline solid (yield: 18%). The collected analytical data are in accordance with those reported in literature.[281]

^{1}H NMR (300 MHz, $CDCl_3$): δ 8.82 (s, 8H, $H_{\beta pyrr}$), 8.34 (d, *J* = 8.1 Hz, 8H, H_{Ar}), 8.05 (d, *J* = 8.1 Hz, 8H, H_{Ar}), and -2.95 ppm (s, 2H, NH).

2.6 Synthesis of *meso*-tetrakis(4-carboxylphenyl) porphyrin 4-COOH-TPPH$_2$ (46)

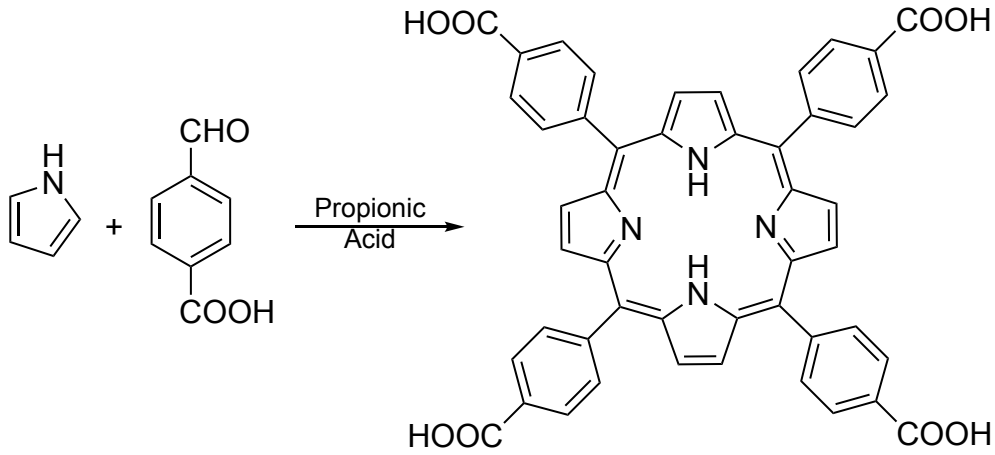

4-Carboxy benzaldehyde (2.96 g, 1.97 x 10^{-2} mol) and dry pyrrole (1.34 g, 2.00 x 10^{-2} mol) were added dropwise in 15 minutes to boiling propionic acid (50 mL). The dark mixture was refluxed for 45 min and then cooled to RT. The precipitate was collected in a filter and washed several times with water and one time with cold methanol. The powder obtained was dried under vacuum at 100 °C. The desired product was obtained as a dark blue crystalline solid (yield: 21%). The collected analytical data are in accordance with those reported in literature.[282]

^{1}H NMR (300 MHz, DMSO-d^6): δ 13.37 (4H, s, COOH) 8.77 (s, 8H, $H_{\beta pyrr}$), 8.31 (d, *J* = 8.0 Hz, 8H, H_{Ar}), 8.23 (d, *J* = 8.0 Hz, 8H, H_{Ar}), and -2.99 ppm (s, 2H, NH).

2.7 Synthesis of 5-(pentafluorophenyl)-10,15,20-triphenyl porphyrin F$_5$-TPPH$_2$ (47)

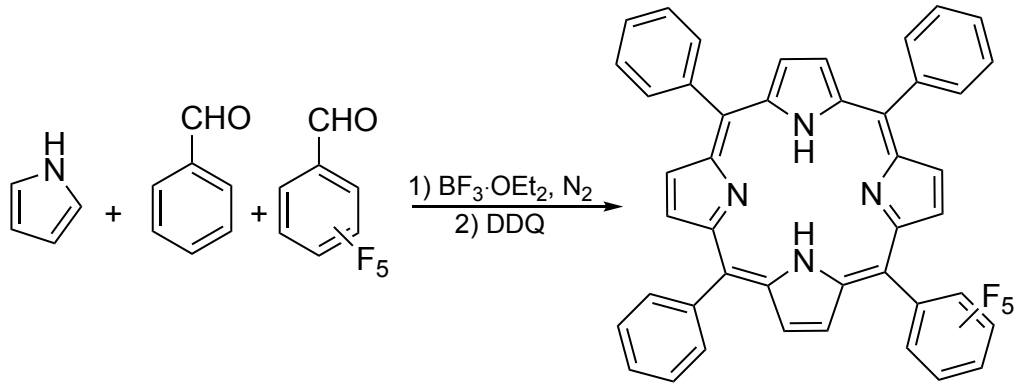

Reaction under nitrogen atmosphere. Dry pyrrole (0.36 g, 5.00 x 10^{-3} mol), benzaldehyde (0.36 g, 3.75 x 10^{-3} mol), and pentafluorobenzaldehyde (0.10 g, 1.25 x 10^{-3} mol) were dissolved in dry CH_2Cl_2 (400 mL). The mixture was protected from light, then $BF_3{\cdot}OEt_2$ (0.72 g, 5.00 x 10^{-4} mol) was added. The reaction mixture was stirred at RT overnight, then 2,3-dichloro-5,6-dicyano-1,4-benzoquinone (DDQ) (0.56 mg, 2.51 x 10^{-3} mol) was added, and the reaction mixture was refluxed 12 h in air. Then, the reaction mixture was cooled down to RT and triethylamine (TEA) (0.076 g, 7.50 x 10^{-4} mol) was added. The solvent was removed under vacuum to dryness and the crude was purified by silica filtration and successively by flash chromatography (silica gel, 60 µm, starting from hexane to hexane/CH_2Cl_2 8:2). The product fraction was evaporated to dryness and under vacuum at 100 °C. The product was obtained as a purple solid (yield: 21%). The collected analytical data are in accordance with those reported in literature.[283]

^{1}H NMR (300 MHz, $CDCl_3$): δ 9.01 (d, *J* = 4.8 Hz, 2H, $H_{\beta pyrr}$), 8.92 (s, 4H, $H_{\beta pyrr}$), 8.85 (d, *J* = 4.6 Hz, 2H, $H_{\beta pyrr}$), 8.27 (m, 6H, H_{Ar}), 7.80 - 7.75 (m, 9H, H_{Ar}), and -2.66 ppm (s, 2H, NH).

2.8 Synthesis of *meso*-tetrakis(pentafluorophenyl) porphyrin F_{20}-TPPH_2 (48)

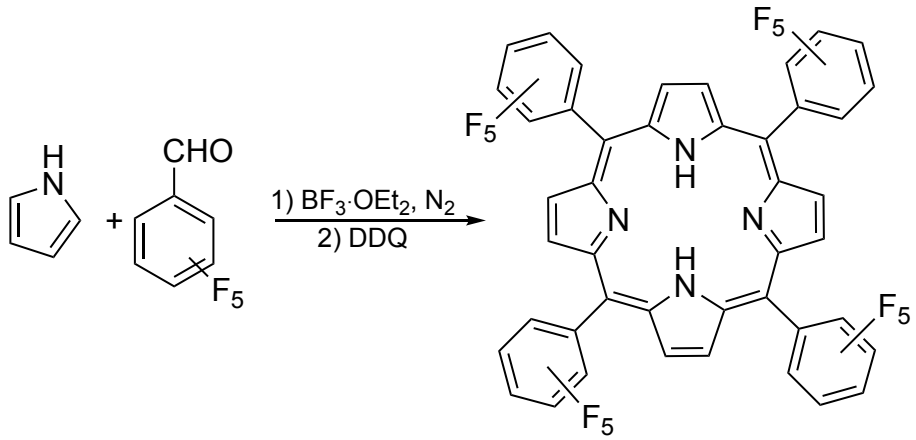

Reaction under nitrogen atmosphere. Dry pyrrole (0.54 g, 8.05 x 10^{-3} mol) and pentafluorobenzaldehyde (0.98 g, 5.00 x 10^{-3} mol) were dissolved in dry CH_2Cl_2 (250 mL). The mixture was protected from light, then, $BF_3{\cdot}OEt_2$ (0.21 g, 1.50 x 10^{-3} mol) was added. The reaction mixture was refluxed for 4 h, then cooled to RT. DDQ (0.56 mg, 2.51 x 10^{-3} mol) was added, and the reaction was refluxed for 12 h on air. At this point the reaction was

cooled down to RT and TEA (0.076 g, 7.50 x 5.00 x 10^{-4} mol) was added. The solvent was removed under vacuum to dryness and the crude was purified by silica filtration and successively by flash chromatography (silica gel, 60 µm, gradient from hexane to hexane/CH_2Cl_2 9:1). The product fraction was evaporated to dryness and under vacuum at 100 °C. The product was obtained as a purple solid (yield: 12%). The collected analytical data are in accordance with those reported in literature.[284]

^{1}H NMR (400 MHz, $CDCl_3$): δ 8.97 (s, 8H, $H_{\beta pyrr}$) and -2.85 ppm (s, 2H, NH).

2.9 Synthesis of octaethylporphyrin $OEPH_2$ (49)

2.9.1 Synthesis of 4-nitro-3-hexhanol

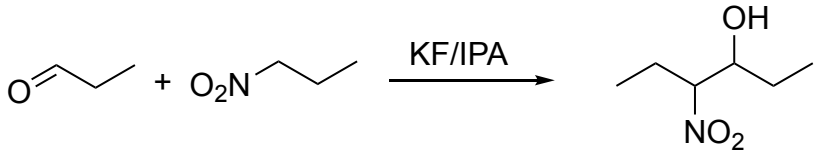

Propionaldehyde (17.40 g, 0.30 mol) was dissolved in isopropyl alcohol (IPA) (45 mL). The solution was stirred and KF (2.50 g, 1.50 x 10^{-2}) was added. The reaction mixture was cooled with an ice bath and 1-nitropropane (26.73 g, 0.30 mol) was added dropwise in 30 minutes. The so-obtained solution was stirred for 30 minutes at 0°C and then brought to RT. After 18 h, KF was filtered, and the volume reduced under reduced pressure. Water (50 mL) was added, and the obtained mixture was extracted with diethyl ether (3 x 30 mL). The organic phases were dried over sodium sulphate and the solvent was removed under reduced pressure. The obtained liquid was distilled and the fraction which boils between 88°C and 90°C was gathered obtaining the desired product (yield: 65%).

2.9.2 Synthesis of 4-acetoxy-3-nitrohexane

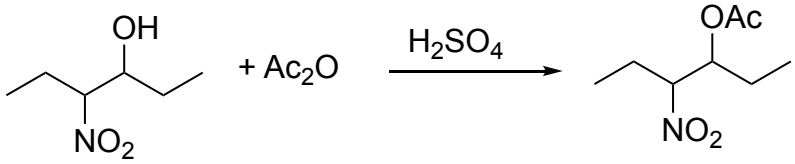

4-Nitro-3-hexanol (33.06 g, 0.22 mol) and sulfuric acid (0.1 mL) were stirred in an ice bath. The acetic anhydride (24.00 g, 0.23 mol) was added stepwise keeping the temperature under 60 °C. Then, the reaction mixture was stirred for 1 h. The low boiling components were distilled under 25 mm Hg, then the desired product was distilled under 10 mm Hg and 107-110 °C (yield: 90%).

2.9.3 Synthesis of 3,4-diethylpyrrole

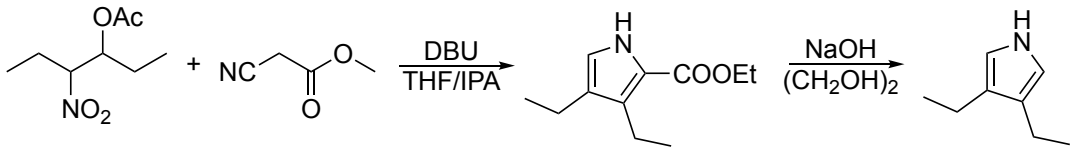

4-acetoxy-3-nitrohexane (10.30 g, 5.4 x 10^{-2} mol) and ethyl isocyanoacetate (5.07 g, 4.5 x 10^{-2} mol) were dissolved in dry tetrahydrofuran (THF) (32 mL) and IPA (13 mL). DBU (15.20 g, 0.10 mol) was added keeping the temperature between 20 and 30°C. The so-obtained orange solution was stirred at RT for 4 h. The solvent was removed to dryness and the obtained product was diluted in water (30 mL). The aqueous phase was extracted with diethyl ether (3 x 30 mL) and the organic phases were washed with a 10% w/w solution of HCl in water (2 x 30 mL). Then, the organic phase was dried over sodium sulphate and the solvent was removed to dryness under reduced pressure. The so-obtained oil was reacted with sodium hydroxide (3.00 g, 7.5 x 10^{-2} mol) in ethylene glycol (30 mL). The reaction mixture was refluxed for 1 h under nitrogen atmosphere and then cooled to RT. Water (50 mL) and hexane (60 mL) were added to the solution, the phases were separated, and the aqueous phase was extracted with hexane (2 x 60 mL). The organic phases were dried over magnesium sulphate and the solvent was removed to dryness under reduced pressure. The product was obtained by distillation (100°C/25 mm Hg) (yield: 40%).

2.9.4 Synthesis of octaethylporphyrin

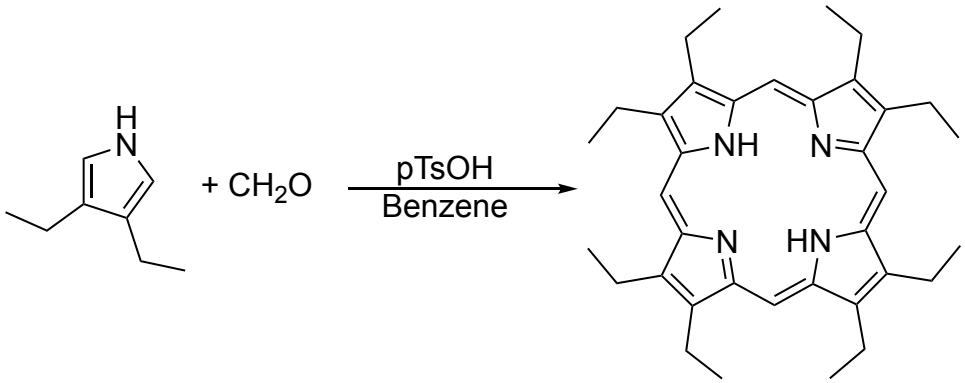

3,4-Diethylpyrrole (1.00 g, 8.12 x 10^{-3} mol) and formaldehyde in water 37% (0.73 mL, 8.12 x 10^{-3} mol) were dissolved in dry benzene (300 mL). The reaction mixture was protected from light and p-toluenesulfonic acid (0.030 g, 1.7 x 10^{-3} mol) was added under nitrogen atmosphere. The reaction mixture was refluxed 8 h, then cooled to room temperature, and stirred 24 h bubbling oxygen in the solution. The solvent was removed under reduced pressure and the crude was dissolved in chloroform (20 mL). The so-obtained solution was washed with a NaOH solution 1 M in water (40 mL) and water (2 x 40 mL). The solution volume was reduced to 5 mL and the desired product was crystalized from methanol. The so-obtained solid was purified by double crystallization from chloroform/*n*-hexane. The final product was collected in a filter and dried under vacuum at 100 °C (yield: 66%). The collected analytical data are in accordance with those reported in literature.[285]

^{1}H NMR: (300 MHz, CDCl3) δ 10.12 (s, 4 H, H_{meso}), 4.12 (q, 16 H, H_{CH2}), 1.95 (t, 24 H, H_{CH3}), and -3.72 ppm (s, 2 H, NH).

2.10 Synthesis of porphyrin 57

2.10.1 Synthesis of (R)-2-methoxy-2-phenylacetic chloride

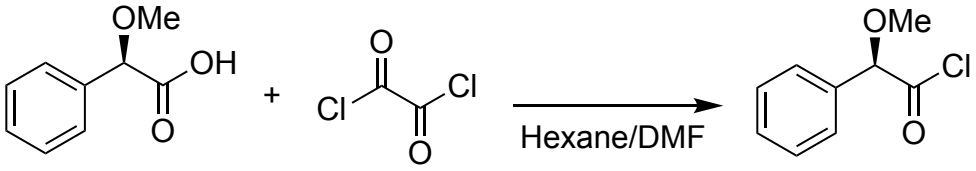

(R)-2-Methoxy-2-phenylacetic acid (0.50 g, 3.00 x 10^{-3} mol) was dissolved in *n*-hexane (5 mL) and DMF (23.0 μL). Oxalyl chloride (3.81 g, 3.00 x 10^{-2} mol) was added dropwise, and the reaction was stirred overnight. The solvent was removed under reduced pressure and the crude was utilized without further purification.

2.10.2 Synthesis of (S)-2-acetoxy-2-phenylacetic acid

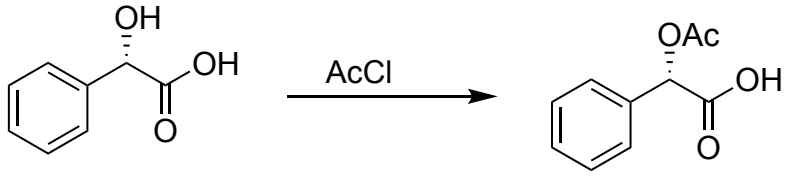

(S)-Mandelic acid (2.15 g, 1.40 x 10^{-2} mol) was dissolved in acetyl chloride (AcCl) (2.48 mL). The reaction mixture was stirred overnight at RT. The AcCl was removed by reduced pressure and the product was obtained as a yellow oil (yield: 95%). The collected analytical data are in accordance with those reported in literature.[286]

^{1}H NMR (400 MHz, $CDCl_3$): δ 11.45 (br, 1H, H_{COOH}); 7.50 - 7.40 (m, 5H, H_{Ph}), 5.95 (s, 1H, H_{CH}), and 2.20 ppm (s, 3H, H_{CH3}).

2.10.3 Synthesis of (S)-2-acetoxy-2-phenylaceti chloride

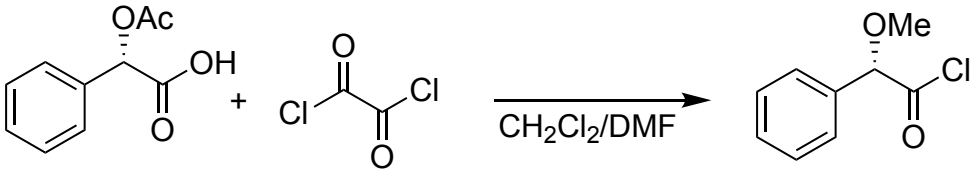

(S)-2-Acetoxy-2-phenyl chloride (0.54 g, 2.80 x 10^{-3} mol) was dissolved in CH_2Cl_2 (12 mL) and DMF (70 μL). Oxalyl chloride (0.35 g, 2.80 x 10^{-3} mol) was added dropwise, and the reaction mixture was stirred overnight. The solvent was removed under reduced pressure and the crude was utilized without further purification.

2.10.4 Synthesis of 5-methoxy-2-nitrobenzaldehyde

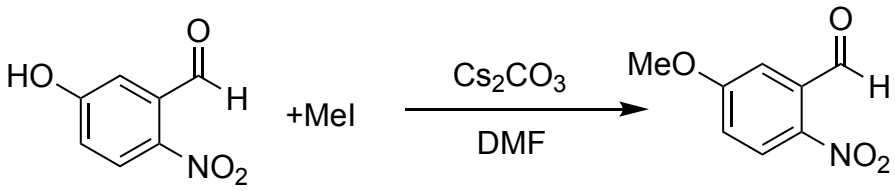

5-Hydroxy-2-nitrobenzaldehyde (25.00 g, 1.5 x 10^{-1} mol) and cesium carbonate (48.90 g, 1.5 x 10^{-1} mol) were dissolved in DMF (25 mL). The orange solution was cooled to 0 °C and methyl iodide (MeI) (2.13 g, 1.5 x 10^{-1} mol) was added dropwise. The reaction mixture was stirred for three days at RT, then, water (200 mL) and ethyl acetate (200 mL) were added. The aqueous phase was washed with ethyl acetate (3 x 100 mL). The organic phases were washed with water (200 mL) and dried over sodium sulphate. The solvent was removed under reduced pressure and the product was obtained as a yellow oil. The crude was washed different times with diethyl ether until a withe solid was obtained (yield: 67%). The collected analytical data are in accordance with those reported in literature.[286]

^{1}H NMR (400 MHz, $CDCl^3$): δ 10.49 (s, 1H, H_{CHO}), 8.17 (d, 1H, *J* = 9.05 Hz, H_m), 7.33 (d, 1H, ^4J = 2.87 Hz, H_o), 7.15 (dd, 1H, *J* = 9.06, 2.88 Hz, H_p), and 3.96 ppm (s, 1H, H_{OCH3}).

2.10.5 Synthesis of (R)-2,2'-dimethoxy-1-1'-binaphtalene

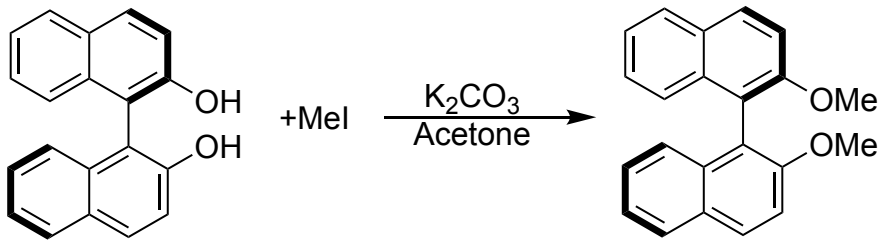

(R)-(+)-1-1'-Bi(2-naphthol) (3.01 g, 1.05·10^{-2} mol) was suspended in acetone (45 mL) and the resulting suspension was heated at 50 °C to give a homogeneous solution. Then, MeI

(3.92 mL, $6.30 \cdot 10^{-2}$ mol) and potassium carbonate (4.95 g, $3.50 \cdot 10^{-2}$ mol) were added to the mixture. At this point the reaction was refluxed for 12 h. The reaction mixture was concentrated to 10 mL, the residue was cooled to room temperature, and 50 mL of water were added. The so-obtained mixture was stirred for 8 h and a white solid precipitated. The resulting solid was collected in a filter, washed with water several times, and finally dried under vacuum to afford (R)-2,2'-dimethoxy-1,1'-dinaphthalene as a white powder (yield: 87%). The collected analytical data are in accordance with those reported in literature.[286]

^{1}H NMR (300 MHz, DMSO-d6): δ 8.06 (d,2H, *J* = 9.0 Hz, H_{Ar}), 7.94 (d, 2H, *J* = 8.0 Hz, H_{Ar}), 7.60 (d, 2H, *J* = 9.0 Hz, H_{Ar}), 7.31 (t, 2H, *J* = 7.3 Hz, H_{Ar}), 7.21 (t, 2H, *J* = 7.6 Hz, H_{Ar}), 6.89 (d, 2H, *J* = 8.4 Hz, H_{Ar}), and 3.70 ppm (s, 6H, H_{CH3}).

2.10.6. Synthesis of (*R*)-2,2'-dimethoxy-1,1'-binaphthyl-3,3'-diboronic acid

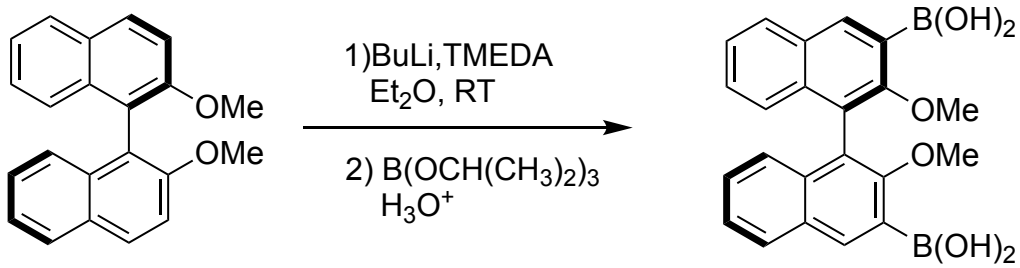

Reaction under nitrogen atmosphere. A solution 1.6 M of butyl lithium in *n*-hexane (3.04 mL, $4.87 \cdot 10^{-3}$ mol) was added to a solution of tetramethylethylenediamine (TMEDA) (0.75 g, $6.49 \cdot 10^{-3}$ mol) in diethyl ether (25 mL). The reaction mixture was stirred at room temperature for 30 minutes. Then, (R)-2,2'-dimethoxy-1,1'-dinaphthalene (0.51 g, $1.62 \cdot 10^{-3}$ mol) was added and the reaction mixture was stirred for 3 h. A light brown suspension was obtained, and it was cooled to -78°C. Triisopropyl borate (1.83 g, $9.73 \cdot 10^{-3}$ mol) was added dropwise in 10 minutes. The reaction mixture was allowed to get back to room temperature and the solution was stirred for 12 h. Then, the suspension was cooled to 0°C and a solution 1 M of HCl in water (15 mL) was added. The resulting solution was stirred at room temperature for 2 hours. The organic layer was washed with a solution 1 M of HCl in water (15 mL), then it was washed with brine (3 x 30 mL), and finally dried

over sodium sulphate. The solvent was evaporated to dryness under vacuum and the product was obtained (yield: 99%). The collected analytical data are in accordance with those reported in literature.[286]

^{1}H NMR (300 MHz, CDCl3): δ 8.62 (s, 2H, H_{Ar}), 7.99 (d, 2H, *J* = 8.1Hz, H_{Ar}), 7.44 (t, 2H, *J* = 7.2 Hz, H_{Ar}), 7.32 (t, 2H, *J* = 7.4 Hz, H_{Ar}), 7.16 (d, 2H, *J* = 8.7 Hz, H_{Ar}), 6.03 (s, 2H, H_{Ar}), and 3.31 ppm (s, 6H, H_{CH3}).

2.10.7. Synthesis of *meso*-tetra(2-nitrophenyl) porphyrin o-TNPPH$_2$

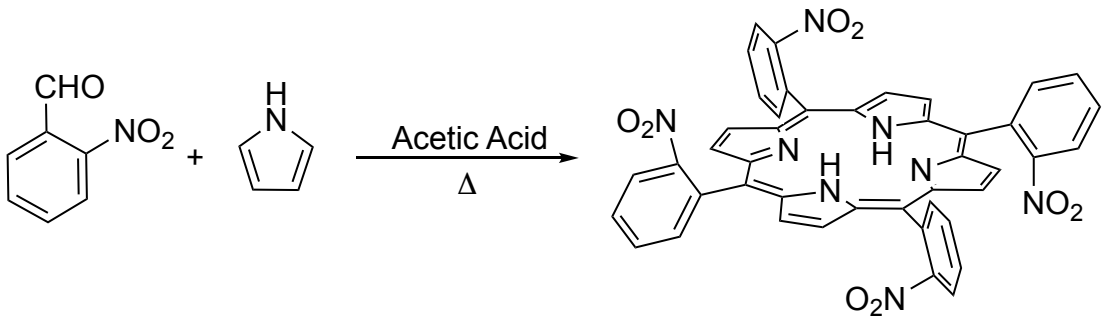

2-Nitrobenzaldehyde (10.10 g, $6.72 \cdot 10^{-2}$ mol) was dissolved in acetic acid (200 mL). Dry pyrrole (4.42 g mL, $6.59 \cdot 10^{-2}$ mol) was added to the refluxing solution in about 15 minutes. Then, the reaction mixture was refluxed for 45 minutes. The so-obtained dark solution was allowed to cool to 60 °C and chloroform (50 mL) was added. After this addition a dark precipitate was formed. The solid was collected in a filter, washed with CH_2Cl_2 (200 mL), and dried in vacuo (yield: 8.2%). The so-obtained product was utilized without further purification.

2.10.8 Synthesis of $\alpha_2\beta_2$ meso-tetra(2-aminophenyl) porphyrin o-TAPPH$_2$

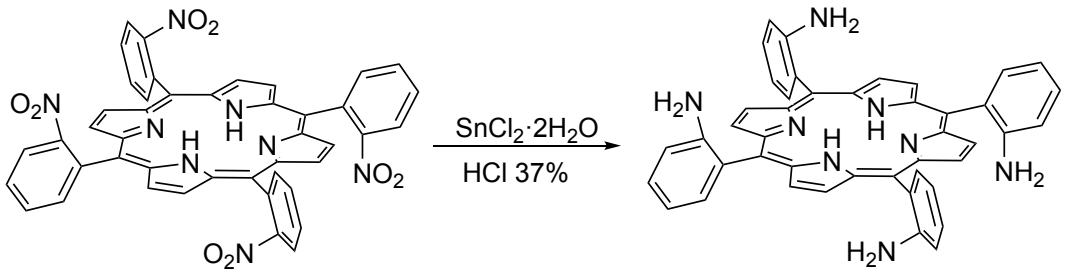

Meso-tetra(2-nitrophenyl) porphyrin (3.60 g, $4.53 \cdot 10^{-3}$ mol) was dissolved in a water

solution of HCl 37% (150 mL) under vigorous magnetic stirring. Then, $SnCl_2 \cdot 2H_2O$ (15.30 g, $6.79 \cdot 10^{-2}$ mol) was gradually added and the so-obtained green solution was stirred at room temperature for 2 days. 100 mL of chloroform were added, and the reaction mixture was stirred for 15 minutes. Then, the solution was cooled with an ice bath and a saturated solution of KOH was added until getting to a pH = 10. At this point, the organic phase was separated, and the solid was collected in a filter. The aqueous phase was extracted with chloroform (5 x 100 mL). The organic phases were dried over sodium sulphate and the solvent was removed under reduced pressure. A purple solid containing the four atropoisomers was obtained. The desired $\alpha_2\beta_2$ atropoisomer was isolated by flash chromatography (silica gel, 15 μm gradient from CH_2Cl_2 to CH_2Cl_2/MeOH 95:5). The collected analytical data are in accordance with those reported in literature.[286]

^{1}H NMR (400 MHz, $CDCl_3$): δ 8.92 (s, 8H, $H_{\beta pyrr}$), 7.86 (d, 4H, *J* = 7.4 Hz, H_{Ar}), 7.26 (t, 4H, *J* = 7.8 Hz, H_{Ar}), 7.18 (t, 4H, *J* = 7.4 Hz, H_{Ar}), 7.14 (d, 2H, *J* = 8.1 Hz, HAr), 3.58 (s, 8H, NH_2), and -2.65 ppm (s, 2H, NH).

2.10.9 Synthesis of $\alpha_2\beta_2$-bis{2,2'-[3,3'-(2,2'-dimethoxy-(1,1'-binaphthyl)benzoyl amido)}phenyl) porphyrin (57)

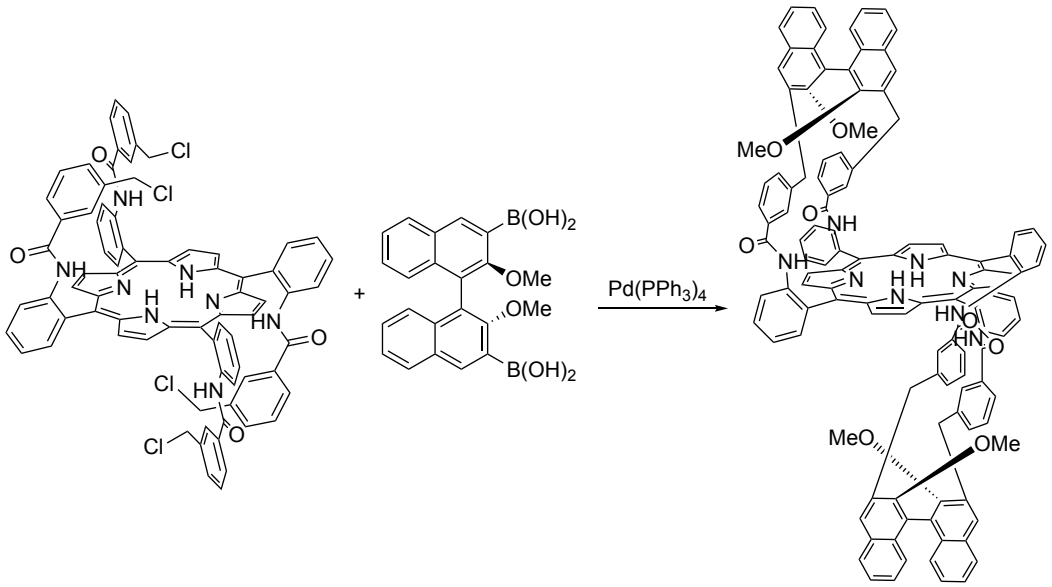

$\alpha_2\beta_2$-Tetra{2-[(3-chloromethyl)benzoylamido]phenyl} porphyrin (0.300 g, $2.33\cdot10^{-5}$ mol), (R)-2,2'-dimethoxy-1,1'-binaphthyl-3,3'-diboronic acid (0.23 g, $5.60\cdot10^{-4}$ mol), tetrakis((triphenyl)phosphine) palladium(0) (0.11 g, $9.34\cdot10^{-5}$ mol), and potassium carbonate (0.52 g, $3.71\cdot10^{-3}$ mol) were dissolved in a solution composed by 16 mL of toluene, 5 mL of ethanol, and 8 mL of water. The reaction mixture was refluxed 4 h until the complete consumption of the starting porphyrin which was monitored by TLC (SiO_2, 1% MeOH in CH_2Cl_2). The resulting biphasic solution was cooled to RT. 50 mL of a saturated aqueous solution of NH_4Cl were added. Then, the aqueous phase was extracted with dichloromethane (3 x 50 mL), and the combined organic phases were washed first with water (50 mL), then with a saturated aqueous solution of sodium bicarbonate (50 mL). The organic phase was dried over sodium sulphate, filtered, and the solvent was removed under reduced pressure. The so-obtained solid was purified by flash chromatography (silica gel, 15 µm, 0.5% MeOH in CH_2Cl_2) to obtain the desired product (yield: 35 %). The collected analytical data are in accordance with those reported in literature.[271]

^{1}H NMR (500 MHz, $CDCl_3$): δ 9.07 (t, 2H, *J* = 8 Hz, $H_{Ar\text{-}meso}$), 9.00 (s, 2H, $H_{\beta pyrr}$), 8.95 (s, 2H, $H_{\beta pyrr}$), 8.94 (d, 2H, *J* = 4 Hz, $H_{\beta pyrr}$), 8.90 (t, 2H, *J* = 8 Hz, $H_{Ar\text{-}meso}$), 8.88 (d, 2H, *J* = 4 Hz, $H_{\beta pyrr}$), 7.98 (dd, 2H, *J* = 8.0, 1.0 Hz, $H_{Ar\text{-}meso}$), 7.89 (dt, 2H, *J* = 8.0, 1.0 Hz $H_{Ar\text{-}meso}$), 7.86 (dt, 2H, *J* = 8.0, 1.0 Hz, $H_{Ar\text{-}meso}$), 7.85 (s, 2H, H_{NHCO}), 7.83 (dd, 2H, *J* = 8.0, 1.0 Hz, $H_{Ar\text{-}meso}$), 7.70 (d, 4H, *J* = 8.0 Hz, $H_{Ar\text{-}binap}$), 7.64 (s, 2H, $H_{Ar\text{-}binap}$), 7.63 (s, 2H, $H_{Ar\text{-}binap}$), 7.62 (s, 2H, H_{NHCO}), 7.51 (dt, 2H, *J* = 8.0, 1.0 Hz, $H_{Ar\text{-}meso}$), 7.49 (dt, 2H, *J* = 8.0, 1.0 Hz, $H_{Ar\text{-}meso}$), 7.32 (s, 2H, $H_{Ar\text{-}strap}$), 7.30 - 7.24 (m, 2H, $H_{Ar\text{-}binap}$), 7.19 (s, 2H, $H_{Ar\text{-}strap}$), 7.10 - 7.03 (m, 2H, $H_{Ar\text{-}binap}$), 6.90 (d, 2H, *J* = 8.0 Hz, $H_{Ar\text{-}binap}$), 6.83 (d, 2H, *J* = 8.0 Hz, $H_{Ar\text{-}binap}$), 6.67 (d, 2H, *J* = 8.0 Hz, $H_{Ar\text{-}strap}$), 6.39 (d, 2H, *J* = 8 .0Hz, $H_{Ar\text{-}strap}$), 6.12 (t, 2H, *J* = 8.0 Hz, $H_{Ar\text{-}strap)}$, 5.98 (t, 2H, *J* = 8.0 Hz, $H_{Ar\text{-}strap)}$, 5.91 (d, 2H, *J* = 8.0 Hz, $H_{Ar\text{-}strap}$), 5.78 (d, 2H, *J* = 8.0 Hz, $H_{Ar\text{-}strap}$), 3.87 (d, 2H, *J* = 8.0 Hz, H_{CH2}), 3.72 (d, 2H, *J* = 8.0 Hz, H_{CH2}), 3.66 (d, 2H, *J* = 8.0 Hz, H_{CH2}), 3.55 (d, 2H, *J* = 8.0 Hz, H_{CH2}), 2.42 (s, 6H, H_{OCH3}), 1.89 (s, 6H, H_{OCH3}),and -2.64 ppm (s, 2H, NH_{pyr}).

2.11 Synthesis of 5-(2-(3-(butyl)$_3$ammoniumpropoxy)phenyl)-10,15,20-trispentafluorophenylporphyrin chloride (58)

2.11.1 Synthesis of 5-(2-(3-bromopropoxy)phenyl)-10,15,20-trispentafluorophenylporphyrin

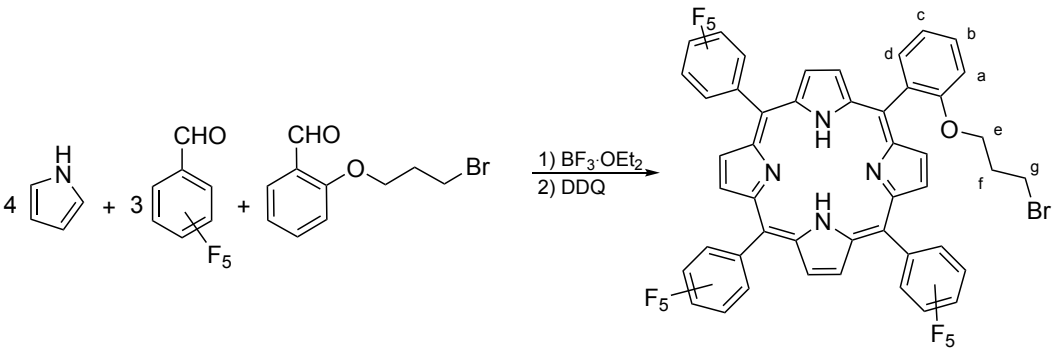

Reaction under nitrogen atmosphere. Dry pyrrole (0.17 g, 2.50 x 10^{-3} mol), 2-(3-bromopropoxy)benzaldehyde (0.15 g, 6.2 x 10^{-4} mol) and pentafluorobenzaldehyde (0.37 g, 1.87 x 10^{-3} mol) were dissolved in dry dichloromethane (250 mL). The reaction flask was protected from light and $BF_3{\cdot}OEt_2$ (0.035 g, 2.5 x 10^{-4} mmol) was added. The so-obtained pale orange solution was stirred for 3 h at RT. Then, p-chloranil (0.61 g, 2.5 x 10^{-3} mol) was added and the reaction mixture was refluxed for 6 h in air. The solvent was removed under reduced pressure obtaining a black solid which was purified by flash column chromatography on silica gel (60 µm, gradient from hexane to hexane/CH_2Cl_2 = 90:10) yielding the desired product as a purple solid (yield: 20%). The collected analytical data are in accordance with those reported in literature.[287]

^{1}H NMR (400 MHz, $CDCl_3$) δ: 8.97 (d, *J* = 4.7 Hz, 2H, $H_{\beta pyrr}$), 8.91 (s, 4H, $H_{\beta pyrr}$), 8.84 (d, *J* = 4.7 Hz, 2H, $H_{\beta pyrr}$), 8.08 (dd, *J* = 7.4 , 1.5 Hz, 1H, H_d), 7.83 (t, *J* = 8.1 Hz, 1H, H_b), 7.44 (t, *J* = 7.6 Hz, 1H, H_c), 7.38 (d, *J* = 8.1 Hz, 1H, H_a), 4.10 (t, *J* = 5.4 Hz, 2H, H_e), 2.26 (t, *J* = 6.0 Hz, 2H, H_g), 1.50 -1.40 (m, 2H, H_f), -2.81 (s, 2H, NH_{pyrr}).

2.11.2 Synthesis of 5-(2-(3-(butyl)$_3$ammoniumpropoxy)phenyl)-10,15,20-trispentafluorophenylporphyrin chloride (58)

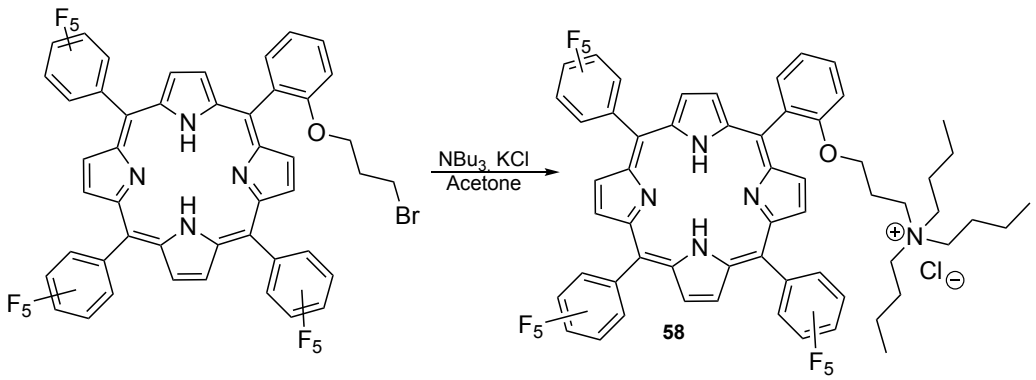

Reaction under nitrogen atmosphere. 5-(2-(3-Bromopropoxy)phenyl-10,15,20-trispentafluorophenylporphyrin (0.10 g, 1.33 x 10^{-3} mol), potassium chloride (0.99 g, 1.33 x 10^{-3} mol) and tributylamine (0.25 g, 1.33 x 10^{-3} mol) were dissolved in freshly distilled acetone (10 mL). The reaction mixture was refluxed for 72 h and the formation of the desired product was checked by TLC (SiO_2, 3% methanol in CH_2Cl_2). Then, the solvent was evaporated to dryness under reduced pressure to obtain a reddish solid. The so-obtained reaction crude was purified by flash chromatography (SiO_2, gradient from CH_2Cl_2 to CH_2Cl_2/methanol 95:5) to obtain the desired product as a purple solid (yield: 25%).

^{1}H NMR (400 MHz, $CDCl_3$): δ 9.01 - 9.00 (m, 2H, $H_{\beta pyrr}$), 8.93 - 8.92 (m, 6H, $H_{\beta pyrr}$), 8.05 - 8.03 (m, 1H, H_{Ar}), 7.88 - 7.83 (m, 1H, H_{Ar}), 7.56 - 7.41 (m, 2H, H_{Ar}), 1.58 - 1.53 (m, 2H, H_{CH2}) 1.47 - 1.38 (m, 10H, H_{CH2}) -0.23 (t, *J* = 6.9 Hz, 9H, H_{CH3}), -0.33 - -0.47(m, 12H, H_{CH2}), -2.88 ppm (s, 2H, NH_{pyrr}). **^{19}F NMR** (376 MHz, $CDCl_3$) δ -136.39 (m, 3F), -137.54 (dd, *J* = 24.6, 8.5 Hz, 1F), -137.79 (m, 2F), -150.71 (t, *J* = 20.9 Hz, 2F), -151.00 (t, *J* = 20.9 Hz, 1F), -160.62 (td, *J* = 22.4, 8.4 Hz, 2F), -160.77 - -161.08 (m, 3F), -161.29 ppm (td, *J* = 22.4, 8.4 Hz, 1F). **^{13}C NMR** (101 MHz, $CDCl_3$) δ 157.67, 147.82, 145.35, 143.65, 141.09, 138.91, 136.45, 134.87, 131.32, 129.76, 121.05, 119.52, 115.48, 113.47, 102.98, 102.32, 77.34, 64.80, 57.08, 54.39, 22.36, 21.85, 17.85, 12.26 ppm. **LR-MS (ESI)**: m/z calcd for ($C_{59}H_{47}ClF_{15}N_5O$): 1162.49, found 1126.6 [M^+], 35.4 [X^-]. **Elemental Analysis** calcd. for ($C_{59}H_{47}ClF_{15}N_5O$): C (60.96), H (4.08), N (6.02), found: C (61.78), H (4.95), N (6.65). **UV-Vis** λmax (DCM)/nm (log ε): 414 (5.18), 508

(4.00), 539 (3.17) 584 (3.52) 637 (2.89). **IR** ν_{max} (DCM)/cm^{-1}: 3322, 3058, 2986, 2961, 2931, 2874, 2860, 1650, 1519, 1499, 1482, 1266, 990. **MP**> 350 °C.

2.12 Synthesis of $TPPH_2$@SBA-15 (71)

2.12.1 Synthesis 3-azidopropyltriethoxy silane (69)

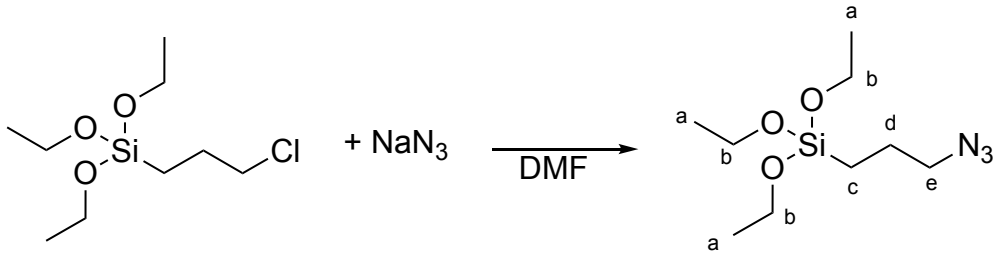

Reaction under argon atmosphere. 3-Chloropropyltriethoxysilane (3.00 g, 1.25 x 10^{-2} mol) was dissolved in dry DMF (25 mL). Sodium azide (4.05 g, 6.23 x 10^{-2} mol) was suspended in the solution and the reaction mixture was stirred for 3 days at 50 °C. The sodium azide was rapidly filtered, then water (50 mL) and ethyl acetate (50 mL) were added to the solution. The two phases were separated and the aqueous one was extracted with ethyl acetate (4 x 50 mL). The organic phases were dried over sodium sulphate, filtered, and the solvent was removed under reduced pressure. The obtained pale-yellow oil was stored under argon at 5 °C (yield: 48%). The collected analytical data are in accordance with those reported in literature.[288]

^{1}H NMR (500 MHz, $CDCl_3$): δ 3.80 (q, 6H, *J* = 6.9 Hz, H_a), 3.25 (t, 2H, *J* = 7.2 Hz, H_c), 1.66 - 1.73 (m, 2H, H_d), 1.21 (t, 9H, *J* = 6.9 Hz, H_b), 0.66 ppm (t, 2H, *J* = 8.2 Hz, H_e).

2.12.2 Synthesis of azide functionalized SBA-15 silica N3@SBA-15 (68)

Pluronic P123 (8.00 g, 1.37 x 10^{-3} mol) was added in a solution 2.00 M of HCl in water (250 mL) and the resulting mixture was heated to 40 °C. The solution was stirred till the complete dissolution of the polymer, then tetraethoxysilane (TEOS) (16.77 g, 8.05 x 10^{-2} mol) was added dropwise. The reaction mixture was stirred 30 minutes, then 3-azidopropyltriethoxysilane (1.00 g, 3.99 x 10^{-3} mol) was added and the solution was stirred at 40 °C for 24 h. Then, the reaction mixture was transferred into a steal autoclave

and aged for 24 h at 100 °C. The autoclave was cooled to RT and the resulting white solid was collected in a filter, washed first with slightly acidic water, then with ethanol, and finally dried for 15 h at 60 °C in the oven. The so-obtained powder was further purified by Soxhlet extraction using acetonitrile for 48 h to remove Pluronic P123. The final product was obtained as a white powder after a further drying at 80 °C in the oven for 12 h.

2.12.3 Synthesis of 4-(3-methyl-3-hydroxybut-1-yn-1yl) benzaldehyde

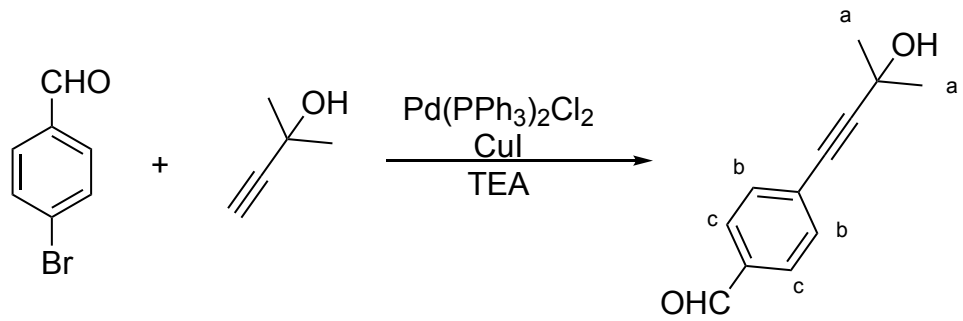

Reaction under argon atmosphere. 4-Bromobenzaldehyde (3.00 g, 1.62 x10^{-2} mol), $Pd(PPh_3)_2Cl_2$ (0.11 g, 1.70 x 10^{-4} mol) and CuI (0.016 g, 8.4 x 10^{-5} mol) were dissolved in freshly distilled TEA (32 mL). Then, 2-methylbut-3-yn-2-ol (1.63 g, 1.94 x 10^{-2} mol) was added. The reaction mixture was stirred for 2 h at 40 °C, then, the solvent was removed under reduced pressure. The crude was purified by flash chromatography (SiO_2, gradient from hexane/CH_2Cl_2 8:2 to CH_2Cl_2) and the product was obtained as a pale-yellow oil (yield: 62%). The collected analytical data are in accordance with those reported in literature.[289]

^{1}H NMR (400 MHz $CDCl_3$): δ 9.02 (s, 1H, H_{CHO}), 7.79 (d, *J* = 8.1 Hz, 2H, H_c), 7.52 (d, J = 8.1 Hz, 2H, H_d), 1.61 (s, 6H, H_{Me}), 2.23 ppm (br s, 1H, OH).

2.12.4 5-(4-ethynylphenyl)-10,15,20-triphenylporphyrin EtTPPH$_2$

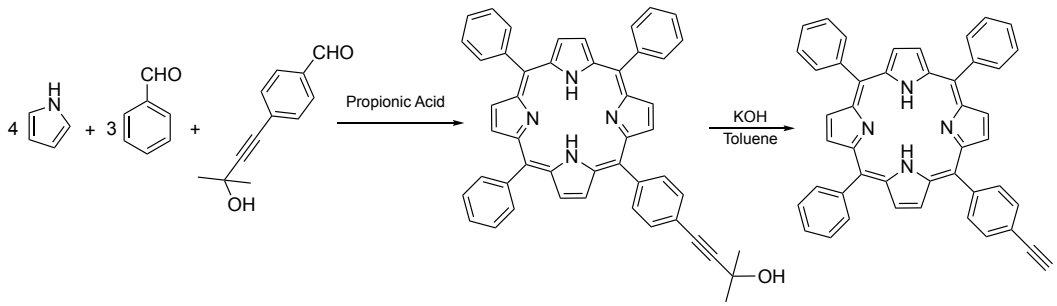

4-(3-Hydroxy-3-methyl-1-butynyl)-benzaldehyde (0.92 g, 4.88 x 10^{-3} mmol) and benzaldehyde (1.56 g, 1.47 10 x 10^{-2} mol) were dissolved in propionic acid (50 mL). The solution was heated to reflux, then pyrrole (1.32 g, 1.95 x 10^{-2} mol) was added over 5 min. The reaction mixture was stirred at reflux for 3 h. The solvent was removed under reduced pressure, then the crude was purified by flash chromatography (SiO_2, gradient elution from *n*-hexane to *n*-hexane/dichloromethane 7:3) as the second spot. The obtained reddish solid was dissolved in dry toluene under argon, potassium hydroxide (6.00 g, 0.11 mol) was added, and the reaction mixture was refluxed for 4 h to remove the ethynyl protecting group. Brine (50 mL) was added, and the organic phase was extracted with brine (3 x 50 mL). The organic phases were dried over sodium sulphate and the solvent was removed to dryness under reduced pressure. The so-obtained solid was purified by flash chromatography (SiO_2, gradient from hexane/CH_2Cl_2 7:3 to hexane/ CH_2Cl_2 1:1) and the desired product was obtained as a reddish solid (yield: 17%). The collected analytical data are in accordance with those reported in literature.[290]

^{1}H NMR (300 MHz, $CDCl_3$): δ 8.85 (m, 8H, $H_{\beta pyrr}$), 8.20 (m, 8 H, H_{Ar}), 7.89 (d, *J* = 8.1 Hz, 2 H, H_{Ar}), 7.77 (m, 9 H, H_{Ar}), 3.32 (s, 1H, $H_{ethynyl}$), -2.80 ppm (s, 2H, NH).

2.12.5 Zn(5-(4-ethynylphenyl)-10,15,20-triphenylporphyrin) ZnEtTPP (70)

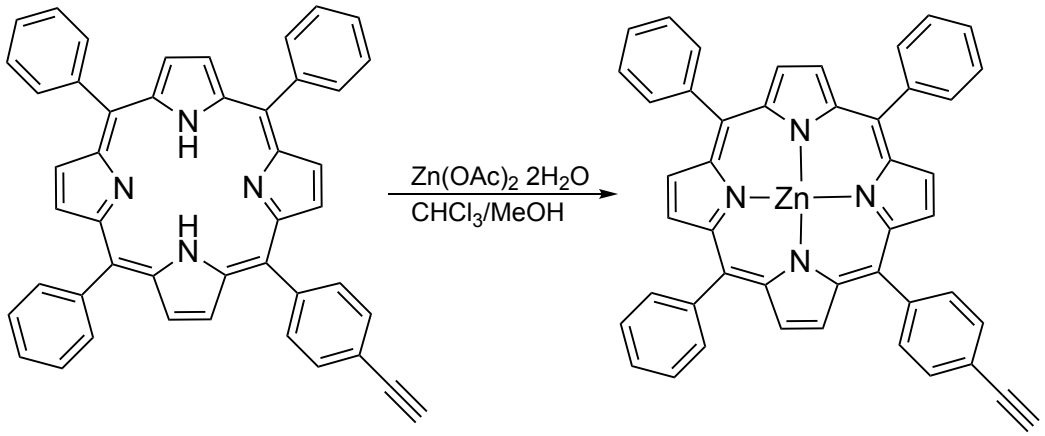

$EtTPPH_2$ (0.25 g, 3.90 x 10^{-4} mmol) was dissolved in chloroform (65 mL) and a methanol (35 mL) solution of zinc acetate dihydrate (0.87 g, 3.95 x 10^{-3} mol) was added. The reaction mixture was refluxed 3 h then, the solvents was removed under reduced pressure. The crude was dissolved in dichloromethane (30 mL) and the solution was washed with water (3 x 30 mL). The organic phase was dried over sodium sulphate, filtered and the solvent was removed under reduced pressure to obtain the desired product as a bright pink powder (yield: 100%).

^{1}H NMR (300 MHz, $CDCl_3$) δ 9.56 - 8.58 (m, 8H, $H_{\beta pyrr}$), 8.39 - 8.06 (m, 8H, $H_{Ar\text{-}o}$), 7.97 - 7.83 (m, 2H, $H_{Ar\text{-}ortoEthynyl}$), 7.83 - 7.68 (m, 9H, $H_{Ar\text{-}m+p}$), 3.31 ppm (s, 1H, $H_{Ethynyl}$). **^{13}C NMR** (75 MHz, $CDCl_3$) δ 150.34, 150.30, 150.24, 149.82, 143.54, 142.74, 142.72, 134.44, 134.37, 132.26, 132.15, 132.11, 131.69, 130.42, 129.86, 127.58, 126.61, 121.44, 121.35, 121.33, 119.99, 83.79, 78.17 ppm. **LR-MS (ESI)**: m/z ($C_{46}H_{28}N_4Zn$) calcd 700.16, found $[M]^+$ 700.38. **Elemental Analysis** calcd. for ($C_{46}H_{28}N_4Zn$): C (78.69), H (4.02), N (7.98), found: C (78.87), H (4.86), N (7.51). **UV-Vis** λ_{max} (DCM)/nm (log ε): 420 (5.42), 548 (4.11), 587 (3.49). **IR** ν_{max} (DCM)/cm^{-1}: 718, 796, 810, 994, 1002, 1069, 1338 (C-N), 1340 (C-N), 2852, 2921, 3399 (C-H alkyne).

2.12.6 Synthesis of $TPPH_2$@SBA-15 (71)

N_3@SBA-15 (1.00 g, 2.4 x 10^{-4} mol of azide) was suspended in dry toluene (40 mL) under argon atmosphere. Then ZnEtTPP (0.34 g, 4.8 x 10^{-4} mol) and TEA (0.61 g, 6.00 x 10^{-3} mol)

were added to the suspension. The reaction mixture was stirred for 30 minutes at RT, then, copper iodide (0.23 g, 1.20 x 10^{-3} mol) was added. The reaction mixture was stirred at RT for 4 days. The obtained purple powder was collected in a filter and washed with THF (3 x 30 mL) to recover the porphyrin in excess. Then, the so-obtained powder was suspended in methanol (40 mL) and *N*,*N*-diethyldithiocarbamate sodium trihydrate (0.90 g, 3.99 x 10^{-3} mol) was added to remove the copper catalyst. The reaction mixture become black, and the so-obtained suspension was stirred for 2 h. Then, the purple-powder was filtrated off and washed firstly with methanol, then with THF, and finally with acetone. In order to remove the zinc atom from the porphyrin core, the solid was washed with a 0.5 M solution of HCl in water (5 x 20 mL). The so-obtained green-powder was further washed with water until it become brown to remove acid traces, then with ethanol and successively with acetone to remove water. Finally, the obtained product was dried overnight at 80 °C in the oven.

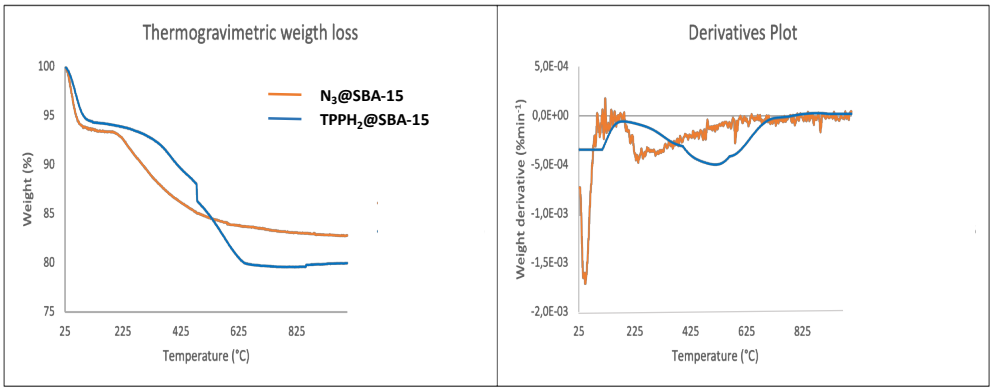

Representative thermogravimetric weight loss curves and derivatives plots for ***N_3@SBA-15*** *and* ***$TPPH_2$@SBA-15****.*

3 ^{1}H, ^{13}C and ^{19}F NMR spectra of unpublished catalysts

Compound (58): ^{1}H NMR (400 MHz, $CDCl_3$)

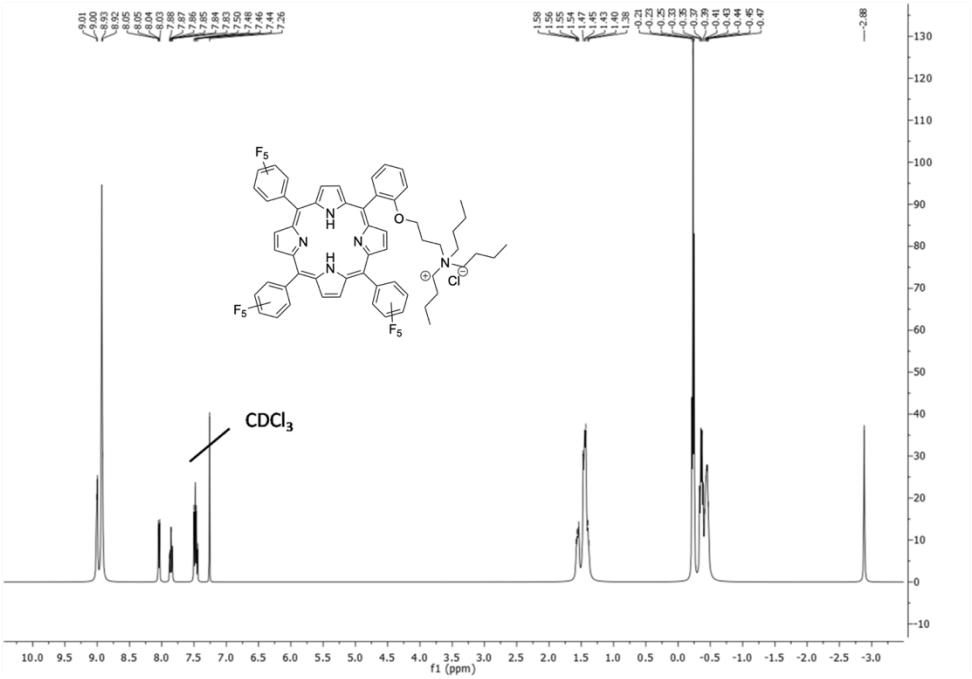

Compound (58): ^{13}C NMR (101 MHz, $CDCl_3$)

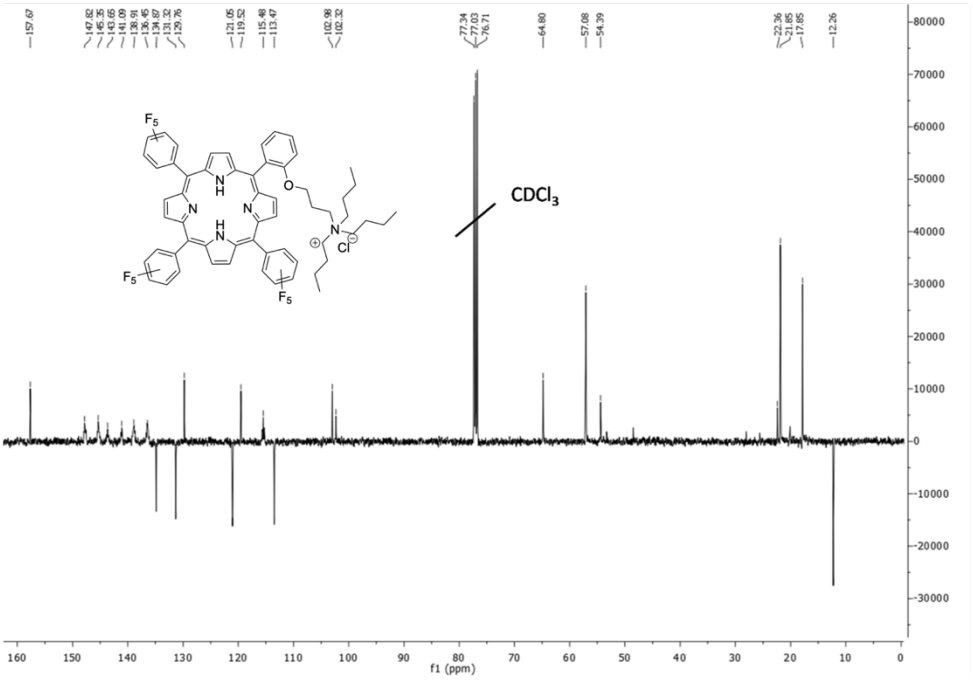

Compound (58): ^{19}F NMR (376 MHz, $CDCl_3$)

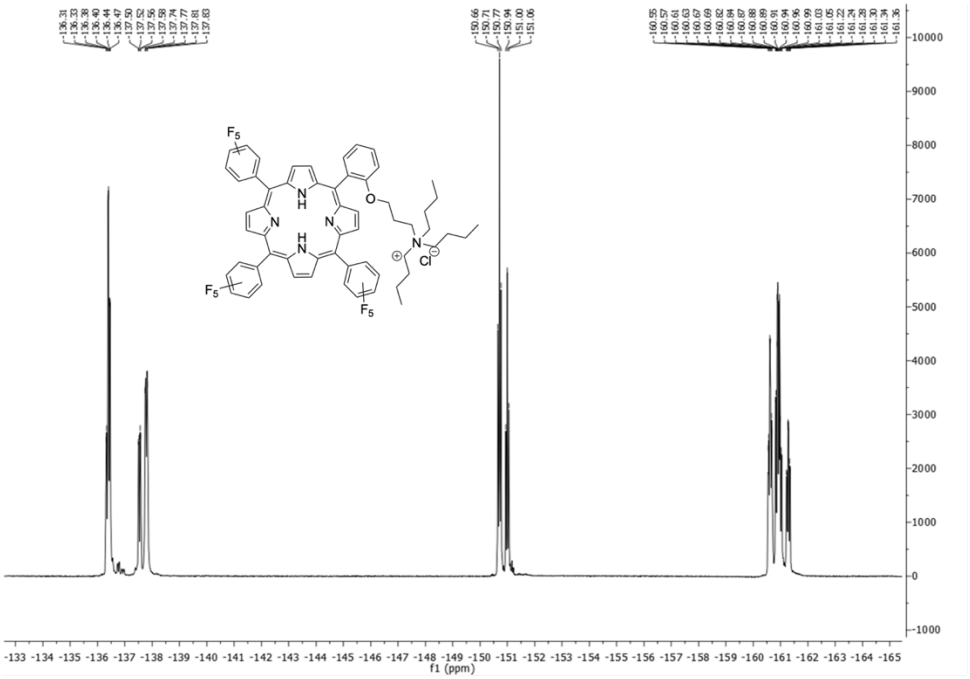

Compound (70): ^{1}H NMR (300 MHz, $CDCl_3$)

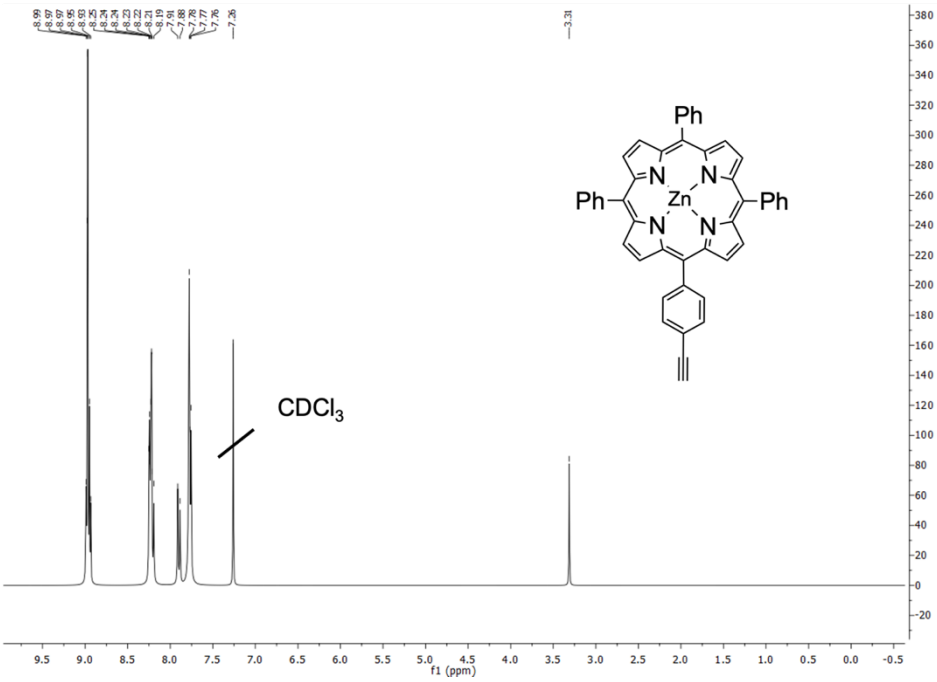

Compound (70): ^{1}H NMR (300 MHz, $CDCl_3$)

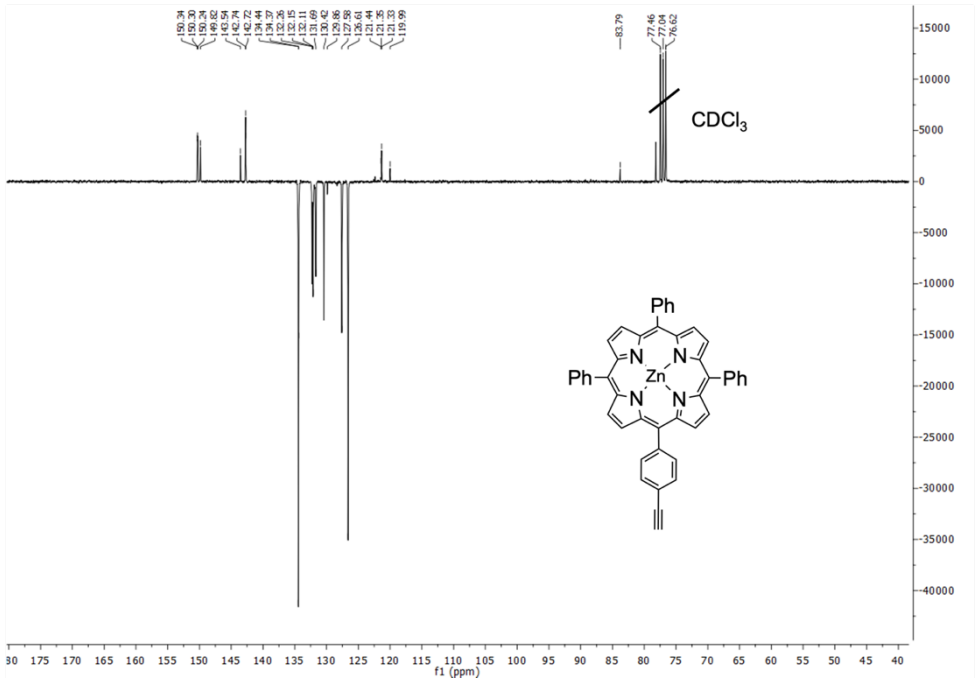

4 Synthesis of *N*-aryl aziridines

4.1 Synthesis of aril azides

4.1.1 General procedure

The desired aniline (9.98 x 10^{-2} mol) was dissolved in a HCl water solution 18.5% (100 mL). The reaction mixture was cooled to 0 °C in an ice bath and a solution of sodium nitrite (6.90 g, 0.10 mol) in water (25 mL) was added dropwise. The so-obtained reaction mixture was stirred for 2 h. Then, urea (0.66 g, 1.10 x 10^{-2} mol) was added in one portion. A sodium azide (6.5 g, 0.10 mol) solution in water (30 mL) was added dropwise in about 30 minutes under vigorous stirring. The reaction was stirred for further 30 minutes at 0°C and for additional 3 h at RT. The aqueous phase was extracted with diethyl ether (3 x 50 mL) and the so-obtained organic phase was dried over sodium sulphate, filtered, and the solvent was removed under reduced pressure to obtain the desired product.

4.1.2 Synthesis of 3,5-*bis*-(trifluoromethyl) phenylazide

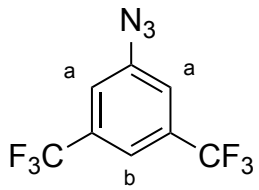

The product was obtained as an orange oil from 3,5-*bis*-(trifluoromethyl)aniline (yield: 83%). The collected analytical data were in accordance with those reported in literature.[291]

^{1}H NMR (300 MHz, $CDCl_3$): δ 7.64 (s, 1H, H_b), and 7.44 ppm (s, 2H, H_a).

4.1.3 Synthesis of 4-*tert*-butylphenylazide

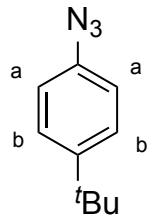

The product was obtained as a reddish oil from 4-*tert*-butyl phenylaniline (yield: 92%). The collected analytical data were in accordance with those reported in literature.[291]

^{1}H NMR (300 MHz, $CDCl_3$): δ 7.37 (d, *J* = 7.2, Hz 2H, H_b), 6.98 (d, *J* = 7.2 Hz, 2H, H_a), and 1.32 ppm (s, 9H, H_{tBu}).

4.1.4 Synthesis of 4-bromophenylazide

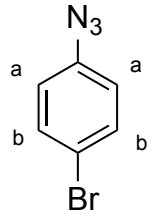

The product was obtained as a pale brown solid from 4-bromophenyl aniline (yield: 83%). The collected analytical data were in accordance with those reported in literature.[292]

^{1}H NMR (300 MHz, $CDCl_3$) δ 7.46 (d, *J* = 8.8 Hz, 2H, H_b) and 6.90 ppm (d, *J* = 8.8 Hz, 2H, H_a).

4.1.5 Synthesis of 4-chlorophenylazide

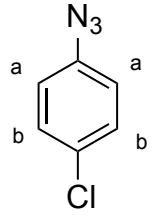

The product was obtained as an opalescent yellow oil from 4-chlorophenyl aniline (yield: 88%). The collected analytical data were in accordance with those reported in literature.[292]

^{1}H NMR (400 MHz, $CDCl_3$) δ 7.31 (d, *J* = 8.7 Hz, 2H, H_b) and 6.96 ppm (d, *J* = 8.7 Hz, 2H, H_a).

4.1.6 Synthesis of 3,5-dichlorophenylazide

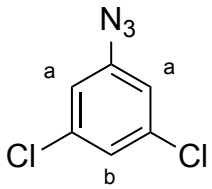

The product was obtained starting as a light brown solid from 3,5-dichlorophenyl aniline (yield: 88%). The collected analytical data were in accordance with those reported in literature.[293]

^{1}H NMR (300 MHz, $CDCl_3$): δ 7.13 (s, 1H, H_b) and 6.91 ppm (s, 2H, H_a).

4.1.7 Synthesis of 2-nitrophenylazide

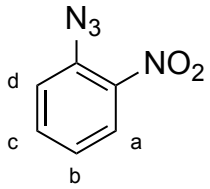

The product was obtained as a yellow powder from 2-nitrophenyl aniline (yield: 84%). The collected analytical data were in accordance with those reported in literature.[291]

^{1}H NMR (300 MHz, $CDCl_3$) δ 7.98 - 7.84 (m, 1H, H_a), 7.63 (pst, *J* = 7.8 Hz, 1H, H_c), 7.40 - 7.25 (m, 1H, H_d), and 7.26 ppm (pst, *J* = 7.8 Hz, 1H, H_b).

4.1.8 Synthesis of 4-nitrophenylazide

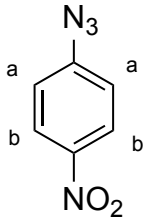

The product was obtained as a yellow powder from 4-nitrophenyl aniline (yield: 87%). The collected analytical data were in accordance with those reported in literature.[291]

^{1}H NMR (300 MHz, C_6D_6) δ 7.62 (d, *J* = 9.1 Hz, 2H, H_b) and 6.15 ppm (d, *J* = 9.1 Hz, 2H, H_a).

4.1.9 Synthesis of 3,5-dinitrophenylazide

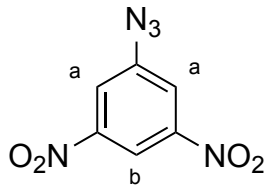

The product was obtained as a yellow powder from 3,5-dinitrophenyl aniline (yield: 89%). The collected analytical data were in accordance with those reported in literature.[267]

^{1}H NMR (400 MHz, $CDCl_3$): δ 8.80 (s, 1H, H_b) and 8.19 ppm (s, 2H, H_a).

4.1.10 Synthesis of 4-methoxyphenylazide

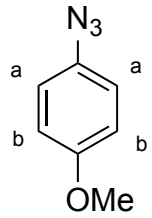

The product was obtained as a deep red oil from 4-methoxyphenyl aniline (yield: 68%). The collected analytical data were in accordance with those reported in literature.[291]

^{1}H NMR (400 MHz, C_6D_6) δ 6.80 (d, *J* = 8.5 Hz, 2H, H_b), 6.68 (d, *J* = 8.5 Hz, 2H, H_a), and 3.35 ppm (s, 3H, H_{OMe}).

4.1.11 Synthesis of 3-methoxyphenylazide

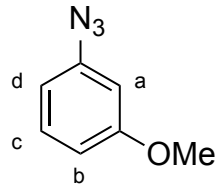

The product was obtained as a red oil from 3-methoxyphenyl aniline (yield: 62 %). The collected analytical data were in accordance with those reported in literature.[294]

^{1}H NMR (400 MHz, $CDCl_3$) δ 7.28 (pst, *J* = 8.1 Hz, 1H, H_c), 6.78 - 6.64 (m, 2H, H_{b+d}), 6.61 - 6.55 (m, 1H, H_a), and 3.83 ppm (s, 3H, H_{OMe}).

4.2 Synthesis of *N*-aryl aziridines

4.2.1 General procedure

Reactions performed under nitrogen atmosphere. [Ru(TPP)(CO)] (0.25 g, 3.37 x 10^{-5} mol), the desired styrene (8.40 x 10^{-3} mol) and the desired aryl azide (1.68 x 10^{-3} mol) were refluxed in dry benzene (50 mL). When the starting aryl azide was completely consumed, the reaction solvent was removed under reduced pressure and the desired product was isolated by flash-chromatography (silica gel, hexane/ethyl acetate 9:1, 0.5% of triethylamine was added in order to deactivate the silica).

4.2.2 Synthesis of 1-(3,5-*bis*-trifluoromethylphenyl)-2-phenylaziridine (2)

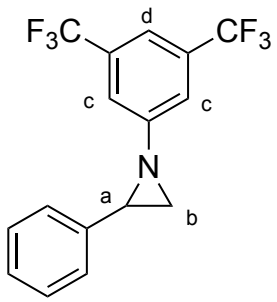

The product was obtained as a purple-brown solid by refluxing 3,5-*bis*-trifluoromethylphenylazide and styrene for 2 h (yield: 99 %). The collected analytical data were in accordance with those reported in literature.[267]

^{1}H NMR (300 MHz, $CDCl_3$) δ 7.49 (s, 1H, H_d), 7.44 (s, 2H, H_c), 7.39 - 7.36 (m, 5H, H_{Ph}), 3.24 (dd, *J* = 6.6, 3.3 Hz, 1H, H_a), 2.57 (d, *J* = 6.6 Hz, 1H, H_b), 2.54 ppm (d, *J* = 3.3 Hz, 1H, $H_{b'}$).

4.2.3 Synthesis of 1-(4-nitrophenyl)-2-phenyilaziridine (5)

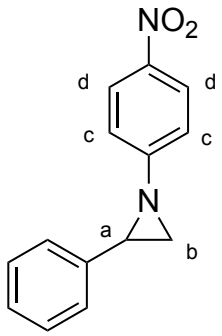

The product was obtained as a yellow powder by refluxing 4-nitrophenylazide and styrene for 1 h (yield: 93%). The collected analytical data were in accordance with those reported in literature.[267]

^{1}H NMR (400 MHz, $CDCl_3$) δ 8.14 (d, *J* = 9.0 Hz, 2H, H_d), 7.40 - 7.32 (m, 5H, H_{Ph}), 7.10 (d, *J* = 9.0 Hz, 2H, H_c), 3.25 (dd, *J* = 6.4, 2.6 Hz, 1H, H_a), 2.58 (d, *J* = 6.4 Hz, 1H, H_b), 2.55 ppm (d, *J* = 2.6 Hz, 1H, $H_{b'}$).

4.2.4 Synthesis of 1-(3,5-*bis*-(trifluoromethyl)phenyl)-2-(4-methylphenyl) aziridine (7)

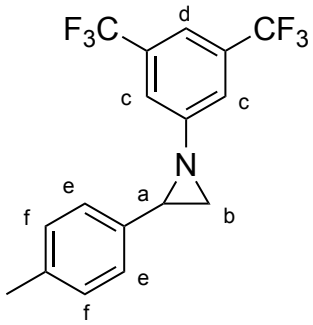

The product was obtained as a purple-brown solid by refluxing 3,5-*bis*-trifluoromethylphenylazide and 4-methylstyrene for 4 h (yield: 98%).

^{1}H NMR (300 MHz, $CDCl_3$) δ 7.49 (s, 1H, H_d), 7.44 (s, 2H, H_c), 7.29 (d, *J* = 8.0 Hz, 2H, H_f), 7.21 (d, *J* = 8.0 Hz, 2H, H_e), 3.21 (dd, *J* = 6.4, 3.6 Hz, 1H, H_a), 2.55 (d, *J* = 6.4 Hz, 1H, H_b), 2.53 (d, *J* = 3.6 Hz, 1H, $H_{b'}$), 2.39 ppm (s, 3H, H_{Me}). **^{13}C NMR** (75 MHz, $CDCl_3$) δ 156.28 (C), 138.12 (C), 135.24 (C), 132.82 (q, *J* = 33.3 Hz, two overlapping CF_3), 129.75 (two overlapping CH), 126.42 (two overlapping CH), 125.42 (C), 121.81 (C), 121.05 (two overlapping CH), 116.30, (CH), 42.35 (CH), 38.27 (CH_2), 21.51 ppm (CH_3). **^{19}F NMR** (282 MHz, $CDCl_3$) δ -63.32 ppm (s). **LR-MS (ESI):** m/z ($C_{17}H_{13}F_6N$) calcd 345.10, found $[M+H]^+$ 346.25. **Elemental Analysis** calcd. for $C_{17}H_{13}F_6N$: C (59.13), H (3.79), N (4.06), found: C (58.83), H (3.55), N (4.14). **UV-Vis** λ_{max} (DCM)/nm (log ε): 248 (4.35). **IR** ν_{max} (DCM)/cm^{-1}: 1004, 1136, 1179, 1244, 1391, 1465, 1613, 3685.

4.2.5 Synthesis of 1-(3,5-*bis*-(trifluoromethyl)phenyl)-2-(4-*tert*-butylphenyl) aziridine (9)

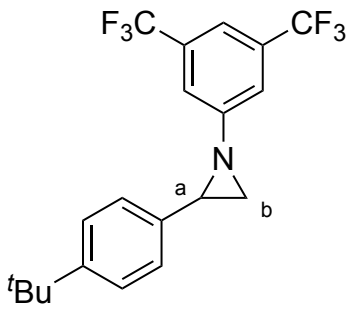

The product was obtained as a brown oil by refluxing 3,5-*bis*-trifluoromethylphenylazide and 4-*tert*-butyl styrene for 4 h (yield: 95%).

^{1}H NMR (400 MHz, $CDCl_3$) δ 7.49 - 7.32 (m, 7H, H_{Ar}), 3.23 (dd, *J* = 6.0, 3.2 Hz, 1H, H_a), 2.57 - 2.55 (m, 2H, H_b), 1.36 ppm (s, 9H, H_{tBu}). **^{13}C NMR** (100 MHz, $CDCl_3$) δ 155.90 (C), 151.08 (C), 134.84 (C), 132.41 (q, *J* = 33.3 Hz, two overlapping CF_3), 126.87 (CH), 125.73 (CH), 124.58 (C), 121.87 (C), 120.70 (CH), 115.90 (CH), 112.97 (C), 112.35 (CH), 41.88 (CH), 37.88 (CH_2), 34.60 (C), 31.33 ppm (three overlapping CH_3). **^{19}F NMR** (376 MHz, $CDCl_3$) δ -62.98 ppm (s). **LR-MS (ESI):** m/z ($C_{20}H_{19}F_6N$) calcd 387.14, found $[M+H]^+$ 388.27. **Elemental Analysis** calcd. for ($C_{20}H_{19}F_6N$): C (62.01), H (4.94), N (3.62), found: C (62.27), H (5.33), N (3.54). **UV-Vis** λ_{max} (DCM)/nm (log ε): 249 (4.26). **IR** ν_{max} (DCM)/cm^{-1}: 947, 1002, 1135, 1180, 1376, 1391, 1466, 1614, 1616.

4.2.6 Synthesis of 1-(4-nitrophenyl)-2-(4-methylphenyl) aziridine (11)

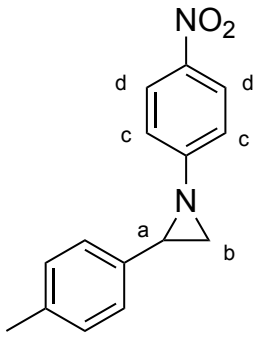

The product was obtained as a yellow powder by refluxing 4-nitrophenylazide and 4-methyl styrene for 2 h (yield: 90%). The collected analytical data were in accordance with those reported in literature.[267]

^{1}H NMR (300 MHz, $CDCl_3$) δ 8.14 (d, *J* = 9.0 Hz, 2H, H_d), 7.26 - 7.20 (m, 4H, H_{Ar}), 7.09 (d, *J* = 9.0 Hz, 2H, H_c), 3.21 (dd, *J* = 6.3, 3.3 Hz, 1H, H_a), 2.56 - 2.52 (m, 2H, H_b), 2.37 ppm (s, 3H, H_{Me}).

4.2.7 Synthesis of 1-(3,5-*bis*-(trifluoromethyl)phenyl)-2-(4-bromophenyl) aziridine (13)

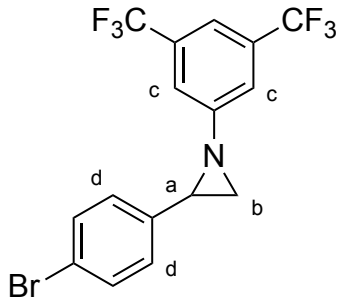

The product was obtained as a brown oil by refluxing 3,5-*bis*-trifluoromethylphenylazide and 4-bromostyrene for 3 h. (yield: 77%). The collected analytical data were in accordance with those reported in literature.[295]

^{1}H NMR (300 MHz, $CDCl_3$) δ 7.52-7.49 (m, 3H, H_{Ar}), 7.41 (s, 2H, H_c), 7.27 - 7.25 (m, 2H, H_d), 3.19 (dd, *J* = 4.8, 2.6 Hz, 1H, H_a) 2.56 (dd, *J* = 4.8, 0.6 Hz, 1H, H_b), 2.48 ppm (dd, *J* = 2.6, 0.6 Hz, 1H, $H_{b'}$).

4.2.8 Synthesis of 1-(3,5-*bis*-(trifluoromethyl)phenyl)-2-(2,3,4,5,6-pentafluorophenyl) aziridine (15)

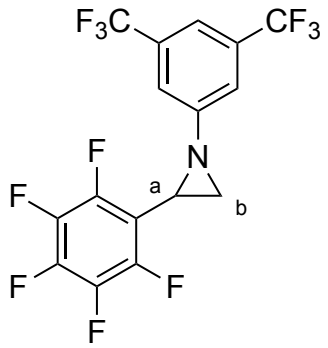

The product was obtained as a light brown solid by refluxing 3,5-*bis*-trifluoromethylphenylazide and 2,3,4,5,6-pentafluoro styrene for 4 h (yield: 97%). **^{1}H NMR** (300 MHz, $CDCl_3$) δ 7.55 (s, 3H, H_{Ar}), 3.29 (dd, *J* = 6.3, 3.6 Hz, 1H, H_a), 2.96 (d, *J* = 3.6 Hz, 1H, H_b), 2.63 ppm (d, *J* = 6.6 Hz, 1H, $H_{b'}$). **^{13}C NMR** (75 MHz, $CDCl_3$) δ 155.05 (C), 148.13 (m, C-F), 144.83 (m, C-F), 143.29 (m, C-F), 139.90 (m, C- F), 136.39 (m, C-F), 133.10 (q, *J* = 33.4 Hz, two overlapping CF_3), 128.88 (C), 125.27 (C), 121.65 (C), 121.10 (CH), 117.23 (CH), 34.36 (CH), 32.81 ppm (CH_2). **^{19}F NMR** (282 MHz, $CDCl_3$) δ -63.49 (s, 6F, F_{CF3}), -143.14 (d, *J* = 20.3 Hz, 2F, F_o), -153.88 - -154.06 (m, 1F, F_p), -161.86 - -162.01 (m, 2F, F_m). **LR-MS (ESI):** m/z ($C_{16}H_6F_{11}N$) calcd 421.03, found $[M+H]^+$ 422.25. **Elemental Analysis** calcd. for ($C_{16}H_6F_{11}N$): C (45.62), H (1.44), N (3.33), found: C (45.44), H (1.68), N (3.42). **UV-Vis** λ_{max} (DCM)/nm (log ε): 248 (4.35). **IR** ν_{max} (DCM)/cm^{-1}: 1138, 1182, 1395,1465, 1502, 1525,1607, 3599, 3685.

4.2.9 Synthesis of 1-(4-*tert*-butylphenyl)-2-(2,3,4,5,6-pentafluorophenyl) aziridine (17)

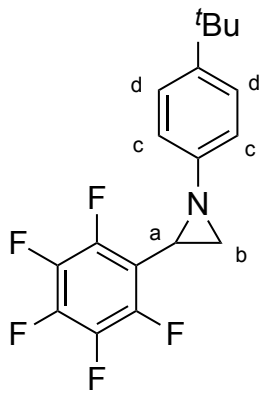

The product was obtained as a brown oil by refluxing 4-*tert*-butylphenylazide and 2,3,4,5,6-pentafluoro styrene for 24 h (yield: 57%).

^{1}H NMR (300 MHz, $CDCl_3$) δ 7.32 (d, *J* = 8.7 Hz, 2H, H_d), 7.08 (d, *J* = 8.7 Hz, 2H, H_c), 3.13 (dd, *J* = 6.3, 3.3 Hz, 1H, H_a), 2.80 (d, *J* = 3.3 Hz, 1H, H_b), 2.49 (d, *J* = 6.3 Hz, 1H, $H_{b'}$), 1.31 ppm (s, 9H, H_{tBu}). **^{13}C NMR** (75 MHz, $CDCl_3$) δ 151.15 (C), 148.25 (m, C-F), 146.55 (C), 144.79 (m, C-F), 142.83 (m, C- F), 139.47 (m, C-F), 136.28 (m, C-F), 126.42 (CH), 126.37 (CH) 122.83 (CH) 120.50 (CH), 34.67 (C), 34.10 (CH_2), 32.27 (CH), 31.82 ppm (three overlapping CH_3). One quaternary carbon was not detected. **^{19}F NMR** (282 MHz, $CDCl_3$) δ -143.02 (dd, *J* = 22.1,

8.0 Hz, 2F, F_o), -155.20 - -155.35 (m, 1F, F_p), - 162.62 - -162.72 ppm (m, $2F_m$). **LR-MS (ESI):** m/z ($C_{18}H_{16}F_5N$) calcd 341.12, found $[M+H]^+$ 342.05. **Elemental Analysis** calcd. for ($C_{18}H_{16}F_5N$): C (63.34), H (4.72), N (4.10), found: C (62.97), H (4.76), N (4.08). **UV-Vis** λ_{max} (DCM)/nm (log ε): 233 (3.14). **IR** ν_{max} (DCM)/cm^{-1}: 909, 915, 920, 1244, 1500, 1523, 1606, 3686.

4.2.10 Synthesis of 1-(4-methoxyphenyl)-2-phenylaziridine (19)

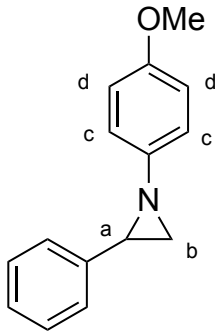

The product was obtained as an orange oil by refluxing 4-methoxyphenylazide and styrene for 6 h (yield 65%). The collected analytical data were in accordance with those reported in literature.[267]

^{1}H NMR (400 MHz, $CDCl_3$) δ 7.36 - 7.28 (m, 5H, H_{Ph}), 6.95 (d, *J* = 8.8 Hz, 2H, H_d), 6.77 (d, *J* = 8.8 Hz, 2H, H_c), 3.73 (s, 3H, H_{OMe}), 3.01 - 2.98 (m, 1H, H_a), 2.37 (d, *J* = 6.3 Hz, 1H, H_b), 2.33 ppm (d, *J* = 2.4 Hz, 1H, $H_{b'}$).

4.2.11 Synthesis of 1-(4-*tert*-butylphenyl)-2-phenylaziridine (21)

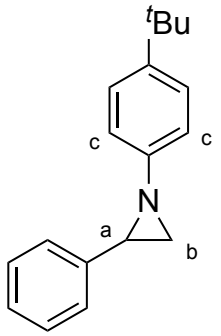

The product was obtained as a brown oil by refluxing 4-*tert*-butylphenylazide and styrene for 4 h (yield: 84%). The collected analytical data were in accordance with those reported in literature.[267]

^{1}H NMR (400 MHz, $CDCl_3$) δ 7.43 - 7.30 (m, 7H, H_{Ar}), 7.03 (d, *J* = 8.4 Hz, 2H, H_c) 3.12 (dd, *J* = 8.8, 4.4 Hz, 1H, H_a), 2.48 (d, *J* = 8.8 Hz, 1H, H_b), 2.41 (d, *J* = 4.4 Hz, 1H, $H_{b'}$), 1.35 ppm (s, 9H, H_{tBu}).

4.2.12 Synthesis of 1-(4-bromophenyl)-2-phenylaziridine (23)

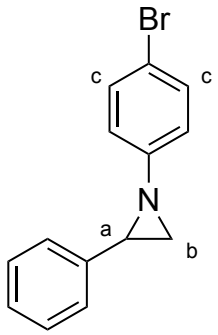

The product was obtained as a light brown solid by refluxing 4-bromophenylazide and styrene for 3 h (yield: 97%). The collected analytical data were in accordance with those reported in literature.[267]

^{1}H NMR (400 MHz, $CDCl_3$) δ 7.36 - 7.32 (m, 7H, H_{Ar}), 6.91 (d, *J* = 11.2 Hz, 2H, H_c), 3.07 (dd, *J* = 8.0, 4.4 Hz, 1H, H_a), 2.42 - 2.40 ppm (m, 2H, H_b).

4.2.13 Synthesis of 1-(4-chlorophenyl)-2-phenylaziridine (25)

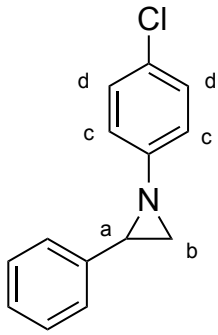

The product was obtained as a brown oil by refluxing 4-chlorophenylazide and styrene for 3 h (yield: 90%). The collected analytical data were in accordance with those reported in literature.[267]

^{1}H NMR (400 MHz, $CDCl_3$) δ 7.37 - 7.36 (m, 5H, H_{Ph}), 7.20 (d, *J* = 8.8 Hz, 2H, H_c), 6.97 (d, *J* = 8.8 Hz, 2H, H_d), 3.08 (dd, *J* = 6.4, 3.6 Hz, 1H, H_a), 2.44 - 2.41 ppm (m, 2H, H_b).

4.2.14 Synthesis of 1-(2-nitrophenyl)-2-phenylaziridine (27)

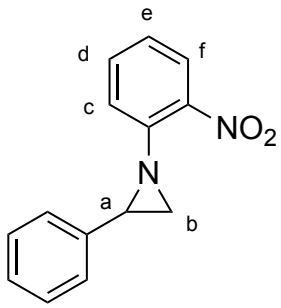

The product was obtained as a yellow oil by refluxing 2-nitrophenylazide and styrene for 4 h (yield: 95%). The collected analytical data were in accordance with those reported in literature.[267]

^{1}H NMR (300 MHz, $CDCl_3$) δ 7.93 (d, *J* = 8.1 Hz, 1H, H_f), 7.46 (pst, *J* = 7.5, Hz 1H, H_d), 7.35 - 7.24 (m, 5H, H_{Ph}), 7.19 - 7.16 (m, 1H, H_c), 7.06 (pst, *J* = 7.8 Hz, 1H, H_e), 3.32 (dd, *J* = 6.2, 3.5 Hz, 1H, H_a), 2.66 (d, *J* = 3.5 Hz, 1H, H_b), 2.47 ppm (d, *J* = 6.2 Hz, 1H, $H_{b'}$).

4.2.15 Synthesis of 1-(3-methoxyphenyl)-2-phenylaziridine (29)

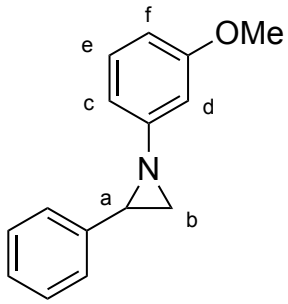

The product was obtained as a reddish oil by refluxing 3-methoxyphenylazide and styrene for 72 h (yield: 43%). The collected analytical data were in accordance with those reported in literature.[267]

^{1}H NMR (400 MHz, $CDCl_3$) δ 7.49 - 7.24 (m, 5H, H_{Ph}), 7.14 (pst, *J* = 8.0 Hz, 1H, H_e), 6.64 (ddd, *J* = 7.9, 2.1, 1.0 Hz, 1H, H_d), 6.60 (pst, *J* = 2.2 Hz, 1H, H_c), 6.53 (ddd, *J* = 8.3, 2.5, 1.0 Hz, 1H, H_f), 3.76 (s, 3H, H_{OMe}), 3.09 (dd, *J* = 6.5, 3.3 Hz, 1H, H_a), 2.45 (dd, *J* = 6.5, 1.2 Hz, 1H, H_b), 2.37 ppm (dd, *J* = 3.3, 1.2 Hz, 1H, $H_{b'}$).

4.2.16 Synthesis of 1-(3,5-dichlorophenyl)-2-phenylaziridine (30)

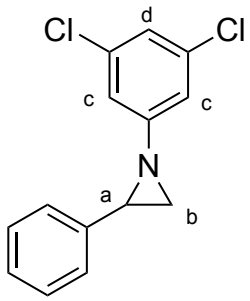

The product was obtained as a brown oil by refluxing 3,5-dichorophenylazide and styrene for 4 h (yield: 96%). The collected analytical data were in accordance with those reported in literature.[267]

^{1}H NMR (300 MHz, $CDCl_3$) δ 7.40 - 7.31 (m, 5H, H_{Ph}), 6.98 (s, 1H, H_d), 6.93 (s, 2H, H_C), 3.14 (dd, *J* = 6.4, 3.4 Hz, 1H, H_a), 2.48 (d, *J* = 6.4 Hz, 1H, H_b), 2.43 ppm (d, *J* = 3.4 Hz, 1H, $H_{b'}$).

4.2.17 Synthesis of 1-(3,5-dinitrophenyl)-2-phenylaziridine (32)

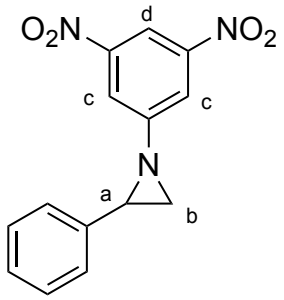

The product was obtained as a yellow powder by refluxing 3,5-dinitrophenylazide and styrene 4 h (yield: 94%).

^{1}H NMR (300 MHz, $CDCl_3$) δ 8.64 (t, *J* = 2.0 Hz, 1H, H_d), 8.15 (d, *J* = 2.0 Hz, 2H, H_c), 7.42 - 7.36 (m, 5H, H_{Ph}), 3.36 (dd, *J* = 6.6, 3.6 Hz, 1H, H_a), 2.68 (d, *J* = 6.6 Hz, 1H, H_b), 2.66 ppm (d, *J* = 3.6 Hz, 1H, $H_{b'}$). **^{13}C NMR** (75 MHz, $CDCl_3$) δ 156.87 (C), 149.00 (C), 136.87 (two overlapping C), 128.83 (two overlapping CH), 128.28 (CH), 126.15 (two overlapping CH), 120.74 (two overlapping CH) 112.39 (CH), 42.71 (CH), 38.46 ppm (CH_2). **LR-MS (ESI):** m/z ($C_{14}H_{11}N_3O_4$) calcd 285.07, found $[M+H]^+$ 286.08. Elemental Analysis calcd. for ($C_{14}H_{11}N_3O_4$): C (58.95), H (3.89), N (14.73), found: C (58.73), H (3.62), N (14.71). **UV-Vis** λ_{max} (DCM)/nm (log ε): 233 (4.40). **IR** ν_{max} (DCM)/cm^{-1}: 1009, 1078, 1137, 1172, 1255, 1346, 1394, 1464, 1543, 1605, 1712.

4.2.18 Synthesis of 1-(3,5-*bis*-trifluoromethylphenyl)-2-phenyl-3-methyl aziridine (34)

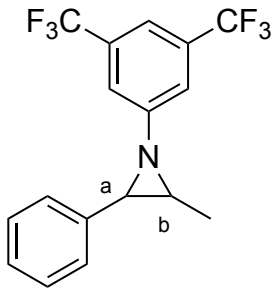

The product was obtained as a brown oil by refluxing 3,5-*bis*-trifluoromethylphenylazide and *trans*-β-methyl styrene for 4 h (yield: 62%).

^{1}H NMR (300 MHz, $CDCl_3$) δ 7.45 - 7.30 (m, 8H, H_{Ph}), 3.06 (d, *J* = 2.7 Hz, 1H, H_a), 2.77 - 2.70 (m, 1H, H_b), 1.29 ppm (d, *J* = 5.7 Hz, 3H, H_{Me}). **^{13}C NMR** (75 MHz, $CDCl_3$) δ 151.67 (C), 137.59 (C), 132.62 (q, *J* = 33.1 Hz, two overlapping CF_3), 129.00 (two overlapping CH), 128.21 (CH), 126.76 (two overlapping CH), 125.48 (C), 121.11 (CH), 121.07 (CH), 115.77 (CH), 48.90 (CH), 44.64 (CH), 15.43 ppm (three overlapping CH_3). One quaternary carbon not detected. **^{19}F NMR** (282 MHz, $CDCl_3$) δ -63.34 ppm (s). **LR-MS (ESI):** m/z ($C_{14}H_{11}F_6N$) calcd 345.10, found $[M+H]^+$ 346.30. **Elemental Analysis** calcd. for ($C_{14}H_{11}F_6N$): C (59.13), H (3.79), N (4.06), found: C (58.75), H (3.84), N (4.03). **UV-Vis** λ_{max} (DCM)/nm (log ε): 251 (4.18). **IR** ν_{max} (DCM)/cm^{-1}: 1003, 1040, 1136, 1179, 1385, 1465, 1612, 3599.

4.2.19 Synthesis of 1-(4-*tert*-butylphenyl)-2-phenyl-3-methyl aziridine (36)

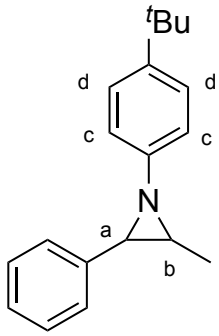

The product was obtained as a brown oil by refluxing 4-*tert*-butylphenylazide and *trans*-β-methyl styrene for 16 h (yield: 48%).

^{1}H NMR (300 MHz, $CDCl_3$) δ 7.33 - 7.31 (m, 5H, H_{Ph}), 7.25 - 7.22 (m, 2H, H_d), 6.86 (d, *J* = 8.4 Hz, 2H, H_c), 2.90 (d, *J* = 2.7 Hz, 1H, H_a), 2.56 (qd, *J* = 5.7, 2.7 Hz, 1H, H_b), 1.28 (s, 9H, H_{tBu}), 1.21 ppm (d, *J* = 5.7 Hz, 1H, H_{Me}). **^{13}C NMR** (75 MHz, $CDCl_3$) δ 147.14 (C), 145.11 (C), 139.76 (C), 128.73 (CH), 127.48 (CH), 126.79 (CH), 126.03 (two overlapping CH), 120.78 (two overlapping CH), 48.09 (CH), 44.15 (CH), 34.56 (C) 31.91 (three overlapping CH_3), 15.16 ppm (CH_3). **LR-MS (ESI):** m/z ($C_{19}H_{23}N$) calcd 265.18, found $[M+H]^+$ 266.27. **Elemental Analysis** calcd. for ($C_{19}H_{23}N$): C (85.99), H (8.74), N (5.27), found: C (85.97), H (9.02), N (5.01). **UV-Vis** λ_{max} (DCM)/nm (log ε): 246 (4.16). **IR** ν_{max} (DCM)/cm^{-1}: 909, 913, 918, 923, 927, 933, 939, 1255, 1417, 1510, 1517, 1605, 3599, 3686.

4.2.20 Synthesis of 1-(3,5-bis(trifluoromethyl)phenyl)-2-methyl-2-phenylaziridine

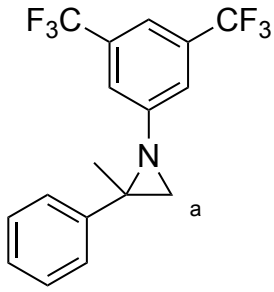

The product was obtained by refluxing 3,5-*bis*-trifluoromethylphenylazide and α-methyl styrene for 1 h (yield: 99 %). The collected analytical data were in accordance with those reported in literature.[267]

^{1}H NMR (400 MHz, $CDCl_3$) δ 7.53 - 7.29 (m, 8H, H_{Ar}), 2.65 (s, 1H, H_a), 2.38 (s, 1H, $H_{a'}$), 1.45 ppm (s, 3H, H_{Me}).

5 ^{1}H, ^{13}C and ^{19}F NMR spectra of unreported *N*-aryl aziridines

Compound (7): ^{1}H NMR (300 MHz, $CDCl_3$)

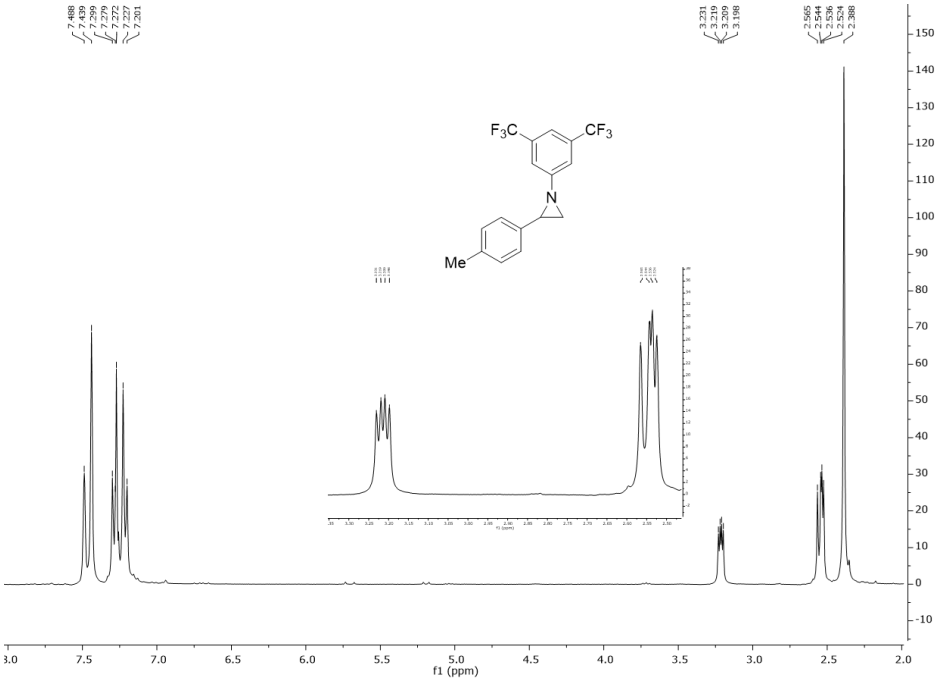

Compound (7): ^{13}C NMR (75 MHz, $CDCl_3$)

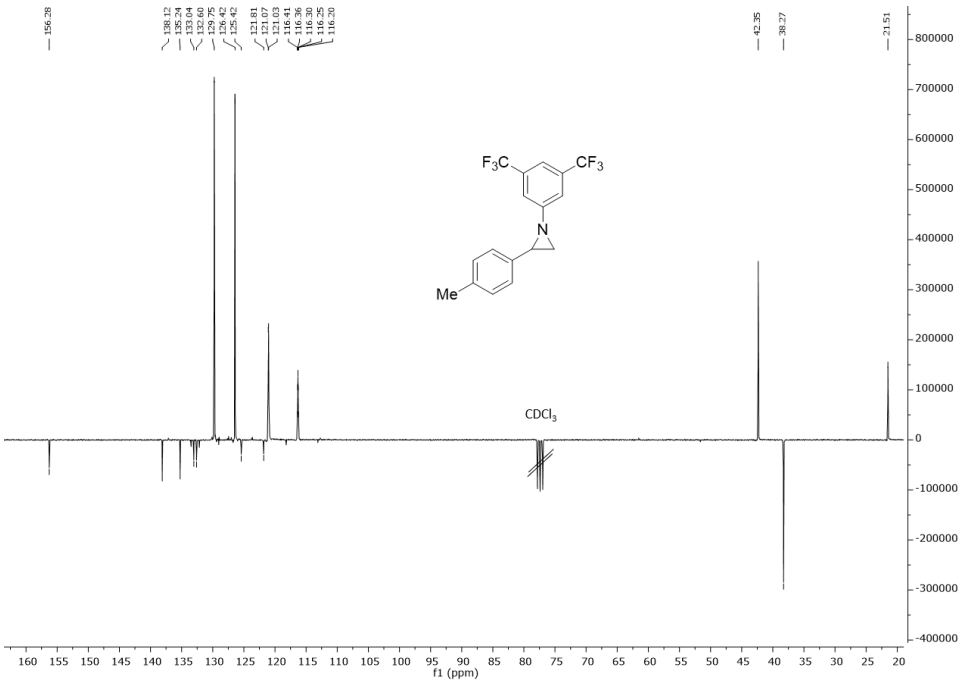

Compound (7): ^{19}F NMR (282 MHz, $CDCl_3$)

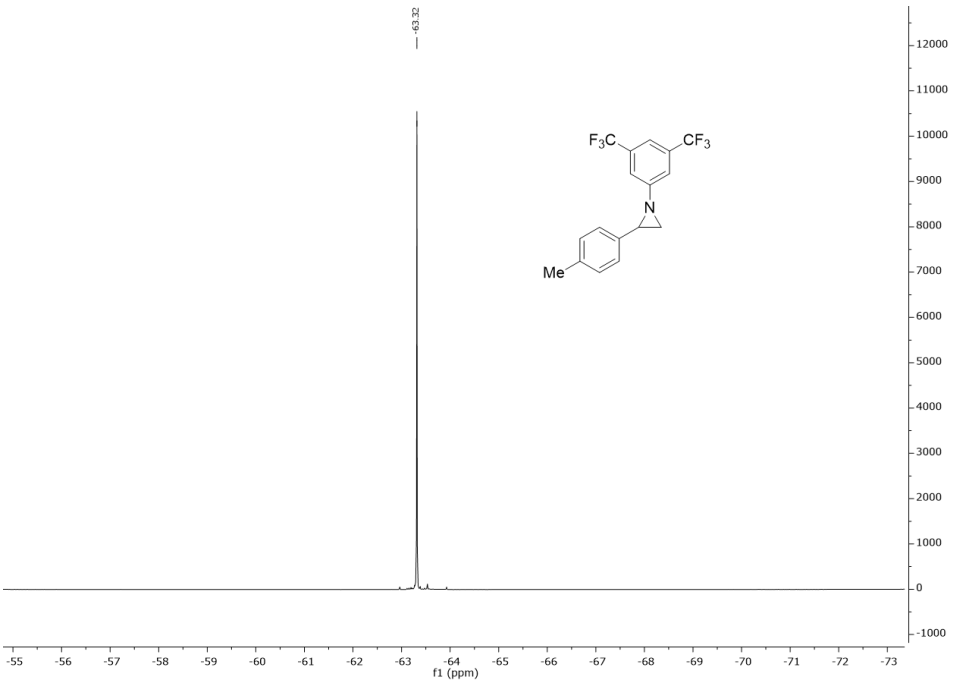

Compound (9): ^{1}H NMR (400 MHz, $CDCl_3$)

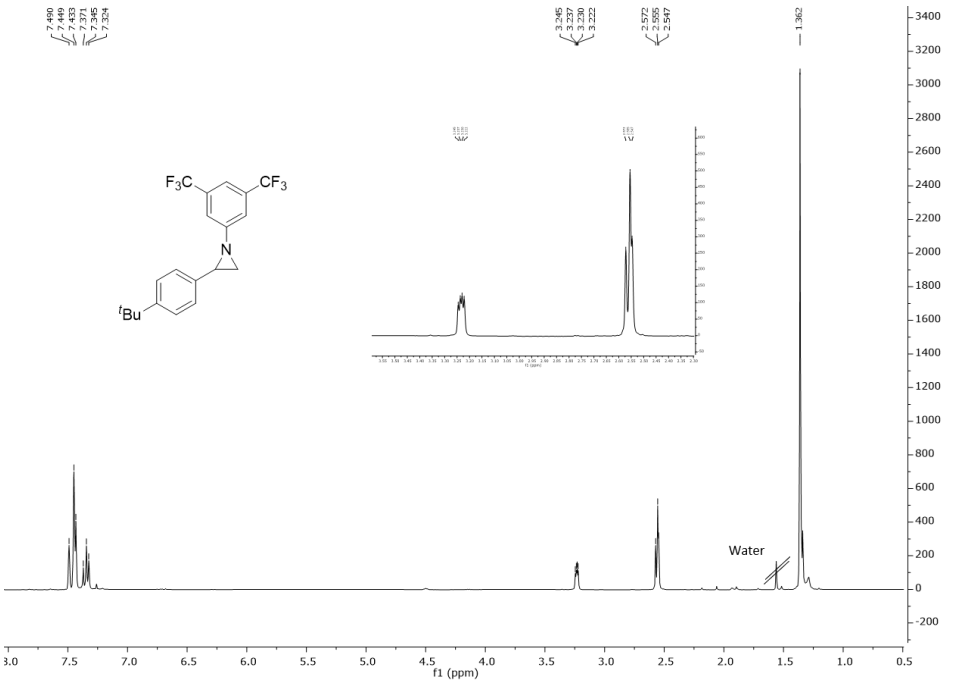

Compound (9): ^{13}C NMR (100 MHz, $CDCl_3$)

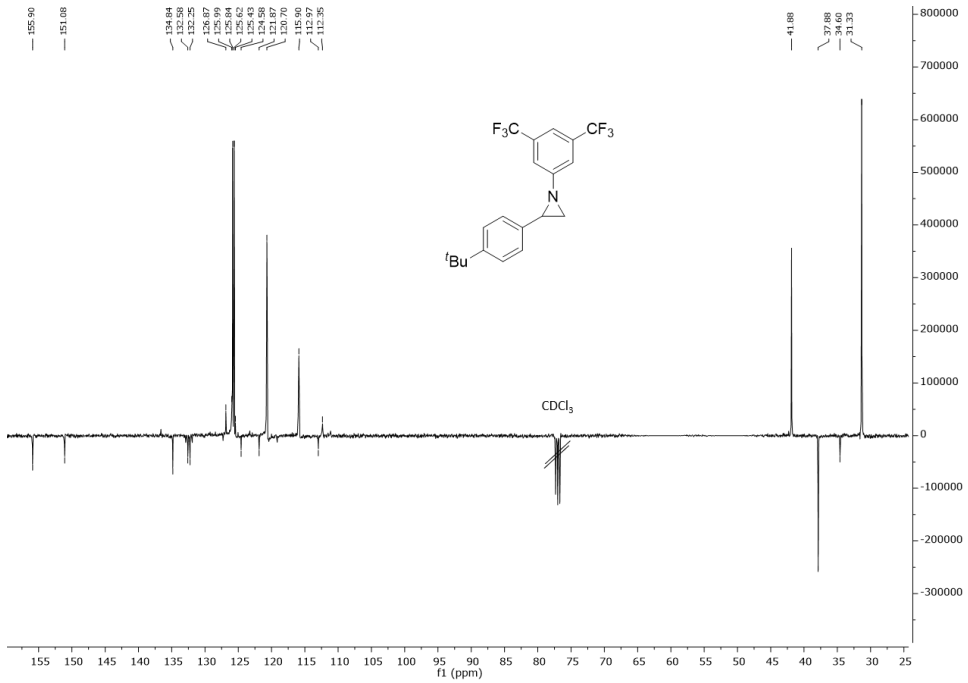

Compound (9): ^{19}F NMR (376 MHz, $CDCl_3$)

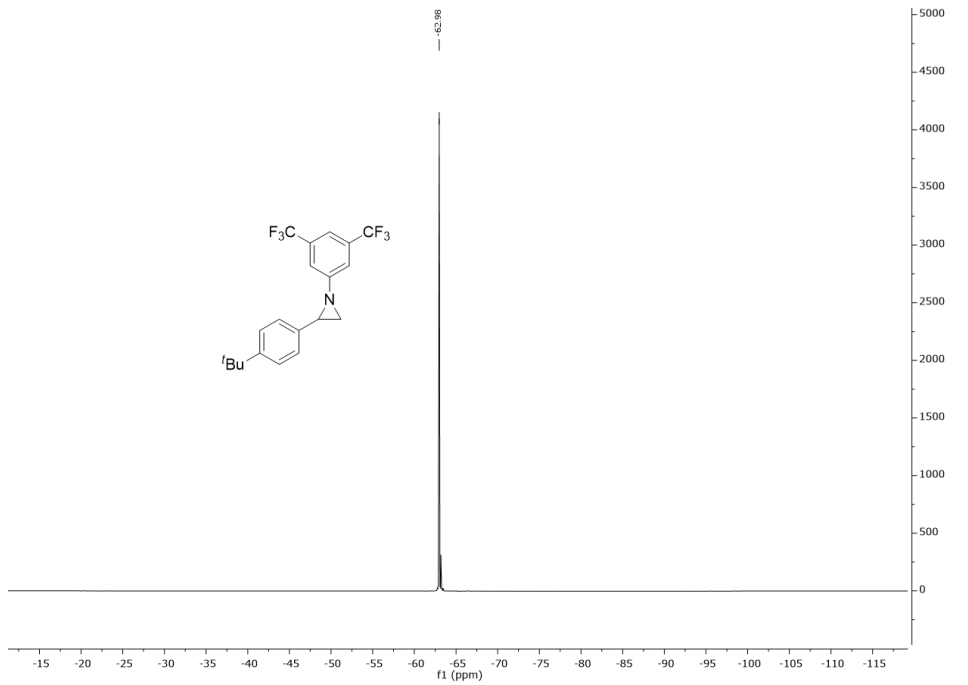

Compound (15): ^{1}H NMR (300 MHz, $CDCl_3$)

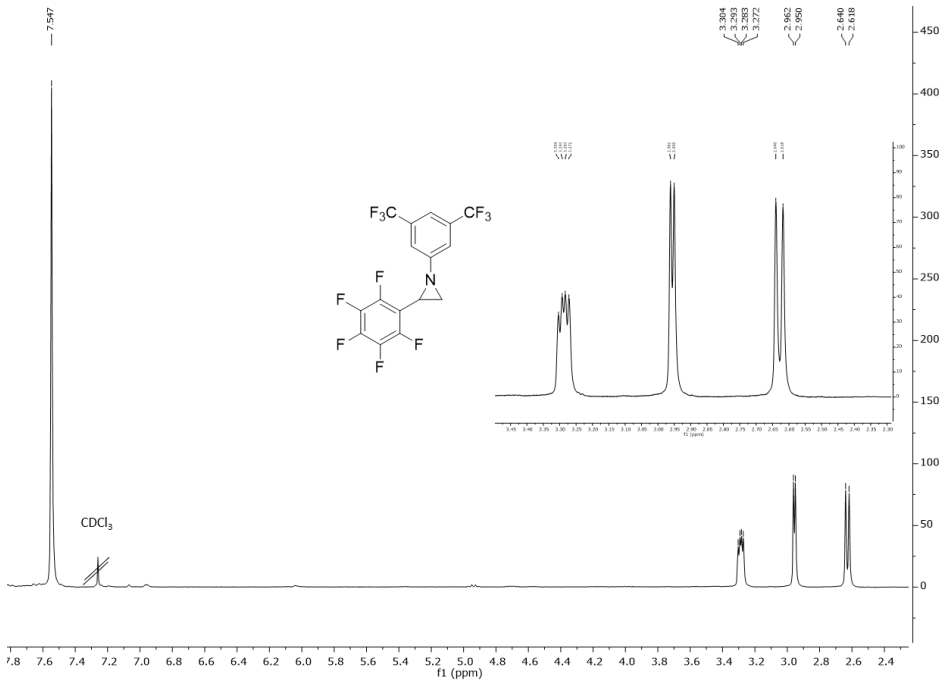

Compound (15): ^{13}C NMR (75 MHz, $CDCl_3$)

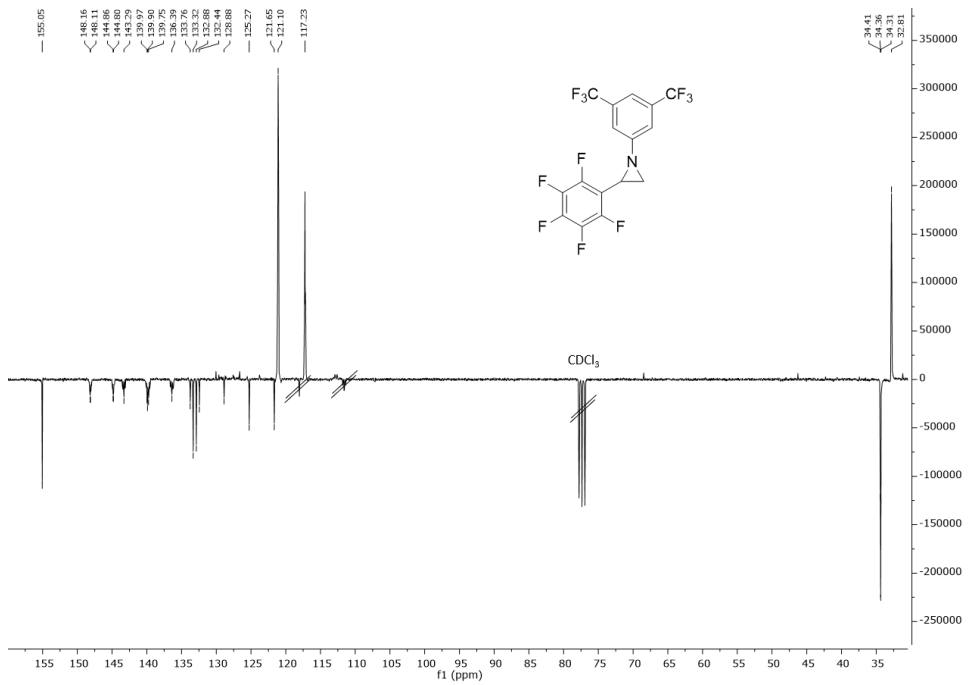

Compound (15): ^{19}F NMR (282 MHz, $CDCl_3$)

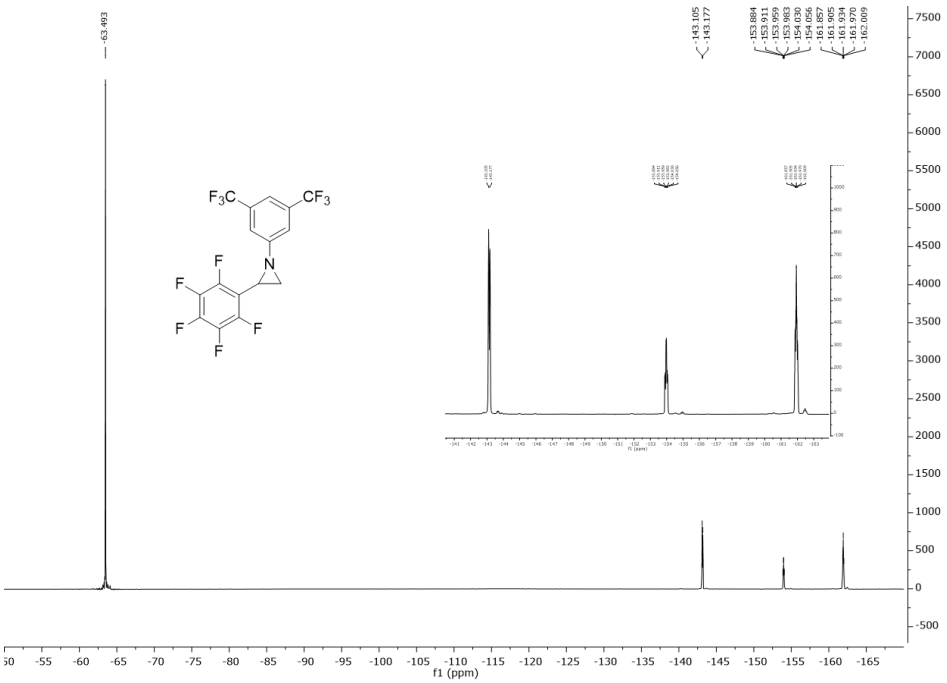

Compound (17): ^{1}H NMR (300 MHz, $CDCl_3$)

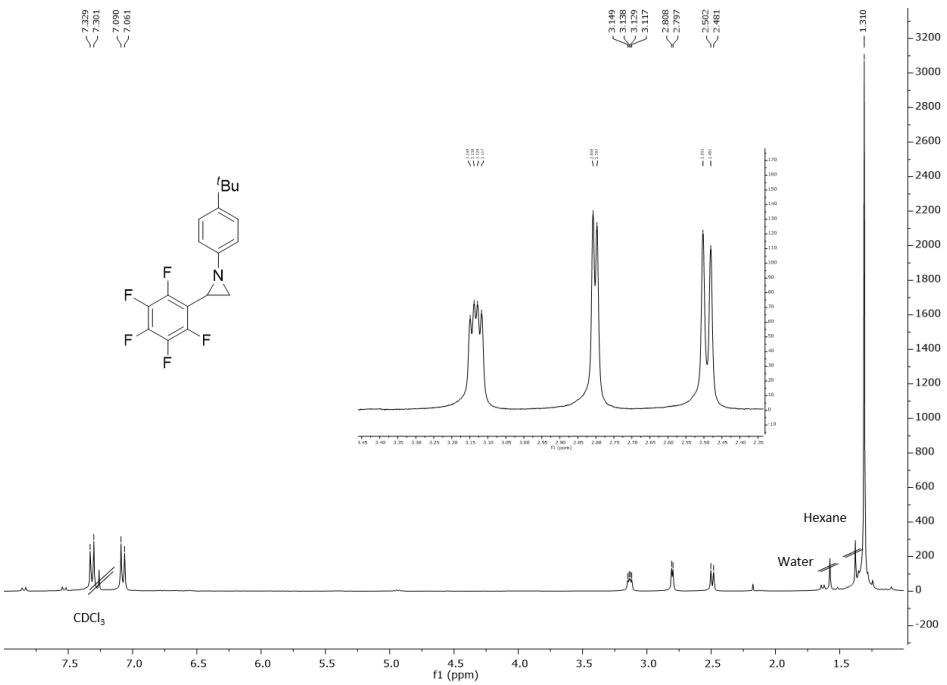

Compound (17): ^{13}C NMR (75 MHz, $CDCl_3$)

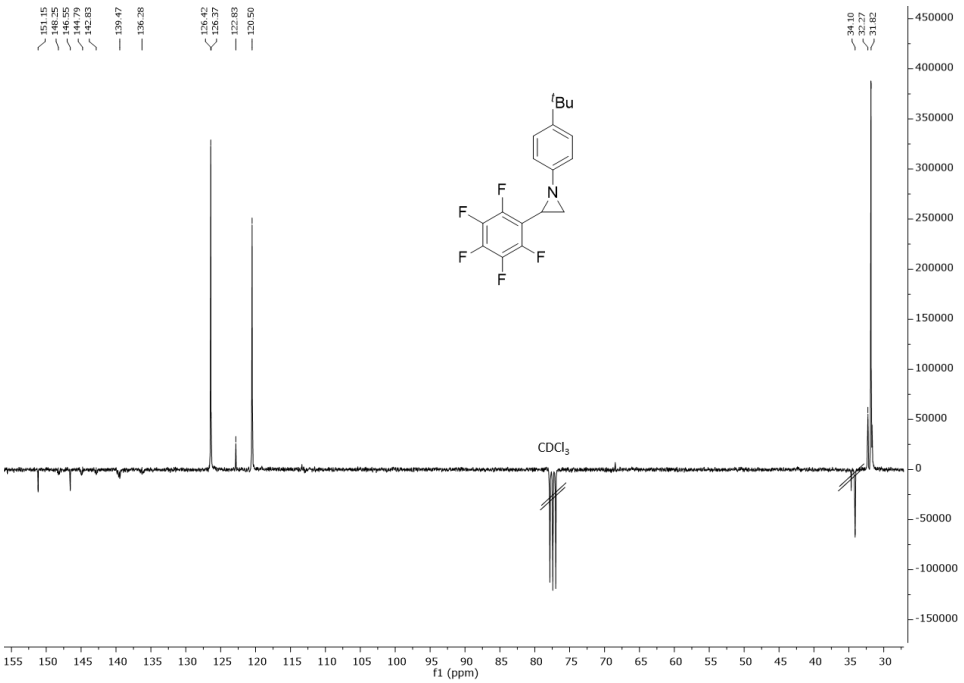

Compound (17): ^{19}F NMR (282 MHz, $CDCl_3$)

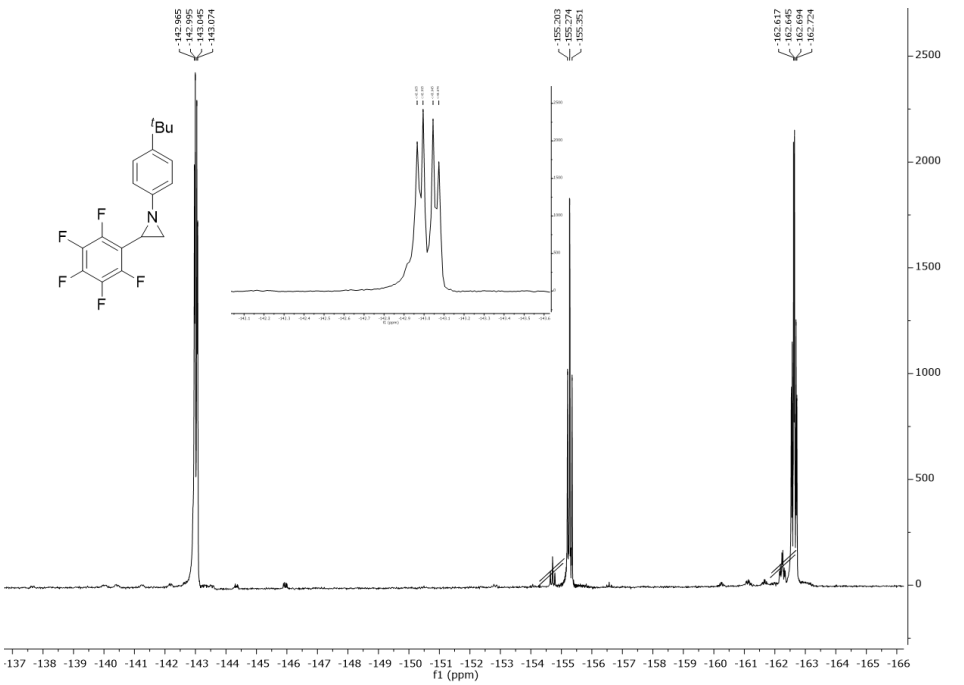

Compound (32): ^{1}H NMR (300 MHz, $CDCl_3$)

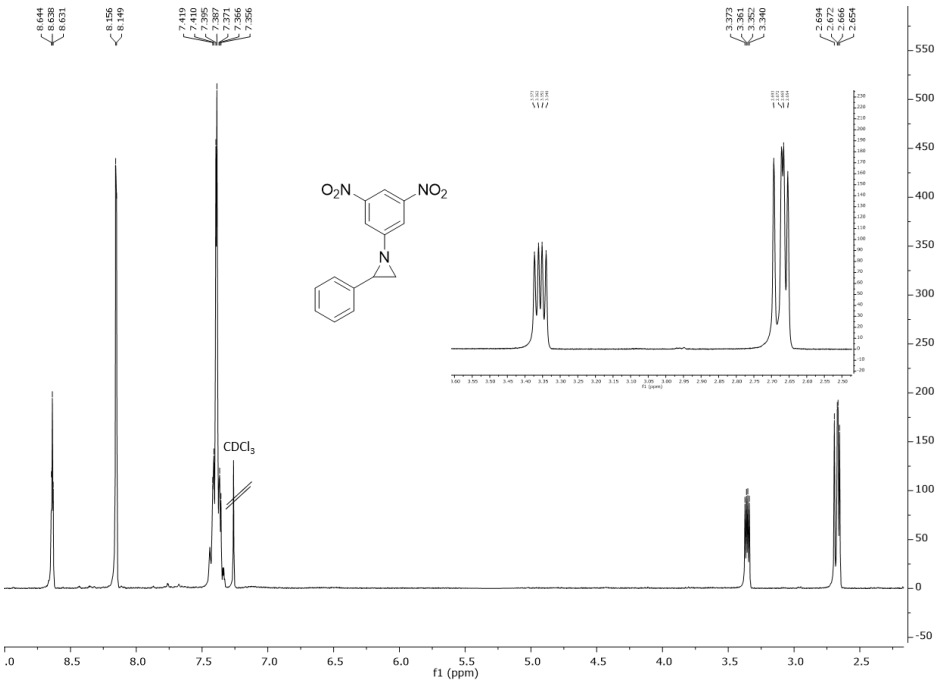

Compound (32): ^{13}C NMR (75 MHz, $CDCl_3$)

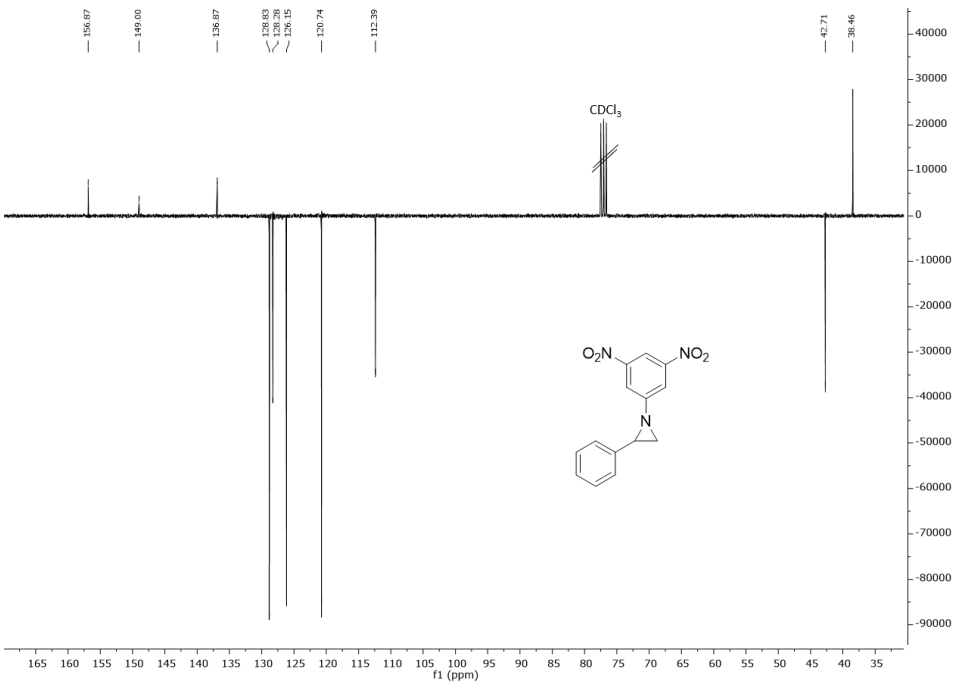

Compound (34): ^{1}H NMR (300 MHz, $CDCl_3$)

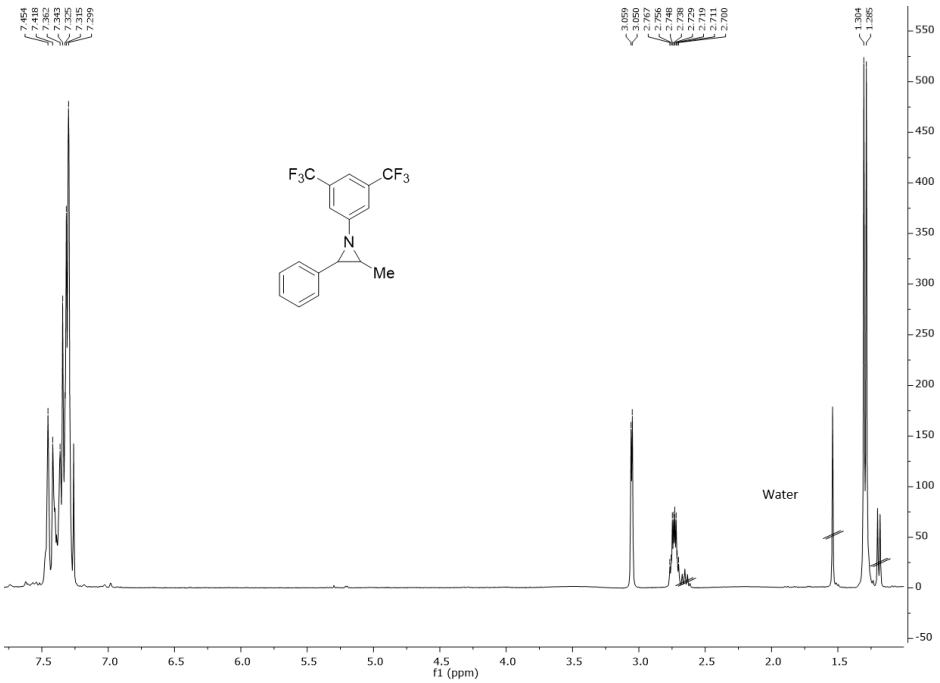

Compound (34): ^{13}C NMR (75 MHz, $CDCl_3$)

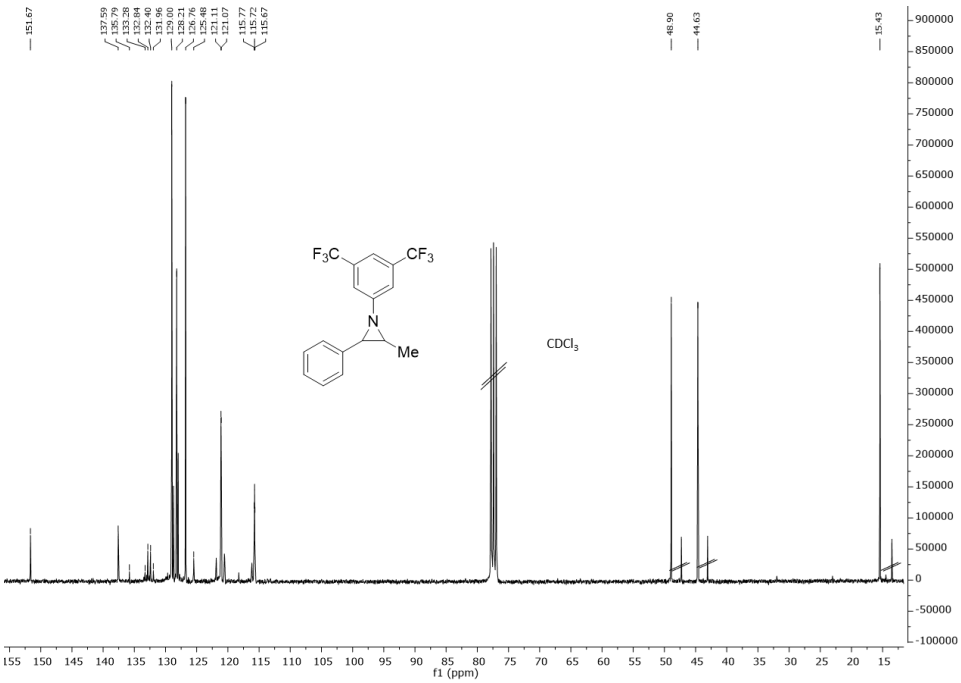

Compound (34): ^{19}F NMR (282 MHz, $CDCl_3$)

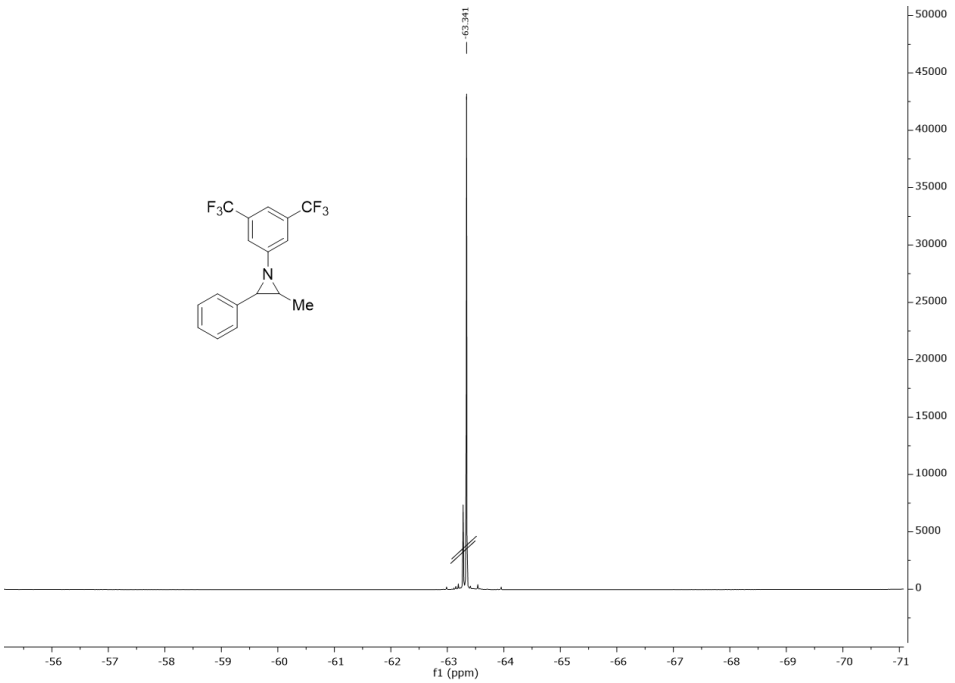

Compound (36): ^{1}H NMR (300 MHz, $CDCl_3$)

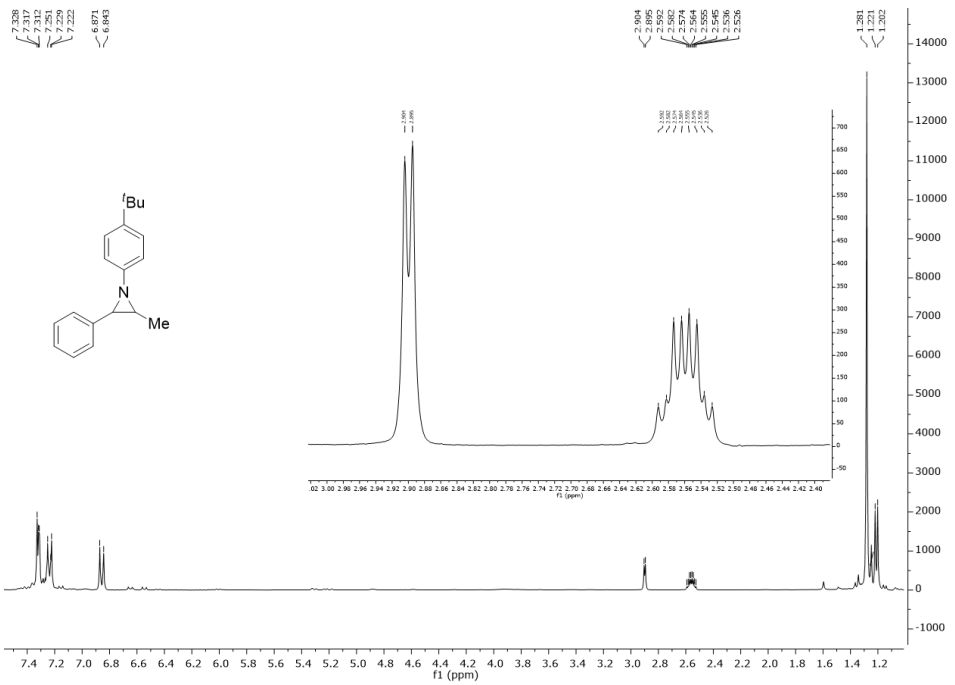

Compound (36): ^{13}C NMR (75 MHz, $CDCl_3$)

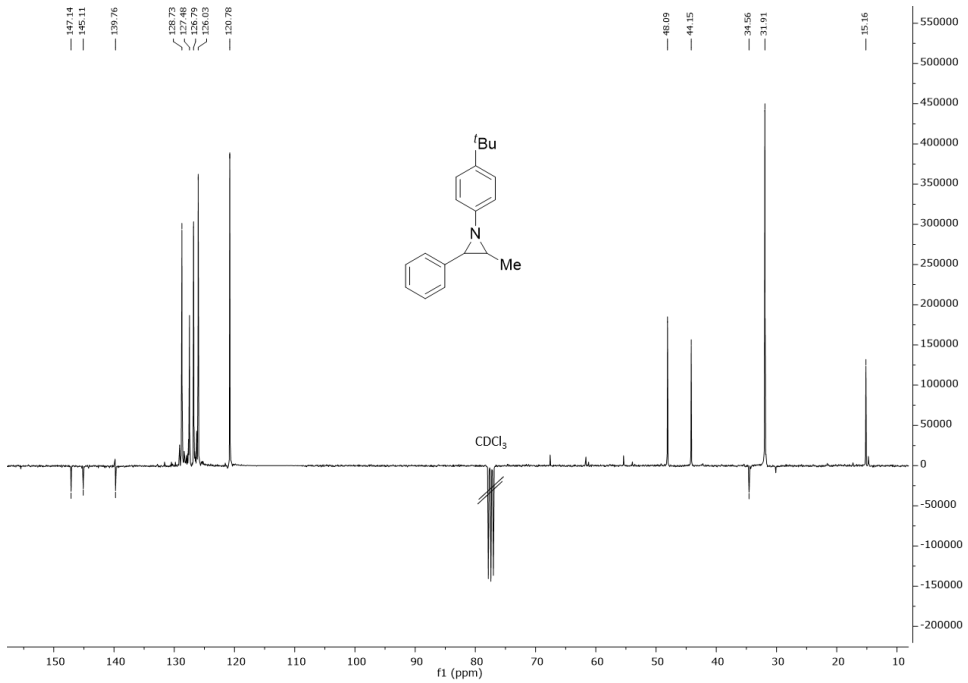

6 Synthesis of *N*-alkyl aziridines

6.1 General procedure

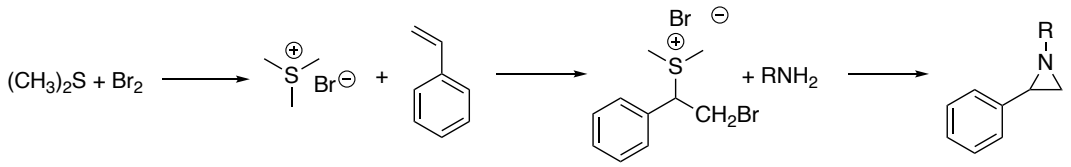

General procedure: dimethyl sulphide (12.42 g, 0.20 mol) was dissolved in acetonitrile (90 mL) and the solution was placed in an ice bath. Then, a solution of bromine (31.96 mL, 0.20 mol) in acetonitrile (10 mL) was added dropwise over 30 minutes. During the addition, light orange crystals of bromodimethyl sulfonium bromide was formed. The reaction was stirred for further 10 minutes, then styrene (20.83 g, 0.20 mol) was added to the solution dropwise. The so-obtained reaction mixture was stirred for 30 minutes, then diethyl ether (70 mL) was added to favour the precipitation of a white solid. The so-obtained powder was collected by filtration, washed several times with diethyl ether and dried under reduced pressure. The white crystals of styrene sulphonium bromide ($8.62 \cdot 10^{-3}$ mol) were suspended in water (20 mL) and a solution of the desired amine ($4.30 \cdot 10^{-2}$ mol) in water (5 mL) was added dropwise. The resulting reaction mixture was stirred overnight. Then, brine (20 mL) and diethyl ether (20 mL) were added, and the phases were separated. The aqueous phase was washed with diethyl ether (3 x 30 mL) and the combined organic phases were dried over sodium sulphate. The solvent was removed under reduced pressure and the crude was purified by flash chromatography (silica gel, hexane/ethyl acetate 9:1, 0.5% of triethylamine was added in order to deactivate the silica).

6.2 Synthesis of 1-*n*butyl-2-phenylaziridine (42)

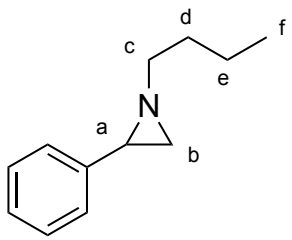

The general procedure was followed by using *normal*-butylamine to obtain the product as a yellowish oil (yield: 72%). The collected analytical data were in accordance with those reported in literature.[96]

^{1}H NMR (400 MHz, $CDCl_3$): δ 7.29 - 7.12 (5H, m, H_{Ph}), 2.45 (dt, *J* = 11.5 Hz, 7.3 Hz, 1H, H_c), 2.28 (dt, *J* = 11.5, 7.3 Hz, 1H, $H_{c'}$), 2.23 (dd, *J* = 6.4, 3.2 Hz, 1H, H_a), 1.83 (d, *J* = 3.2 Hz, 1H, H_b), 1.59 (d, *J* = 6.5 Hz, 1H, $H_{b'}$), 1.67 - 1.55 (m, 2H, H_d), 1.44 - 1.34 (m, 2H, H_e), 0.91 ppm (t, *J* = 7.3 Hz, 3H, H_f).

6.3 Synthesis of 1-*i*butyl-2-phenylaziridine (72)

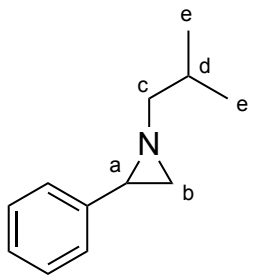

The general procedure was followed by using *iso*-butylamine to obtain the product as a yellowish oil (yield: 86%). The collected analytical data were in accordance with those reported in literature.

^{1}H NMR (300 MHz, $CDCl_3$): δ 7.34 - 7.21 (m, 5H, H_{Ph}), 2.46 (dd, *J* = 11.5, 7.1 Hz, 1H, H_a), 2.30 (dd, *J* = 6.5, 3.3 Hz, 1H, H_b), 2.09 (dd, *J* = 11.5, 6.5 Hz 1H, $H_{b'}$), 1.97 - 1.86 (m, 2H, $H_{d+c'}$), 1.67 (d, *J* = 6.4 Hz, 1H, H_c), 1.02 - 0.96 ppm (m, 6H, H_e).

6.4 Synthesis of 1-*s*butyl-2-phenylaziridine (73)

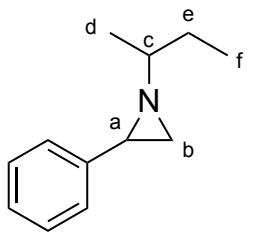

The general procedure was followed by using *sec*-butylamine to obtain the product as a yellowish oil (yield: 81%).

^{1}H NMR (300 MHz, $CDCl_3$) δ 7.29 - 7.16 (m, 5H, H_{Ph}), 2.34 and 2.28 (dd, *J* = 6.6, 3.3 Hz, 1H, H_a) 1.90 and 1.84 (d, *J* = 3.3 Hz, 1H, H_b), 1.60 - 1.36 (m, 4H, $H_{b',c\ and}$), 1.14 and 1.12 (d, *J* = 3.8 Hz, 1H, H_d), 0.94 and 0.88 ppm (t, *J* = 7.3 Hz, 1H, H_f). **^{13}C NMR** (75 MHz, $CDCl_3$) δ 114.12 and 114.01 (C), 128.66 (CH), 127.15 (CH), 126.88 and 126.78 (CH), 68.22 and 67.96 (CH), 42.06 and 40.24 (CH), 37.86 and 36.31 (CH_2), 30.27 and 29.91(CH_2), 20.22 and 19.66 (CH_3), 11.29 and 11.11 ppm (CH_3). **Elemental Analysis** calcd. for $C_{12}H_{17}N$: C (82.23), H (9.78), N (7.99), found: C (82.02), H (9.70), N (7.83). **LR-MS (ESI)**: m/z ($C_{12}H_{17}N$) calcd 175.1, found $[M+H]^+$ 176.23 **UV-Vis** λ_{max} (DCM)/nm (log ε): 231 (3.56). **IR** ν_{max} (DCM)/cm^{-1}: 1008, 1029, 1074, 1086, 1097, 1158, 1176, 1205, 1344, 1376, 1464, 1497, 1605, 2825, 2827, 2933.

6.5 Synthesis of 1-^{t}butyl-2-phenylaziridine (75)

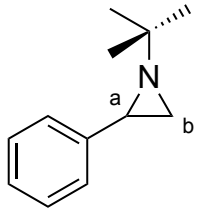

The general procedure was followed by using *tert*-butylamine to obtain the product as a yellowish oil (yield: 64%). The collected analytical data were in accordance with those reported in literature.[95]

^{1}H NMR (400 MHz, $CDCl_3$): δ 7.37 - 7.24 (m, 5H, H_{Ph}), 2.67 (dd, *J* = 6.3, 2.9 Hz, 1H, H_a), 1.93 (d, *J* = 6.4 Hz, 1H, H_b), 1.69 (d, *J* = 2.9 Hz, 1H, $H_{b'}$), 1.10 ppm (s, 9H, H_{tBu}).

6.6 Synthesis of 1-cyclpopentyl-2-phenylaziridine (76)

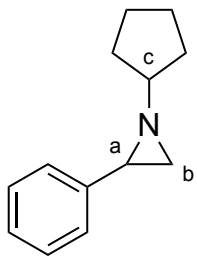

The general procedure was followed by using cyclopentylamine to obtain the product as a yellowish oil (yield: 81%). The collected analytical data were in accordance with those reported in literature.[296]

^{1}H NMR (300 MHz, $CDCl_3$): δ 7.26 - 7.24 (m, 4H, H_{Ph}), 7.18 - 7.15 (m, 1H, $H_{Ph\text{-}para}$), 2.34 (dd, *J* = 6.5, 3.3 Hz, 1H, H_a), 2.09 - 2.00 (m, 1H, H_c), 1.81 (d, *J* = 3.1 Hz, 1H, H_b), 1.79 - 1.74 (m, 1H, $H_{cyclopentyl}$), 1.72 - 1.66 (m, 4H, $H_{cyclopentyl}$), 1.64 (d, *J* = 6.5 Hz, 1H, $H_{b'}$), 1.53 - 1.49 ppm (m, 2H, $H_{cyclopentyl}$).

6.7 Synthesis of 1-cyclohexyl-2-phenylaziridine (77)

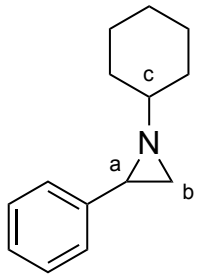

The general procedure was followed by using cyclohexylamine to obtain the product as a yellowish oil (yield: 77%). The collected analytical data were in accordance with those reported in literature.[96]

^{1}H NMR (400 MHz, $CDCl_3$): δ 7.24 - 7.20 (m, 4H, H_{Ph}), 7.19 - 7.12 (m, 1H, $H_{Ph\text{-}para}$), 2.30 (dd, *J* = 6.5, 3.3 Hz, 1H, H_a), 1.85 - 1.80 (m, 1H, H_c), 1.83 (d, *J* = 3.1 Hz, 1H, H_b), 1.82 - 1.70 (m, 2H, $H_{cyclohexyl}$), 1.61 (d, *J* = 6.5 Hz, 1H, $H_{b'}$), 1.47 - 1.37 (m, 2H, $H_{cyclohexyl}$), 1.28 - 1.15 ppm (m, 6H, $H_{cyclohexyl}$).

6.8 Synthesis of 1-cyclohexylmethyl-2-phenylaziridine (78)

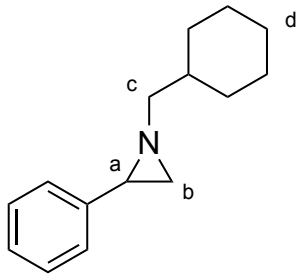

The general procedure was followed by using cyclohexylmethylamine to obtain the product as a yellowish oil (yield: 82%). The collected analytical data were in accordance with those reported in literature.[96]

^{1}H NMR (300 MHz, $CDCl_3$): δ 7.30 - 7.17 (m, 5H, H_{Ph}), 2.42 (dd, *J* = 11.7, 7.0 Hz, 1H, H_c), 2.25 (dd, *J* = 6.4, 3.2 Hz, 1H, H_a), 2.09 (dd, *J* = 11.7, 6.4 Hz, 1H, $H_{c'}$), 1.85 (d, *J* = 6.5 Hz, 1H, H_b), 1.79 - 1.58 (m, 5H, $H_{cyclohexyl}$), 1.62 (d, *J* = 6.5 Hz, $H_{b'}$), 1.20 - 1.10 (m, 3H, $H_{cyclohexyl}$), 0.98 - 0.90 ppm (m, 2H, H_d).

6.9 Synthesis of 1-benzyl-2-phenylaziridine (80)

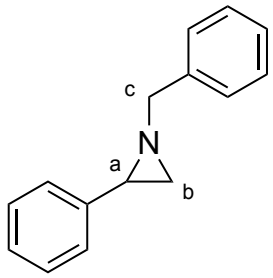

The general procedure was followed by using benzylamine to obtain the product as a yellowish oil (yield: 80%). The collected analytical data were in accordance with those reported in literature.[96]

^{1}H NMR (400 MHz, $CDCl_3$): δ 7.47 - 7.28 (m, 10H, H_{Ar}), 3.74 (q, *J* = 13.7 Hz, 2H, H_c), 2.59 (dd, *J* = 6.4, 3.3 Hz, 1H, H_a), 2.07 (d, *J* = 3.3 Hz, 1H, H_b), 1.93 ppm (d, *J* = 6.5 Hz, 1H, $H_{b'}$).

6.10 Synthesis of 1-(4-methoxy)benzyl-2-phenylaziridine (81)

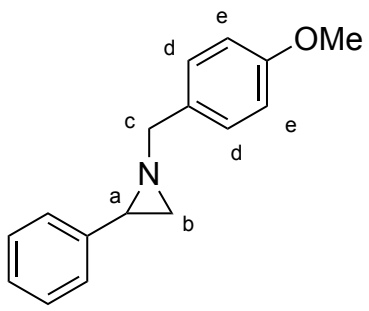

The general procedure was followed by using 4-(methoxy)benzylamine to obtain the product as a yellowish oil (yield: 80%). The collected analytical data were in accordance with those reported in literature.[297]

^{1}H NMR (300 MHz, $CDCl_3$): δ 7.29 - 7.18 (m, 7H, H_{Ph+d}), 6.84 (d, *J* = 8.6 Hz, 2H, H_e), 3.77 (s, 3H, H_{OMe}), 3.57 (q, *J* = 13.4 Hz, 2H, H_c), 2.48 (dd, *J* = 6.5, 3.3 Hz 1H, H_a), 1.95 (d, *J* = 3.3 Hz, 1H, H_b), 1.82 ppm (d, *J* = 6.5 Hz, 1H, $H_{b'}$).

6.11 Synthesis of 1-*i*amyl-2-phenylaziridine (82)

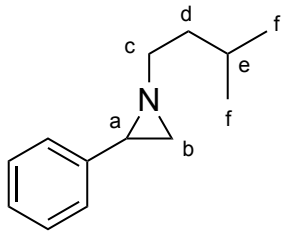

The general procedure was followed by using *iso*-amylamine to obtain the product as a yellowish oil (yield: 71%). The collected analytical data were in accordance with those reported in literature.[95]

^{1}H NMR (400 MHz, $CDCl_3$): δ 7.37 - 7.31 (m, 4H, H_{Ar}), 7.29 - 7.24 (m, 1H, H_{Ar}), 2.61 - 250 (m, 1H, H_c), 2.48 - 2.37 (m, 1H, $H_{c'}$), 2.35 (dd, 1H, *J* = 6.5, 3.3 Hz, H_a), 1.94 (d, 1H, J=3.1 Hz, H_b), 1.77 (heptet, 1H, *J* = 6.6 Hz, H_e), 1.70 (d, 1H, *J* = 6.5 Hz, $H_{b'}$), 1.65 - 1.55 (m, 2H, H_d), 0.99 ppm (dd, 6H, *J* = 6.9 Hz, 1.6 Hz, H_f).

7 ^{1}H and ^{13}C spectra of unpublished *N*-alkyl aziridines

Compound (73): ^{1}H NMR (300 MHz, $CDCl_3$)

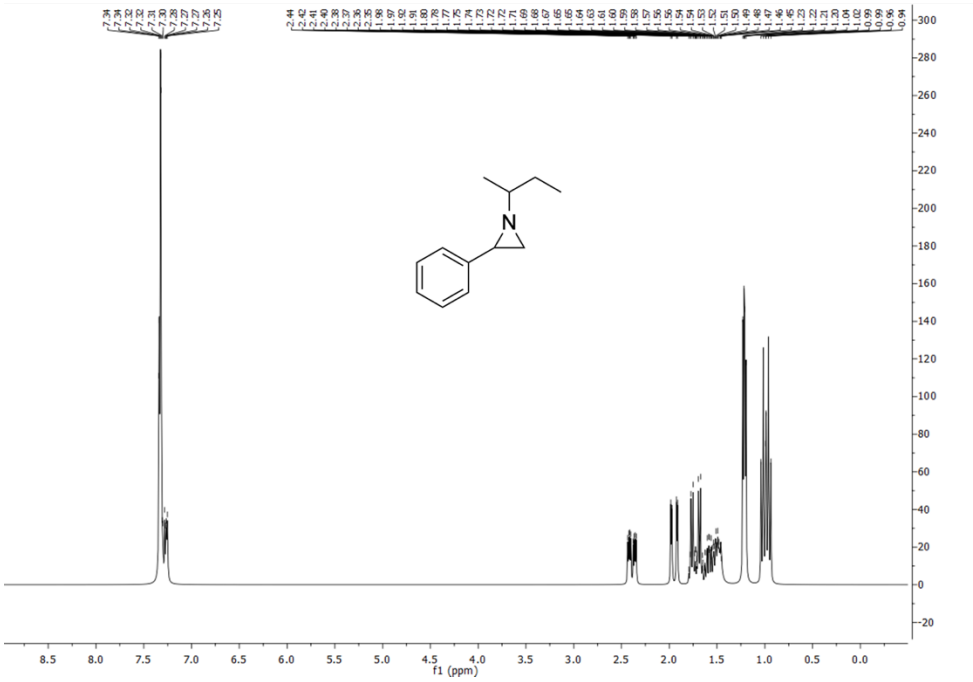

Compound (73): ^{13}C NMR (75 MHz, $CDCl_3$)

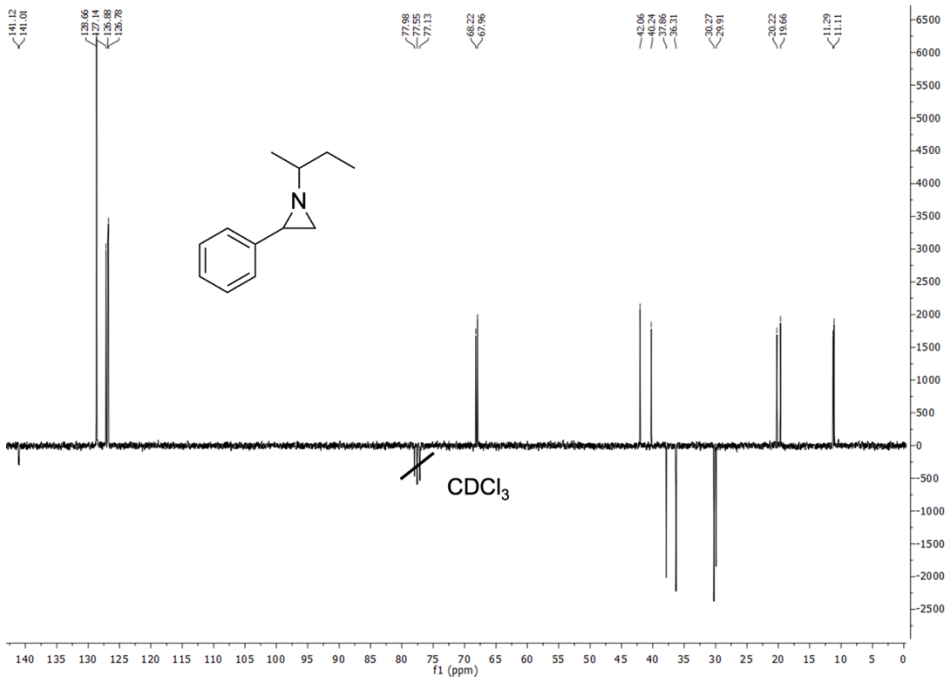

8 Carbon dioxide cycloaddition to *N*-aryl aziridines

8.1 General procedure

a) General procedure for homogenous catalysts: *meso*-tetraphenylporphyrin (2.3 mg, 3.75 x 10^{-6} mol), tetrabutyl ammonium chloride (2.6 mg, 1.88 x 10^{-5} mol) and the aziridine (3.75 x 10^{-4} mol) were dissolved in THF (0.25 mL) in a 2 mL glass liner equipped with a screw cap and glass wool. The vessel was transferred into a stainless-steel autoclave under nitrogen atmosphere and three vacuum-nitrogen cycles were performed. 1.2 MPa of CO_2 was charged at room temperature and the autoclave was placed in a preheated oil bath at 125 °C and stirred for 8 h. Then, the autoclave was cooled at room temperature and slowly vented. The solvent was evaporated to dryness and the crude analyzed by ^{1}H NMR spectroscopy by using 2,4-dinitrotoluene as the internal standard. The product was purified by flash chromatography (silica gel, hexane/ethyl acetate 9:1).

b) General procedure for heterogeneous catalysts: $TPPH_2$@SBA-15 (3.75 x 10^{-6} mol), tetrabutyl ammonium chloride (2.6 mg, 1.88 x 10^{-5} mol) and the aziridine (3.75 x 10^{-4} mol) were dissolved in THF (0.25 mL) in a 2 mL glass liner equipped with a screw cap and glass wool. The vessel was transferred into a stainless-steel autoclave under nitrogen atmosphere and three vacuum-nitrogen cycles were performed. 1.2 MPa of CO_2 was charged at room temperature and the autoclave was placed in a preheated oil bath at 125°C and stirred for 16 h. Then, the autoclave was cooled at room temperature and slowly vented. The solvent was evaporated to dryness and the crude analyzed by ^{1}H NMR spectroscopy by using 2,4-dinitrotoluene as the internal standard.

c) Recycling of the heterogeneous catalyst: the procedure **b** was applied and at the end of the reaction the catalyst was collected in a filter, washed with DCM, and dried in the oven. Then, the isolated catalyst was used for the next reaction cycle.

8.1.2 Optimization of the catalytic conditions: the general procedure reported for synthesizing **4** was repeated by varying the following experimental conditions:

a) the aziridine concentration at 1.2 MPa CO_2, 100 °C for 15 h: [**2**] = 0.075 M, 30% yield; [**2**] = 0.16 M, 45% yield; [**2**] = 0.33 M, 58% yield; [**2**] = 0.66 M, 69% yield; [**2**] = 1.00 M, 80% yield; [**2**] = 1.50 M, 86% yield; [**2**] = 2.0 M, 89% yield.

b) the CO_2 pressure at 1.5 M of **2**, 100 °C for 15 h: CO_2 pressure = 0.1 MPa, 56% yield; CO_2 pressure = 0.4 MPa, 57% yield; CO_2 pressure = 0.6 MPa, 74% yield; CO_2 pressure = 1.2 MPa 86% yield; CO_2 pressure = 1.8 MPa, 75% yield.

c) the reaction temperature at 1.5 M of aziridine, 1.2 MPa CO_2 for 15 h: T = 25 °C, 8% yield; T = 50 °C, 9% yield; T = 75 °C, 32% yield; T = 100 °C, 70% yield; T = 125 °C, 99% yield; T = 150 °C, 99% yield.

8.2 Synthesis of 3-(3,5-*bis*-(trifluoromethyl)phenyl-5-phenyloxazalidin-2-one (4)

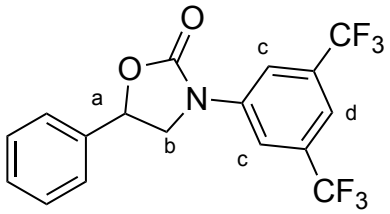

The general procedure was followed by using aziridine **2** to obtain the product as a purple-brown solid.

^{1}H NMR (400 MHz, $CDCl_3$) δ 8.06 (s, 2H, H_c), 7.64 (s, 1H, H_d), 7.45 - 7.41 (m, 5H, H_{Ph}), 5.72 (pst, *J* = 8.0 Hz, 1H, H_a), 4.47 (pst, *J* = 8.8 Hz, 1H, H_b), 4.03 ppm (pst, *J* = 7.6 Hz, 1H, $H_{b'}$). **^{13}C NMR** (100 MHz, $CDCl_3$) δ 154.49 (C=O), 140.02 (C), 137.55 (C), 132.92 (q, *J* = 33.7, two overlapping CF_3), 129.85 (CH), 129.57 (two overlapping CH), 125.96 (two overlapping CH), 124.73 (C), 122.02 (C), 117.97 (CH), 117.94 (CH), 117.58 (CH), 74.69 (CH), 52.68 ppm (CH_2). **^{19}F NMR** (376 MHz, $CDCl_3$) δ -62.97 ppm (s). **LR-MS (ESI):** m/z ($C_{17}H_{11}F_6NO_2$) calcd 375.07, found $[M+H]^+$ 376.11. **Elemental Analysis** calcd. for ($C_{17}H_{11}F_6NO_2$): C (54.41), H (2.95), N (3.73), found: C (54.09), H (3.25), N (3.61). **UV-Vis** λ_{max} (DCM)/nm (log ε): 244 (4.22). **IR** ν_{max} (DCM)/cm^{-1}:1140 1184, 1403, 1476, 1764 (C=O), 2976.

8.3 Synthesis of 3-(4-nitrophenyl)-5-phenyloxazalidin-2-one (6)

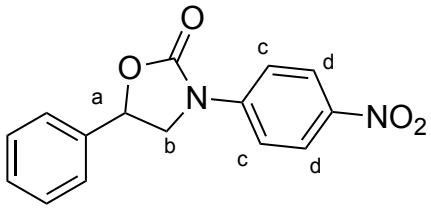

The general procedure was followed by using aziridine **5** to obtain the product as a yellow powder.

^{1}H NMR (400 MHz, $CDCl_3$) 8.27 - 8.24 (m, 2H, H_d), 7.74 (d, *J* = 9.3 Hz, 2H, H_c), 7.46 - 7.42 (m, 5H, H_{Ph}) 5.71 (pst, *J* = 8.2 Hz, 1H, H_a), 4.47 (pst, *J* = 8.8 Hz, 1H, H_b), 4.03 ppm (dd, *J* = 8.8, 7.6 Hz, 1H, $H_{b'}$). **^{13}C NMR** (100 MHz, $CDCl_3$) δ 154.05 (C=O), 143.65 (C), 143.41 (C), 137.23 (C), 129.53 (CH), 129.24 (two overlapping CH), 125.66 (two overlapping CH), 125.02 (two overlapping CH), 117.55 (two overlapping CH), 74.30 (CH), 52.42 ppm (CH_2). **LR-MS (ESI):** m/z ($C_{15}H_{12}N_2O_4$) calcd 284.08, found $[M+H]^+$ 285.02. **Elemental Analysis** calcd. for ($C_{15}H_{12}N_2O_4$): C (63.38), H (4.25), N (9.85), found: C (63.01), H (4.29), N (9.80). **UV-Vis** λ_{max} (DCM)/nm (log ε): 317 (4.28). **IR** ν_{max} (DCM)/cm^{-1}:1143, 1205, 1220, 1298, 1333, 1344, 1369, 1395, 1417, 1482, 1503, 1520, 1599, 1764 (C=O).

8.4 3-(3,5-bis-(trifluoromethyl)phenyl-5-(4-methylphenyl)oxazalidin-2-one (8)

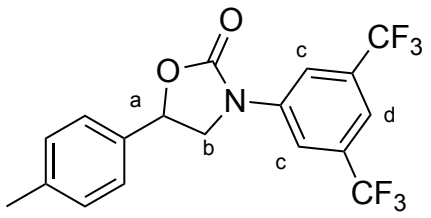

The general procedure was followed by using aziridine **7** to obtain the product as a purple-brown solid.

^{1}H NMR (300 MHz, $CDCl_3$) δ 8.05 (s, 2H, H_c), 7.64 (s, 1H, H_s), 7.35 - 7.24 (m, 4H, H_{Ar}), 5.68 (pst, *J* = 8.1 Hz, 1H, H_a), 4.43 (pst, *J* = 8.7 Hz, 1H, H_b), 4.01 (pst, *J* = 8.1 Hz, 1H, $H_{b'}$), 2.38 ppm (s, 3H, H_{Me}). **^{13}C NMR** (75 MHz, $CDCl_3$) δ 154.20 (C=O), 139.72 (C), 134.12 (C), 132.80 (q, *J* = 33.4 Hz, two overlapping CF_3), 129.86 (two overlapping CH), 125.69 (two overlapping CH), 124.85 (C), 121.23 (C), 117.62 (two overlapping CH), 117.16 (CH), 74.40 (CH), 52.38

(CH_2), 21.22 ppm (CH_3). **^{19}F NMR** (282 MHz, $CDCl_3$) δ -63.26 ppm (s). **LR-MS (ESI):** m/z ($C_{18}H_{13}F_6NO_2$) calcd 389.09, found $[M+H]^+$ 390.13. **Elemental Analysis** calcd. for ($C_{18}H_{13}F_6NO_2$): C (55.53), H (3.37), N (3.60), found: C (55.17), H (3.42), N (3.57). **UV-Vis** λ_{max} (DCM)/nm (log ε): 244 (4.17). **IR** ν_{max} (DCM)/cm^{-1}: 1141, 1185, 1246, 1403, 1476, 1763 (C=O).

8.5 Synthesis of 3-(3,5-*bis*-(trifluoromethyl)phenyl)-5-(4-*tert*-butylphenyl)oxazalidin-2-one (10)

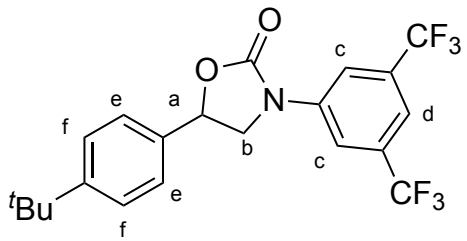

The general procedure was followed by using aziridine **9** to obtain the product as a light brown oil.

^{1}H NMR (300 MHz, $CDCl_3$) δ 8.05 (s, 2H, H_c), 7.64 (s, 1H, H_d), 7.47 (d, *J* = 8.4 Hz, 2H, H_f), 7.36 (d, *J* = 8.4 Hz, 2H, H_e), 5.70 (pst, *J* = 7.7 Hz, 1H, H_a), 4.44 (pst, *J* = 8.6 Hz, 1H, H_b), 4.03 (dd, *J* 8.6, 7.7 Hz, 1H, $H_{b'}$), 1.33 ppm (s, 9H, H_{tBu}). **^{13}C NMR** (75 MHz, $CDCl_3$) 140.12 (C), 134.52 (C) 132.95 (q, *J* = 33.7 Hz, two overlapping CF_3), 126.54 (two overlapping CH), 125.86 (two overlapping CH), 125.24 (C), 121.62 (C), 117.95 (two overlapping CH), 117.58 (CH), 74.70 (CH), 52.73 (CH_2), 35.15 (C), 31.62 ppm (three overlapping CH_3). C=O was not detected. **^{19}F NMR** (282 MHz, $CDCl_3$) δ -63.27 ppm (s). **LR-MS (ESI):** m/z ($C_{21}H_{19}F_6NO_2$) calcd 431.16, found $[M+Na]^+$ 454.16 **Elemental Analysis** calcd. for ($C_{21}H_{19}F_6NO_2$): C (58.47), H (4.44), N (3.25), found: C (58.17), H (4.47), N (3.23). **UV-Vis** λ_{max} (DCM)/nm (log ε): 245 (3.90). **IR** ν_{max} (DCM)/cm^{-1}: 895, 922, 1136, 1183, 1245, 1420, 1476, 1609, 1762 (C=O).

8.6 Synthesis of 3-(4-nitrophenyl)-5-(4-methylphenyl)oxazalidin-2-one (12)

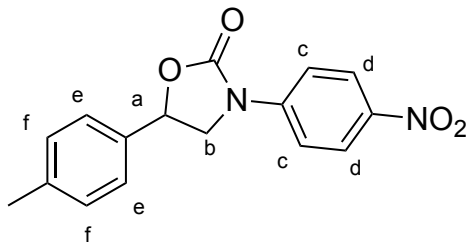

The general procedure was followed by using aziridine **11** to obtain the product as a yellow powder.

^{1}H NMR (400 MHz, $CDCl_3$) δ 8.29 (d, *J* = 9.2 Hz, 2H, H_d), 7.77 (d, *J* = 9.2 Hz, 2H, H_c), 7.35 (d, *J* = 8.0 Hz, 2H, H_e), 7.29 (d, *J* = 8.0 Hz, 2H, H_f), 5.71 (pst, *J* = 8.0 Hz, 1H, H_a), 4.47 (pst, *J* = 8.8 Hz, 1H, H_b), 4.05 - 4.03 (m, 1H, $H_{b'}$), 2.42 ppm (s, 3H, H_{Me}). **^{13}C NMR** (100 MHz, $CDCl_3$) δ 143.73 (C), 143.34 (C), 139.61 (C), 134.14 (C), 129.86 (two overlapping CH), 125.78 (two overlapping CH), 125.00 (two overlapping CH), 117.53 (two overlapping CH), 74.41 (CH), 52.42 (CH_2), 21.24 ppm (CH_3). C=O was not detected. **LR-MS (ESI):** m/z ($C_{16}H_{14}N_2O_4$) calcd 298.10, found $[M+H]^+$ 299.00. **Elemental Analysis** calcd. for ($C_{16}H_{14}N_2O_4$): C (64.42), H (4.73), N (9.39), found: C (64.04), H (4.77), N (9.33). **UV-Vis** λ_{max} (DCM)/nm (log ε): 320 (4.72). **IR** ν_{max} (DCM)/cm^{-1}:1113, 1143, 1311, 1331, 1393, 1422, 1503, 1519, 1598, 1764 (C=O).

8.7 Synthesis of 3-(3,5-*bis*-(trifluoromethyl)phenyl)-5-(4-bromophenyl)oxazalidin-2-one (14)

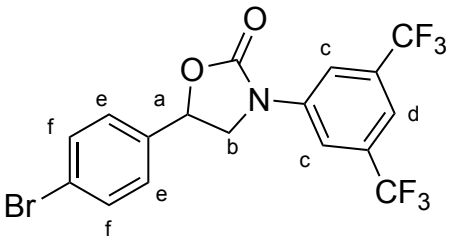

The general procedure was followed by using aziridine **13** to obtain the product as a brown solid.

^{1}H NMR (400 MHz, $CDCl_3$) δ 8.04 (s, 2H, H_c), 7.65 (s, 1H, H_d), 7.60 - 7.57 (m, 2H, H_f), 7.31 (d, *J* = 8.4 Hz, 2H, H_e), 5.68 (pst, *J* = 8.0 Hz, 1H, H_a), 4.48 (pst, *J* = 8.8 Hz, 1H, H_b), 3.99 ppm (dd,

J = 8.4, 7.2 Hz, 1H, $H_{b'}$). **^{13}C NMR** (100 MHz, $CDCl_3$) δ 153.88 (C=O), 139.48 (C), 136.20 (C), 132.47 (q, *J* = 33.8 Hz, two overlapping CF_3), 132.44 (two overlapping CH), 127.27 (two overlapping CH), 124.34 (C), 123.64 (C), 121.63 (C), 117.62 (two overlapping CH), 117.43 (CH), 73.66 (CH), 52.16 ppm (CH_2). **^{19}F NMR** (376 MHz, $CDCl_3$) δ -62.95 ppm (s). **LR-MS (ESI)**: m/z ($C_{17}H_{10}BrF_6NO_2$) calcd 452.98, found $[M+H]^+$ 454.08**. Elemental Analysis** calcd. for ($C_{17}H_{10}BrF_6NO_2$): C (44.96), H (2.22), N (3.08), found: C (44.74), H (2.26), N (3.05). **UV-Vis** λ_{max} (DCM)/nm (log ε): 241 (4.04). **IR** ν_{max} (DCM)/cm^{-1}: 917, 1142, 1185, 1476, 1622, 1767 (C=O).

8.8 Synthesis of 3-(3,5-*bis*-(trifluoromethyl)phenyl)-5-(2,3,4,5,6-pentafluorophenyl)oxazalidin-2-one (16)

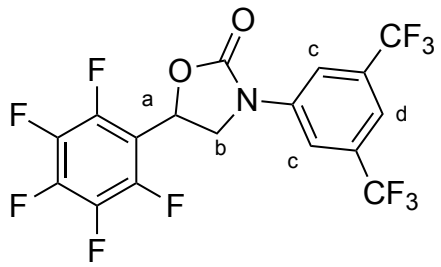

The general procedure was followed by using aziridine **15** to obtain the product as a brown oil.

^{1}H NMR (400 MHz, $CDCl_3$) δ 8.06 (s, 2H, H_c), 7.69 (s, 1H, H_d), 6.06 (dd, *J* = 9.6, 7.2 Hz, 1H, H_a), 4.55 (pst, *J* = 9.4 Hz, 1H, H_b), 4.24 - 4.20 ppm (m, 1H, $H_{b'}$). **^{13}C NMR** (100 MHz, $CDCl_3$) δ 152.91 (C=O), 139.09 (C), 132.98 (q, *J* = 33.6 Hz, two overlapping CF_3), 124.30 (m, two overlapping C-F), 121.58 (C-F), 117.70 (two overlapping CH), 112.79 (CH), 64.44 (CH), 49.71 ppm (CH_2). Three quaternary carbons were not detected. **^{19}F NMR** (282 MHz, $CDCl_3$) δ -63.32 (s, 6F, F_{CF3}), -142.64 (d, *J* = 15.3 Hz, 2F, F_o), -149.66 (t, *J* = 20.5 Hz, 1F, F_p), -159.69 - -159.81 ppm (m, 2F, F_m). **LR-MS (ESI):** m/z ($C_{17}H_6F_6NO_2$) calcd 465.02, found $[M+H]^+$ 466.11. **Elemental Analysis** calcd. for ($C_{17}H_6F_6NO_2$): C (43.89), H (1.30), N (3.01), found: C (43.65), H (1.35), N (2.99). **UV-Vis** λ_{max} (DCM)/nm (log ε): 242 (3.68). **IR** ν_{max} (DCM)/cm^{-1}: 1422, 1511, 1604, 1774 (C=O), 3057.

8.9 Synthesis of 3-(4-*tert*-butylphenyl-5-(2,3,4,5,6-pentafluorophenyl)oxazalidin-2-one (18)

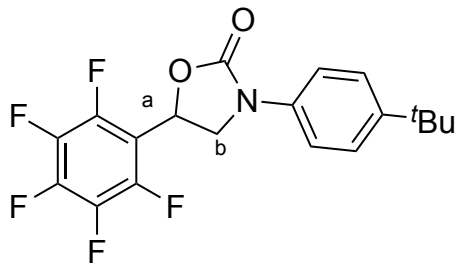

The general procedure was followed by using aziridine **17** to obtain the product as a brown oil.

^{1}H NMR (300 MHz, $CDCl_3$) δ 7.49 - 7.41 (m, 4H, H_{Ar}), 5.97 (dd, *J* = 9.6, 6.9 Hz, 1H, H_a), 4.44 (pst, *J* = 9.3 Hz, 1H, H_b), 4.15- 4.09 (m, 1H, $H_{b'}$), 1.33 ppm (s, 9H, H_{tBu}). **^{13}C NMR** (75 MHz, $CDCl_3$) δ 154.04 (C=O), 148.27 (C), 144.24 (C), 135.36 (C), 126.52 (two overlapping CH), 118.96 (two overlapping CH), 64.65 (CH), 50.69 (CH_2), 34.79 (C), 31.69 ppm (three overlapping CH_3). Five C-F quaternary carbons were not detected. **^{19}F NMR** (282 MHz, $CDCl_3$) δ -142.65 (dd, *J* = 21.9, 10.1 Hz, 1F, F_o), -150.95 (pst, *J* = 20.5 Hz, 1F, F_p), -160.42 - -160.56 ppm (m, 1F, F_m). **LR-MS** (ESI): m/z ($C_{19}H_{16}F_5NO_2$) calcd 385.11, found $[M+Na]^+$ 408.22. **Elemental Analysis** calcd. for ($C_{17}H_6F_6NO_2$): C (59.22), H (4.19), N (3.64), found: C (58.88), H (4.23), N (3.61). **UV-Vis** λ_{max} (DCM)/nm (log ε): 240 (4.26). **IR** ν_{max} (DCM)/cm^{-1}: 978, 1135, 1230, 1308, 1379, 1511, 1765 (C=O).

8.10 Synthesis of 3-(4-methoxyphenyl)-5-phenyloxazalidin-2-one (20)

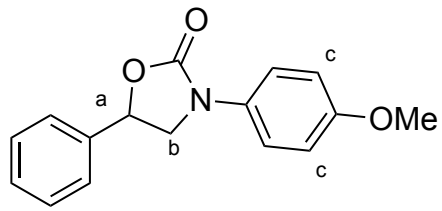

The general procedure was followed by using aziridine **19** to obtain the product as a reddish oil.

^{1}H NMR (300 MHz, $CDCl_3$) δ 7.47 - 7.41 (m, 7H, H_{Ar}), 6.92 (d, *J* = 9.0 Hz, 2H, H_c), 5.66-5.60 (m, 1H, H_a), 4.35 (pst, *J* = 8.8 Hz, 1H, H_b), 3.96 - 3.90 (m, 1H, $H_{b'}$), 3.80 ppm (s, 3H, H_{OMe}).

^{13}C NMR (75 MHz, $CDCl_3$) δ 156.91 (C), 155.41 (C=O), 138.69 (C), 131.75 (C), 129.43 (three overlapping CH), 126.06 (two overlapping CH), 120.77 (two overlapping CH), 114.76 (two overlapping CH), 74.40 (CH), 55.92 (CH_2), 53.65 ppm (CH_3). **LR-MS (ESI):** m/z ($C_{16}H_{15}NO_3$) calcd 269.11, found $[M+H]^+$ 269.95. **Elemental Analysis** calcd. for ($C_{16}H_{15}NO_3$): C (71.36), H (5.61), N (5.20), found: C (71.00), H (5.64), N (5.17). **UV-Vis** λ_{max} (DCM)/nm (log ε): 244 (3.97). **IR** ν_{max} (DCM)/cm^{-1}: 1420, 1514, 1647, 1754 (C=O).

8.11 Synthesis of 3-(4-*tert*-butylphenyl)-5-phenyloxazalidin-2-one (22)

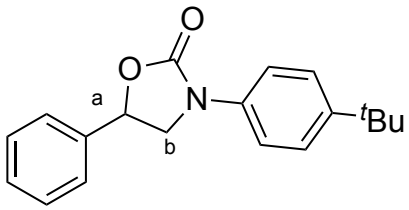

The general procedure was followed by using aziridine **21** to obtain the product as a brown oil.

^{1}H NMR (400 MHz, $CDCl_3$) δ 7.49 - 7.39 (m, 9H, H_{Ar}), 5.63 (dd, *J* = 8.4, 7.2 Hz, 1H, H_a), 4.37 (pst, *J* = 8.8 Hz 1H, H_b), 3.97 - 3.93 (m, 1H, $H_{b'}$), 1.31 ppm (s, 9H, H_{tBu}). **^{13}C NMR** (100 MHz, $CDCl_3$) δ 154.85 (C=O), 147.26 (C), 138.26 (C), 135.55 (C), 129.10 (two overlapping CH), 129.05 (two overlapping CH), 125.99 (two overlapping CH), 125.71 (CH), 118.19 (two overlapping CH), 74.07 (CH), 52.84 (CH_2), 34.36 (C), 31.34 (three overlapping CH_3). **LR-MS (ESI):** m/z ($C_{19}H_{21}NO_2$) calcd 295.16, found $[M+H]^+$ 296.07. **Elemental Analysis** calcd. for ($C_{19}H_{21}NO_2$): C (77.26), H (7.17), N (4.74), found: C (76.92), H (7.19), N (4.72). **UV-Vis** λ_{max} (DCM)/nm (log ε): 241 (4.19). **IR** ν_{max} (DCM)/cm^{-1}: 906, 915, 1276, 1420, 1518, 1756 (C=O).

8.12 Synthesis of 3-(4-bromophenyl)-5-phenyloxazalidin-2-one (24)

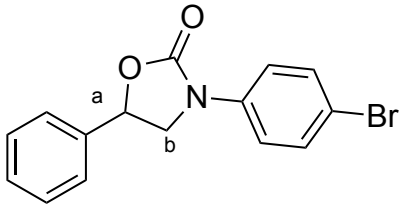

The general procedure was followed by using aziridine **23** to obtain the product as a brown oil.

^{1}H NMR (300 MHz, $CDCl_3$) δ 7.51 - 7.39 (m, 9H, H_{Ar}), 5.65 (pst, *J* = 8.1 Hz, 1H, H_a), 4.35 (pst, *J* = 8.7 Hz, 1H, H_b), 3.93 ppm (pst, *J* = 7.8 Hz, 1H, $H_{b'}$). **^{13}C NMR** (75 MHz, $CDCl_3$) δ 154.86 (C=O), 138.24 (C), 137.69 (C), 132.47 (two overlapping CH), 129.64 (CH), 129.56 (CH), 129.51 (CH) 126.05 (two overlapping CH), 120.15 (two overlapping CH), 117.43 (C), 74.46 (CH), 52.96 ppm (CH_2). **LR-MS (ESI):** m/z ($C_{15}H_{12}BrNO_2$) calcd 317.01, found $[M+H]^+$ 318.30. **Elemental Analysis** calcd. for ($C_{15}H_{12}BrNO_2$): C (56.62), H (3.80), N (4.40), found: C (56.31), H (3.86), N (4.38). **UV-Vis** λ_{max} (DCM)/nm (log ε): 247 (4.28). **IR** ν_{max} (DCM)/cm^{-1}: 1077, 1140, 1369, 1397, 1418, 1493, 1758 (C=O).

8.13 Synthesis of 3-(4-clorophenyl)-5-phenyloxazalidin-2-one (26)

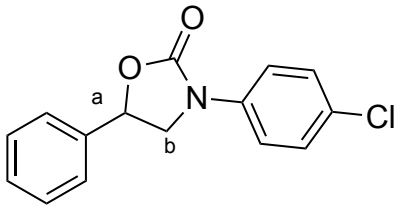

The general procedure was followed by using aziridine **25** to obtain the product as a brown oil.

^{1}H NMR (300 MHz, $CDCl_3$) δ 7.52 - 7.33 (m, 9H, H_{Ar}), 5.65 (pst, *J* = 8.7 Hz 1H, H_a), 4.36 (pst, *J* = 8.8 Hz, 1H, H_b), 3.94 ppm (dd, *J* = 8.7, 7.5 Hz, 1H, $H_{b'}$). **^{13}C NMR** (75 MHz, $CDCl_3$) δ 154.91 (C=O), 138.26 (C), 137.17 (C), 129.63 (CH), 129.53 (two overlapping CH), 129.51 (two overlapping CH), 126.04 (two overlapping CH), 119.83(two overlapping CH), 74.45 (CH), 53.04 ppm (CH_2). One quaternary carbon was not detected. **LR-MS (ESI):** m/z ($C_{15}H_{12}ClNO_2$) calcd 273.06, found $[M+H]^+$ 274.27. **Elemental Analysis** calcd. for ($C_{15}H_{12}ClNO_2$): C (65.82), H (4.42), N (5.12), found: C (65.46), H (4.46), N (5.09). **UV-Vis** λ_{max} (DCM)/nm (log ε): 245 (4.16). **IR** ν_{max} (DCM)/cm^{-1}: 1096, 1142, 1223, 1368, 1398, 1420, 1496, 1599, 1758 (C=O).

8.14 Synthesis of 3-(2-nitrophenyl)-5-phenyloxazalidin-2-one (28)

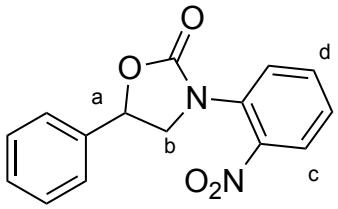

The general procedure was followed by using aziridine **27** to obtain the product as a yellow oil.

^{1}H NMR (300 MHz, $CDCl_3$) δ 8.05 (dd, *J* = 8.1, 1.5 Hz, 1H, H_c), 7.67 - 7.64 (m, 1H, H_d), 7.52 - 7.41 (m, 7H, H_{Ar}), 5.76 (pst, *J* = 8.2 Hz, 1H, H_a), 4.39 (pst, *J* = 8.6 Hz, 1H, H_b), 4.01 ppm (pst, *J* = 8.1 Hz, 1H, $H_{b'}$). **^{13}C NMR** (75 MHz, $CDCl_3$) δ 137.92 (C), 134.34 (CH), 131.71 (C), 129.71 (CH), 129.48 (two overlapping CH), 128.56 (CH), 128.33 (CH), 126.43 (two overlapping CH), 76.25 (CH), 55.20 ppm (CH_2). Two quaternary carbons were not detected. **LR-MS (ESI):** m/z ($C_{15}H_{12}N_2O_4$) calcd 284.08, found $[M+Na]^+$ 307.08. **Elemental Analysis** calcd. for ($C_{15}H_{12}N_2O_4$): C (63.38), H (4.25), N (9.85), found: C (63.04), H (4.29), N (9.80). **UV-Vis** λ_{max} (DCM)/nm (log ε): 231 (3.75). **IR** ν_{max} (DCM)/cm^{-1}: 1015, 1095, 1276, 1422, 1535, 1607, 1765 (C=O).

8.15 Synthesis of 3-(3,5-diclorophenyl)-5-phenyloxazalidin-2-one (31)

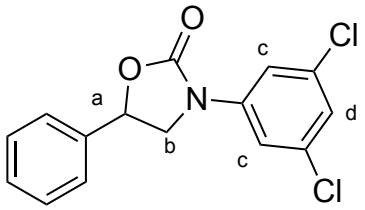

The general procedure was followed by using aziridine **30** to obtain the product as a brown oil.

^{1}H NMR (300 MHz, $CDCl_3$) δ 7.52 (d, *J* = 1.5 Hz, 2H, H_c), 7.44 - 7.42 (m, 5H, H_{Ph}),7.14 - 7.13 (m, 1H, H_d), 5.66 (pst, *J* = 8.0 Hz, 1H, H_a), 4.35 (pst, *J* = 8.8 Hz, 1H, H_b), 3.92 ppm (dd, *J* = 8.7, 7.5 Hz, 1H, $H_{b'}$). **^{13}C NMR** (75 MHz, $CDCl_3$) δ 154.47 (C=O), 140.35 (C), 137.84 (C), 135.95 (two overlapping C), 129.79 (CH), 129.58 (two overlapping CH), 126.01 (two overlapping CH), 124.42 (CH), 116.76 (two overlapping CH), 74.56 (CH), 52.81 ppm (CH_2). **LR-MS (ESI):**

m/z ($C_{15}H_{12}Cl_2NO_2$) calcd 307.02, found $[M+Na]^+$ 330.30. **Elemental Analysis** calcd. for ($C_{15}H_{12}ClNO_2$): C (58.46), H (3.60), N (4.55), found: C (58.12), H (3.64), N (4.51). **UV-Vis** λ_{max} (DCM)/nm (log ε): 245 (3.16). **IR** ν_{max} (DCM)/cm^{-1}: 1148, 1208, 1366, 1392, 1426, 1455, 1569, 1493, 1763 (C=O).

8.16 Synthesis of 3-(3,5-dinitrophenyl-5-phenyloxazalidin-2-one (33)

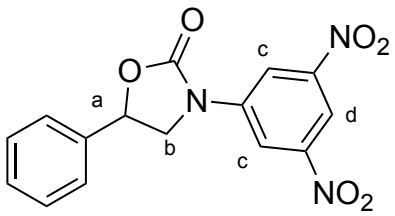

The general procedure was followed by using aziridine **32** to obtain the product as a yellow powder.

^{1}H NMR (400 MHz, $CDCl_3$) δ 8.81 - 8.80 (m, 3H, H_{c+d}), 7.50 - 7.43 (m, 5H, H_{Ph}), 5.79 (pst, *J* = 8.0 Hz, 1H, H_a), 4.55 (pst, *J* = 8.8 Hz, 1H, H_b), 4.13 - 4.08 ppm (m, 1H, $H_{b'}$). **^{13}C NMR** (100 MHz, $CDCl_3$) δ 140.55 (C), 136.70 (C), 129.75 (CH), 129.35 (two overlapping CH), 125.58 (two overlapping CH), 117.30 (two overlapping CH), 113.72 (C), 113.32 (CH) 107.80 (C), 74.54 (CH), 52.40 ppm (CH_2). C=O was not detected. **LR-MS (ESI):** m/z ($C_{15}H_{12}N_3O_6$) calcd 329.06, found $[M+H]^+$ 329.94. **Elemental Analysis** calcd. for ($C_{15}H_{12}N_2O_4$): C (54.72), H (3.37), N (12.76), found: C (54.47), H (3.40), N (12.70). **UV-Vis** λ_{max} (DCM)/nm (log ε): 232 (4.34). **IR** ν_{max} (DCM)/cm^{-1}: 1158, 1206, 1347, 1395, 1423, 1478, 1547, 1768 (C=O).

8.17 Synthesis of 3-(3,5-*bis*-(trifluoromethyl)phenyl)-4-methyl-5-phenyloxazalidin-2-one (35)

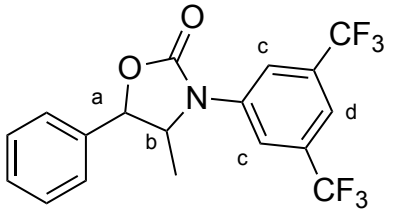

The general procedure was followed by using aziridine **33** to obtain the product as a brown solid.

^{1}H NMR (300 MHz, $CDCl_3$) δ 7.92 (s, 2H, H_c), 7.68 (s, 1H, H_d), 7.47 - 7.40 (m, 5H, H_{Ph}), 5.19 (d, *J* = 6.3 Hz, 1H, H_a), 4.41 (psp, *J* = 6.1 Hz, 1H, H_b), 1.51 ppm (d, *J* = 6.3 Hz, 3H, H_{Me}). **^{13}C NMR** (75 MHz, $CDCl_3$) δ 154.85 (C=O), 138.87 (C), 137.29 (C), 133.06 (q, *J* = 33.7 Hz, two overlapping CF_3), 129.94 (CH), 129.63 (CH), 126.29 (CH), 126.09 (CH), 125.17 (C), 121.56 (C), 121.20 (CH), 118.61 (CH), 82.57 (CH), 60.13 (CH), 18.23 (CH_3). **^{19}F NMR** (276 MHz, $CDCl_3$) δ -63.27 ppm (s). **LR-MS (ESI):** m/z ($C_{18}H_{13}F_6NO_2$) calcd 389.09, found $[M+H]^+$ 390.12. **Elemental Analysis** calcd. for ($C_{18}H_{13}F_6NO_2$): C (55.53), H (3.37), N (3.60), found: C (55.32), H (3.40), N (3.57). **UV-Vis** λ_{max} (DCM)/nm (log ε): 244 (3.87). **IR** ν_{max} (DCM)/cm^{-1}: 1158, 1206, 1347, 1395, 1423, 1478, 1547, 1768 (C=O).

8.18 Synthesis of 3-(4-*tert*-butylphenyl)-4-methyl-5-phenyloxazalidin-2-one (37)

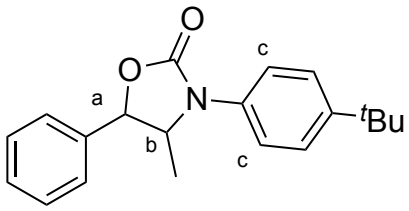

The general procedure was followed by using aziridine **36** to obtain the product as a brown oil.

^{1}H NMR (400 MHz, $CDCl_3$) δ 7.44 - 7.40 (m, 7H, H_{Ar}), 7.30 (d, *J* = 8.8 Hz, 2H, H_c), 5.11 (d, *J* = 6.8 Hz, 1H, H_a), 4.27 (psp, *J* = 6.4 Hz, 1H, H_b), 1.42 (d, *J* = 6.0 Hz, 3H, H_{Me}), 1.32 (s, 9H, H_{tBu}). **^{13}C NMR** (100 MHz, $CDCl_3$) δ 129.11 (CH), 129.01 (two overlapping CH), 126.11 (two overlapping CH), 125.86 (two overlapping CH), 122.23(two overlapping CH), 82.19 (CH), 60.55 (CH), 31.32 (three overlapping CH_3), 18.11 (CH_3). Quaternary carbons were not detected. **LR-MS (ESI):** m/z ($C_{20}H_{23}NO_2$) calcd 309.17, found $[M+H]^+$ 310.00. **Elemental Analysis** calcd. for ($C_{20}H_{26}NO_2$): C (77.64), H (7.49), N (4.23), found: C (77.82), H (7.86), N (4.02). **UV-Vis** λ_{max} (DCM)/nm (log ε): 240 (4.30). **IR** ν_{max} (DCM)/cm^{-1}: 1369, 1394, 1519, 1607, 1753 (C=O).

8.19 Synthesis of 3-(3-methoxyphenyl)-5-(4-fluorophenyl)oxazalidin-2-one (41) by the tandem procedure

8.19.1 Synthesis of 1-(3-methoxyphenyl)-2-(4-fluorophenyl) aziridine

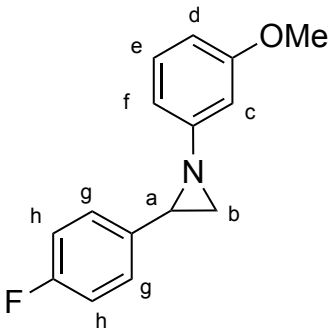

The product was obtained by refluxing 3-methoxyphenylazide and 4-fluorostyrene for 72 hours (Yield: 37 %).

^{1}H NMR (400 MHz, $CDCl_3$) δ 7.35 (m, 2H, H_h), 7.17 (pst, *J* = 8.0 Hz, 1H, H_e), 7.05 (m, 2H, H_g), 6.73 - 6.63 (m, 1H, H_F), 6.61 (s, 1H, H_c), 6.59 - 6.53 (m, 1H, H_d), 3.79 (s, 3H, H_{OMe}), 3.10 (dd, *J* = 6.3, 3.3 Hz, 1H, H_a), 2.46 (psd, *J* = 6.4 Hz, 1H, H_b), 2.35 ppm (psd, *J* = 3.2 Hz, 1H, $H_{b'}$).

8.19.2 Synthesis of 3-(3-methoxyphenyl)-5-(4-fluorophenyl)oxazalidin-2-one (41)

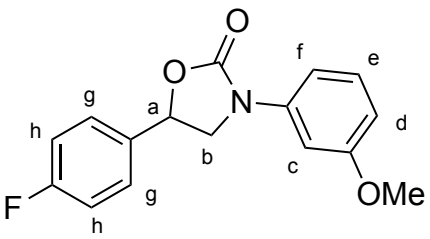

The product was prepared from 1-(3-methoxyphenyl)-2-phenyl aziridine by using the reaction crude following the general procedure (Yield: 35%). The aziridine amount was determined by ^{1}H NMR on a fraction of the reaction mixture using 2,4-dinitrotoluene as the internal standard. The collected analytical data were in accordance with those reported in literature.[268]

^{1}H NMR (400 MHz, $CDCl_3$) δ 7.43 - 7.40 (m, 2H, H_h), 7.30 - 7.27 (m, 2H, H_g), 7.15 - 7.13 (m, 2H, H_{e+f}), 7.03 (ddd, *J* = 8.3, 2.2, 0.8 Hz, 1H, H_c), 6.71 (ddd, *J* = 8.4, 2.5, 0.8 Hz, 1H, H_d), 5.61

(pst, *J* = 8.0 Hz, 1H, H_a), 4.36 (pst, *J* = 8.8 Hz, 1H, H_b), 3.92 (dd, *J* = 8.8, 7.6 Hz, 1H, $H_{b'}$), 3.83 ppm (s, 1H, H_{OMe}).

1. ^{1}H, ^{13}C and ^{19}F NMR spectra of unreported *N*-aryl oxazolidinones

Compound (4a): ^{1}H NMR (400 MHz, $CDCl_3$)

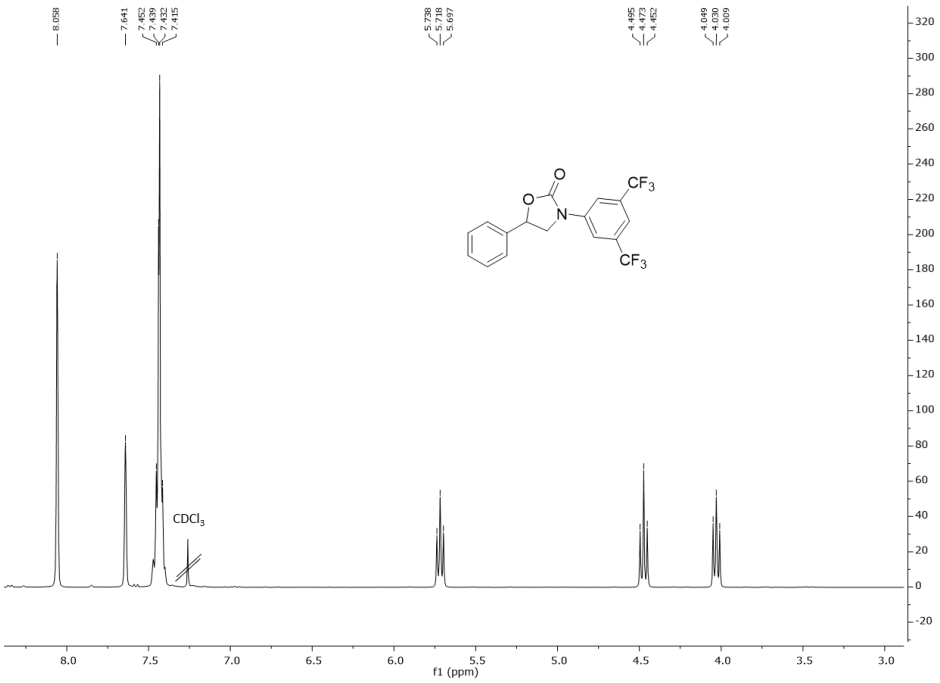

Compound (4a): ^{13}C NMR (100 MHz, $CDCl_3$)

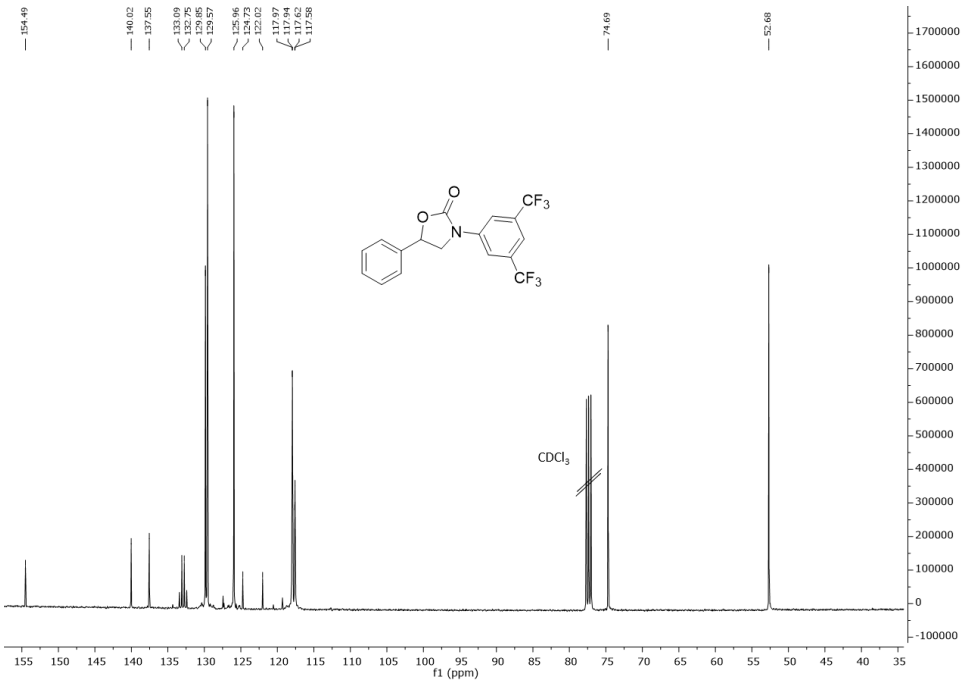

Compound (4a): ^{19}F NMR (376 MHz, $CDCl_3$)

Compound (6a): ^{1}H NMR (400 MHz, $CDCl_3$)

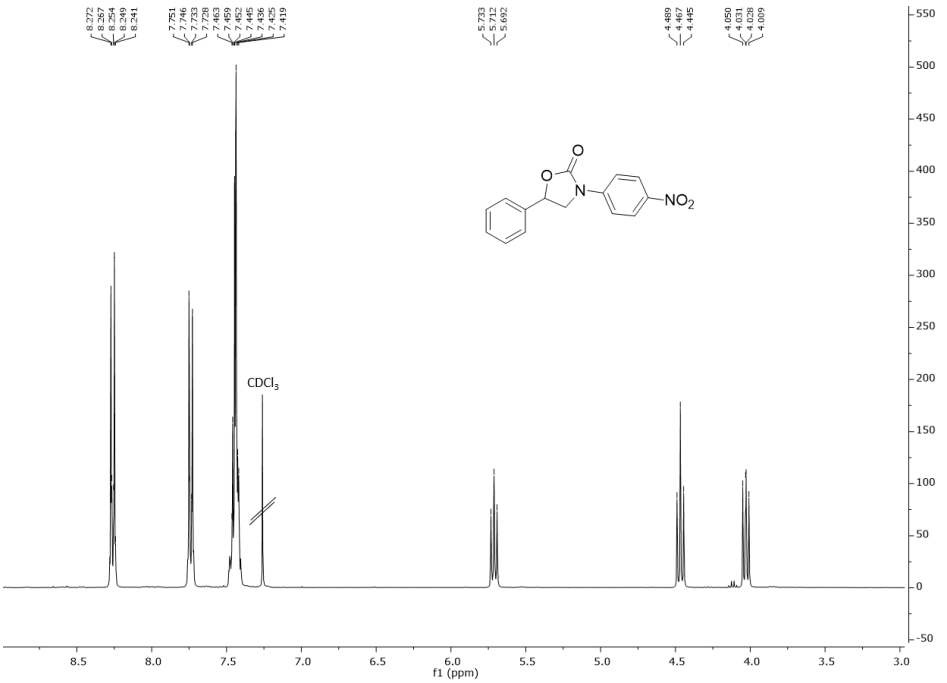

Compound (6a): ^{13}C NMR (100 MHz, $CDCl_3$)

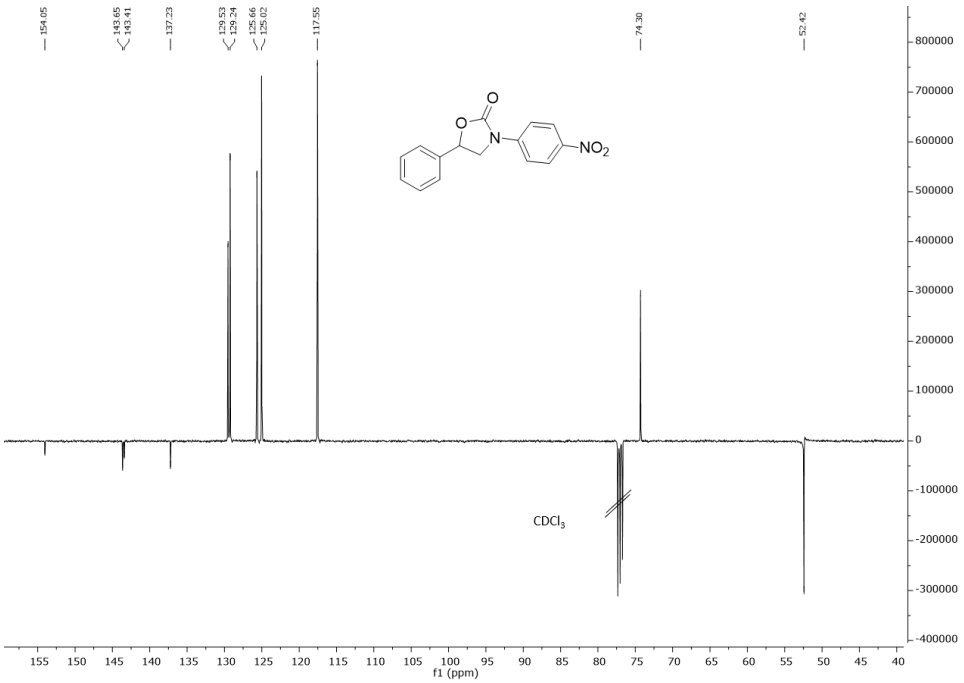

Compound (8a): ^{1}H NMR (300 MHz, $CDCl_3$)

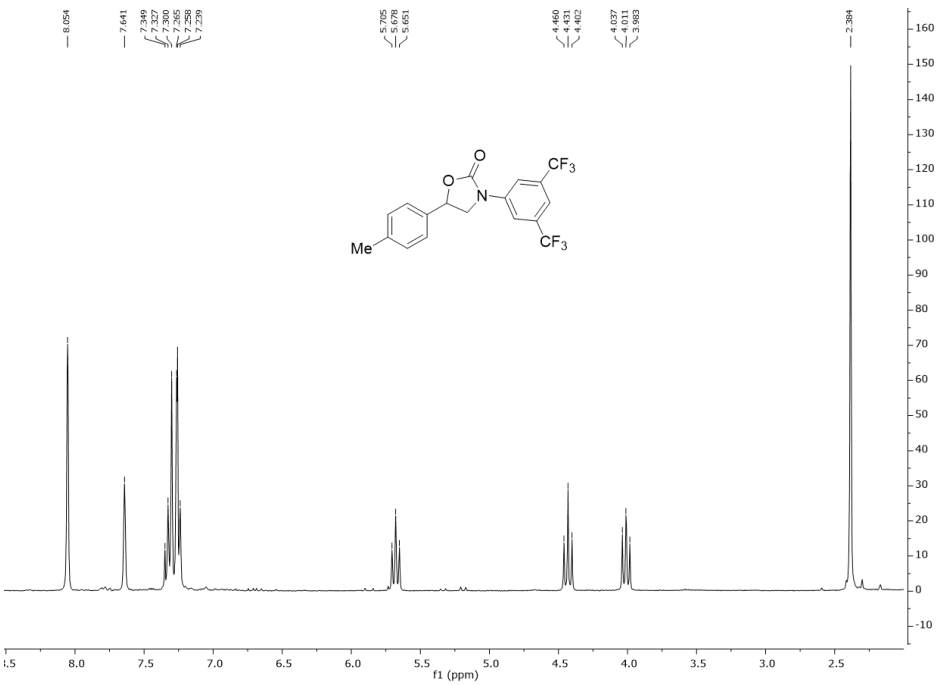

Compound (8a): ^{13}C NMR (75 MHz, $CDCl_3$)

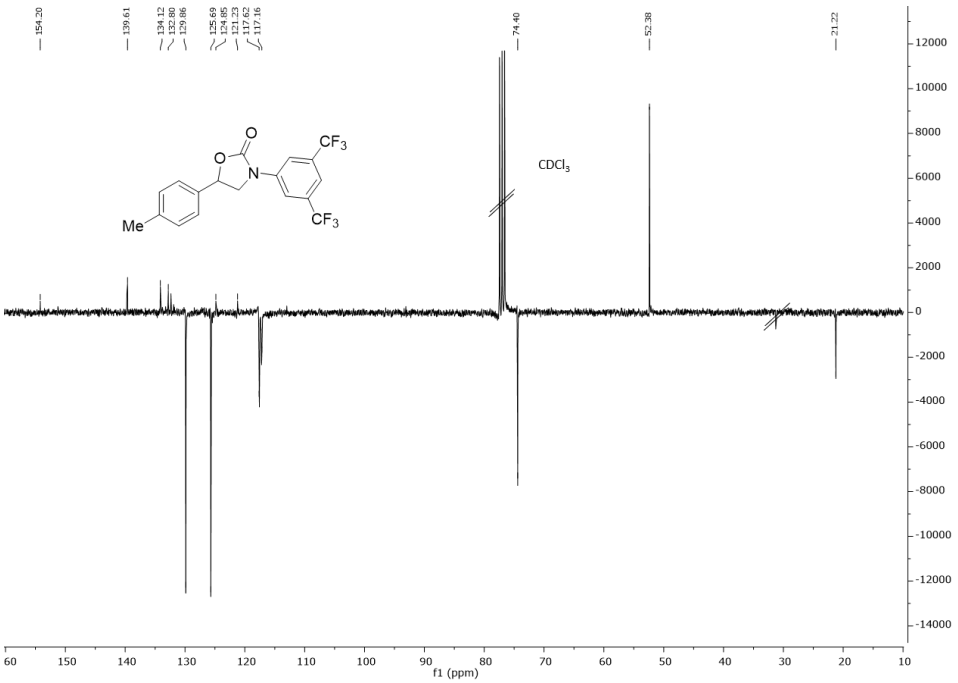

Compound (8a): ^{19}F NMR (282 MHz, $CDCl_3$)

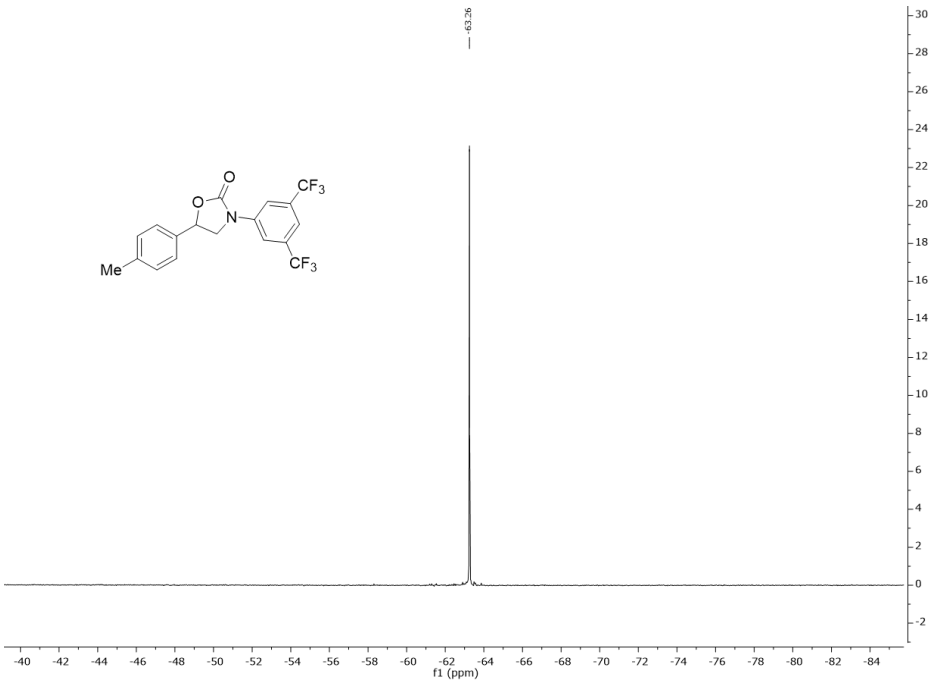

Compound (10a): ^{1}H NMR (300 MHz, $CDCl_3$)

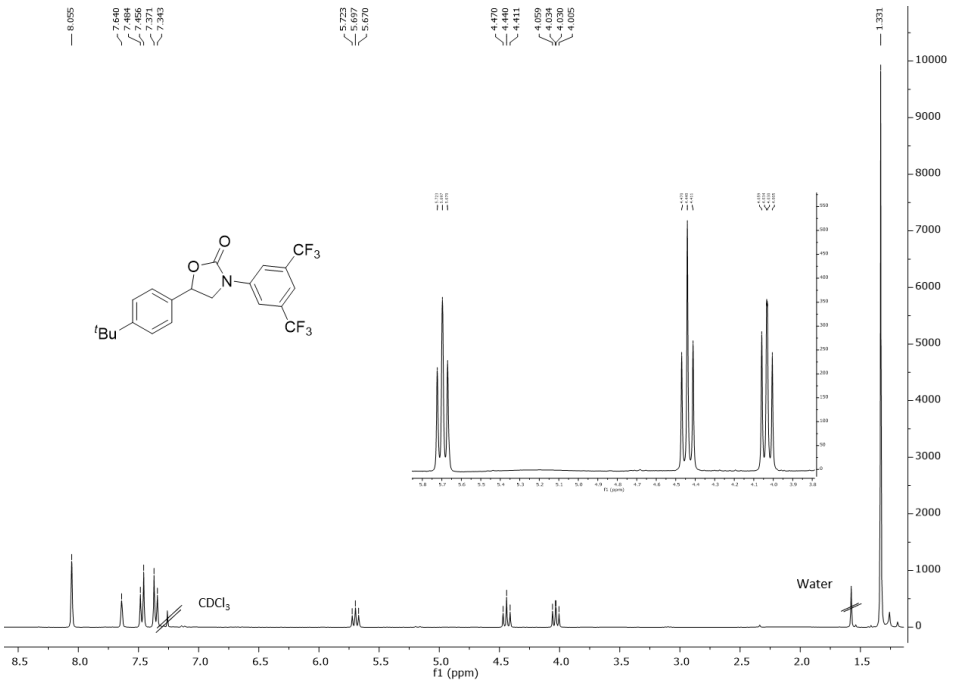

Compound (10a): ^{13}C NMR (75 MHz, $CDCl_3$)

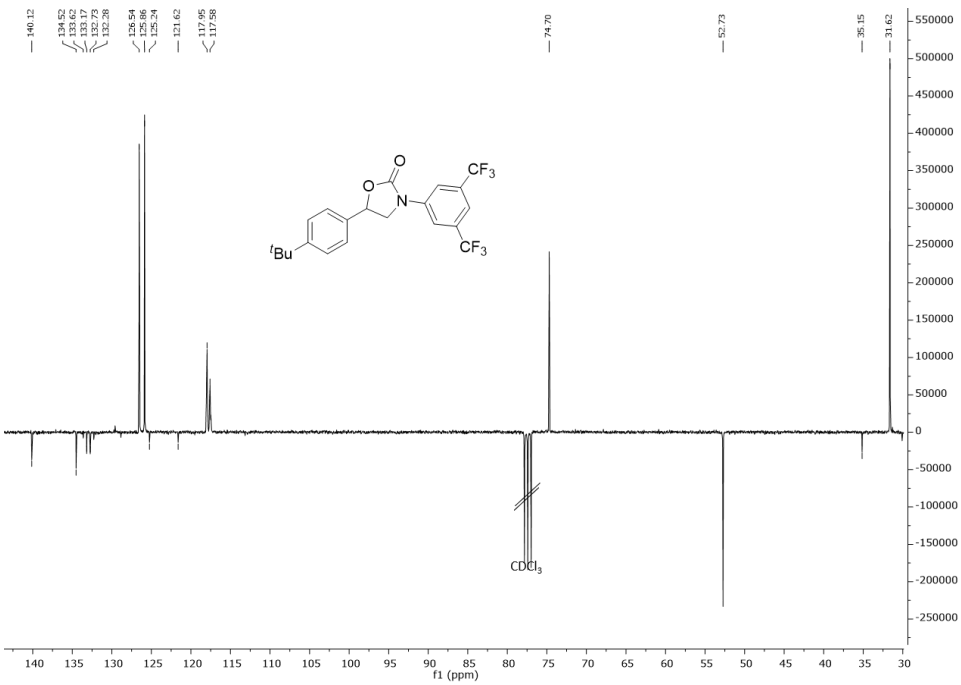

Compound (10a): ^{19}F NMR (282 MHz, $CDCl_3$)

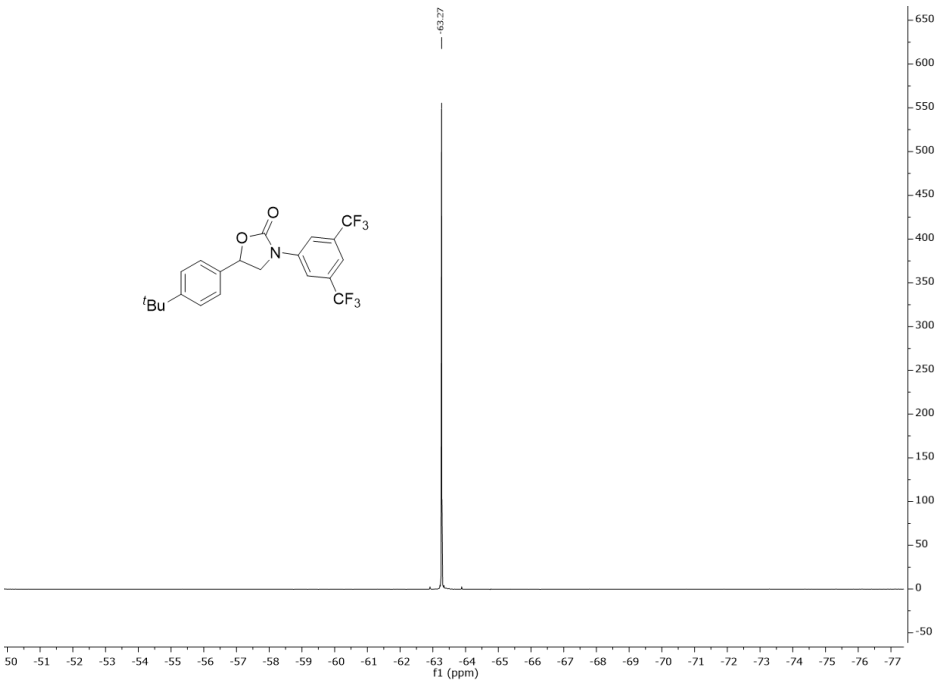

Compound (12a): ^{1}H NMR (400 MHz, $CDCl_3$)

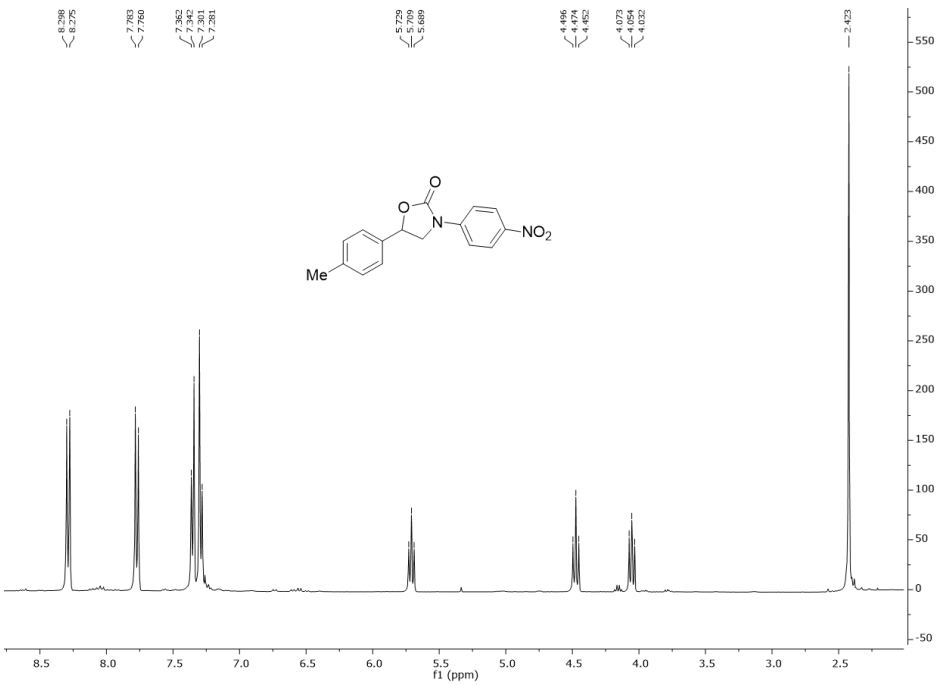

Compound (12a): ^{13}C NMR (100 MHz, $CDCl_3$)

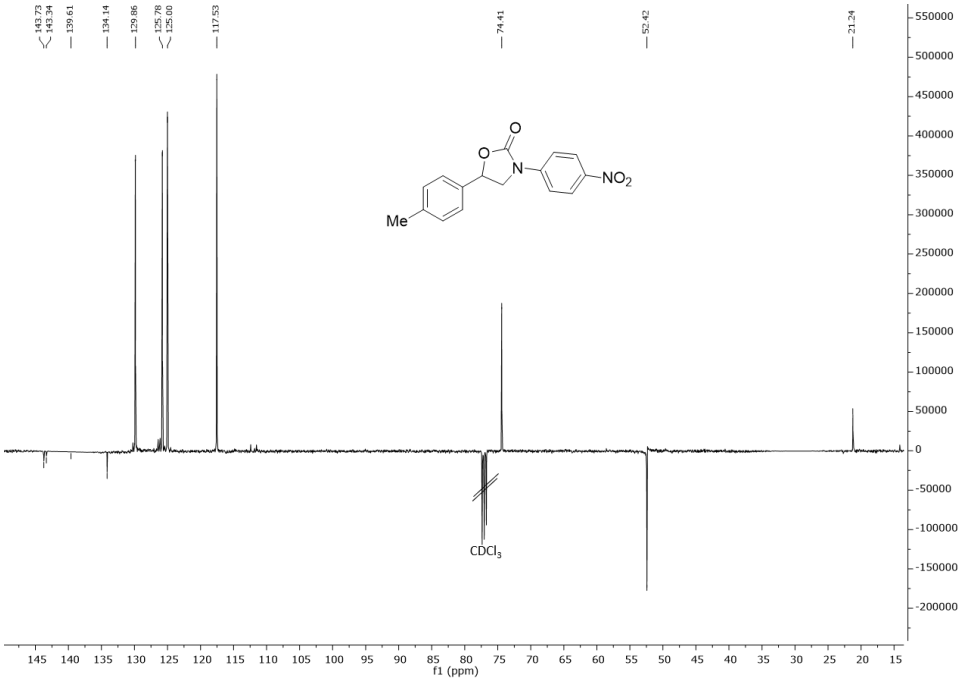

Compound (14a): ^{1}H NMR (400 MHz, $CDCl_3$)

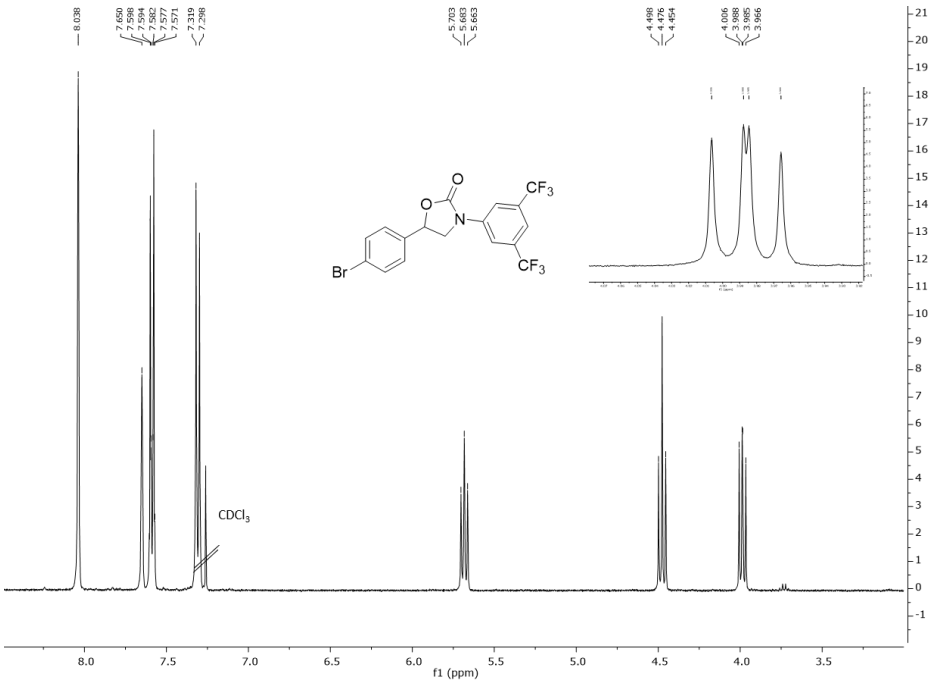

Compound (14a): ^{13}C NMR (100 MHz, $CDCl_3$)

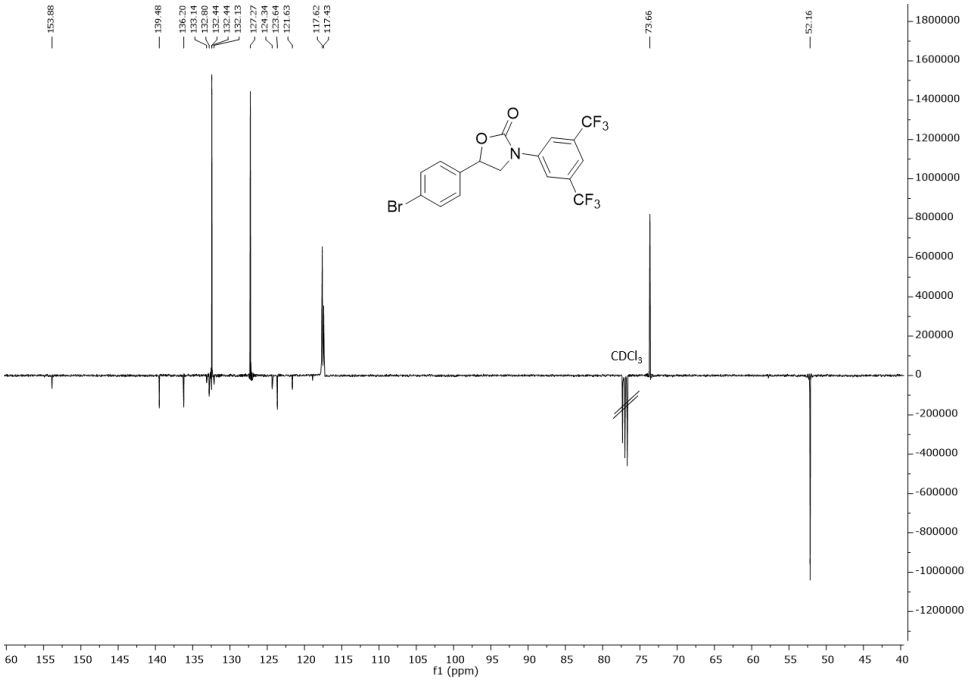

Compound (14a): ^{19}F NMR (376 MHz, $CDCl_3$)

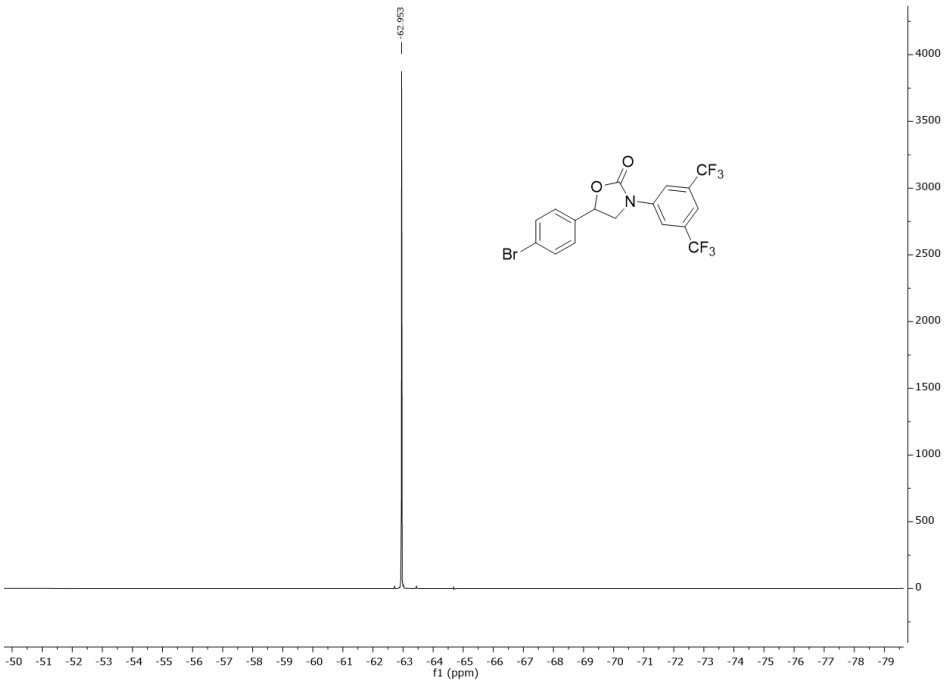

Compound (16a): ^{1}H NMR (400 MHz, $CDCl_3$)

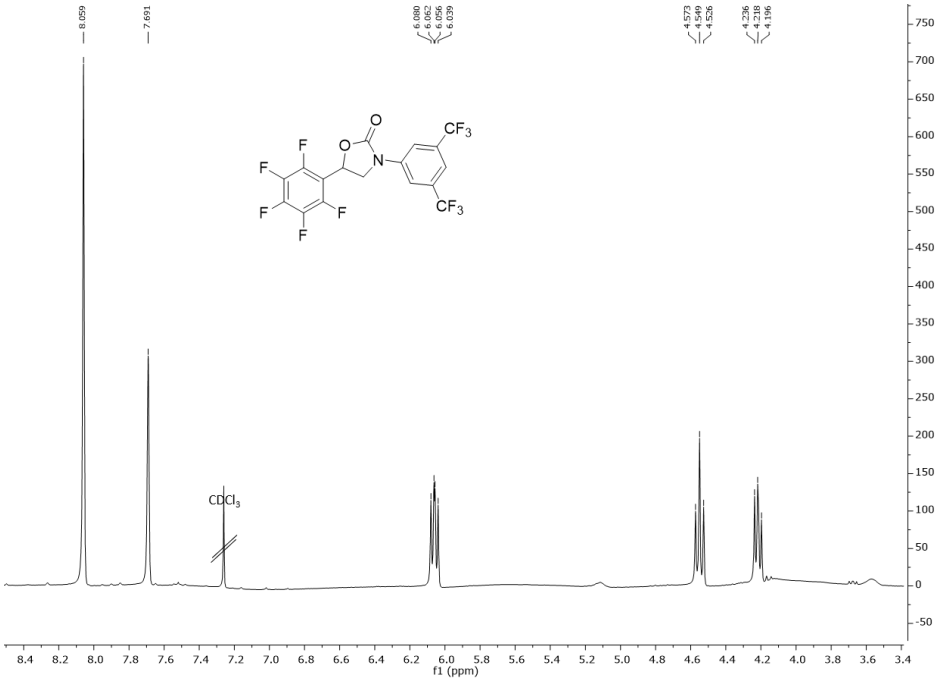

Compound (16a): ^{13}C NMR (100 MHz, $CDCl_3$)

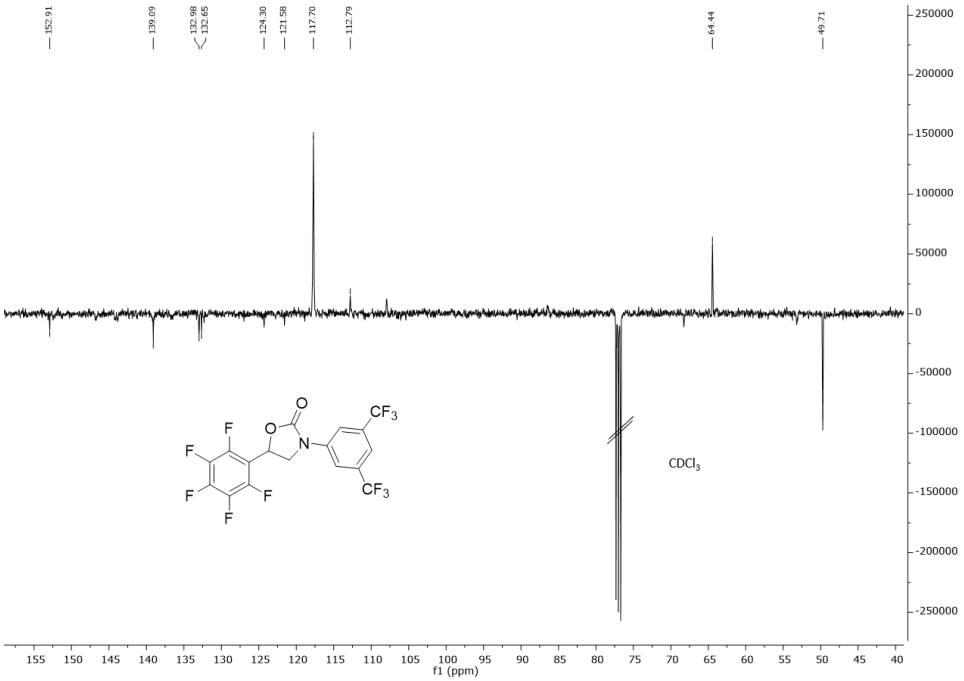

Compound (16a): ^{19}F NMR (376 MHz, $CDCl_3$)

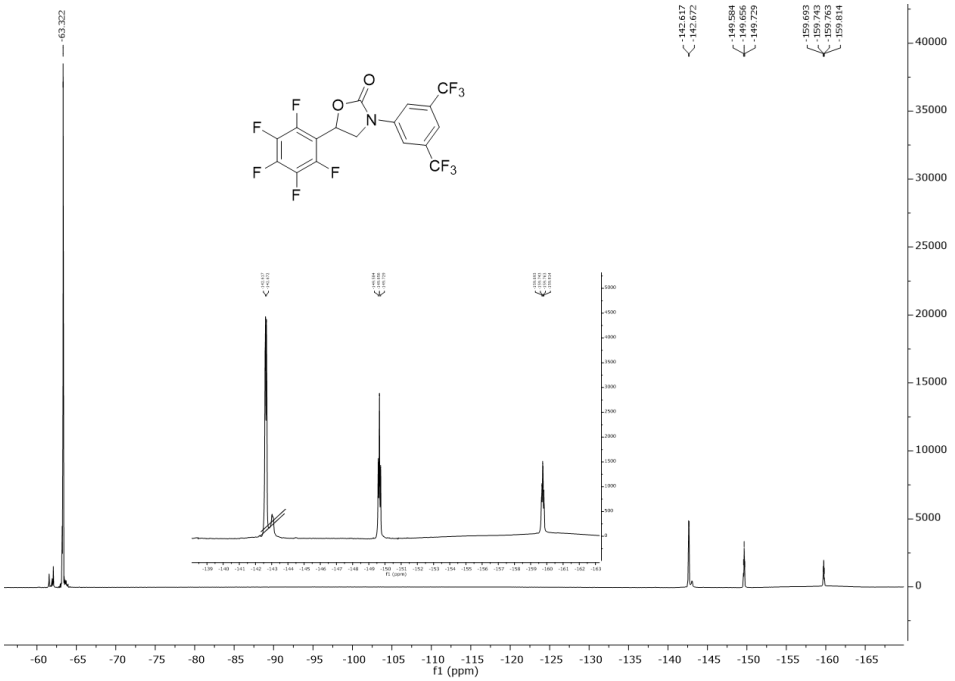

Compound (18a): ^{1}H NMR (300 MHz, $CDCl_3$)

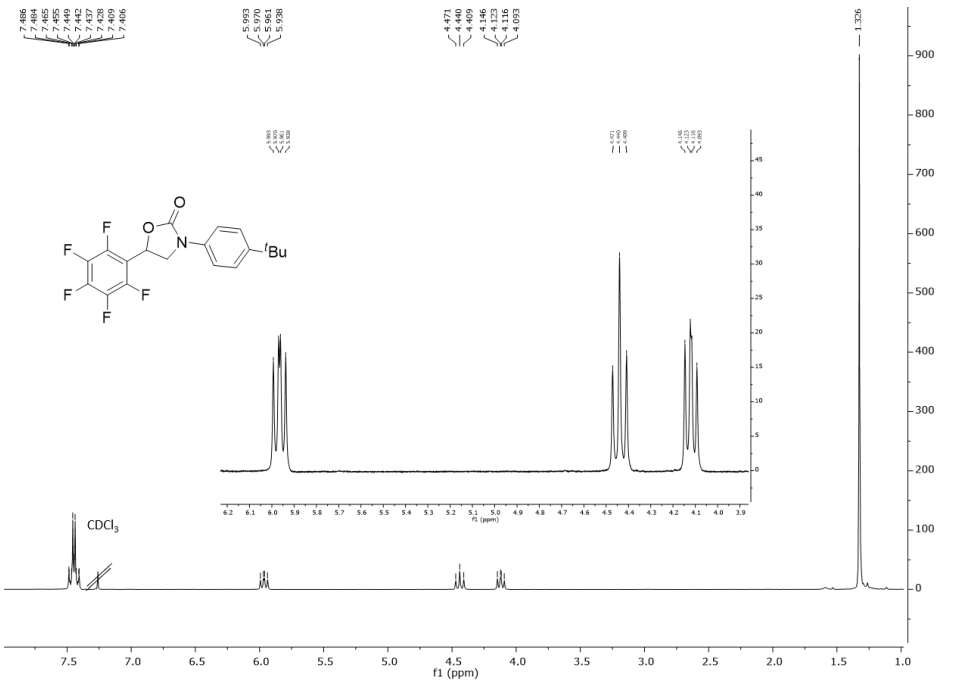

Compound (18a): ^{13}C NMR (75 MHz, $CDCl_3$)

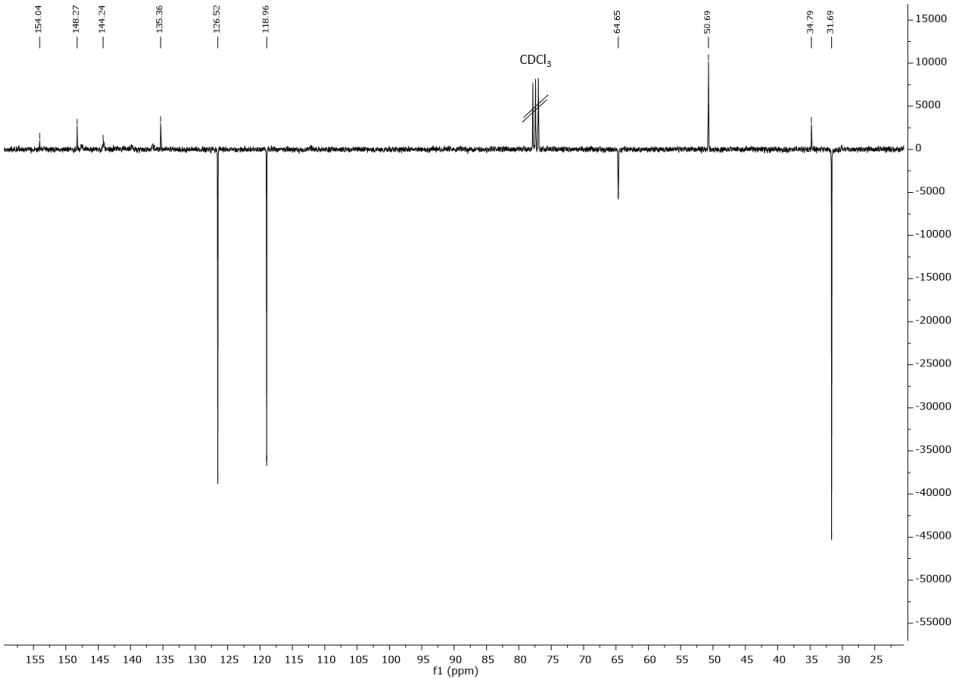

Compound (18a): ^{19}F NMR (282 MHz, $CDCl_3$)

Compound (20a): ^{1}H NMR (300 MHz, $CDCl_3$)

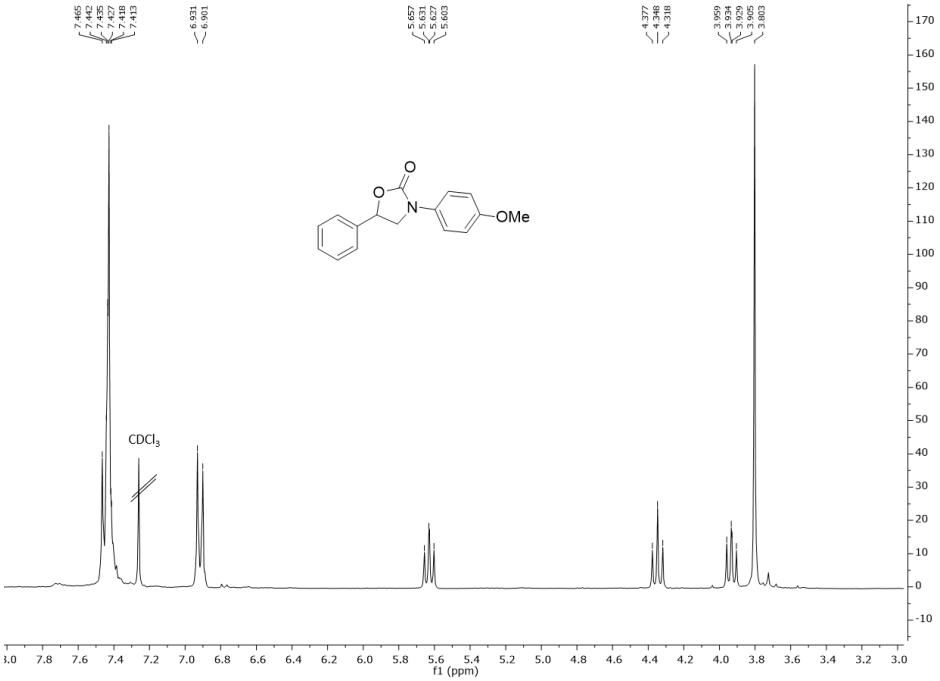

Compound (20a): ^{13}C NMR (75 MHz, $CDCl_3$)

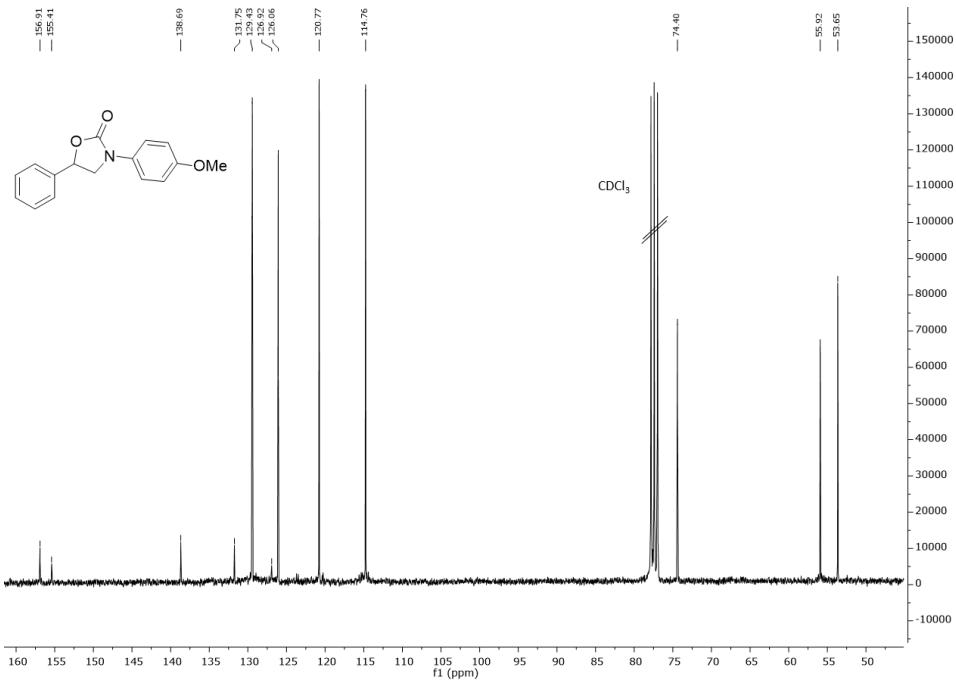

Compound (22a): ^{1}H NMR (400 MHz, $CDCl_3$)

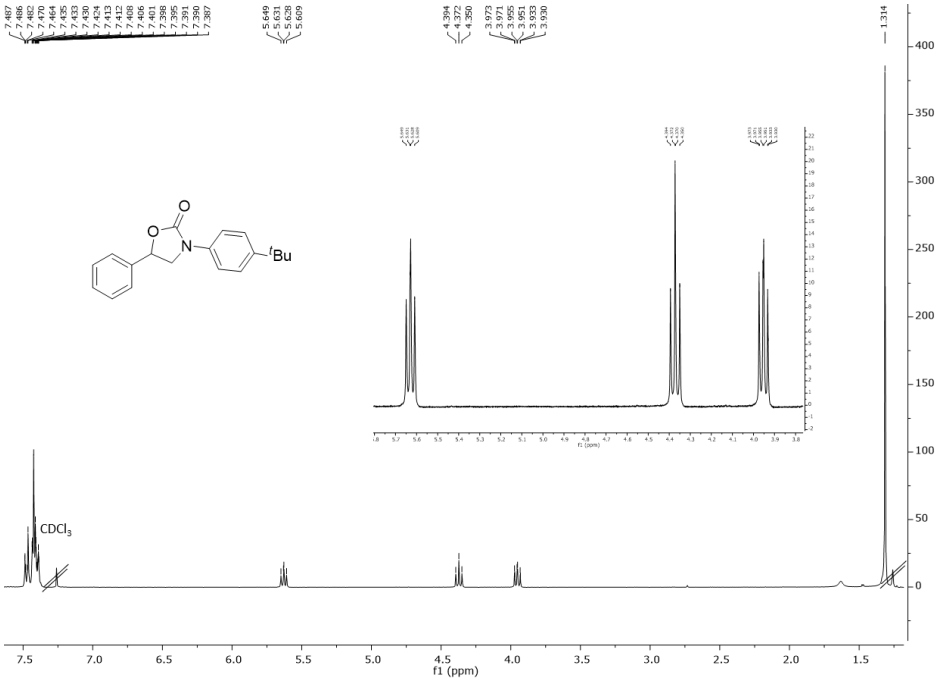

Compound (20a): ^{13}C NMR (100 MHz, $CDCl_3$)

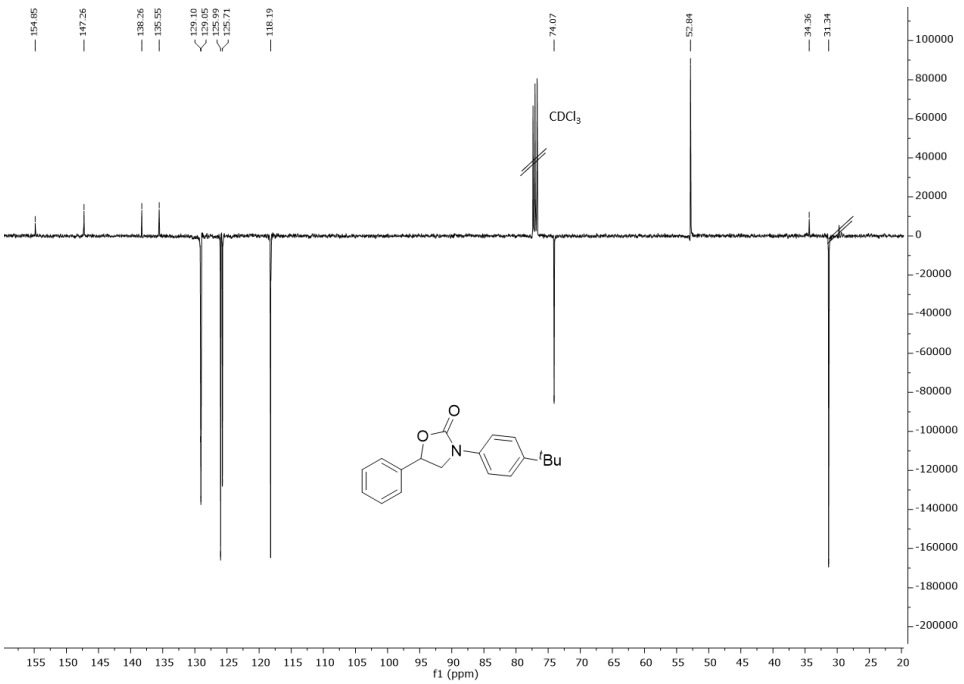

Compound (24a): ^{1}H NMR (300 MHz, $CDCl_3$)

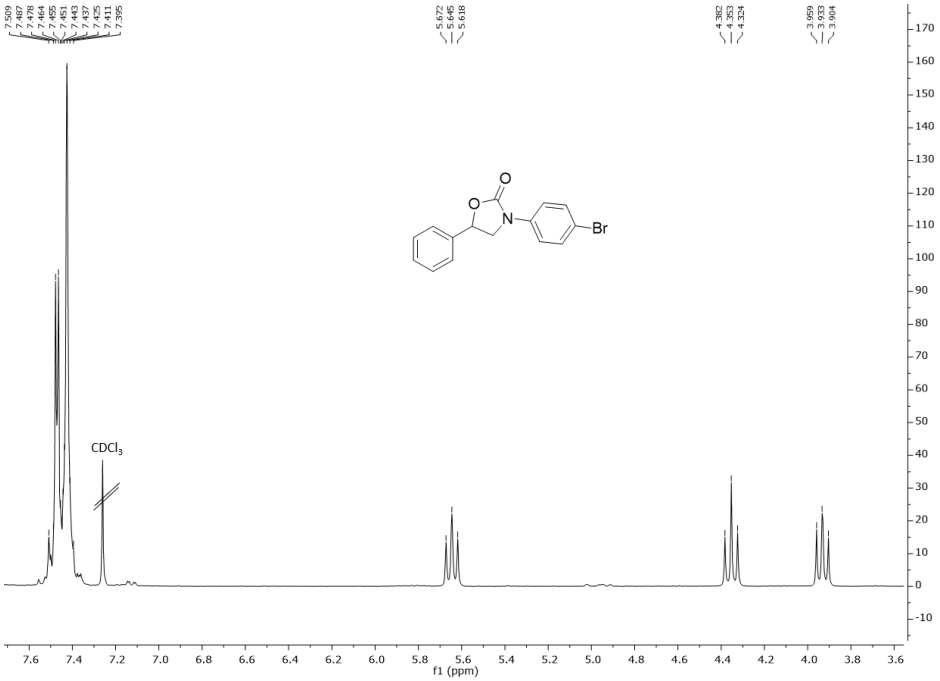

Compound (24a): ^{13}C NMR (75 MHz, $CDCl_3$)

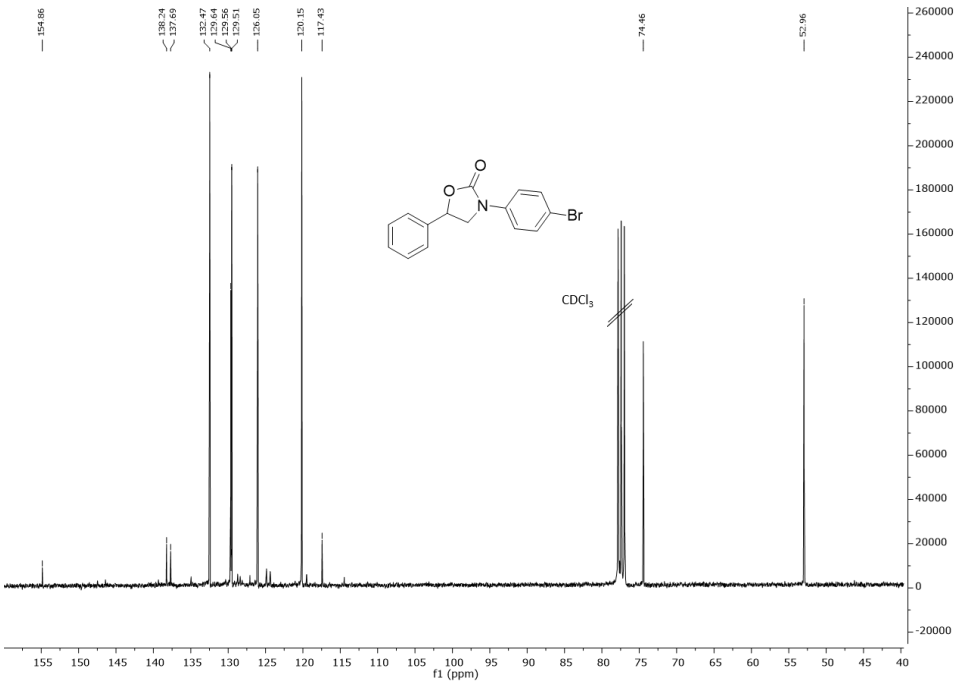

Compound (26a): ^{1}H NMR (300 MHz, $CDCl_3$)

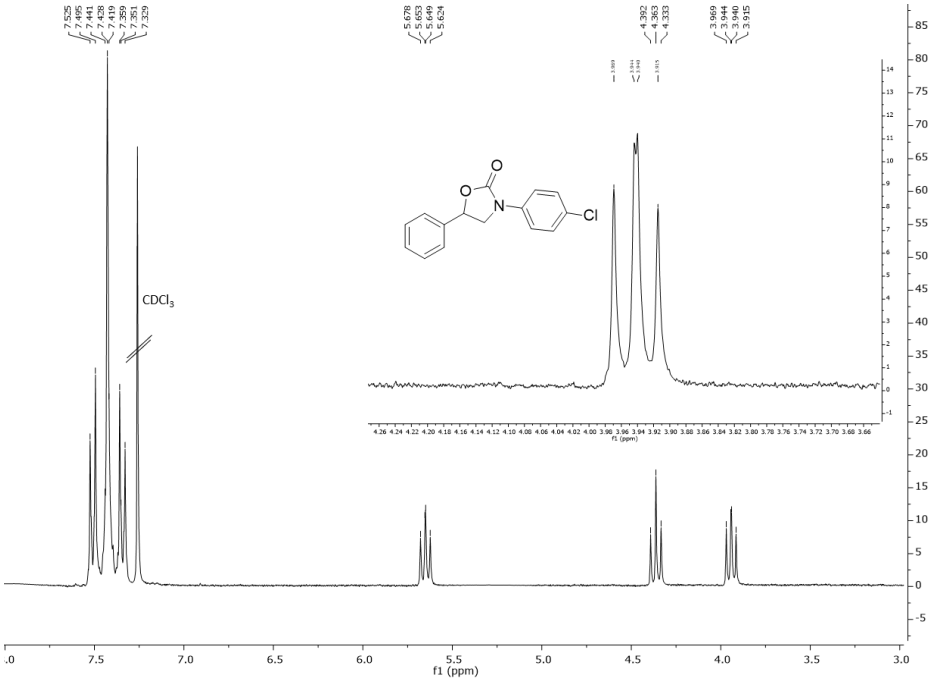

Compound (26a): ^{13}C NMR (75 MHz, $CDCl_3$)

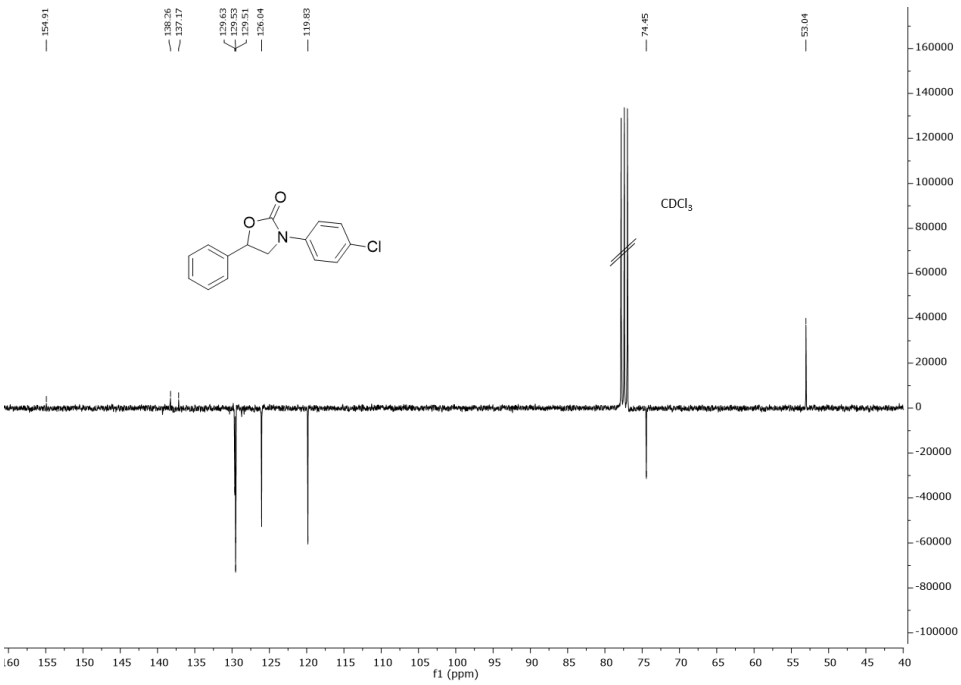

Compound (28a): ^{1}H NMR (300 MHz, $CDCl_3$)

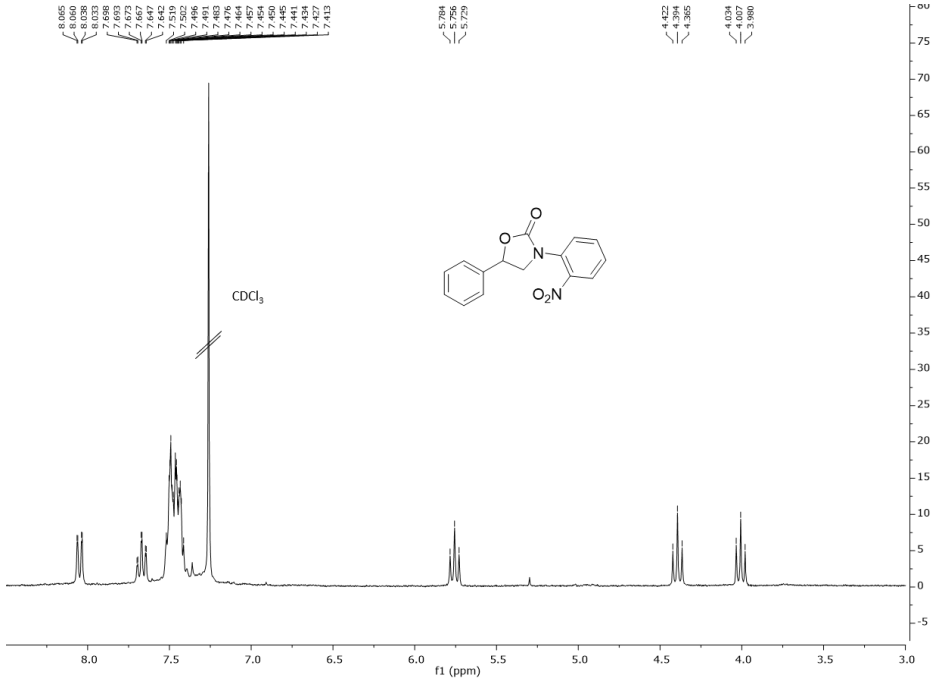

ù

Compound (28a): ^{13}C NMR (75 MHz, $CDCl_3$)

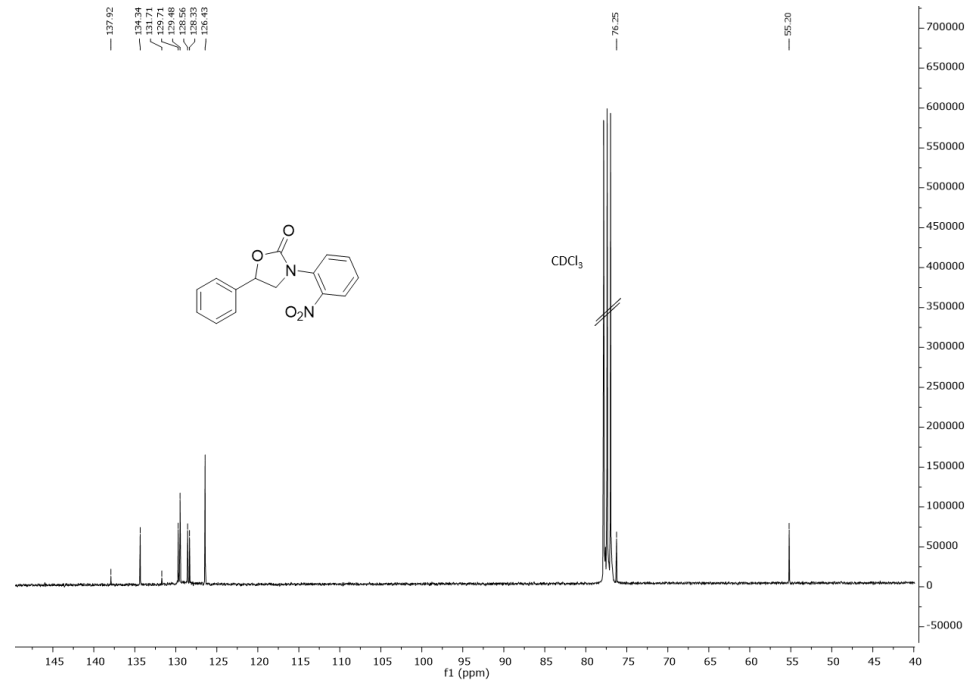

Compound (31a): ^{1}H NMR (300 MHz, $CDCl_3$)

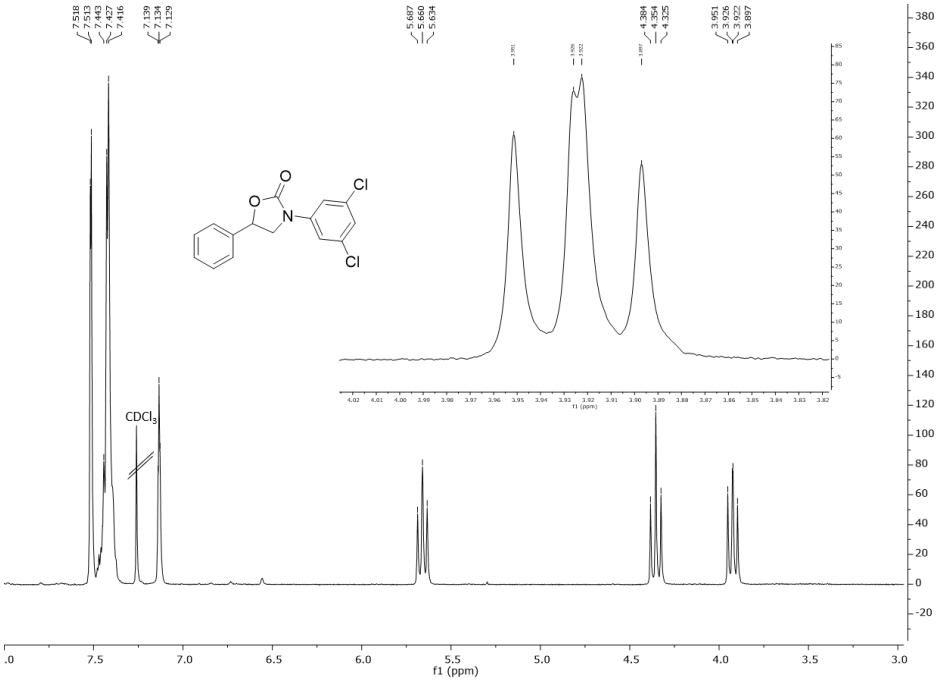

Compound (31a): ^{13}C NMR (75 MHz, $CDCl_3$)

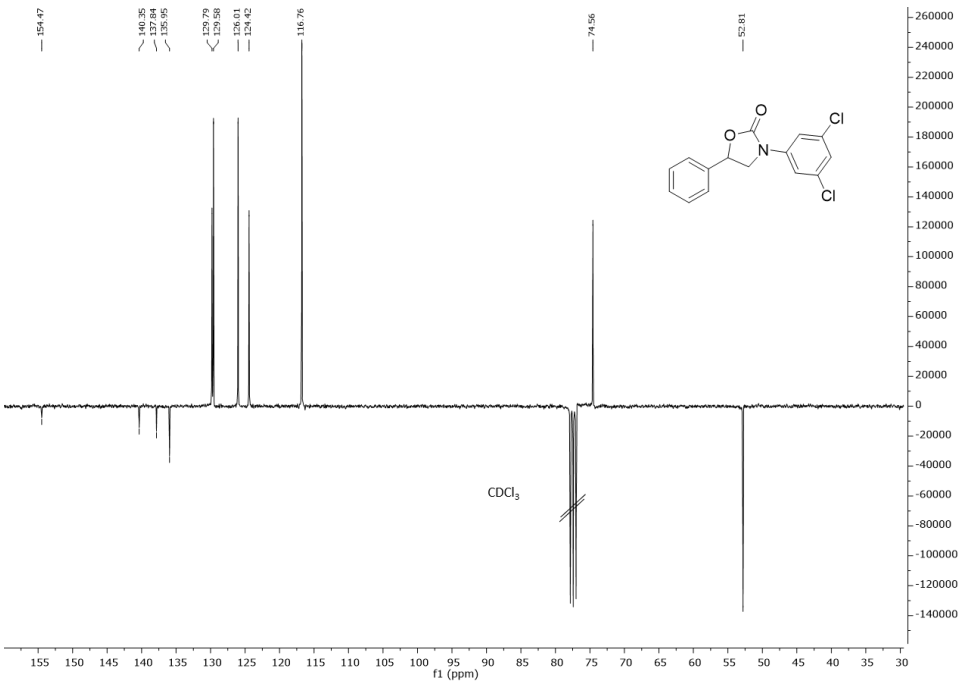

Compound (33a): ^{1}H NMR (400 MHz, $CDCl_3$)

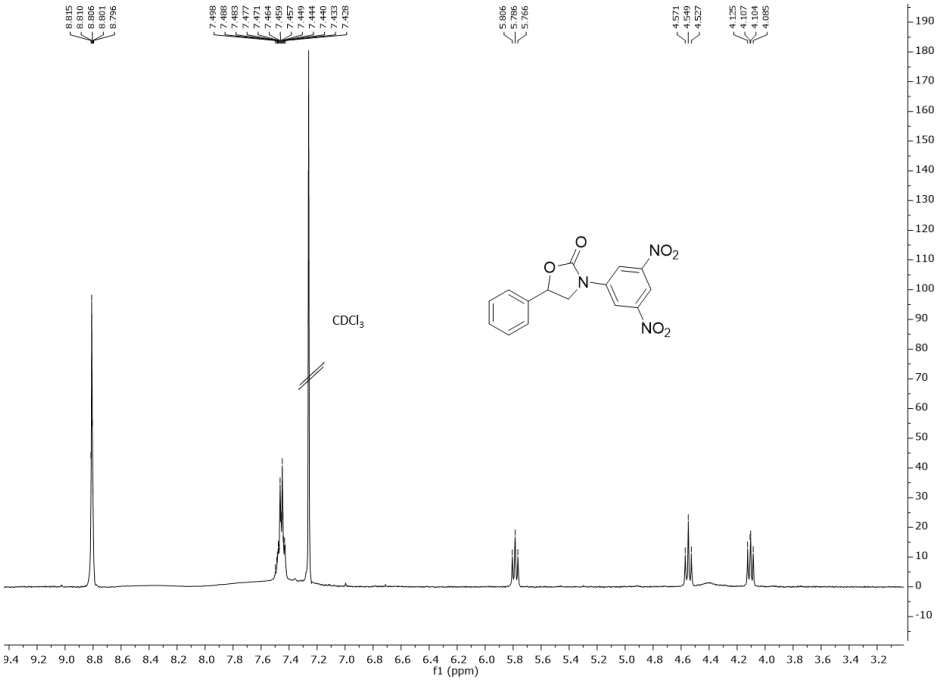

Compound (33a): ^{13}C NMR (100 MHz, $CDCl_3$)

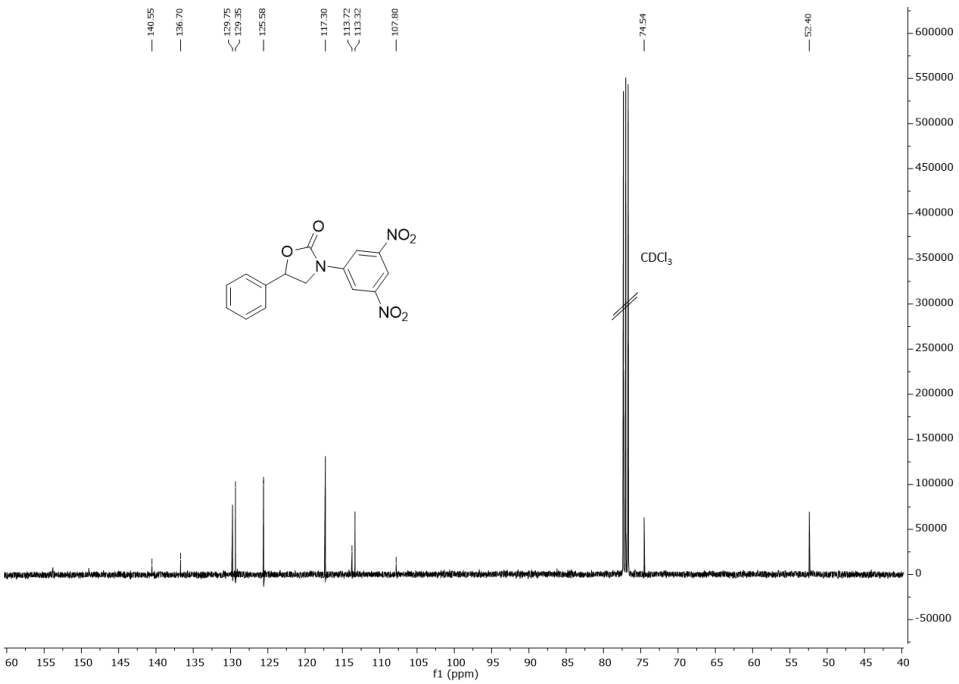

Compound (35a): ^{1}H NMR (300 MHz, $CDCl_3$)

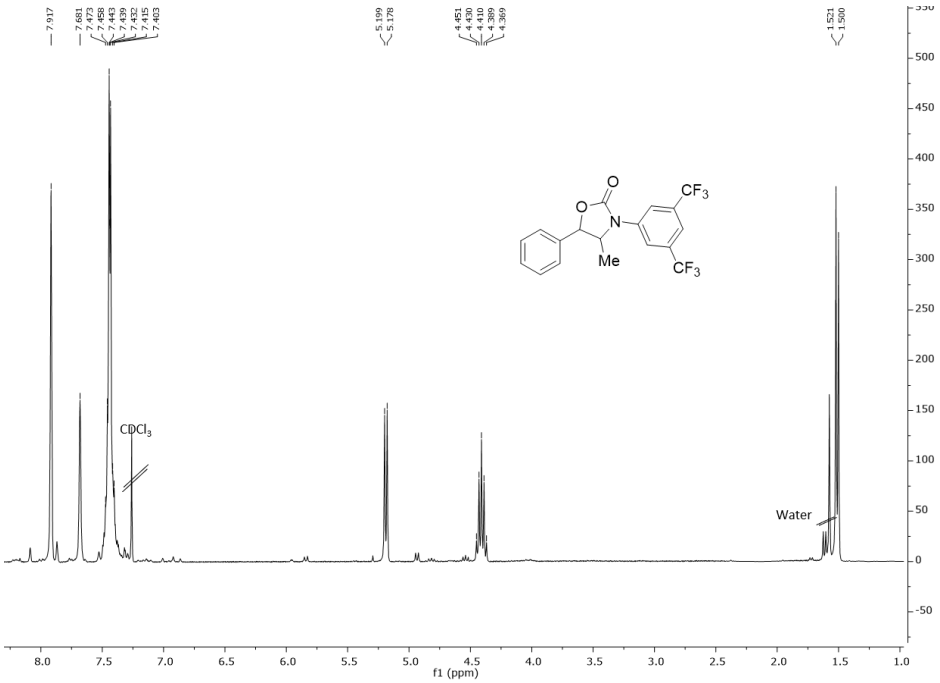

Compound (35a): ^{13}C NMR (75 MHz, $CDCl_3$)

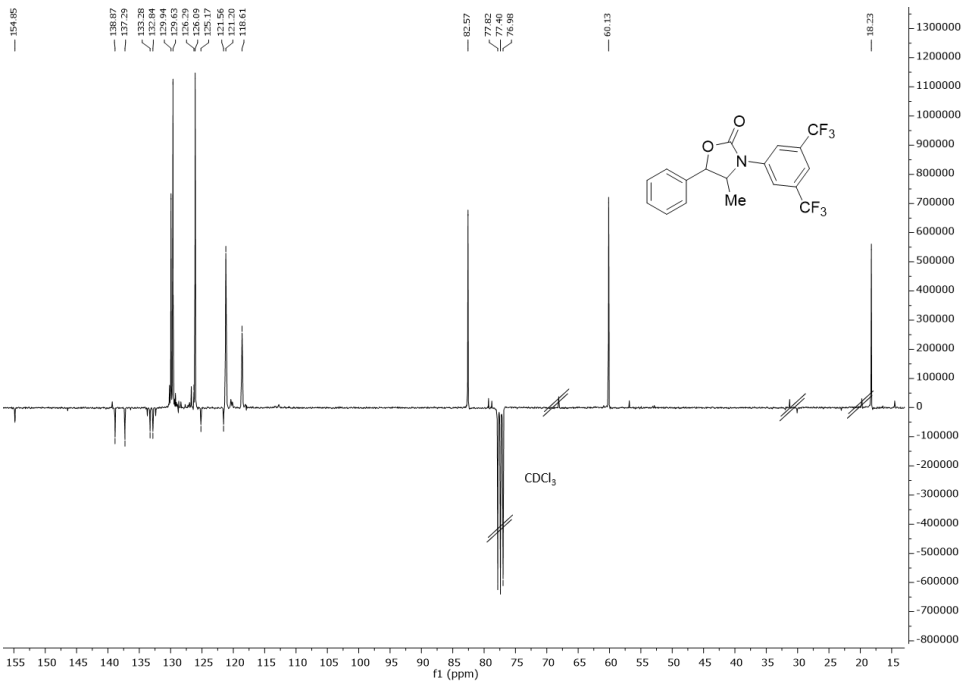

Compound (35a): ^{19}F NMR (282 MHz, $CDCl_3$)

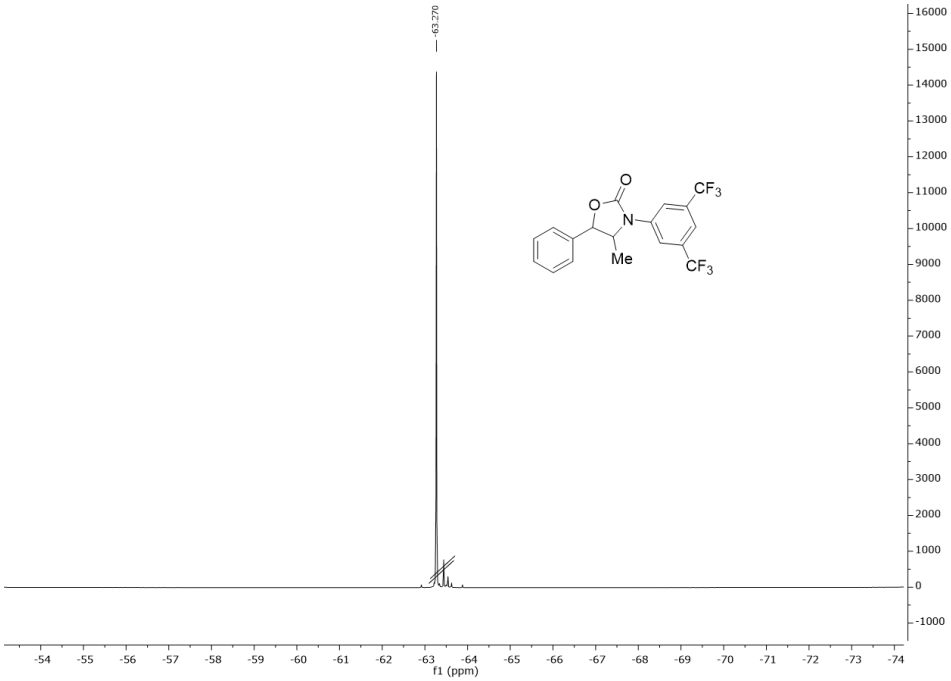

Compound (37a): ^{1}H NMR (400 MHz, $CDCl_3$)

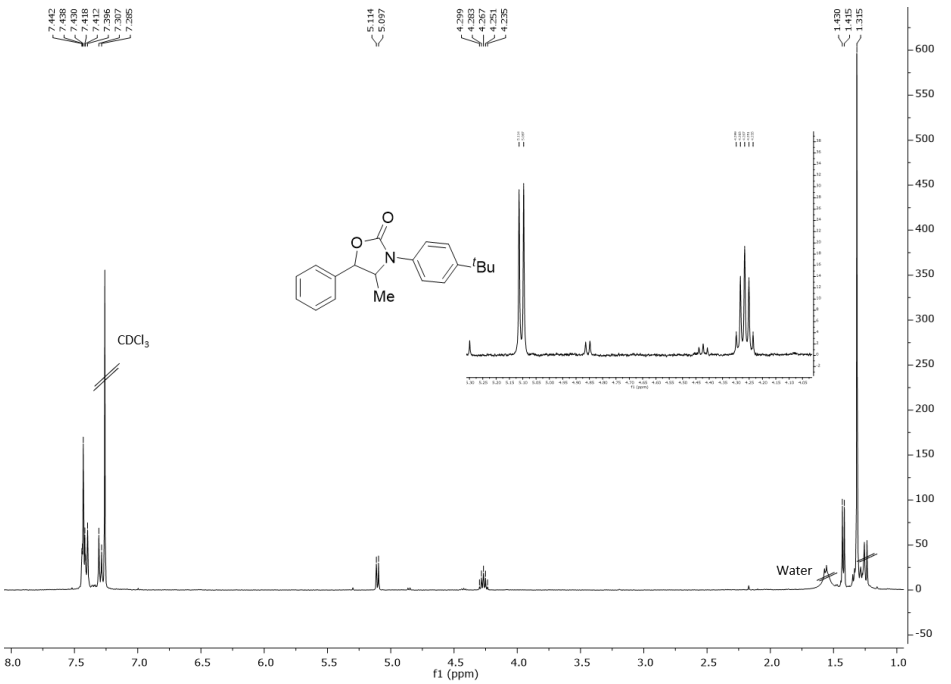

Compound (37a): ^{13}C NMR (100 MHz, $CDCl_3$)

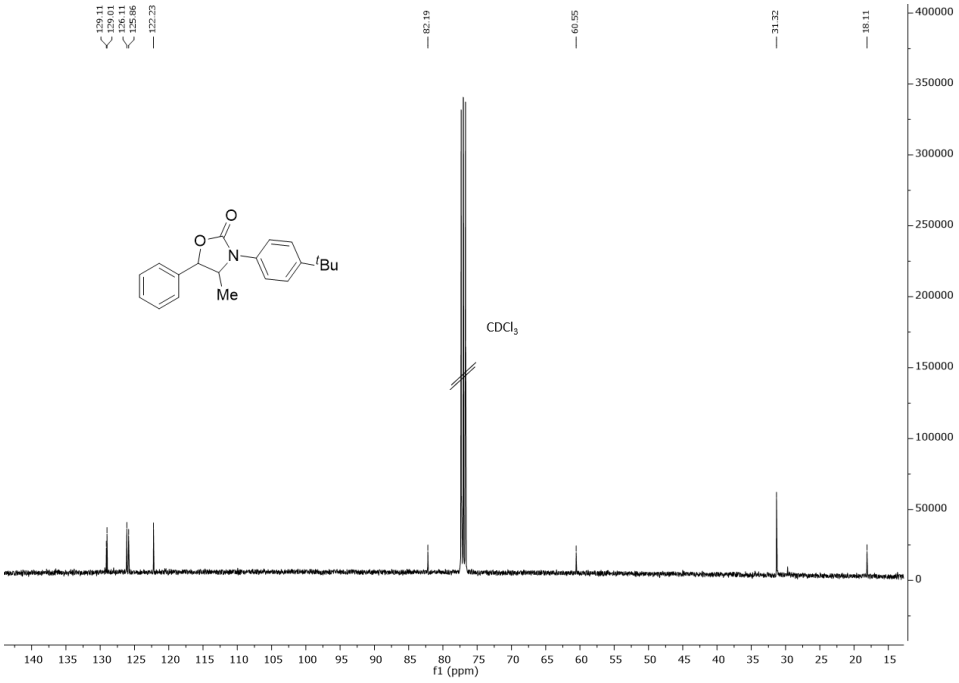

9 Carbon dioxide cycloaddition to *N*-alkyl aziridines

9.1 General procedure

a) General procedure for homogenous catalysts: *meso*-tetraphenylporphyrin (2.3 mg, 3.75 x 10^{-6} mol), tetrabutyl ammonium chloride (2.6 mg, 1.88 x 10^{-5} mol) and the aziridine (3.75 x 10^{-4} mol) were dissolved in THF (0.25 mL) in a 2 mL glass liner equipped with a screw cap and glass wool. The vessel was transferred into a stainless-steel autoclave under nitrogen atmosphere and three vacuum-nitrogen cycles were performed. 1.2 MPa of CO_2 was charged at room temperature and the autoclave was placed in a preheated oil bath at 125 °C and stirred for 8 h. Then, the autoclave was cooled at room temperature and slowly vented. The solvent was evaporated to dryness and the crude analyzed by ^{1}H NMR spectroscopy by using 2,4-dinitrotoluene as the internal standard. The product was purified by flash chromatography (silica gel, hexane/ethyl acetate 9:1).

b) General procedure for heterogeneous catalysts: $TPPH_2$@SBA-15 (3.75 x 10^{-6} mol), tetrabutyl ammonium iodide (6.9 mg, 1.88 x 10^{-5} mol) and the aziridine (9.38 x 10^{-4} mol) were dissolved in THF (0.25 mL) in a 3 mL glass liner equipped with a screw cap and glass wool. The vessel was transferred into a stainless-steel autoclave under nitrogen atmosphere and three vacuum-nitrogen cycles were performed. 1.2 MPa of CO_2 was charged at room temperature and the autoclave was placed in a preheated oil bath at 125 °C and stirred for 16 h. Then, the autoclave was cooled at room temperature and slowly vented. The solvent was evaporated to dryness and the crude analyzed by ^{1}H NMR spectroscopy by using 2,4-dinitrotoluene as the internal standard.

c) Recycling of the heterogeneous catalyst: the procedure **b** was applied and at the end of the reaction the catalyst was collected in a filter, washed with DCM, and dried in the oven. Then, the so-isolated catalyst was used for the next reaction cycle.

9.2 Synthesis of 3-normalbutyl-5-phenyl oxazolidine-2-one (43)

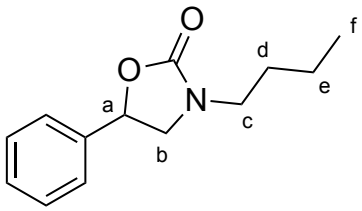

The general procedure was followed by using aziridine **42** to obtain the product as a light-brown oil. The collected analytical data are in accordance with those reported in literature.[95]

^{1}H NMR (300 MHz, $CDCl_3$) δ 7.41 - 7.34 (m, 5H, H_{Ph}), 5.48 (dd, *J* = 8.8, 7.4 Hz, 1H, H_a), 3.91 (pt, *J* = 8.7 Hz, 1H, H_b), 3.42 (dd, *J* = 8.7, 7.4 Hz, 1H, $H_{b'}$), 3.36 - 3.21 (m, 2H, H_c), 1.59 - 1.49 (m, 2H, H_d), 1.41 - 1.29 (m, 2H, H_e), 0.94 ppm (t, *J* = 7.3 Hz, 3H, H_f).

9.3 Synthesis of 3-isobutyl-5-phenyl oxazolidine-2-one (50)

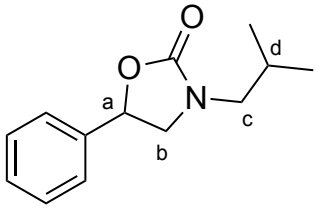

The general procedure was followed by using aziridine **72** to obtain the product as a yellow oil. The collected analytical data are in accordance with those reported in literature.[96]

H NMR (300 MHz, $CDCl_3$) δ 7.40 - 7.32 (m, 5H, H_{Ph}), 5.46 (dd, *J* = 8.8, 7.3 Hz, 1H, H_a) 3.90 (pt, *J* = 8.8 Hz, 1H, H_b), 3.40 (dd, *J* = 8.8, 7.3 Hz, 1H, $H_{b'}$), 3.15 - 3.01 (m, 2H, H_c), 1.91 - 1.82 (m, 1H, H_d), 0.92 (d, *J* = 4.9 Hz, 3H, H_{CH3}), 0.90 ppm (d, *J* = 5.0 Hz, 3H, H_{CH3}).

9.4 Synthesis of 3-tertbutyl-5-phenyl oxazolidine-2-one (51)

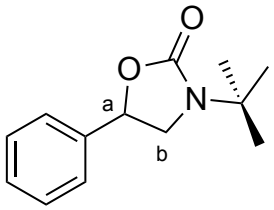

The general procedure was followed by using aziridine **75** to obtain the product as a light-yellow oil. The collected analytical data are in accordance with those reported in literature.[96]

^{1}H NMR (300 MHz, $CDCl_3$) δ 7.32 - 7.41 (m, 5H, H_{Ph}), 5.36 (pt, *J* = 8.1 Hz, 1H, H_a), 3.95 (pt, *J* = 8.7 Hz, 1H, H_b), 3.45 (pt, *J* = 8.4 Hz, 1H, $H_{b'}$), 1.41 ppm (s, 9H, H_{tBu}).

9.5 Synthesis of 3-isoamyl-5-phenyl oxazolidine-2-one (52)

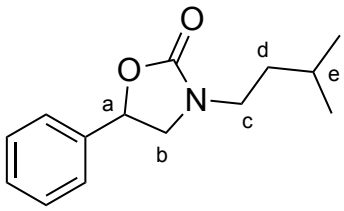

The general procedure was followed by using aziridine **82** to obtain the product as a light-brown oil. The collected analytical data are in accordance with those reported in literature.[95]

^{1}H NMR (400 MHz, CDCl3) δ 7.43 - 7.32 (m, 5H, H_{Ph}), 5.47 (pt, *J* = 8.1 Hz, 1H, H_a), 3.90 (pt, *J* = 8.7 Hz, 1H, H_b), 3.41 (pt, *J* = 8.0, 1H, $H_{b'}$), 3.37 - 3.20 (m, 2H, H_c), 1.66 - 1.54 (m, 1H, H_e), 1.49 - 1.39 (m, 2H, H_d), 0.94 (d, *J* = 3.3 Hz, 3H, H_{CH3}), 0.92 ppm (d, *J* = 3.4 Hz, 3H, H_{CH3}).

9.6 Synthesis of 3-cyclopentyl-5-phenyl oxazolidine-2-one (53)

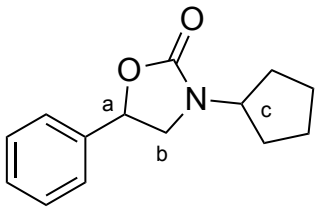

The general procedure was followed by using aziridine **76** to obtain the product as a brown oil. The collected analytical data are in accordance with those reported in literature.[298]

^{1}H NMR (400 MHz, $CDCl_3$) δ 7.41 - 7.25 (m, 5H, H_{Ph}), 5.48 (dd, *J* = 8.7, 7.5 Hz, 1H, H_a), 4.33 - 4.27 (m, 1H, H_c), 3.91 - 3.86 (m, 1H, H_b), 3.40 (dd, *J* = 8.7, 7.5 Hz, 1H, $H_{b'}$), 1.95 - 1.86 (m, 2H, $H_{cyclopentyl}$), 1.70 - 1.46 ppm (m, 6H, $H_{cyclopentyl}$).

9.7 Synthesis of 3-isobutyl-5-phenyl oxazolidine-2-one (54)

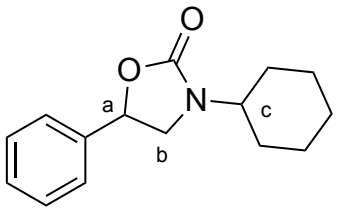

The general procedure was followed by using aziridine **77** to obtain the product as a brown oil. The collected analytical data are in accordance with those reported in literature.[96]

^{1}H NMR (300 MHz, $CDCl_3$) δ 7.39 - 7.25 (m, 5H, H_{Ph}), 5.45 (pt, *J* = 8.4 Hz, 1H, H_a), 3.92 - 3.84 (m, 1H, H_b), 3.70 - 3.73 (m, 1H, H_c), 3.39 (dd, *J* = 8.6, 7.4 Hz, 1H, $H_{b'}$), 1.88 - 0.93 ppm (m, 10H, $H_{cyclohexyl}$).

9.8 Synthesis of 3-benzyl-5-phenyl oxazolidine-2-one (55)

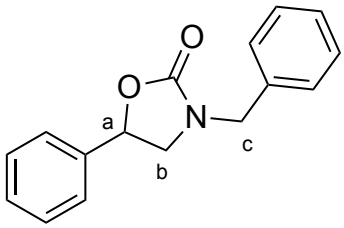

The general procedure was followed by using aziridine **80** to obtain the product as a pale-yellow oil. The collected analytical data are in accordance with those reported in literature.[95]

^{1}H NMR (400 MHz, $CDCl_3$) δ 7.38 - 7.28 (m, 10H, H_{Ar}), 5.47 (dd, *J* = 8.7, 7.6 Hz, 1H, H_a), 4.55 (d, *J* = 14.8 Hz, 1H, H_c), 4.40 (d, *J* = 14.9 Hz, 1H, $H_{c'}$), 3.76 (pt, *J* = 8.8 Hz, 1H, H_b), 3.31 ppm (dd, *J* = 8.7, 7.5 Hz, 1H, $H_{b'}$).

9.9 Synthesis of 3-(4-methoxy)benzyl-5-phenyl oxazolidine-2-one (56)

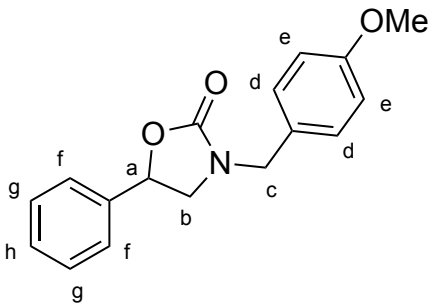

The general procedure was followed by using aziridine **81** to obtain the product as a pale-yellow oil. The collected analytical data are in accordance with those reported in literature.[297]

^{1}H NMR (400 MHz, $CDCl_3$) δ 7.38 - 7.32 (m, 3H, H_{g+h}), 7.31 - 7.28 (m, 2H, H_f), 7.21 (d, *J* = 8.6 Hz, 2H, H_e), 6.87 (d, *J* = 8.6 Hz, 2H, H_d), 5.45 (pt, *J* = 8.2 Hz, 1H, H_a), 4.47 (d, *J* = 14.7 Hz, 1H, H_c), 4.35 (d, *J* = 14.7 Hz, 1H, $H_{c'}$), 3.80 (s, 3H, H_{OCH3}), 3.74 (pt, *J* = 8.8 Hz, 1H, H_b), 3.28 ppm (dd, *J* = 8.7, 7.6 Hz, 1H, $H_{b'}$).

9.10 Synthesis of 3-secbutyl-5-phenyl oxazolidine-2-one (74)

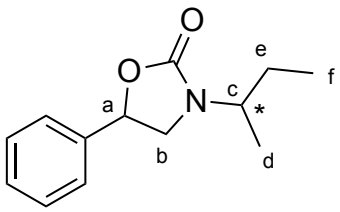

The general procedure was followed by using aziridine **73** to obtain the product as a yellowish oil.

^{1}H NMR (400 MHz, $CDCl_3$) δ 7.43 - 7.30 (m, 5H, H_{Ph}), 5.47 (m, 1H, H_a), 3.95 - 3.83 (m, 2H, H_{b+c}), 3.78 - 3.76 and 3.36 - 3.27 (m, 1H, H_b) 1.58 - 1.39 (m, 2H, H_e), 1.18 and 1.13 (d, *J* = 6.8 Hz, 3H, H_d), 0.94 and 0.85 ppm (t, *J* = 7.4 Hz, 3H, H_f). **^{13}C NMR** (101 MHz, $CDCl_3$) δ 157.62 (C), 139.31 and 138.98 (C), 128.90 (CH), 128.70 (CH), 125.51 (CH), 74.60 and 74.42 (CH), 50.71 and 50.62 (CH), 47.42 (CH_2), 27.25 and 27.00 (CH_2), 18.01 and 17.62 (CH_3), 11.00 and 10.88 ppm (CH_3). **Elemental Analysis** calcd. for $C_{13}H_{17}NO_2$: C (71.21), H (7.81), N (6.39), found: C (71.02), H (8.01), N (6.28). **LR-MS (ESI)**: m/z ($C_{13}H_{17}NO_2$) calcd 219.13, found

$[M+Na]^+$ 242.26. **UV-Vis** λ_{max} (DCM)/nm (log ε): 229 (2.61). **IR** ν_{max} (DCM)/cm^{-1}: 935, 951, 991, 1014, 1359, 1505, 1539, 1557, 1748 (C=O).

9.11 Synthesis of 3-cyclohexylmethyl-5-phenyl oxazolidine-2-one (79)

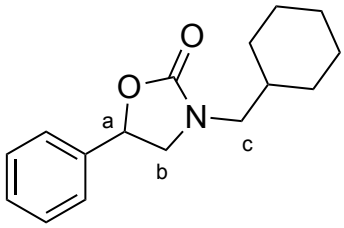

The general procedure was followed by using aziridine **78** to obtain the product as a yellowish oil. The collected analytical data are in accordance with those reported in literature.[296]

^{1}H NMR (400 MHz, $CDCl_3$): δ 7.41 - 7.34 (m, 5H, H_{Ph}), 5.49 (pt, *J* = 8.2 Hz, 1H, H_a), 3.91 (pt, *J* = 8.8 Hz, 1H, H_b), 3.42 (dd, *J* = 8.7, 7.6 Hz, 1H, $H_{b'}$), 3.22 - 3.03 (m, 2H, H_c), 1.77 - 1.54 (m, 6H, $H_{cyclohexyl}$), 1.25 - 1.13 (m, 3H, $H_{cyclohexyl}$), 1.04 - 0.91 ppm (m, 2H, $H_{cyclohexyl}$).

10 ^{1}H and ^{13}C NMR spectra of unreported *N*-alkyl oxazolidinones

Compound (74a): ^{1}H NMR (300 MHz, $CDCl_3$)

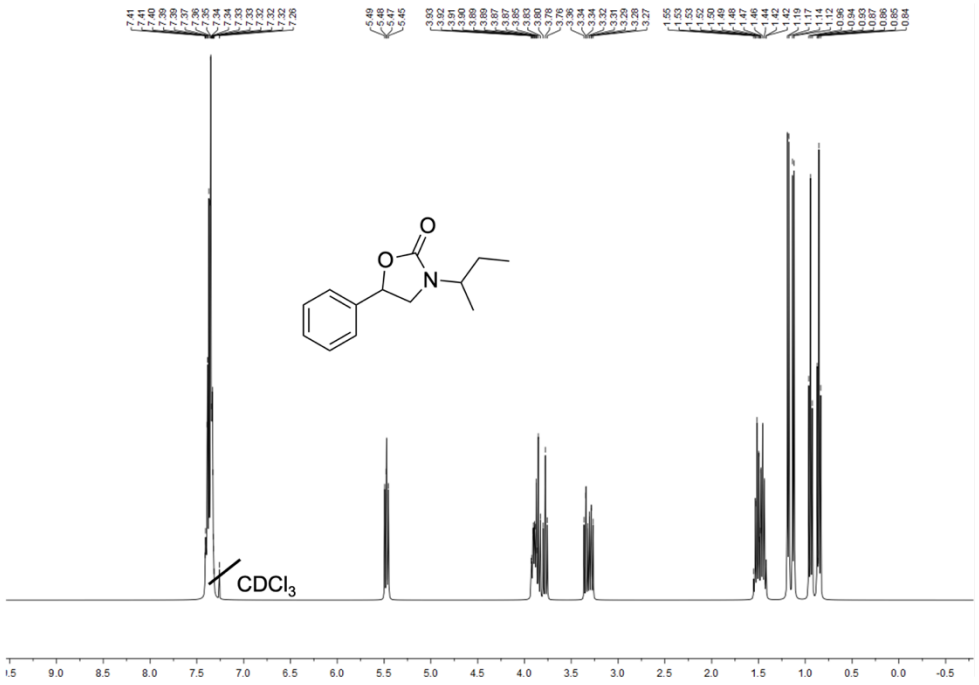

Compound (74a): ^{13}C NMR (75 MHz, $CDCl_3$)

11. Carbon dioxide cycloaddition to epoxides

11.1 General procedure

a) General procedure for homogenous catalysts: *meso*-tetraphenylporphyrin (0.64 mg, 1.12 x 10^{-6} mol) and tetrabutyl ammonium chloride (0.29 mg, 1.12 x 10^{-5} mol) were dissolved in the epoxide (2.18 x 10^{-3} mol) in a 2 mL glass liner equipped with a screw cap and glass wool. The vessel was transferred into a stainless-steel autoclave and three vacuum-carbon dioxide cycles were performed. 0.6 MPa of CO_2 was charged at room temperature and the autoclave heated to 150 °C and stirred for 2 h. Then, the autoclave was cooled at room temperature and slowly vented. The solvent was evaporated to dryness and the crude analyzed by ^{1}H NMR spectroscopy by using 2,4-dibromomesitylene as the internal standard

b) General procedure for heterogeneous catalysts: $TPPH_2$@SBA-15 (5.50 mg, 1.12 x 10^{-6} mol) and tetrabutyl ammonium iodide (0.41 mg, 1.12 x 10^{-5} mol) were suspended in the epoxide (2.18 x 10^{-3} mol) in a 2 mL glass liner equipped with a screw cap and glass wool. The vessel was transferred into a stainless-steel autoclave and three vacuum-carbon dioxide cycles were performed. 0.6 MPa of CO_2 was charged at room temperature and the autoclave heated to 150 °C and stirred for 2 h. Then, the autoclave was cooled at room temperature and slowly vented. The solvent was evaporated to dryness and the crude analyzed by ^{1}H NMR spectroscopy by using 2,4-dibromomesitylene as the internal standard

11.1.2 Optimization of the catalytic conditions in homogeneous phase: the above general procedure was repeated using styrene oxide by varying the following experimental conditions:

a) ***The reaction time*** at 1.2 MPa CO_2 and 125 °C, $TPPH_2$/TBACl/SO: 1/5/10000

t = 1.50 h, 6% yield; t = 1.75 h, 14% yield; t = 2.00, 33% yield; t = 3.00 h, 36 % yield; t = 4.00 h, 35% yield; t = 6.00 h, 34% yield.

b) ***The temperature*** at 1.2 MPa, $TPPH_2$/TBACl/SO: 1/5/10000 for 1.50 h

T = 80 °C, 1% yield; T = 100 °C, 2% yield; T = 125 °C, 6% yield; T = 150 °C, 14% yield; T = 175 °C, 13% yield.

c) *The $TPPH_2$/TBACl/SO ratio* at 1.2 MPa CO_2, 125 °C for 1.5 h

$TPPH_2$/TBACl/SO: 1/5/10000, 6% yield; $TPPH_2$/TBACl/SO: 2/5/1000, 6% yield; $TPPH_2$/TBACl/SO: 3/5/10000, 10% yield; $TPPH_2$/TBACl/SO: 4/5/1000, 11% yield; $TPPH_2$/TBACl/SO: 5/5/10000, 12% yield.

d) *The reaction time* at 1.2 MPa CO_2 and 150 °C, $TPPH_2$/TBACl/SO: 5/5/10000

t = 1 h, 18% yield; t = 2 h, 29% yield; t = 3 h, 29% yield.

e) *The CO_2 pressure* at $TPPH_2$/TBACl/SO: 5/5/1000, 150 °C for 1.h

P_{CO2} = 0.2 MPa, 16% yield; P_{CO2} = 0.3 MPa, 18% yield; P_{CO2} = 0.6 MPa, 20% yield; P_{CO2} = 0.9 MPa, 19% yield; P_{CO2} = 1.2 MPa, 18% yield.

11.2 Synthesis of 4-phenyl-1,3-dioxolan-2-one (60)

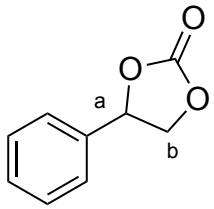

The product was obtained from styrene oxide by following the general procedure. The collected analytical data are in accordance with those reported in literature.[262]

^{1}H NMR (300 MHz, $CDCl_3$): δ 7.47 - 7.34 (m, 5H, H_{Ph}), 5.67 (pt, *J* = 8.0 Hz, 1H, H_a), 4.79 (pt, *J* = 8.4 Hz, 1H, H_b), 4.33 ppm (pt, *J* = 8.0 Hz, 1H, $H_{b'}$).

11.3 Synthesis of 4-(methoxymethyl)-1,3-dioxolan-2-one (61)

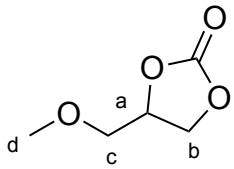

The product was obtained from methyl glycidyl ether by following the general procedure. The collected analytical data are in accordance with those reported in literature.[79]

^{1}H NMR (400 MHz, $CDCl_3$): δ 4.81 - 4.74 (m, 1H, H_a), 4.49 (pt, *J* = 8.4 Hz, 1H, H_b), 4.37 (dd, *J* = 6.1; 8.4 Hz, 1H, $H_{b'}$), 3.52 - 3.60 (m, 2H, H_c), 3.43 ppm (s, 3H, H_d).

11.4 Synthesis of 4-phenyl-1,3-dioxolan-2-one (62)

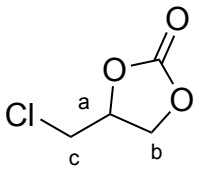

The product was obtained from epichlorohydrin by following the general procedure. The collected analytical data are in accordance with those reported in literature.[262]

^{1}H NMR (400 MHz, $CDCl_3$): δ 5.09 - 4.89 (m, 1H, H_a), 4.61 (t, *J* = 8.5 Hz, 1H, H_b), 4.45 - 4.38 (m, 1H, $H_{b'}$), 3.75 ppm (d, *J* = 5.1, 2H, H_c).

11.5 Synthesis of 4-butyl-1,3-dioxolan-2-one (63)

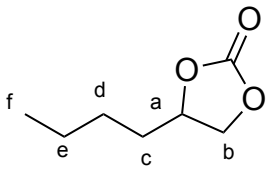

The product was obtained from 1-hexene oxide by following the general procedure. The collected analytical data are in accordance with those reported in literature.[79]

^{1}H NMR (400 MHz, $CDCl_3$): δ 4.76 - 4.60 (m, 1H, H_a), 4.52 (dd, *J* = 7.8; 8.4 Hz, 1H, H_b), 4.06 (pt, *J* = 8.4 Hz, 1H, $H_{b'}$)1.88 - 1.64 (m, 2H, H_c), 1.50 - 1.24 (m, 4H, H_d + H_e), 0.92 ppm (t, *J* = 7.0 Hz, 3H, H_f).

11.6 Synthesis of 4-ethyl-1,3-dioxolan-2-one (64)

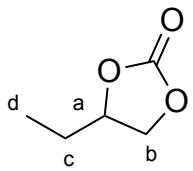

The product was obtained from 1-butene oxide by following the general procedure. The collected analytical data are in accordance with those reported in literature.[262]

^{1}H NMR (400 MHz, $CDCl_3$): δ 4.66 - 4.60 (m, 1H, H_a), 4.46 (pt, *J* = 8.2 Hz, 1H, H_b), 3.98 (pt, *J* = 8.0 Hz, 1H, $H_{b'}$), 1.60 - 1.66 (m, 2H, H_c), 0.97 ppm (t, *J* = 7.4 Hz, 3H, H_d).

11.7 Synthesis of 4,4-dimethyl-1,3-dioxolan-2-one (65)

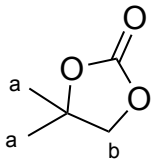

The product was obtained from 2,2-dimethyl oxirane by following the general procedure. The collected analytical data are in accordance with those reported in literature.[262]

^{1}H NMR (400 MHz, $CDCl_3$): δ 4.13 (s, 2H, H_b), 1.91 ppm (s, 6H, H_a).

11.8 Synthesis of tetrahydro-4H-cyclopenta[d][1,3]dioxol-2-one (66)

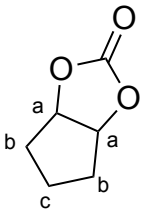

The product was obtained from cyclopentene oxide by following the general procedure. The collected analytical data are in accordance with those reported in literature.[262]

^{1}H NMR (400 MHz, $CDCl_3$): δ 5.13 - 5.09 (m, 2H, H_a), 2.24 - 2.08 (m, 2H, H_c), 1.86 - 1.56 ppm (m, 4H, H_b).

11.9 Synthesis of hexahydrobenzo[d][1,3]dioxol-2-one (67)

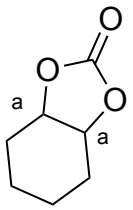

The product was obtained from cyclohexene oxide by following the general procedure. The collected analytical data are in accordance with those reported in literature.[262]

^{1}H NMR (300 MHz, $CDCl_3$): δ 4.69 - 4.64 (m, 2H, H_a), 1.91 - 1.79 (m, 2H, $H_{cyclohexene}$), 1.72 - 1.33 ppm (m, 6H, $H_{cyclohexene}$).

References

(1) MassonDelmotte, V., P. Zhai, A. Pirani, S.L. Connors, C. Péan, S. Berger, N. Caud, Y. Chen, L. Goldfarb, M.I. Gomis, M. Huang, K. Leitzell, E. Lonnoy, J.B.R. Matthews, T.K. Maycock, T. Waterfield, O. Yelekçi, R. Yu, and B. Zhou *IPCC, 2021: Summary for Policymakers.* In: Climate Change 2021: The Physical Science Basis. Contribution of Working Group I to the Sixth Assessment Report of the Intergovernmental Panel on Climate Change. Cambridge University Press. In Press.

(2) Hannart, A.; Naveau, P. Probabilities of Causation of Climate Changes. *J. Clim.* **2018**, *31* (14), 5507–5524.

(3) Guinotte, J. M.; Fabry, V. J. Ocean Acidification and Its Potential Effects on Marine Ecosystems. *Ann. N. Y. Acad. Sci.* **2008**, *1134*, 320–342.

(4) United Nations Framework Convention on Climate Change (UNFCCC). *The Paris Agreement **2015***.

(5) COP26. COP26: The Glasgow Cimate Pact. **2021**, 28.

(6) Ellen MacArthur Foundation. *Towards the Circular Economy Vol 1. Economic and business rational for an accelerated transition* **2013**.

(7) Dobbs, R.; Oppenheim, J.; Thompson, F.; Brinkman, M.; Zornes, M. *Resource Revolution : Meeting the World ' s Energy , Materials , Food , and Water Needs.* McKinsey Global Institute. **2011**.

(8) McDonough W.and Braungart M. *Cradle to Cradle: Remaking the Way We Make Things*, First.; Nort Point Press: New York, 2002.

(9) Anastas, P. T.; Warner, J. C. *Green Chemistry: Theory and Practice*; Oxford University Press: New York, 1998.

(10) He, M.; Sun, Y.; Han, B. Green Carbon Science: Scientific Basis for Integrating Carbon Resource Processing, Utilization, and Recycling. *Angew. Chemie - Int. Ed.* **2013**, *52* (37), 9620–9633.

(11) Edenhofer, O., R. Pichs-Madruga, Y. Sokona, E. Farahani, S. Kadner, K. Seyboth, A. Adler, I. Baum, S. Brunner, P. Eickemeier, B. Kriemann, J. Savolainen, S. Schlömer, C. von Stechow, T. Z. and J. C. M. *IPCC, 2014: Climate Change 2014: Mitigation of Climate Change. Contribution of Working Group III to the Fifth Assessment Report of the Intergovernmental Panel on Climate Change*; Cambridge University Press: New York, 2014.

(12) Rebecca, L. Climate Change: Atmospheric Carbon Dioxide | NOAA Climate.Gov. *NOAA Clim.* **2018**, 1–7.

(13) Bui, M.; Adjiman, C. S.; Bardow, A.; Anthony, E. J.; Boston, A.; Brown, S.; Fennell, P. S.; Fuss, S.; Galindo, A.; Hackett, L. A.; Hallett, J. P.; Herzog, H. J.; Jackson, G.; Kemper, J.; Krevor, S.; Maitland, G. C.; Matuszewski, M.; Metcalfe, I. S.; Petit, C.; Puxty, G.; Reimer, J.; Reiner, D. M.; Rubin, E. S.; Scott, S. A.; Shah, N.; Smit, B.; Trusler, J. P. M.; Webley, P.; Wilcox, J.; Mac Dowell, N. Carbon Capture and Storage (CCS): The Way Forward. *Energy Environ. Sci.* **2018**, *11* (5), 1062–1176.

(14) Gaurina-Međimurec, N.; Novak Mavar, K. Carbon Capture and Storage (CCS):

Geological Sequestration of CO_2. In *CO2 Sequestration*; IntechOpen, 2020.
(15) Adu, E.; Zhang, Y.; Liu, D. Current Situation of Carbon Dioxide Capture, Storage, and Enhanced Oil Recovery in the Oil and Gas Industry. *Can. J. Chem. Eng.* **2019**, *97* (5), 1048–1076.
(16) Osman, A. I.; Hefny, M.; Abdel Maksoud, M. I. A.; Elgarahy, A. M.; Rooney, D. W. Recent Advances in Carbon Capture Storage and Utilisation Technologies: A Review. *Environ. Chem. Lett.* **2021**, *19* (2), 797–849.
(17) Babin, A.; Vaneeckhaute, C.; Iliuta, M. C. Potential and Challenges of Bioenergy with Carbon Capture and Storage as a Carbon-Negative Energy Source: A Review. *Biomass and Bioenergy* **2021**, *146* 105968.
(18) Fajardy, M.; Mac Dowell, N. Can BECCS Deliver Sustainable and Resource Efficient Negative Emissions? *Energy Environ. Sci.* **2017**, *10* (6), 1389–1426.
(19) Liu, Q.; Wu, L.; Jackstell, R.; Beller, M. Using Carbon Dioxide as a Building Block in Organic Synthesis. *Nat. Commun.* **2015**, *6* (1), 5933.
(20) Kondratenko, E. V.; Mul, G.; Baltrusaitis, J.; Larrazábal, G. O.; Pérez-Ramírez, J. Status and Perspectives of CO_2 Conversion into Fuels and Chemicals by Catalytic, Photocatalytic and Electrocatalytic Processes. *Energy Environ. Sci.* **2013**, *6* (11), 3112–3135.
(21) Artz, J.; Müller, T. E.; Thenert, K.; Kleinekorte, J.; Meys, R.; Sternberg, A.; Bardow, A.; Leitner, W. Sustainable Conversion of Carbon Dioxide: An Integrated Review of Catalysis and Life Cycle Assessment. *Chem. Rev.* **2018**, *118* (2), 434–504.
(22) Aresta, M.; Dibenedetto, A.; Angelini, A. Catalysis for the Valorization of Exhaust Carbon: From CO_2 to Chemicals, Materials, and Fuels. Technological Use of CO_2. *Chem. Rev.* **2014**, *114* (3), 1709–1742.
(23) Kleij, A. W.; North, M.; Urakawa, A. CO_2 Catalysis. *ChemSusChem* **2017**, *10* (6), 1036–1038.
(24) Truong, C. C.; Mishra, D. K. Catalyst-Free Fixation of Carbon Dioxide into Value-Added Chemicals: A Review. *Environ. Chem. Lett.* **2021**, *19* (2), 911–940.
(25) Song, C. Global Challenges and Strategies for Control, Conversion and Utilization of CO_2 for Sustainable Development Involving Energy, Catalysis, Adsorption and Chemical Processing. *Catal. Today* **2006**, *115* (1–4), 2–32.
(26) Drees, M.; Cokoja, M.; Kühn, F. E. Recycling CO_2? Computational Considerations of the Activation of CO_2 with Homogeneous Transition Metal Catalysts. *ChemCatChem* **2012**, *4* (11), 1703–1712.
(27) Palmer, D. A.; Van Eldik, R. The Chemistry of Metal Carbonato and Carbon Dioxide Complexes. *Chem*. Rev. **1983**, 6, 651–731
(28) Gibson, D. H. The Organometallic Chemistry of Carbon Dioxide. *Chem. Rev.* **1996**, *96*, 2063–2095.
(29) Intrieri, D.; Damiano, C.; Sonzini, P.; Gallo, E. Porphyrin-Based Homogeneous Catalysts for the CO_2 Cycloaddition to Epoxides and Aziridines . *J. Porphyr. Phthalocyanines* **2019**, *23* (04n05), 305–328.
(30) Vaitla, J.; Guttormsen, Y.; Mannisto, J. K.; Nova, A.; Repo, T.; Bayer, A.; Hopmann, K. H. Enantioselective Incorporation of CO_2: Status and Potential. *ACS Catal.* **2017**, *7* (10), 7231–7244.

(31) Kolbe, H. Ueber Synthese Der Salicylsäure. *Justus Liebigs Ann. Chem.* **1860**, *113* (1), 125–127.

(32) Ogden Baixe, G. F. Adamson, J. W. Barton, Z J. L. Fitch, D. R. Swayampati, A. H. J. A Study of the Kolbe-Schmitt Reaction. II. The Carbonation of Phenols. *J. Org. Chem.* **1953**, 19, 510–514.

(33) Schmitt, R. Beitrag Zur Kenntniss Der Kolbe'schen Salicyl- Saure-Synthese. *J. für Prakt. Chemie* **1885**, *31*, 397.

(34) Huang, K.; Sun, C. L.; Shi, Z. J. Transition-Metal-Catalyzed C–C Bond Formation through the Fixation of Carbon Dioxide. *Chem. Soc. Rev.* **2011**, *40* (5), 2435–2452.

(35) Mizuno, T.; Ishino, Y. Highly Efficient Synthesis of 1H-Quinazoline-2,4-Diones Using Carbon Dioxide in the Presence of Catalytic Amount of DBU. *Tetrahedron* **2002**, *58* (16), 3155–3158.

(36) Mizuno, T.; Iwai, T.; Ishino, Y. The Simple Solvent-Free Synthesis of 1H-Quinazoline-2,4-Diones Using Supercritical Carbon Dioxide and Catalytic Amount of Base. *Tetrahedron Lett.* **2004**, *45* (38), 7073–7075.

(37) Das Neves Gomes, C.; Jacquet, O.; Villiers, C.; Thuéry, P.; Ephritikhine, M.; Cantat, T. A Diagonal Approach to Chemical Recycling of Carbon Dioxide: Organocatalytic Transformation for the Reductive Functionalization of CO_2. *Angew. Chemie* **2012**, *124* (1), 191–194.

(38) Bruneau, C.; Dixneuf, P. H. Catalytic Incorporation of CO_2 into Organic Substrates: Synthesis of Unsaturated Carbamates, Carbonates and Ureas. *J. Mol. Catal.* **1992**, *74* (1–3), 97–107.

(39) Kayaki, Y.; Yamamoto, M.; Ikariya, T.; October, R. V. Stereoselective Formation of r -Alkylidene Cyclic Carbonates via Carboxylative Cyclization of Propargyl Alcohols in Supercritical Carbon Dioxide Ates or Precursors in Organic Synthesis 12 and Polymer Chemis- Internal Propargylic Alcohols Leading to R -Alk. *J. Org. Chem.* **2007**, 72, 647–649.

(40) Fournier, J.; Bruneau, C.; Dixneuf, P. H. Phosphine Catalysed Synthesis of Unsaturated Cyclic Carbonates from Carbon Dioxide and Propargylic Alcohols. *Tetrahedron Lett.* **1989**, *30* (30), 3981–3982.

(41) Kayaki, Y.; Yamamoto, M.; Ikariya, T. N-Heterocyclic Carbenes as Efficient Organocatalysts for CO_2 Fixation Reactions . *Angew. Chemie* **2009**, *121* (23), 4258–4261.

(42) Bresciani, G.; Bortoluzzi, M.; Pampaloni, G.; Marchetti, F. Diethylammonium Iodide as Catalyst for the Metal-Free Synthesis of 5-Aryl-2-Oxazolidinones from Aziridines and Carbon Dioxide. *Org. Biomol. Chem.* **2021**, *19* (18), 4152–4161.

(43) Yang, Z. Z.; He, L. N.; Gao, J.; Liu, A. H.; Yu, B. Carbon Dioxide Utilization with C-N Bond Formation: Carbon Dioxide Capture and Subsequent Conversion. *Energy Environ. Sci.* **2012**, *5* (5), 6602–6639.

(44) Tamura, M.; Honda, M.; Nakagawa, Y.; Tomishige, K. Direct Conversion of CO_2 with Diols, Aminoalcohols and Diamines to Cyclic Carbonates, Cyclic Carbamates and Cyclic Ureas Using Heterogeneous Catalysts. *J. Chem. Technol. Biotechnol.* **2014**, *89* (1), 19–33.

(45) Kindermann, N.; Jose, T.; Kleij, A. W. Synthesis of Carbonates from Alcohols and

CO_2. *Top. Curr. Chem.* **2017**, *375* (1).
(46) Calabrese, C.; Giacalone, F.; Aprile, C. Hybrid Catalysts for CO_2 Conversion into Cyclic Carbonates. *Catalysts* **2019**, *9* (4), 1–30.
(47) Tamura, M.; Ito, K.; Honda, M.; Nakagawa, Y.; Sugimoto, H.; Tomishige, K. Direct Copolymerization of CO_2 and Diols. *Sci. Rep.* **2016**, *6*, 1–9.
(48) Zhang, Z.; Ye, J. H.; Wu, D. S.; Zhou, Y. Q.; Yu, D. G. Synthesis of Oxazolidin-2-Ones from Unsaturated Amines with CO_2 by Using Homogeneous Catalysis. *Chem.: An Asian J.* **2018**, *13* (17), 2292–2306.
(49) Jiang, H. F.; Zhao, J. W. Silver-Catalyzed Activation of Internal Propargylic Alcohols in Supercritical Carbon Dioxide: Efficient and Eco-Friendly Synthesis of 4-Alkylidene-1,3-Oxazolidin-2-Ones. *Tetrahedron Lett.* **2009**, *50* (1), 60–62.
(50) Feng, L.; Li, X.; Xu, C.; Sadeghzadeh, S. M. Green Synthesis of $Dy_2Ce_2O_7$ Nanoparticles Immobilized on Fibrous Nano-Silica for Synthesis of 3-Aryl-2-Oxazolidinones from Alkenes, Amines, and Carbon Dioxide. *Catal. Letters* **2020**, *150* (6), 1729–1740.
(51) Niemi, T.; Perea-Buceta, J. E.; Fernández, I.; Hiltunen, O. M.; Salo, V.; Rautiainen, S.; Räisänen, M. T.; Repo, T. A One-Pot Synthesis of N-Aryl-2-Oxazolidinones and Cyclic Urethanes by the Lewis Base Catalyzed Fixation of Carbon Dioxide into Anilines and Bromoalkanes. *Chem. Eur. J.* **2016**, *22* (30), 10355–10359.
(52) Mei, C.; Zhao, Y.; Chen, Q.; Cao, C.; Pang, G.; Shi, Y. Synthesis of Oxazolidinones and Derivatives through Three-Component Fixation of Carbon Dioxide. *ChemCatChem* **2018**, *10* (14), 3057–3068.
(53) Seo, U. R.; Chung, Y. K. Potassium Phosphate-Catalyzed One-Pot Synthesis of 3-Aryl-2-Oxazolidinones from Epoxides, Amines, and Atmospheric Carbon Dioxide. *Green Chem.* **2017**, *19* (3), 803–808.
(54) Wang, B.; Elageed, E. H. M.; Zhang, D.; Yang, S.; Wu, S.; Zhang, G.; Gao, G. One-Pot Conversion of Carbon Dioxide, Ethylene Oxide, and Amines to 3-Aryl-2-Oxazolidinones Catalyzed with Binary Ionic Liquids. *ChemCatChem* **2014**, *6* (1), 278–283.
(55) Xu, B.; Wang, P.; Lv, M.; Yuan, D.; Yao, Y. Transformation of Carbon Dioxide into Oxazolidinones and Cyclic Carbonates Catalyzed by Rare-Earth-Metal Phenolates. *ChemCatChem* **2016**, *8* (15), 2466–2471.
(56) Wang, B.; Luo, Z.; Elageed, E. H. M.; Wu, S.; Zhang, Y.; Wu, X.; Xia, F.; Zhang, G.; Gao, G. DBU and DBU-Derived Ionic Liquid Synergistic Catalysts for the Conversion of Carbon Dioxide/Carbon Disulfide to 3-Aryl-2-Oxazolidinones/[1,3]Dithiolan-2-Ylidenephenyl- Amine. *ChemCatChem* **2016**, *8* (4), 830–838.
(57) Lv, M.; Wang, P.; Yuan, D.; Yao, Y. Conversion of Carbon Dioxide into Oxazolidinones Mediated by Quaternary Ammonium Salts and DBU. *ChemCatChem* **2017**, *9* (24), 4451–4455.
(58) Xie, Y. F.; Guo, C.; Shi, L.; Peng, B. H.; Liu, N. Bifunctional Organocatalysts for the Conversion of CO_2, Epoxides and Aryl Amines to 3-Aryl-2-Oxazolidinones. *Org. Biomol. Chem.* **2019**, *17* (14), 3497–3506.
(59) McGhee, W.; Riley, D.; Christ, K.; Pan, Y.; Parnas, B. Carbon Dioxide as a Phosgene Replacement: Synthesis and Mechanistic Studies of Urethanes from Amines, CO_2,

and Alkyl Chlorides. *J. Org. Chem.* **1995**, *60* (9), 2820–2830.
(60) L. Goncalves, A. A.; C. Fonseca, A.; J. Coelho, J. F.; C. Serra, A. Supported Catalysis in Carbon Dioxide Activation. *Curr. Green Chem.* **2015**, *2* (1), 43–65.
(61) Shaikh, R. R.; Pornpraprom, S.; D'Elia, V. Catalytic Strategies for the Cycloaddition of Pure, Diluted, and Waste CO_2 to Epoxides under Ambient Conditions. *ACS Catal.* **2018**, *8* (1), 419–450.
(62) Comerford, J. W.; Ingram, I. D. V.; North, M.; Wu, X. Catalytic Cyclic Carbonate Synthesis with Sustainable Metals. *Encycl. Inorg. Bioinorg. Chem.* **2016**, 1–13.
(63) Pulla, S.; Felton, C. M.; Ramidi, P.; Gartia, Y.; Ali, N.; Nasini, U. B.; Ghosh, A. Advancements in Oxazolidinone Synthesis Utilizing Carbon Dioxide as a C1 Source. *J. CO2 Util.* **2013**, *2*, 49–57.
(64) Lamb, K. J.; Ingram, I. D. V.; North, M.; Sengoden, M. Valorization of Carbon Dioxide into Oxazolidinones by Reaction with Aziridines. *Curr. Green Chem.* **2019**, *6* (1), 32–43.
(65) Sengoden, M.; North, M.; Whitwood, A. C. Synthesis of Oxazolidinones by Using Carbon Dioxide as a C1 Building Block and an Aluminium-Based Catalyst. *ChemSusChem* **2019**, *12* (14), 3296–3303.
(66) Miller, A. W.; Nguyen, S. B. T. (Salen)Chromium(III)/DMAP: An Efficient Catalyst System for the Selective Synthesis of 5-Substituted Oxazolidinones from Carbon Dioxide and Aziridines. *Org. Lett.* **2004**, *6* (14), 2301–2304.
(67) Sweeney, J. B. Aziridines: Epoxides' Ugly Cousins? *Chem. Soc. Rev.* **2002**, *31* (5), 247–258.
(68) Sakakura, T.; Choi, J. C.; Yasuda, H. Transformation of Carbon Dioxide. *Chem. Rev.* **2007**, *107* (6), 2365–2387.
(69) Pescarmona, P. P.; Taherimehr, M. Challenges in the Catalytic Synthesis of Cyclic and Polymeric Carbonates from Epoxides and CO_2. *Catal. Sci. Technol.* **2012**, *2* (11), 2169–2187.
(70) S, H. W.; Guo, L. Mechanistic Insights into Cycloaddition of CO_2 with Epoxide Catalyzed by a Bimetallic (Salen)Fe(II)Cl_2 Complex with/without a Cocatalyst. *ChemistrySelect* **2020**, 5, 2516–2521.
(71) Wu, G. P.; Wei, S. H.; Ren, W. M.; Lu, X. B.; Li, B.; Zu, Y. P.; Darensbourg, D. J. Alternating Copolymerization of CO_2 and Styrene Oxide with Co(III)-Based Catalyst Systems: Differences between Styrene Oxide and Propylene Oxide. *Energy Environ. Sci.* **2011**, *4* (12), 5084–5092.
(72) Li, X.; Cheetham, A. K.; Jiang, J. CO_2 Cycloaddition with Propylene Oxide to Form Propylene Carbonate on a Copper Metal-Organic Framework: A Density Functional Theory Study. *Mol. Catal.* **2019**, *463*, 37–44.
(73) North, M.; Pasquale, R. Mechanism of Cyclic Carbonate Synthesis from Epoxides and CO_2. *Angew. Chemie - Int. Ed.* **2009**, *48* (16), 2946–2948.
(74) Liu, Y.; Hou, H.; Wang, B. Theoretical Study on Cycloaddition Reaction of Epoxides with CO_2 Catalyzed by Metal-Porphrin Complexes: Reaction Mechanisms and Structure Impacts on Catalytic Activity. *J. Organomet. Chem.* **2020**, *911*, 121123.
(75) Wang, T. T.; Xie, Y.; Deng, W. Q. Reaction Mechanism of Epoxide Cycloaddition to CO_2 Catalyzed by Salen-M (M = Co, Al, Zn). *Journal of Physical Chemistry A*. **2014**,

118, 39, 9239–9243.

(76) Carvalho Rocha, C.; Onfroy, T.; Pilmé, J.; Denicourt-Nowicki, A.; Roucoux, A.; Launay, F. Experimental and Theoretical Evidences of the Influence of Hydrogen Bonding on the Catalytic Activity of a Series of 2-Hydroxy Substituted Quaternary Ammonium Salts in the Styrene Oxide/CO_2 Coupling Reaction. *J. Catal.* **2016**, *333*, 29–39.

(77) Cheng, W.; Xiao, B.; Sun, J.; Dong, K.; Zhang, P.; Zhang, S.; Ng, F. T. T. Effect of Hydrogen Bond of Hydroxyl-Functionalized Ammonium Ionic Liquids on Cycloaddition of CO_2. *Tetrahedron Lett.* **2015**, *56* (11), 1416–1419.

(78) He, J.; Wu, T.; Zhang, Z.; Ding, K.; Han, B.; Xie, Y.; Jiang, T.; Liu, Z. Cycloaddition of CO_2 to Epoxides Catalyzed by Polyaniline Salts. *Chem. Eur. J.* **2007**, *13* (24), 6992–6997.

(79) Della Monica, F.; Buonerba, A.; Grassi, A.; Capacchione, C.; Milione, S. Glycidol: An Hydroxyl-Containing Epoxide Playing the Double Role of Substrate and Catalyst for CO_2 Cycloaddition Reactions. *ChemSusChem* **2016**, *9* (24), 3457–3464.

(80) North, M.; Pasquale, R.; Young, C. Synthesis of Cyclic Carbonates from Epoxides and CO_2. *Green Chem.* **2010**, *12* (9), 1514–1539..

(81) Wang, J. Q.; Sun, J.; Cheng, W. G.; Shi, C. Y.; Dong, K.; Zhang, X. P.; Zhang, S. J. Synthesis of Dimethyl Carbonate Catalyzed by Carboxylic Functionalized Imidazolium Salt via Transesterification Reaction. *Catal. Sci. Technol.* **2012**, *2* (3), 600–605.

(82) Cokoja, M.; Wilhelm, M. E.; Anthofer, M. H.; Herrmann, W. A.; Kühn, F. E. Synthesis of Cyclic Carbonates from Epoxides and Carbon Dioxide by Using Organocatalysts. *ChemSusChem* **2015**, *8* (15), 2436–2454.

(83) Yoshida, M.; Komatsuzaki, Y.; Ihara, M. Synthesis of 5-Vinylideneoxazolidin-2-Ones by DBU-Mediated CO_2-Fixation Reaction of 4-(Benzylamino)-2-Butynyl Carbonates and Benzoates. *Org. Lett.* **2008**, *10* (10), 2083–2086.

(84) Zhou, H.; Zhang, W. Z.; Liu, C. H.; Qu, J. P.; Lu, X. B. CO_2 Adducts of N-Heterocyclic Carbenes: Thermal Stability and Catalytic Activity toward the Coupling of CO_2 with Epoxides. *J. Org. Chem.* **2008**, *73* (20), 8039–8044.

(85) Hancock, M. T.; Pinhas, A. R. Synthesis of Oxazolidinones and 1,2-Diamines from N-Alkyl Aziridines. *Synthesis (Stuttg).* **2004**, 14, 2347–2355.

(86) Hancock, M. T.; Pinhas, A. R. A Convenient and Inexpensive Conversion of an Aziridine to an Oxazolidinone. *Tetrahedron Lett.* **2003**, *44* (29), 5457–5460.

(87) Sudo, A.; Morioka, Y.; Koizumi, E.; Sanda, F.; Endo, T. Highly Efficient Chemical Fixations of Carbon Dioxide and Carbon Disulfide by Cycloaddition to Aziridine under Atmospheric Pressure. *Tetrahedron Lett.* **2003**, *44* (43), 7889–7891.

(88) Matsuda, H.; Ninagawa, A.; Hasegawa, H. Reaction of Carbon Dioxide with 1-Phenylaziridine Catalyzed by Organo-Antimony and -Tin Compounds. *Bull. Chem. Soc. Jpn.* **1985**, *58* (9), 2717–2718.

(89) Wu, Y.; He, L. N.; Du, Y.; Wang, J. Q.; Miao, C. X.; Li, W. Zirconyl Chloride: An Efficient Recyclable Catalyst for Synthesis of 5-Aryl-2-Oxazolidinones from Aziridines and CO_2 under Solvent-Free Conditions. *Tetrahedron* **2009**, *65* (31), 6204–6210.

(90) Ren, W. M.; Liu, Y.; Lu, X. B. Bifunctional Aluminum Catalyst for CO_2 Fixation: Regioselective Ring Opening of Three-Membered Heterocyclic Compounds. *J. Org. Chem.* **2014**, *79* (20), 9771–9777.

(91) Ma, T. Y.; Qiao, S. Z. Acid-Base Bifunctional Periodic Mesoporous Metal Phosphonates for Synergistically and Heterogeneously Catalyzing CO_2 Conversion. *ACS Catal.* **2014**, *4* (11), 3847–3855.

(92) Lin, X. Z.; Yang, Z. Z.; He, L. N.; Yuan, Z. Y. Mesoporous Zirconium Phosphonates as Efficient Catalysts for Chemical CO_2 Fixation. *Green Chem.* **2015**, *17* (2), 795–798.

(93) Wang, X.; Gao, W. Y.; Niu, Z.; Wojtas, L.; Perman, J. A.; Chen, Y. S.; Li, Z.; Aguila, B.; Ma, S. A Metal-Metalloporphyrin Framework Based on an Octatopic Porphyrin Ligand for Chemical Fixation of CO_2 with Aziridines. *Chem. Commun.* **2018**, *54* (10), 1170–1173.

(94) Xu, H.; Liu, X. F.; Cao, C. S.; Zhao, B.; Cheng, P.; He, L. N. A Porous Metal–Organic Framework Assembled by $[Cu_{30}]$ Nanocages: Serving as Recyclable Catalysts for CO_2 Fixation with Aziridines. *Adv. Sci.* **2016**, *3* (11). 1600048.

(95) Du, Y.; Wu, Y.; Liu, A. H.; He, L. N. Quaternary Ammonium Bromide Functionalized Polyethylene Glycol: A Highly Efficient and Recyclable Catalyst for Selective Synthesis of 5-Aryl-2-Oxazolidinones from Carbon Dioxide and Aziridines under Solvent-Free Conditions. *J. Org. Chem.* **2008**, *73* (12), 4709–4712.

(96) Yang, Z. Z.; Li, Y. N.; Wei, Y. Y.; He, L. N. Protic Onium Salts-Catalyzed Synthesis of 5-Aryl-2-Oxazolidinones from Aziridines and CO_2 under Mild Conditions. *Green Chem.* **2011**, *13* (9), 2351–2353.

(97) Yang, Z. Z.; He, L. N.; Peng, S. Y.; Liu, A. H. Lewis Basic Ionic Liquids-Catalyzed Synthesis of 5-Aryl-2-Oxazolidinones from Aziridines and CO_2 under Solvent-Free Conditions. *Green Chem.* **2010**, *12* (10), 1850–1854.

(98) Watile, R. A.; Bagal, D. B.; Deshmukh, K. M.; Dhake, K. P.; Bhanage, B. M. Polymer Supported Diol Functionalized Ionic Liquids: An Efficient, Heterogeneous and Recyclable Catalyst for 5-Aryl-2-Oxazolidinones Synthesis from CO_2 and Aziridines under Mild and Solvent Free Condition. *J. Mol. Catal. A Chem.* **2011**, *351*, 196–203.

(99) Jiang, H. F.; Ye, J. W.; Qi, C. R.; Huang, L. Bin. Naturally Occurring α-Amino Acid: A Simple and Inexpensive Catalyst for the Selective Synthesis of 5-Aryl-2-Oxazolidinones from CO_2 and Aziridines under Solvent-Free Conditions. *Tetrahedron Lett.* **2010**, *51* (6), 928–932.

(100) Qi, C.; Ye, J.; Zeng, W.; Jiang, H. Polystyrene-Supported Amino Acids as Efficient Catalyst for Chemical Fixation of Carbon Dioxide. *Adv. Synth. Catal.* **2010**, *352* (11–12), 1925–1933.

(101) Mu, W. H.; Chasse, G. A.; Fang, D. C. High Level Ab Initio Exploration on the Conversion of Carbon Dioxide into Oxazolidinones: The Mechanism and Regioselectivity. *J. Phys. Chem. A* **2008**, *112* (29), 6708–6714.

(102) Adhikari, D.; Miller, A. W.; Baik, M.-H.; Nguyen, S. T. Intramolecular Ring-Opening from a CO_2-Derived Nucleophile as the Origin of Selectivity for 5-Substituted Oxazolidinone from the (Salen)Cr-Catalyzed [Aziridine + CO_2] Coupling. *Chem. Sci.* **2015**, *6* (2), 1293–1300.

(103) Arayachukiat, S.; Yingcharoen, P.; Vummaleti, S. V. C.; Cavallo, L.; Poater, A.; D'Elia,

V. Cycloaddition of CO_2 to Challenging N-Tosyl Aziridines Using a Halogen-Free Niobium Complex: Catalytic Activity and Mechanistic Insights. *Mol. Catal.* **2017**, *443*, 280–285.

(104) Hu, T. D.; Ding, Y. H. Mechanism for CO_2 Fixation with Aziridines Synergistically Catalyzed by HKUST-1 and TBAB: A DFT Study. *Organometallics*. **2020**, 39, 4, 505–515.

(105) Shaikh, A. A. G.; Sivaram, S. Organic Carbonates. *Chem. Rev.* **1996**, *96* (3), 951–976.

(106) Claver, C.; Yeamin, M. Bin; Reguero, M.; Masdeu-Bultó, A. M. Recent Advances in the Use of Catalysts Based on Natural Products for the Conversion of CO_2 into Cyclic Carbonates. *Green Chem.* **2020**, *22* (22), 7665–7706.

(107) Schäffner, B.; Schäffner, F.; Verevkin, S. P.; Börner, A. Organic Carbonates as Solvents in Synthesis and Catalysis. *Chem. Rev.* **2010**, *110* (8), 4554–4581.

(108) S. Bello Forero, J.; A. Hernández Muñoz, J.; Jones Junior, J.; M. da Silva, F. Propylene Carbonate in Organic Synthesis: Exploring Its Potential as a Green Solvent. *Curr. Org. Synth.* **2016**, *13* (6), 834–846.

(109) Ding, M. S.; Xu, K.; Jow, T. R. Liquid-Solid Phase Diagrams of Binary Carbonates for Lithium Batteries. *J. Electrochem. Soc.* **2000**, *147* (5), 1688.

(110) Zhao, H.; Park, S.-J.; Shi, F.; Fu, Y.; Battaglia, V.; Ross, P. N.; Liu, G. Propylene Carbonate (PC)-Based Electrolytes with High Coulombic Efficiency for Lithium-Ion Batteries. *J. Electrochem. Soc.* **2014**, *161* (1), A194–A200.

(111) Gennen, S.; Grignard, B.; Tassaing, T.; Jérôme, C.; Detrembleur, C. CO_2-Sourced α-Alkylidene Cyclic Carbonates: A Step Forward in the Quest for Functional Regioregular Poly(Urethane)s and Poly(Carbonate)S . *Angew. Chemie* **2017**, *129* (35), 10530–10534.

(112) Clements, J. H. Reactive Applications of Cyclic Alkylene Carbonates. *Ind. Eng. Chem. Res.* **2003**, *42* (4), 663–674.

(113) Zhang, H.; Liu, H. B.; Yue, J. M. Organic Carbonates from Natural Sources. *Chem. Rev.* **2014**, *114* (1), 883–898.

(114) Guo, W.; Gómez, J. E.; Cristòfol, À.; Xie, J.; Kleij, A. W. Catalytic Transformations of Functionalized Cyclic Organic Carbonates. *Angew. Chemie - Int. Ed.* **2018**, *57* (42), 13735–13747.

(115) Shieh, W. C.; Dell, S.; Repič, O. Nucleophilic Catalysis with 1,8-Diazabicyclo[5.4.0]Undec-7-Ene (DBU) for the Esterification of Carboxylic Acids with Dimethyl Carbonate. *J. Org. Chem.* **2002**, *67* (7), 2188–2191.

(116) Haba, O.; Itakura, I.; Ueda, M.; Kuze, S. Synthesis of Polycarbonate from Dimethyl Carbonate and Bisphenol-A through a Non-Phosgene Process. *J. Polym. Sci. A. Polym. Chem.* **1999**, *37* (13), 2087–2093.

(117) Mallesham, B.; Rajesh, B. M.; Rajamohan Reddy, P.; Srinivas, D.; Trehan, S. Highly Efficient CuI-Catalyzed Coupling of Aryl Bromides with Oxazolidinones Using Buchwald's Protocol: A Short Route to Linezolid and Toloxatone. *Org. Lett.* **2003**, *5* (7), 963–965.

(118) Roger, C.; Roberts, J. A.; Muller, L. Clinical Pharmacokinetics and Pharmacodynamics of Oxazolidinones. *Clin. Pharmacokinet.* **2018**, *57* (5), 559–575.

(119) Niemi, T.; Repo, T. Antibiotics from Carbon Dioxide: Sustainable Pathways to

Pharmaceutically Relevant Cyclic Carbamates. *European J. Org. Chem.* **2019**, *2019* (6), 1180–1188.

(120) Evans, D. A.; Bartroli, J.; Shih, T. L. Enantioselective Aldol Condensations. 2. Erythro-Selective Chiral Aldol Condensations via Boron Enolates. *J. Am. Chem. Soc.* **1981**, *103* (8), 2127–2129.

(121) Zadsirjan, V.; Heravi, M. M. Oxazolidinones as Chiral Auxiliaries in the Asymmetric 1,4-Conjugate Addition Reaction Applied to the Total Synthesis of Natural Products: A Supplemental Mini-Review. *Curr. Org. Synth.* **2018**, *15* (1), 3–20.

(122) Heravi, M. M.; Zadsirjan, V.; Farajpour, B. Applications of Oxazolidinones as Chiral Auxiliaries in the Asymmetric Alkylation Reaction Applied to Total Synthesis. *RSC Adv.* **2016**, *6* (36), 30498–30551.

(123) Moureau, F.; Wouters, J.; Vercauteren, D.; Collin, S.; Evrard, G.; Durant, F.; Ducrey, F.; Koenig, J.; Jarreau, F. A Reversible Monoamine Oxidase Inhibitor, Toloxatone: Structural and Electronic Properties. *Eur. J. Med. Chem.* **1992**, *27* (9), 939–948

(124) Park, C. H.; Brittelli, D. R.; Wang, C. L. J.; Marsh, F. D.; Gregory, W. A.; Wuonola, M. A.; McRipley, R. J.; Eberly, V. S.; Slee, A. M.; Forbes, M. Antibacterials. Synthesis and Structure-Activity Studies of 3-Aryl-2-Oxooxazolidines. 4. Multiply-Substituted Aryl Derivatives. *J. Med. Chem.* **1992**, *35* (6), 1156–

(125) Kaatz, G. W.; Rybak, M. J. Oxazolidinones: New Players in the Battle against Multi-Resistant Gram-Positive Bacteria. *Emerg. Drugs* **2005**, *6* (1), 43–55.

(126) Mai, A.; Artico, M.; Esposito, M.; Sbardella, G.; Massa, S.; Befani, O.; Turini, P.; Giovannini, V.; Mondovi, B. 3-(1H-Pyrrol-1-Yl)-2-Oxazolidinones as Reversible, Highly Potent, and Selective Inhibitors of Monoamine Oxidase Type A. *J. Med. Chem.* **2002**, *45* (6), 1180–1183.

(127) Ali, A.; Reddy, G. S. K. K.; Cao, H.; Anjum, S. G.; Nalam, M. N. L.; Schiffer, C. A.; Rana, T. M. Discovery of HIV-1 Protease Inhibitors with Picomolar Affinities Incorporating N-Aryl-Oxazolidinone-5-Carboxamides as Novel P2 Ligands. *J. Med. Chem.* **2006**, *49* (25), 7342–7356.

(128) Barbachyn, M. R.; Ford, C. W. Oxazolidinone Structure-Activity Relationships Leading to Linezolid. *Angew. Chemie - Int. Ed.* **2003**, *42* (18), 2010–2023.

(129) Bialvaei, A. Z.; Rahbar, M.; Yousefi, M.; Asgharzadeh, M.; Kafil, H. S. Linezolid: A Promising Option in the Treatment of Gram-Positives. *J. Antimicrob. Chemother.* **2017**, *72* (2), 354–364.

(130) McBride, D.; Krekel, T.; Hsueh, K.; Durkin, M. J. Pharmacokinetic Drug Evaluation of Tedizolid for the Treatment of Skin Infections. *Expert Opin. Drug Metab. Toxicol.* **2017**, *13* (3), 331–337.

(131) Barona-Castaño, J. C.; Carmona-Vargas, C. C.; Brocksom, T. J.; De Oliveira, K. T.; Graça, M.; Neves, P. M. S.; Amparo, M.; Faustino, F. Porphyrins as Catalysts in Scalable Organic Reactions. *Molecules* **2016**, *21* (3), 310–337

(132) Sternberg, E. D.; Dolphin, D.; Brückner, C. Porphyrin-Based Photosensitizers for Use in Photodynamic Therapy. *Tetrahedron* **1998**, *54* (17), 4151–4202.

(133) Geraldes, C. F. G. C.; Castro, M. M. C. A.; Peters, J. A. Mn(III) Porphyrins as Potential MRI Contrast Agents for Diagnosis and MRI-Guided Therapy. *Coord. Chem. Rev.* **2021**, *445*, 214069.

(134) Aggarwal, A.; Bhupathiraju, N. V. S. D. K.; Farley, C.; Singh, S. Applications of Fluorous Porphyrinoids: An Update†. *Photochem. Photobiol.* **2021**, *97* (6), 1241–1265.
(135) Monti, D.; Nardis, S.; Stefanelli, M.; Paolesse, R.; Di Natale, C.; D'Amico, A. Porphyrin-Based Nanostructures for Sensing Applications. *J. Sensors* **2009**, 2009, 856063.
(136) Nicolau, K. C.; Sorensen, E. J. *Classics in Total Synthesis: Targets, Strategies, Methods*; **1996**.
(137) Fischer, H.; Zeile, K. Synthese Des Hämatoporphyrins, Protoporphyrins Und Hämins. *Justus Liebig's Ann. der Chemie* **1929**, *468* (1), 98–116.
(138) Arsenault, G. P.; Bullock, E.; MacDonald, S. F. Pyrromethanes and Porphyrins Therefrom. *J. Am. Chem. Soc.* **1960**, *82* (16), 4384–4389.
(139) Boudif, A.; Momenteau, M. Synthesis of a Porphyrin-2,3-Diacrylic Acid Using a New "3 + 1" Type Procedure. *J. Chem. Soc. Chem. Commun.* **1994**, 18, 2069–2070.
(140) Rothemund, P. Formation of Porphyrins from Pyrrole and Aldehydes. *J. Am. Chem. Soc.* **1935**, *57* (10), 2010–2011.
(141) Rothemund, P.; Menotti, A. R. Porphyrin Studies IV. The Synthesis of TPP. *J. Am. Chem. Soc.* **1941**, *63*, 267–270.
(142) Adler, A. D.; Longo, F. R.; Finarelli, J. D.; Goldmacher, J.; Assour, J.; Korsakoff, L. A Simplified Synthesis for Meso-Tetraphenylporphine. *J. Org. Chem.* **1967**, *32* (2), 476–476.
(143) Liu, M. O.; Tai, C. H.; Wang, W. Y.; Chen, J. R.; Hu, A. T.; Wei, T. H. Microwave-Assisted Synthesis and Reverse Saturable Absorption of Phthalocyanines and Porphyrins. *J. Organomet. Chem.* **2004**, *689* (6), 1078–1084.
(144) Lindsey, J. S.; Schreiman, I. C.; Hsu, H. C.; Kearney, P. C.; Marguerettaz, A. M. Rothemund and Adler-Longo Reactions Revisited: Synthesis of Tetraphenylporphyrins under Equilibrium Conditions. *J. Org. Chem.* **1987**, *52* (5), 827–836.
(145) Lindsey, J. S.; MacCrum, K. A.; Tyhonas, J. S.; Chuang, Y. Y. Investigation of a Synthesis of Meso-Porphyrins Employing High Concentration Conditions and an Electron Transport Chain for Aerobic Oxidation. *J. Org. Chem.* **1994**, *59* (3), 579–587.
(146) Brothers, P. J.; Collman, J. P. The Organometallic Chemistry of Transition-Metal Porphyrin Complexes. *Acc. Chem. Res.* **1986**, *19* (7), 209–215.
(147) Dolphin, D. *The Porphyrins V1 Structure and Synthesis, Part A*; Elsevier Science, 2012.
(148) Kadish, K.; Smith, K. M.; Guilard, M. *The Porphyrin Handbook*; Elsevier Science, 2000.
(149) Alan D.Adler, Frederick R.Longo, Frank Kampas, J. K. On the Preparation of Metalloporphyrins. *J. Inor., Nucl.* **1970**, *32* (7), 2443–2445.
(150) Darensbourg, D. J.; Holtcamp, M. W. Catalysts for the Reactions of Epoxides and Carbon Dioxide. *Coord. Chem. Rev.* **1996**, *153*, 155–174.
(151) Lang, X.-D.; He, L.-N. Green Catalytic Process for Cyclic Carbonate Synthesis from Carbon Dioxide under Mild Conditions. *Chem. Rec.* **2016**, *16* (3), 1337–1352.

(152) Paddock, R. L.; Nguyen, S. T. Chemical CO_2 Fixation: Cr(III) Salen Complexes as Highly Efficient Catalysts for the Coupling of CO_2 and Epoxides. *J. Am. Chem. Soc.* **2001**, *123* (46), 11498–11499.
(153) Wu, X.; Castro-Osma, J. A.; North, M. Synthesis of Chiral Cyclic Carbonates via Kinetic Resolution of Racemic Epoxides and Carbon Dioxide. *Symmetry (Basel).* **2016**, *8* (1), 4–9.
(154) Takeda, N.; Inoue, S. Activation of Carbon Dioxide by Tetraphenylporphinatoaluminium Methoxide. Reaction with Epoxide. *Bull. Chem. Soc. Jpn.* **1978**, *51* (12), 3564–3567.
(155) Bai, D.; Duan, S.; Hai, L.; Jing, H. Carbon Dioxide Fixation by Cycloaddition with Epoxides, Catalyzed by Biomimetic Metalloporphyrins. *ChemCatChem* **2012**, *4* (11), 1752–1758.
(156) Qin, Y.; Guo, H.; Sheng, X.; Wang, X.; Wang, F. An Aluminum Porphyrin Complex with High Activity and Selectivity for Cyclic Carbonate Synthesis. *Green Chem.* **2015**, *17* (5), 2853–2858.
(157) Ahmadi, F.; Tangestaninejad, S.; Moghadam, M.; Mirkhani, V.; Mohammadpoor-Baltork, I.; Khosropour, A. R. Highly Efficient Chemical Fixation of Carbon Dioxide Catalyzed by High-Valent Tetraphenylporphyrinatotin(IV) Triflate. *Inorg. Chem. Commun.* **2011**, *14* (9), 1489–1493.
(158) Peng, J.; Geng, Y.; Yang, H. J.; He, W.; Wei, Z.; Yang, J.; Guo, C. Y. Efficient Solvent-Free Fixation of CO_2 into Cyclic Carbonates Catalyzed by Bi(III) Porphyrin/TBAI at Atmospheric Pressure. *Mol. Catal.* **2017**, *432*, 37–46.
(159) Kruper, W. J.; Dellar, D. V. Catalytic Formation of Cyclic Carbonates from Epoxides and CO_2 with Chromium Metalloporphyrinates. *J. Org. Chem.* **1995**, *60* (3), 725–727.
(160) Paddock, R. L.; Hiyama, Y.; McKay, J. M.; Nguyen, S. B. T. Co(III) Porphyrin/DMAP: An Efficient Catalyst System for the Synthesis of Cyclic Carbonates from CO2 and Epoxides. *Tetrahedron Lett.* **2004**, *45* (9), 2023–2026.
(161) Jin, L.; Jing, H.; Chang, T.; Bu, X.; Wang, L.; Liu, Z. Metal Porphyrin/Phenyltrimethylammonium Tribromide: High Efficient Catalysts for Coupling Reaction of CO_2 and Epoxides. *J. Mol. Catal. A Chem.* **2007**, *261* (2), 262–266.
(162) Farhadian, A.; Gol Afshani, M. B.; Babaei Miyardan, A.; Nabid, M. R.; Safari, N. A Facile and Green Route for Conversion of Bifunctional Epoxide and Vegetable Oils to Cyclic Carbonate: A Green Route to CO_2 Fixation. *ChemistrySelect* **2017**, *2* (4), 1431–1435.
(163) Jin, L.; Chang, T.; Jing, H. Coupling of Epoxides with Carbon Dioxide Catalyzed by Ruthenium Porphyrin Complex. *Chin. J. Catal.* **2007**, *28* (4), 287–288.
(164) Bai, D.; Wang, X.; Song, Y.; Li, B.; Zhang, L.; Yan, P.; Jing, H. Bifunctional Metalloporphyrins-Catalyzed Coupling Reaction of Epoxides and CO_2 to Cyclic Carbonates. *Chin. J. Catal.* **2010**, *31* (2), 176–180.
(165) Sharma, N.; Dhankhar, S. S.; Nagaraja, C. M. Environment-Friendly, Co-Catalyst-And Solvent-Free Fixation of CO_2 Using an Ionic Zinc(II)-Porphyrin Complex Immobilized in Porous Metal-Organic Frameworks. *Sustain. Energy Fuels* **2019**, *3*

(11), 2977–2982.
(166) Jiang, X.; Gou, F.; Fu, X.; Jing, H. Ionic Liquids-Functionalized Porphyrins as Bifunctional Catalysts for Cycloaddition of Carbon Dioxide to Epoxides. *J. CO_2 Util.* **2016**, *16*, 264–271.
(167) Ema, T.; Miyazaki, Y.; Koyama, S.; Yano, Y.; Sakai, T. A Bifunctional Catalyst for Carbon Dioxide Fixation: Cooperative Double Activation of Epoxides for the Synthesis of Cyclic Carbonates. *Chem. Commun.* **2012**, *48* (37), 4489–4491.
(168) Maeda, C.; Taniguchi, T.; Ogawa, K.; Ema, T. Bifunctional Catalysts Based on M-Phenylene-Bridged Porphyrin Dimer and Trimer Platforms: Synthesis of Cyclic Carbonates from Carbon Dioxide and Epoxides. *Angew. Chemie - Int. Ed.* **2015**, *54* (1), 134–138.
(169) Rehman, A.; Saleem, F.; Javed, F.; Ikhlaq, A.; Ahmad, S. W.; Harvey, A. Recent Advances in the Synthesis of Cyclic Carbonates via CO_2 cycloaddition to Epoxides. *J. Environ. Chem. Eng.* **2021**, *9* (2), 105113.
(170) Caló, V.; Nacci, A.; Monopoli, A.; Fanizzi, A. Cyclic Carbonate Formation from Carbon Dioxide and Oxiranes in Tetrabutylammonium Halides as Solvents and Catalysts. *Org. Lett.* **2002**, *4* (15), 2561–2563.
(171) Wang, J. Q.; Dong, K.; Cheng, W. G.; Sun, J.; Zhang, S. J. Insights into Quaternary Ammonium Salts-Catalyzed Fixation Carbon Dioxide with Epoxides. *Catal. Sci. Technol.* **2012**, *2* (7), 1480–1484.
(172) Steinbauer, J.; Kubis, C.; Ludwig, R.; Werner, T. Mechanistic Study on the Addition of CO_2 to Epoxides Catalyzed by Ammonium and Phosphonium Salts: A Combined Spectroscopic and Kinetic Approach. *ACS Sustain. Chem. Eng.* **2018**, *6* (8), 10778–10788.
(173) Jutz, F.; Andanson, J. M.; Baiker, A. Ionic Liquids and Dense Carbon Dioxide: A Beneficial Biphasic System for Catalysis. *Chem. Rev.* **2011**, *111* (2), 322–353. https://doi.org/10.1021/cr100194q.
(174) Zhou, H.; Wang, G. X.; Zhang, W. Z.; Lu, X. B. CO2 Adducts of Phosphorus Ylides: Highly Active Organocatalysts for Carbon Dioxide Transformation. *ACS Catal.* **2015**, *5* (11), 6773–6779.
(175) Toda, Y.; Komiyama, Y.; Kikuchi, A.; Suga, H. Tetraarylphosphonium Salt-Catalyzed Carbon Dioxide Fixation at Atmospheric Pressure for the Synthesis of Cyclic Carbonates. *ACS Catal.* **2016**, *6* (10), 6906–6910.
(176) Sun, J.; Ren, J.; Zhang, S.; Cheng, W. Water as an Efficient Medium for the Synthesis of Cyclic Carbonate. *Tetrahedron Lett.* **2009**, *50* (4), 423–426.
(177) Liu, S.; Suematsu, N.; Maruoka, K.; Shirakawa, S. Design of Bifunctional Quaternary Phosphonium Salt Catalysts for CO_2 Fixation Reaction with Epoxides under Mild Conditions. *Green Chem.* **2016**, *18* (17), 4611–4615
(178) Liu, M.; Wang, X.; Jiang, Y.; Sun, J.; Arai, M. Hydrogen Bond Activation Strategy for Cyclic Carbonates Synthesis from Epoxides and CO_2 : Current State-of-the Art of Catalyst Development and Reaction Analysis. *Catal. Rev. -Sci. Eng.* **2019**, *61* (2), 214–269.
(179) Phung, C.; Ulrich, R. M.; Ibrahim, M.; Tighe, N. T. G.; Lieberman, D. L.; Pinhas, A. R. The Solvent-Free and Catalyst-Free Conversion of an Aziridine to an Oxazolidinone

Using Only Carbon Dioxide. *Green Chem.* **2011**, *13* (11), 3224–3229.
(180) Chen, Y.; Luo, R.; Yang, Z.; Zhou, X.; Ji, H. Imidazolium-Based Ionic Liquid Decorated Zinc Porphyrin Catalyst for Converting CO_2 into Five-Membered Heterocyclic Molecules. *Sustain. Energy Fuels* **2018**, *2* (1), 125–132.
(181) Carminati, D.; Gallo, E.; Damiano, C.; Caselli, A.; Intrieri, D. Ruthenium Porphyrin Catalyzed Synthesis of Oxazolidin-2-Ones by Cycloaddition of CO_2 to Aziridines. *Eur. J. Inorg. Chem.* **2018**, *2018* (48), 5258–5262.
(182) Watile, R. A.; Bagal, D. B.; Patil, Y. P.; Bhanage, B. M. Regioselective Synthesis of 5-Aryl-2-Oxazolidinones from Carbon Dioxide and Aziridines Using $Br^-Ph_3{}^+PPEG_{600}P^+Ph_3Br^-$ as an Efficient, Homogenous Recyclable Catalyst at Ambient Conditions. *Tetrahedron Lett.* **2011**, *52* (48), 6383–6387.
(183) Dai, W. L.; Luo, S. L.; Yin, S. F.; Au, C. T. The Direct Transformation of Carbon Dioxide to Organic Carbonates over Heterogeneous Catalysts. *Appl. Catal. A Gen.* **2009**, *366* (1), 2–12.
(184) Yano, T.; Matsui, H.; Koike, T.; Ishiguro, H.; Fujihara, H.; Yoshihara, M.; Maeshima, T. Magnesium Oxide-Catalysed Reaction of Carbon Dioxide with an Epoxide with Retention of Stereochemistry. *Chem. Commun.* **1997**, *2* (12), 1129–1130.
(185) Bhanage, B. M.; Fujita, S.; Ikushima, Y.; Arai, M. Synthesis of Dimethyl Carbonate and Glycols from Carbon Dioxide, Epoxides, and Methanol Using Heterogeneous Basic Metal Oxide Catalysts with High Activity and Selectivity. *Appl. Catal. A Gen.* **2001**, *219* (1–2), 259–266.
(186) Aresta, M.; Dibenedetto, A.; Gianfrate, L.; Pastore, C. Nb(V) Compounds as Epoxides Carboxylation Catalysts: The Role of the Solvent. *J. Mol. Catal. A Chem.* **2003**, *204–205*, 245–252.
(187) Shi, Y.; Hou, S.; Qiu, X.; Zhao, B. *MOFs-Based Catalysts Supported Chemical Conversion of CO_2*; Springer International Publishing, 2020; Vol. 378.
(188) Song, J.; Zhang, Z.; Hu, S.; Wu, T.; Jiang, T.; Han, B. MOF-5/*n*-Bu_4NBr: An Efficient Catalyst System for the Synthesis of Cyclic Carbonates from Epoxides and CO_2 under Mild Conditions. *Green Chem.* **2009**, *11* (7), 1031–1036.
(189) Ren, Y.; Cheng, X.; Yang, S.; Qi, C.; Jiang, H.; Mao, Q. A Chiral Mixed Metal-Organic Framework Based on a Ni(Saldpen) Metalloligand: Synthesis, Characterization and Catalytic Performances. *Dalt. Trans.* **2013**, *42* (27), 9930–9937.
(190) Cho, H. Y.; Yang, D. A.; Kim, J.; Jeong, S. Y.; Ahn, W. S. CO_2 Adsorption and Catalytic Application of Co-MOF-74 Synthesized by Microwave Heating. *Catal. Today* **2012**, *185* (1), 35–40.
(191) Kumar, S.; Wani, M. Y.; Arranja, C. T.; E Silva, J. D. A.; Avula, B.; Sobral, A. J. F. N. Porphyrins as Nanoreactors in the Carbon Dioxide Capture and Conversion: A Review. *J. Mater. Chem. A* **2015**, *3* (39), 19615–19637.
(192) Dhakshinamoorthy, A.; Asiri, A. M.; Alvaro, M.; Garcia, H. Metal Organic Frameworks as Catalysts in Solvent-Free or Ionic Liquid Assisted Conditions. *Green Chem.* **2018**, *20* (1), 86–107.
(193) Kim, D.; Subramanian, S.; Thirion, D.; Song, Y.; Jamal, A.; Otaibi, M. S.; Yavuz, C. T. Quaternary Ammonium Salt Grafted Nanoporous Covalent Organic Polymer for Atmospheric CO_2 Fixation and Cyclic Carbonate Formation. *Catal. Today* **2020**, *356*

(May), 527–534.
(194) Du, Y.; Wang, J. Q.; Chen, J. Y.; Cai, F.; Tian, J. S.; Kong, D. L.; He, L. N. A Poly(Ethylene Glycol)-Supported Quaternary Ammonium Salt for Highly Efficient and Environmentally Friendly Chemical Fixation of CO_2 with Epoxides under Supercritical Conditions. *Tetrahedron Lett.* **2006**, *47* (8), 1271–1275.
(195) Xiong, Y.; Bai, F.; Cui, Z.; Guo, N.; Wang, R. Cycloaddition Reaction of Carbon Dioxide to Epoxides Catalyzed by Polymer-Supported Quaternary Phosphonium Salts. *J. Chem.* **2013**, *2013*.
(196) Watile, R. A.; Deshmukh, K. M.; Dhake, K. P.; Bhanage, B. M. Efficient Synthesis of Cyclic Carbonate from Carbon Dioxide Using Polymer Anchored Diol Functionalized Ionic Liquids as a Highly Active Heterogeneous Catalyst. *Catal. Sci. Technol.* **2012**, *2* (5), 1051–1055.
(197) Bai, D.; Wang, Q.; Song, Y.; Li, B.; Jing, H. Synthesis of Cyclic Carbonate from Epoxide and CO_2 Catalyzed by Magnetic Nanoparticle-Supported Porphyrin. *Catal. Commun.* **2011**, *12* (7), 684–688.
(198) Chen, A.; Ju, P.; Zhang, Y.; Chen, J.; Gao, H.; Chen, L.; Yu, Y. Highly Recyclable and Magnetic Catalyst of a Metalloporphyrin-Based Polymeric Composite for Cycloaddition of CO_2 to Epoxide. *RSC Adv.* **2016**, *6* (99), 96455–96466.
(199) Dias, L. D.; Carrilho, R. M. B.; Henriques, C. A.; Calvete, M. J. F.; Masdeu-Bultó, A. M.; Claver, C.; Rossi, L. M.; Pereira, M. M. Hybrid Metalloporphyrin Magnetic Nanoparticles as Catalysts for Sequential Transformation of Alkenes and CO_2 into Cyclic Carbonates. *ChemCatChem* **2018**, *10* (13), 2792–2803.
(200) Sun, J.; Wang, J.; Cheng, W.; Zhang, J.; Li, X.; Zhang, S.; She, Y. Chitosan Functionalized Ionic Liquid as a Recyclable Biopolymer-Supported Catalyst for Cycloaddition of CO2. *Green Chem.* **2012**, *14* (3), 654–660.
(201) Roshan, K. R.; Mathai, G.; Kim, J.; Tharun, J.; Park, G. A.; Park, D. W. A Biopolymer Mediated Efficient Synthesis of Cyclic Carbonates from Epoxides and Carbon Dioxide. *Green Chem.* **2012**, *14* (10), 2933–2940.
(202) Asefa, T.; MacLachlan, M. J.; Coombs, N.; Ozin, G. A. Periodic Mesoporous Organosilicas with Organic Groups inside the Channel Walls. *Nature* **1999**, *402* (6764), 867–871.
(203) Melde, B. J.; Holland, B. T.; Blanford, C. F.; Stein, A. Mesoporous Sieves with Unified Hybrid Inorganic/Organic Frameworks. *Chem. Mater.* **1999**, *11* (11), 3302–3308.
(204) Inagaki, S.; Guan, S.; Fukushima, Y.; Ohsuna, T.; Terasaki, O. Novel Mesoporous Materials with a Uniform Distribution of Organic Groups and Inorganic Oxide in Their Frameworks. *J. Am. Chem. Soc.* **1999**, *121* (41), 9611–9614.
(205) Kresge, C. T.; Leonowicz, M. E.; Roth, W. J.; Vartuli, J. C.; Beck, J. S. Ordered Mesoporous Molecular Sieves Synthesized by a Liquid-Crystal Template Mechanism. *Nature* **1992**, *359* (6397), 710–712.
(206) Zhao, D.; Feng, J.; Huo, Q.; Melosh, N.; Fredrickson, G. H.; Chmelka, B. F.; Stucky, G. D. Triblock Copolymer Syntheses of Mesoporous Silica with Periodic 50 to 300 Angstrom Pores. *Science (80-.).* **1998**, *279* (5350), 548–552.
(207) Takahashi, T.; Watahiki, T.; Kitazume, S.; Yasuda, H.; Sakakura, T. Synergistic

Hybrid Catalyst for Cyclic Carbonate Synthesis: Remarkable Acceleration Caused by Immobilization of Homogeneous Catalyst on Silica. *Chem. Commun.* **2006**, 15, 1664–1666.

(208) Hajipour, A. R.; Heidari, Y.; Kozehgary, G. Silica Grafted Ammonium Salts Based on DABCO as Heterogeneous Catalysts for Cyclic Carbonate Synthesis from Carbon Dioxide and Epoxides. *RSC Adv.* **2015**, *5* (29), 22373–22379.

(209) Lagarde, F.; Srour, H.; Berthet, N.; Oueslati, N.; Bousquet, B.; Nunes, A.; Martinez, A.; Dufaud, V. Investigating the Role of SBA-15 Silica on the Activity of Quaternary Ammonium Halides in the Coupling of Epoxides and CO_2. *J. CO2 Util.* **2019**, *34,* 34–39.

(210) Srivastava, R.; Srinivas, D.; Ratnasamy, P. Sites for CO_2 Activation over Amine-Functionalized Mesoporous Ti(Al)-SBA-15 Catalysts. *Microporous Mesoporous Mater.* **2006**, *90*, 314–326.

(211) Srivastava, R.; Srinivas, D.; Ratnasamy, P. CO_2 Activation and Synthesis of Cyclic Carbonates and Alkyl/Aryl Carbamates over Adenine-Modified Ti-SBA-15 Solid Catalysts. *J. Catal.* **2005**, *233* (1), 1–15.

(212) Baleizão, C.; Gigante, B.; Sabater, M. J.; Garcia, H.; Corma, A. On the Activity of Chiral Chromium Salen Complexes Covalently Bound to Solid Silicates for the Enantioselective Epoxide Ring Opening. *Appl. Catal. A Gen.* **2002**, *228* (1–2), 279–288.

(213) Alvaro, M.; Baleizao, C.; Das, D.; Carbonell, E.; García, H. CO_2 Fixation Using Recoverable Chromium Salen Catalysts: Use of Ionic Liquids as Cosolvent or High-Surface-Area Silicates as Supports. *J. Catal.* **2004**, *228* (1), 254–258.

(214) Ramin, M.; Jutz, F.; Grunwaldt, J. D.; Baiker, A. Solventless Synthesis of Propylene Carbonate Catalysed by Chromium-Salen Complexes: Bridging Homogeneous and Heterogeneous Catalysis. *J. Mol. Catal. A Chem.* **2005**, *242* (1–2), 32–39.

(215) Bourda, L.; Jena, H. S.; Van Deun, R.; Kaczmarek, A. M.; Van Der Voort, P. Functionalized Periodic Mesoporous Organosilicas: From Metal Free Catalysis to Sensing. *J. Mater. Chem. A* **2019**, *7* (23), 14060–14069.

(216) Jayakumar, S.; Li, H.; Tao, L.; Li, C.; Liu, L.; Chen, J.; Yang, Q. Cationic Zn-Porphyrin Immobilized in Mesoporous Silicas as Bifunctional Catalyst for CO_2 Cycloaddition Reaction under Cocatalyst Free Conditions. *ACS Sustain. Chem. Eng.* **2018**, *6* (7), 9237–9245.

(217) Barbarini, A.; Maggi, R.; Mazzacani, A.; Mori, G.; Sartori, G.; Sartorio, R. Cycloaddition of CO_2 to Epoxides over Both Homogeneous and Silica-Supported Guanidine Catalysts. *Tetrahedron Lett.* **2003**, *44* (14), 2931–2934.

(218) Zhang, X.; Zhao, N.; Wei, W.; Sun, Y. Chemical Fixation of Carbon Dioxide to Propylene Carbonate over Amine-Functionalized Silica Catalysts. *Catal. Today* **2006**, *115* (1–4), 102–106.

(219) Wang, J. Q.; Yue, X. D.; Cai, F.; He, L. N. Solventless Synthesis of Cyclic Carbonates from Carbon Dioxide and Epoxides Catalyzed by Silica-Supported Ionic Liquids under Supercritical Conditions. *Catal. Commun.* **2007**, *8* (2), 167–172.

(220) Han, L.; Choi, H. J.; Choi, S. J.; Liu, B.; Park, D. W. Ionic Liquids Containing Carboxyl Acid Moieties Grafted onto Silica: Synthesis and Application as Heterogeneous

Catalysts for Cycloaddition Reactions of Epoxide and Carbon Dioxide. *Green Chem.* **2011**, *13* (4), 1023–1028.

(221) Dokhaee, Z.; Ghiaci, M.; Farrokhpour, H.; Buntkowsky, G.; Breitzke, H. SBA-15-Supported Imidazolium Ionic Liquid through Different Linkers as a Sustainable Catalyst for the Synthesis of Cyclic Carbonates: A Kinetic Study and Theoretical DFT Calculations. *Ind. Eng. Chem. Res.* 2020, *59*, 28, 12632–12644.

(222) Sakai, T.; Tsutsumi, Y.; Ema, T. Highly Active and Robust Organic–Inorganic Hybrid Catalyst for the Synthesis of Cyclic Carbonates from Carbon Dioxide and Epoxides. *Green Chem.* **2008**, *10* (3), 337–34.

(223) Motokura, K.; Itagaki, S.; Iwasawa, Y.; Miyaji, A.; Baba, T. Silica-Supported Aminopyridinium Halides for Catalytic Transformations of Epoxides to Cyclic Carbonates under Atmospheric Pressure of Carbon Dioxide. *Green Chem.* **2009**, *11* (11), 1876–1880.

(224) Rehman, A.; Saleem, F.; Javed, F.; Qutab, H. G.; Eze, V. C.; Harvey, A. Kinetic Study for Styrene Carbonate Synthesis via CO_2 Cycloaddition to Styrene Oxide Using Silica-Supported Pyrrolidinopyridinium Iodide Catalyst. *J. CO2 Util.* **2021**, *43*, 101379.

(225) Wang, J. Q.; Kong, D. L.; Chen, J. Y.; Cai, F.; He, L. N. Synthesis of Cyclic Carbonates from Epoxides and Carbon Dioxide over Silica-Supported Quaternary Ammonium Salts under Supercritical Conditions. *J. Mol. Catal. A Chem.* **2006**, *249* (1–2), 143–148.

(226) Mirabaud, A.; Mulatier, J. C.; Martinez, A.; Dutasta, J. P.; Dufaud, V. Investigating Host-Guest Complexes in the Catalytic Synthesis of Cyclic Carbonates from Styrene Oxide and CO_2. *ACS Catal.* **2015**, *5* (11), 6748–6752.

(227) Mirabaud, A.; Martinez, A.; Bayard, F.; Dutasta, J. P.; Dufaud, V. A New Heterogeneous Host-Guest Catalytic System as an Eco-Friendly Approach for the Synthesis of Cyclic Carbonates from CO_2 and Epoxides. *New J. Chem.* **2018**, *42* (20), 16863–16874.

(228) Song, Y.; Sun, Q.; Aguila, B.; Ma, S. Optimizing the Performance of Porous Pyridinium Frameworks for Carbon Dioxide Transformation. *Catal. Today* **2020**, *356*, 557–562.

(229) Chen, X.; Sun, J.; Wang, J.; Cheng, W. Polystyrene-Bound Diethanolamine Based Ionic Liquids for Chemical Fixation of CO_2. *Tetrahedron Lett.* **2012**, *53* (22), 2684–2688.

(230) Liu, A.; He, L.; Peng, S.; Pan, Z.; Wang, J.; Gao, J. Environmentally Benign Chemical Fixation of CO_2 Catalyzed by the Functionalized Ion-Exchange Resins. *Sci. China Chem.* **2010**, *53* (7), 1578–1585.

(231) Kathalikkattil, A. C.; Tharun, J.; Roshan, R.; Soek, H. G.; Park, D. W. Efficient Route for Oxazolidinone Synthesis Using Heterogeneous Biopolymer Catalysts from Unactivated Alkyl Aziridine and CO_2 under Mild Conditions. *Appl. Catal. A Gen.* **2012**, *447–448*, 107–114.

(232) Watile, R. A.; Bhanage, B. M. Chitosan Biohydrogel Beads: A Recyclable, Biodegradable, Heterogeneous Catalyst for the Regioselective Synthesis of 5-Aryl-2-Oxazolidinones from Carbon Dioxide and Aziridines at Mild Conditions. *Indian J.*

Chem **2012**, *51* (9–10), 1354–1360.

(233) Zhao, Y. N.; Yang, Z. Z.; Luo, S. H.; He, L. N. Design of Task-Specific Ionic Liquids for Catalytic Conversion of CO 2 with Aziridines under Mild Conditions. *Catal. Today* **2013**, *200* (1), 2–8.

(234) Zhou, H.; Wang, Y. M.; Zhang, W. Z.; Qu, J. P.; Lu, X. B. N-Heterocyclic Carbene Functionalized MCM-41 as an Efficient Catalyst for Chemical Fixation of Carbon Dioxide. *Green Chem.* **2011**, *13* (3), 644–650.

(235) Nale, D. B.; Rana, S.; Parida, K.; Bhanage, B. M. Amine Functionalized MCM-41 as a Green, Efficient, and Heterogeneous Catalyst for the Regioselective Synthesis of 5-Aryl-2-Oxazolidinones, from CO_2 and Aziridines. *Appl. Catal. A Gen.* **2014**, *469*, 340–349.

(236) Aresta, M.; Quaranta, E.; Ciccarese, A. Direct Synthesis of 1,3-Benzodioxol-2-One from Styrene, Dioxygen and Carbon Dioxide Promoted by Rh(I). *J. Mol. Catal.* **1987**, *41* (3), 355–359.

(237) Aresta, M.; Dibenedetto, A.; Tommasi, I. Direct Synthesis of Organic Carbonates by Oxidative Carboxylation of Olefins Catalyzed by Metal Oxides: Developing Green Chemistry Based on Carbon Dioxide. *Appl. Organomet. Chem.* **2000**, *14* (12), 799–802.

(238) Aresta, M.; Dibenedetto, A. Carbon Dioxide as Building Block for the Synthesis of Organic Carbonates. *J. Mol. Catal. A Chem.* **2002**, *182–183*, 399–409.

(239) Sun, J.; Liang, L.; Sun, J.; Jiang, Y.; Lin, K.; Xu, X.; Wang, R. Direct Synthetic Processes for Cyclic Carbonates from Olefins and CO_2. *Catal. Surv. Asia* **2011**, *15* (1), 49–54.

(240) Calmanti, R.; Selva, M.; Perosa, A. Tandem Catalysis: One-Pot Synthesis of Cyclic Organic Carbonates from Olefins and Carbon Dioxide. *Green Chem.* **2021**, *23* (5), 1921–1941.

(241) Wang, L.; Que, S.; Ding, Z.; Vessally, E. Oxidative Carboxylation of Olefins with CO_2: Environmentally Benign Access to Five-Membered Cyclic Carbonates. *RSC Adv.* **2020**, *10* (15), 9103–9115.

(242) Bai, D.; Jing, H. Aerobic Oxidative Carboxylation of Olefins with Metalloporphyrin Catalysts. *Green Chem.* **2010**, *12* (1), 39–41.

(243) Ono, F.; Qiao, K.; Tomida, D.; Yokoyama, C. Direct Preparation of Styrene Carbonates from Styrene Using an Ionic-Liquid-Based One-Pot Multistep Synthetic Process. *Appl. Catal. A: Gen.* **2007**, *333* (1), 107–113.

(244) Ke, S. C.; Luo, T. T.; Chang, G. G.; Huang, K. X.; Li, J. X.; Ma, X. C.; Wu, J.; Chen, J.; Yang, X. Y. Spatially Ordered Arrangement of Multifunctional Sites at Molecule Level in a Single Catalyst for Tandem Synthesis of Cyclic Carbonates. *Inorg. Chem.* **2020**, *59* (3), 1736–1745.

(245) Qiu, J.; Yu, L.; Ni, J.; Fei, Z.; Li, W.; Sadeghzadeh, S. M. Palladium-Salen-Bridged Ionic Networks Immobilized on Magnetic Dendritic Silica Fibers for the Synthesis of Cyclic Carbonates by Oxidative Carboxylation. *New J. Chem.* **2020**, *44* (4), 1269–1277.

(246) Abassian, M.; Zhiani, R.; Motavalizadehkakhky, A.; Eshghi, H.; Mehrzad, J. A New Class of Organoplatinum-Based DFNS for the Production of Cyclic Carbonates from

Olefins and CO_2. *RSC Adv.* **2020**, *10* (26), 15044–15051.
(247) Ramidi, P.; Felton, C. M.; Subedi, B. P.; Zhou, H.; Tian, Z. R.; Gartia, Y.; Pierce, B. S.; Ghosh, A. C. *J. CO2 Util.* **2015**, *9*, 48–57.
(248) Carvalho Rocha, C.; Onfroy, T.; Launay, F. Towards a Combined Use of Mn(Salen) and Quaternary Ammonium Salts as Catalysts for the Direct Conversion of Styrene to Styrene Carbonate in the Presence of Dioxygen and Carbon Dioxide. *C. R. Chim.* **2015**, *18* (3), 270–276.
(249) Kumar, S.; Singhal, N.; Singh, R. K.; Gupta, P.; Singh, R.; Jain, S. L. Dual Catalysis with Magnetic Chitosan: Direct Synthesis of Cyclic Carbonates from Olefins with Carbon Dioxide Using Isobutyraldehyde as the Sacrificial Reductant. *Dalt. Trans.* **2015**, *44* (26), 11860–11866.
(250) Liu, J.; Yang, G.; Liu, Y.; Wu, D.; Hu, X.; Zhang, Z. Metal-Free Imidazolium Hydrogen Carbonate Ionic Liquids as Bifunctional Catalysts for the One-Pot Synthesis of Cyclic Carbonates from Olefins and CO_2. *Green Chem.* **2019**, *21* (14), 3834–3838.
(251) Yu, K.; Puthiaraj, P.; Ahn, W. S. One-Pot Catalytic Transformation of Olefins into Cyclic Carbonates over an Imidazolium Bromide-Functionalized Mn(III)-Porphyrin Metal–Organic Framework. *Appl. Catal. B Environ.* **2020**, *273* (May), 119059.
(252) Zalomaeva, O. V.; Maksimchuk, N. V.; Chibiryaev, A. M.; Kovalenko, K. A.; Fedin, V. P.; Balzhinimaev, B. S. Synthesis of Cyclic Carbonates from Epoxides or Olefins and CO_2 Catalyzed by Metal-Organic Frameworks and Quaternary Ammonium Salts. *J. Energy Chem.* **2013**, *22* (1), 130–135.
(253) Fang, J.; Li, K.; Wang, Z.; Li, D.; Ma, Y.; Gong, X.; Hou, Z. Direct Oxidative Carboxylation of Olefins into Cyclic Carbonates at Ambient Pressure. *J. CO2 Util.* **2020**, *40*, 101204.
(254) Comès, A.; Poncelet, R.; Pescarmona, P. P.; Aprile, C. Imidazolium-Based Titanosilicate Nanospheres as Active Catalysts in Carbon Dioxide Conversion: Towards a Cascade Reaction from Alkenes to Cyclic Carbonates. *J. CO2 Util.* **2021**, *48* (December 2020).
(255) Zhang, J.; Liu, Y.; Li, N.; Wu, H.; Li, X.; Xie, W.; Zhao, Z.; Wu, P.; He, M. Synthesis of Propylene Carbonate on a Bifunctional Titanosilicate Modified with Quaternary Ammonium Halides. *Chin. J. Catal.* **2008**, *29* (7), 589–591.
(256) Yu, L.; Xing, S.; Zheng, K. The Synthesis of Cyclic Carbonates from Oxidative Carboxylation Under Mild Conditions Using Al/FPS Nanocatalyst. *Catal. Letters* **2021**, *151* (2), 600–611.
(257) Wu, J.; Kozak, J. A.; Simeon, F.; Hatton, T. A.; Jamison, T. F. Mechanism-Guided Design of Flow Systems for Multicomponent Reactions: Conversion of CO_2 and Olefins to Cyclic Carbonates. *Chem. Sci.* **2014**, *5* (3), 1227–1231.
(258) Han, Q.; Qi, B.; Ren, W.; He, C.; Niu, J.; Duan, C. Polyoxometalate-Based Homochiral Metal-Organic Frameworks for Tandem Asymmetric Transformation of Cyclic Carbonates from Olefins. *Nat. Commun.* **2015**, *6*, 10007.
(259) Kong, D. L.; He, L. N.; Wang, J. Q. Facile Synthesis of Oxazolidinones Catalyzed by N-Bu_4NBr_3/*n*-Bu_4NBr Directly from Olefins, Chloramine-T and Carbon Dioxide. *Catal. Commun.* **2010**, *11* (11), 992–995.
(260) Jeong, J. U.; Tao, B.; Sagasser, I.; Henniges, H.; Sharpless, K. B. Bromine-Catalyzed

Aziridination of Olefins. A Rare Example of Atom-Transfer Redox Catalysis by a Main Group Element. *J. Am. Chem. Soc.* **1998**, *120* (27), 6844–6845.

(261) Arshadi, S.; Banaei, A.; Ebrahimiasl, S.; Monfared, A.; Vessally, E. Solvent-Free Incorporation of CO_2 into 2-Oxazolidinones: A Review. *RSC Adv.* **2019**, *9* (34), 19465–19482.

(262) Damiano, C.; Sonzini, P.; Intrieri, D.; Gallo, E. Synthesis of Cyclic Carbonates by Ruthenium(VI) Bis-Imido Porphyrin/TBACl-Catalyzed Reaction of Epoxide with CO_2. *J. Porphyr. Phthalocyanines* **2020**, *24* (5–7), 809–816.

(263) Series, S. D. *Carbon Dioxide in Non–Aqueous Solvents At Pressures Less Than 200 KPA*; Elsevier, 1992; Vol. 50.

(264) Rehman, A.; Saleem, F.; Javed, F.; Ikhlaq, A.; Ahmad, S. W.; Harvey, A. Recent Advances in the Synthesis of Cyclic Carbonates via CO_2 Cycloaddition to Epoxides. *J. Environ. Chem. Eng.* **2021**, *9* (2), 105113.

(265) Li, J.; Rodrigues, M.; Paiva, A.; Matos, H. A.; de Azevedo, E. G. Vapor-Liquid Equilibria and Volume Expansion of the Tetrahydrofuran/CO_2 System: Application to a SAS-Atomization Process. *J. Supercrit. Fluids* **2007**, *41* (3), 343–351.

(266) Monticelli, S.; Castoldi, L.; Murgia, I.; Senatore, R.; Mazzeo, E.; Wackerlig, J.; Urban, E.; Langer, T.; Pace, V. Recent Advancements on the Use of 2-Methyltetrahydrofuran in Organometallic Chemistry. *Monatsh. Chem.* **2017**, *148* (1), 37–48.

(267) Fantauzzi, S.; Gallo, E.; Caselli, A.; Piangiolino, C.; Ragaini, F.; Cenini, S. The (Porphyrin)Ruthenium-Catalyzed Aziridination of Olefins Using Aryl Azides as Nitrogen Sources. *Eur. J. Org. Chem.* **2007**, 36, 6053–6059.

(268) Fujimoto, J.; Okamoto, R.; Noguchi, N.; Hara, R.; Masada, S.; Kawamoto, T.; Nagase, H.; Tamura, Y. O.; Imanishi, M.; Takagahara, S.; Kubo, K.; Tohyama, K.; Iida, K.; Andou, T.; Miyahisa, I.; Matsui, J.; Hayashi, R.; Maekawa, T.; Matsunaga, N. Discovery of 3,5-Diphenyl-4-Methyl-1,3-Oxazolidin-2-Ones as Novel, Potent, and Orally Available Δ-5 Desaturase (D5D) Inhibitors. *J. Med. Chem.* **2017**, *60* (21), 8963–8981.

(269) Phung, C.; Tantillo, D. J.; Hein, J. E.; Pinhas, A. R. The Mechanism of the Reaction between an Aziridine and Carbon Dioxide with No Added Catalyst. *J. Phys. Org. Chem.* **2018**, *31* (1), e3735.

(270) Intrieri, D.; Gac, S. Le; Caselli, A.; Rose, E.; Boitrel, B.; Gallo, E. Highly Diastereoselective Cyclopropanation of α-Methylstyrene Catalysed by a C_2-Symmetrical Chiral Iron Porphyrin Complex. *Chem. Commun.* **2014**, *50* (15), 1811–1813.

(271) Carminati, D. M.; Intrieri, D.; Caselli, A.; Le Gac, S.; Boitrel, B.; Toma, L.; Legnani, L.; Gallo, E. Designing 'Totem' C_2-Symmetrical Iron Porphyrin Catalysts for Stereoselective Cyclopropanations. *Chem. Eur. J.* **2016**, *22* (38), 13599–13612.

(272) Maeda, C.; Sasaki, S.; Ema, T. Electronic Tuning of Zinc Porphyrin Catalysts for the Conversion of Epoxides and Carbon Dioxide into Cyclic Carbonates. *ChemCatChem* **2017**, *9* (6), 946–949.

(273) Lu, Y.; Chang, Z.; Zhang, S.; Wang, S.; Chen, Q.; Feng, L.; Sui, Z. Porous Organic Polymers Containing Zinc Porphyrin and Phosphonium Bromide as Bifunctional

Catalysts for Conversion of Carbon Dioxide. *J. Mater. Sci.* **2020**, *55* (26), 11856–11869.

(274) Beck, J. S.; Vartuli, J. C.; Roth, W. J.; Leonowicz, M. E.; Kresge, C. T.; Schmitt, K. D.; Chu, C. T. W.; Olson, D. H.; Sheppard, E. W.; McCullen, S. B.; Higgins, J. B.; Schlenker, J. L. A New Family of Mesoporous Molecular Sieves Prepared with Liquid Crystal Templates. *J. Am. Chem. Soc.* **1992**, *114* (27), 10834–10843.

(275) Greene, T. W.; Wuts, P. G. M. Protection for the Alkyne –CH. In *Protective Groups in Organic Synthesis* **1999**, Jhon Wiley & Sons, Inc.: New York, USA, Vol. 9, pp 654–659

(276) Milgram, L. R. *The Colours of Life. An Introduction to the Chemistry of Porphyrins and Related Compound*; Oxford Universitary Press: Oxford, 1997.

(277) Clegg, W.; Harrington, R. W.; North, M.; Pasquale, R. Cyclic Carbonate Synthesis Catalysed by Bimetallic Aluminium-Salen Complexes. *Chem. Eur. J.* **2010**, *16* (23), 6828–6843.

(278) Rillema, D. P.; Nagle, J. K.; Barringer, L. F.; Meyer, T. J. Redox Properties of Metalloporphyrin Excited States, Lifetimes, and Related Properties of a Series of Para-Substituted Tetraphenylporphine Carbonyl Complexes of Ruthenium(II). *J. Am. Chem. Soc.* **1981**, *103* (1), 56–62.

(279) Fantauzzi, S.; Gallo, E.; Caselli, A.; Ragaini, F.; Casati, N.; MacChi, P.; Cenini, S. The Key Intermediate in the Amination of Saturated C-H Bonds: Synthesis, X-Ray Characterization and Catalytic Activity of Ru(TPP)$(NAr)_2$ (Ar = 3,5-$(CF_3)_2C_6H_3$). *Chem. Commun.* **2009**, 26, 3952–3954.

(280) Zhuo, C. W.; Qin, Y. S.; Wang, X. H.; Wang, F. S. Steric Hindrance Ligand Strategy to Aluminum Porphyrin Catalyst for Completely Alternative Copolymerization of CO_2 and Propylene Oxide. *Chinese J. Polym. Sci. English Ed.* **2018**, *36* (2), 252–260.

(281) Eaton, S. S.; Eaton, G. R. Rotation of Phenyl Rings in Metal Complexes of Substituted Tetraphenylporphyrins. *J. Am. Chem. Soc.* **1975**, *97* (13), 3660–3666.

(282) Ahmadi, E.; Ramazani, A.; Hamdi, Z.; Mashhadi-Malekzadeh, A.; Mohamadnia, Z. 5,10,15,20-Tetrakis(4-Carboxyphenyl)Porphyrin Covalently Bound to Nano-Silica Surface: Preparation, Characterization and Chemosensor Application to Detect TNT. *Silicon* **2015**, *7* (4), 323–332.

(283) Auras, B. L.; De Lucca Meller, S.; da Silva, M. P.; Neves, A.; Cocca, L. H. Z.; De Boni, L.; da Silveira, C. H.; Iglesias, B. A. Synthesis, Spectroscopic/Electrochemical Characterization and DNA Interaction Study of Novel Ferrocenyl-Substituted Porphyrins. *Appl. Organomet. Chem.* **2018**, *32* (5), 1–12.

(284) Lindsey, J. S.; Wagner, R. W. Investigation of the Synthesis of Ortho-Substituted Tetraphenylporphyrins. *J. Org. Chem.* **1989**, *54* (4), 828–836.

(285) Sessler, J. L.; Mozaffari, A.; Johnson, M. R. 3,4-Diethylpyrrole and 2,3,7,8,12,13,17,18-Octaethylporphyrin. *Org. Synth.* **2003**, 70, 68.

(286) Didier, A.; Michaudet, L.; Ricard, D.; Baveux-Chambenoît, V.; Richard, P.; Boitrel, B. A Versatile and Convenient Method for the Functionalization of Porphyrins. *Eur. J. Org. Chem.* **2001**, 10, 1927–1926.

(287) Intrieri, D.; Damiano, C.; Rizzato, S.; Paolesse, R.; Venanzi, M.; Monti, D.; Savioli, M.; Stefanelli, M.; Gallo, E. Sensing of Diclofenac by a Porphyrin-Based Artificial

Receptor. *New J. Chem.* **2018**, *42* (19), 15778–15783.
(288) Malvi, B.; Sarkar, B. R.; Pati, D.; Mathew, R.; Ajithkumar, T. G.; Sen Gupta, S. "clickable" SBA-15 Mesoporous Materials: Synthesis, Characterization and Their Reaction with Alkynes. *J. Mater. Chem.* **2009**, *19* (10), 1409–1416.
(289) Gryko, D.; Li, J.; Diers, J. R.; Roth, K. M.; Bocian, D. F.; Kuhr, W. G.; Lindsey, J. S. Studies Related to the Design and Synthesis of a Molecular Octal Counter. *J. Mater. Chem.* **2001**, *11* (4), 1162–1180.
(290) Li, F.; Yang, K.; Tyhonas, J. S.; MacCrum, K. A.; Lindsey, J. S.; Greene, T. W.; Wuts, P. G. M.; Vázquez-Arce, A.; Zaragoza-Galán, G.; Aguilar-Ortíz, E.; Morales-Espinoza, E. G.; Rodríguez-Alba, E.; Rivera, E.; Nakazawa, J.; Smith, B. J.; Stack, T. D. P.; Gryko, D.; Li, J.; Diers, J. R.; Roth, K. M.; Bocian, D. F.; Kuhr, W. G.; Lindsey, J. S.; Nakazawa, J.; Smith, B. J.; Stack, T. D. P. Discrete Complexes Immobilized onto Click-SBA-15 Silica: Controllable Loadings and the Impact of Surface Coverage on Catalysis. *J. Am. Chem. Soc.* **2012**, *134* (5), 2750–2759.
(291) Damiano, C.; Gadolini, S.; Intrieri, D.; Lay, L.; Colombo, C.; Gallo, E. Iron and Ruthenium Glycoporphyrins: Active Catalysts for the Synthesis of Cyclopropanes and Aziridines. *Eur. J. Inorg. Chem.* **2019**, *2019* (41), 4412–4420.
(292) Lima-Neto, R. G.; Cavalcante, N. N. M.; Srivastava, R. M.; Mendonça, F. J. B.; Wanderley, A. G.; Neves, R. P.; Dos Anjos, J. V. Synthesis of 1,2,3-Triazole Derivatives and in Vitro Antifungal Evaluation on Candida Strains. *Molecules* **2012**, *17* (5), 5882–5892.
(293) Graßl, S.; Singer, J.; Knochel, P. Iron-Mediated Electrophilic Amination of Organozinc Halides Using Organic Azides. *Angew. Chemie Int. Ed.* **2019**.
(294) Barral, K.; Moorhouse, A. D.; Moses, J. E. Efficient Conversion of Aromatic Amines into Azides: A One-Pot Synthesis of Triazole Linkages. *Org. Lett.* **2007**, *9* (9), 1809–1811.
(295) Rossi, S.; Puglisi, A.; Benaglia, M.; Carminati, D. M.; Intrieri, D.; Gallo, E. Synthesis in Mesoreactors: Ru(Porphyrin)CO-Catalyzed Aziridination of Olefins under Continuous Flow Conditions. *Catal. Sci. Technol.* **2016**, *6* (13), 4700–4704.
(296) Saptal, V. B.; Bhanage, B. M. N-Heterocyclic Olefins as Robust Organocatalyst for the Chemical Conversion of Carbon Dioxide to Value-Added Chemicals. *ChemSusChem* **2016**, *9* (15), 1980–1985.
(297) Carminati, D.; Gallo, E.; Damiano, C.; Caselli, A.; Intrieri, D. Ruthenium Porphyrin Catalyzed Synthesis of Oxazolidin-2-Ones by Cycloaddition of CO2 to Aziridines. *Eur. J. Inorg. Chem.* **2018**, *2018* (48), 5258–5262.
(298) Zhang, Y.; Zhang, Y.; Ren, Y.; Ramström, O. Synthesis of Chiral Oxazolidinone Derivatives through Lipase-Catalyzed Kinetic Resolution. *J. Mol. Catal. B Enzym.* **2015**, *122*, 29–34.

Summary

Chapter I: Introduction

The human influence in the raise of the atmospheric concentration of carbon dioxide registered in the last decades up to the actual alarming situation is clear. The most evident consequence is the global warming, but this is only one of the problems correlated to emissions of greenhouse gases. Unfortunately, almost all the economic sectors play a role in the CO_2 production and the complete elimination of the anthropogenic emissions of carbon dioxide is not possible in the short term. Thus, one of the major scientific challenges of this century is to find a solution to this problem. In addition to the reduction of the emissions, three ways has emerged as the most promising and interesting tools to face the carbon dioxide problem: Carbon Capture and Storage (CCS), Bioenergy from Carbon Capture and Storage (BECCS) and Carbon Capture and Usage (CCU).

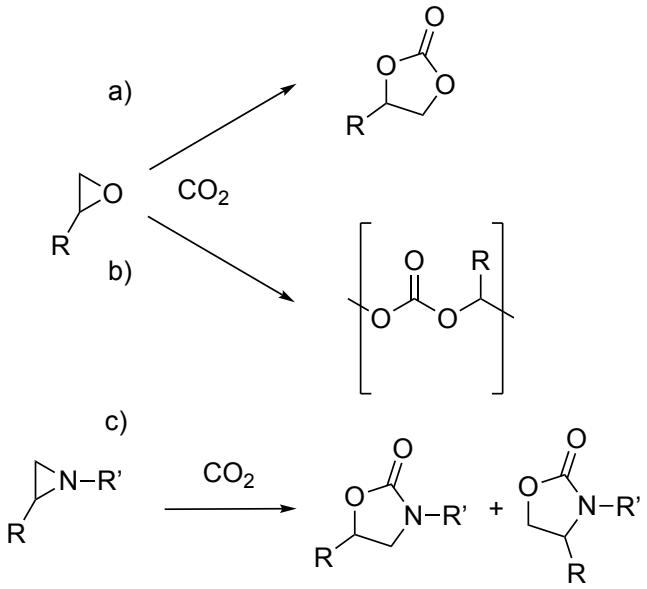

Scheme 1: *The carbon dioxide cycloaddition to three membered heterocycles.*

The carbon dioxide cycloaddition to three membered heterocycles is an example of CCU that can be exploited to mitigate the human influence on the climate change. Moreover, this reaction is very promising because makes possible the synthesis of very useful fine

chemicals such as cyclic carbonates and oxazolidinones from a waste -as CO_2- with a 100% of atom economy. However, carbon dioxide is a very stable molecule and an efficient catalytic species is needed to make the reaction proceeds by avoiding drastic conditions. Even if the reaction between epoxides and CO_2 has been deeply studied in the last 20 years, the analogous carbon dioxide cycloaddition to aziridines has been much less studied and the conversion of *N*-aryl aziridines into corresponding oxazolidinones resulted challenging and only few examples of efficient catalysts have been reported up to now. This work is devoted to the study of porphyrins as organic catalysts of the carbon dioxide cycloaddition both under homogeneous and heterogeneous conditions with the final the goal to improve the sustainability of the production of cyclic carbonates and oxazolidinones.

Chapter II: Homogeneous catalysts for the CO_2 cycloaddition reaction

In this chapter the full organic catalytic *meso*-tetraphenyl porphyrin ($TPPH_2$)/TBACl combination has been studied in the synthesis of oxazolidinones and cyclic carbonates from CO_2 and aziridines or epoxides, respectively. After the initial optimization of the experimental conditions, this catalytic system was applied for converting a plethora of different substrates into corresponding five-membered products. The gathered data made possible to present the first general methodology for the conversion of *N*-aryl aziridines and CO_2 into *N*-aryl oxazolidinones. Then, a tandem methodology for the production of these useful molecules from aryl azides, styrenes and carbon dioxide has been presented. This methodology resulted effective also in the synthesis of the pharmacologically active oxazalidin-2-one **41**.

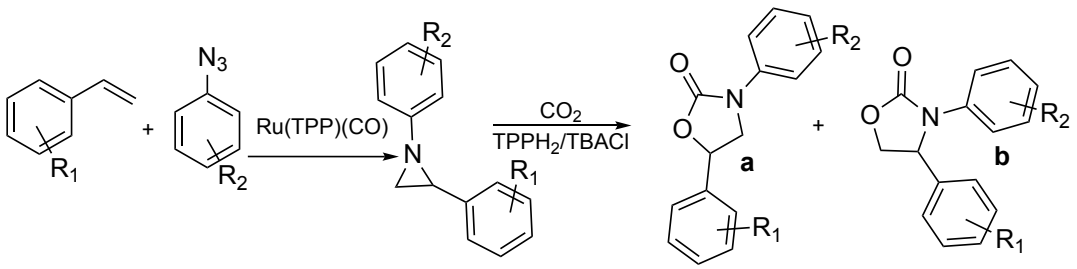

Scheme 2: *tandem procedure for the preparation of oxazolidinones from styrenes, aryl azides and carbon dioxide.*

Encouraged by the good results obtained in these studies, the proposed catalytic procedure was successfully extended to the reaction of CO_2 with *N*-alkyl aziridines and epoxides. Moreover, different catalysts have been tested in combination with TBACl in order to shed some light on the influences of the steric and electronic characteristic of the porphyrins on the reaction productivity. Moreover, a first mechanistic study has been presented in collaboration with Dr. Gabriele Manca of the ICCCOM-CNR of Sesto Fiorentino.

Chapter III: Heterogeneous catalysts for the CO_2 cycloaddition reaction

The heterogenization of the porphyrin onto a SBA-15 silica material has been proposed in this chapter. To improve the reaction sustainability, the synthesis of an active heterogeneous catalyst represents a crucial step to simplify the catalyst recovery and the product purification. The possibility to combine the characteristics of a heterogeneous catalyst with the high activity demonstrated by the $TPPH_2$/TBACl homogeneous catalytic system propelled the preparation of a hybrid material by supporting a free porphyrin onto mesoporous SBA-15 silica trough covalent bondings. This solid support was selected because it is easy to functionalize and the presence of silanols group onto its surface foster the reactivity of epoxides towards CO_2.

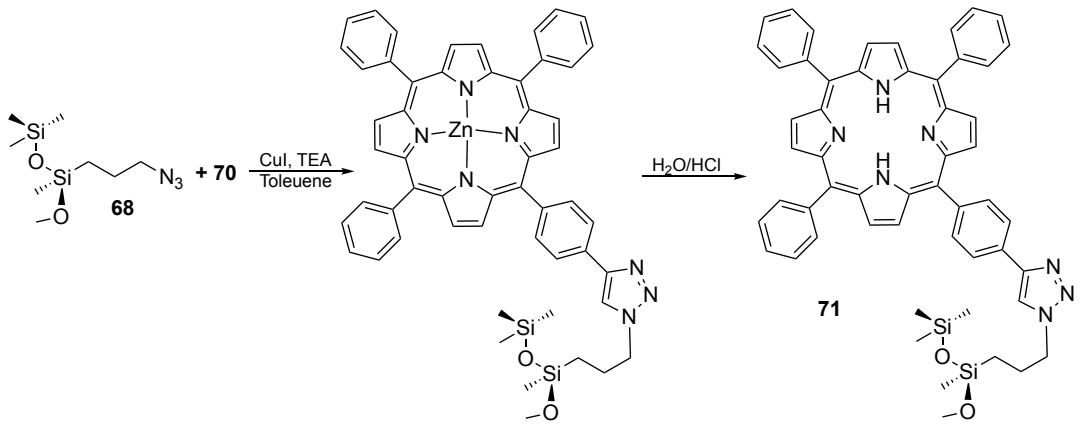

Scheme 3: *Synthesis of the hybrid catalyst* ***71****.*

The so-prepared catalyst, in combination with tetrabutyl ammonium iodide (TBAI) resulted very active in the preparation of cyclic carbonates from the reaction of epoxides with CO_2. Then, the same catalytic system was successfully tested for the carbon dioxide cycloaddition to *N*-alkyl aziridines. Finally, the supported porphyrin, in combination with TBACl, represents the first heterogeneous catalyst active in the conversion of *N*-aryl aziridines into *N*-aryl oxazolidinones.

The good results obtained with the three different classes of substrates, in combination with the recyclability of the heterogeneous catalyst and the possibility to use it with up to 1.00 g of substrate, make this hybrid material an interesting candidate for further industrial applications.